ISABEL CARDOSO

DYNAMICS OF TRANSTHYRETIN FIBRILLOGENESIS: CONTRIBUTION TO THERAPEUTIC APPROACHES IN FAMILIAL AMYLOIDOTIC POLYNEUROPATHY

PORTO

2002

ISABEL CARDOSO

DYNAMICS OF TRANSTHYRETIN FIBRILLOGENESIS: CONTRIBUTION TO THERAPEUTIC APPROACHES IN FAMILIAL AMYLOIDOTIC POLYNEUROPATHY

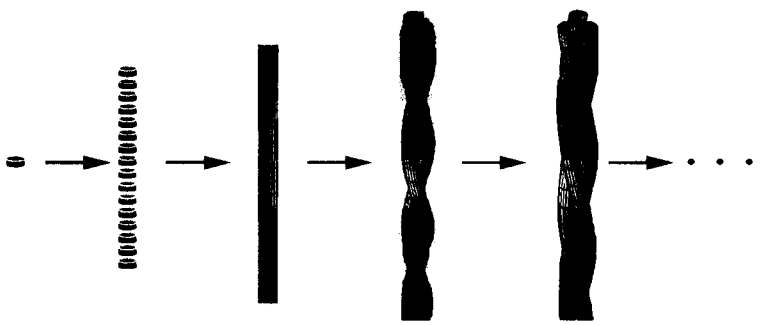

PORTO

2002

ISABEL CARDOSO

DYNAMICS OF TRANSTHYRETIN FIBRILLOGENESIS: CONTRIBUTION TO THERAPEUTIC APPROACHES IN FAMILIAL AMYLOIDOTIC POLYNEUROPATHY

Dissertation for the obtention of a Ph.D degree in Biomedical Sciences, Biochemistry speciality, submitted to the Instituto de Ciências Biomédicas Abel Salazar, Universidade do Porto

Supervisor: Professor Maria João Saraiva

PORTO

2002

De acordo com o nº 2 do Artigo 8º do Decreto-lei nº 388/70 foram utilizados neste trabalho os resultados dos artigos publicados ou em vias de publicação, que em seguida se descrimina:

Cardoso I, Pereira PJB, Damas AM and Saraiva MJ (2000). Aprotinin binding to amyloid fibrils. *Eur J Biochem* **267**: 2307-2311.

Cardoso I, Damas AM and Saraiva MJ (2000). *In vitro* binding of aprotinin/ aprotinin derived peptides to amyloid fibrils: Potencial radiopharmaceuticals in diagnosis of amyloidosis. *Nuclear medicine Communications* **21**: 586.

Palha JA, Ballinari D, Amboldi N, Cardoso I, Fernandes R, Bellotti V, Merlini G and Saraiva MJ (2000). 4'-iodo-4'-deoxydoxorubicin disrupts the fibrillar strucutre of transthyretin amyloid. *Am J pathol* **156**: 1919-1925.

Sousa MM, Cardoso I, Fernandes R, Guimarães A and Saraiva M J (2001). Deposition of transthyretin in early stages of familial amyloidotic polyneuropathy: evidence for toxicity of non-fibrillar aggregates. *Am J Pathol* **159**: 1993-2000.

Cardoso I, Goldsbury CS, Müller SA, Olivieri V, Wirtz S, Damas AM, Aebi U and Saraiva MJ (2002). Transthyretin fibrillogenesis entails the assembly of monomers: A molecular model for *in vitro* assembled transthyretin amyloid-like fibrils. *J Mol Biol* **317**: 687-99.

Cardoso I, Merlini G and Saraiva, MJ. 4'-iodo-4'-Deoxydoxorubicin disrupts transthyretin amyloid fibrils *in vitro* producing non- cytotoxic species. Screening for TTR fibril disrupters. *In preparation.*

Cardoso I, Saraiva MJ. Detecting conformational and morphological changes in TTR. Screening for compounds affecting early amyloidogenic stages. *In preparation.*

No cumprimento do disposto no Decreto-lei acima referido, esclarece-se serem da nossa responsabilidade a execução das experiências que permitiram a obtenção dos resultados apresentados (excepto quando referido em contrário), assim como a sua interpretação e discussão.

Acknowledgements/ Agradecimentos

I hope I'm able to put into words my gratitude to those who supported me and in this manner made possible this thesis. My many thanks go to:

À Professora Maria João Saraiva, por todo o apoio dado durante este trabalho e pela orientação constante. Pela força e vontade transmitidas, ensinando-me a não desistir.

To Professor Robert Kisilevsky for receiving me in his lab, his kindness and all support. I can't forget how he made me fill welcome in Kingston. To all the people in his lab, I thank for their friendship and joy: Ruth, John, Lee, Chris, Runland and Alana.
Special thanks to John DaCosta, not only for helping me with the electron microscopy but also for being such a great friend. For all the coffee breaks in portuguese that encouraged me throughout the rest of the day making me feel closer to home.

To Professor Ueli Aebi for the great opportunity to work in his lab allowing me to learn so much in such a short time. To his team, especially to Claire for all her support in and out of the lab. "No worries" like she says, made my stay in Basel a pleasant journey. But also to Jochan for being such a nice and helpful person and to Martin (the AFM guy).

À Mónica (Louise), por tudo.... o que me ensinou, pelos maus momentos que me ajudou a passar e pelos bons que me fez passar. Pela amizada.

À Rosário, sempre disponível, mesmo nas alturas em que estava mais atarefada.
À Anabela, antes e agora. Pelo apoio e por me fazer ver as coisas de uma outra (melhor) forma.
Ao Paul, pela ajuda e por ter sempre mais um bocadinho de proteína para me dar!
À Joana, pela pronta ajuda sempre que necessário e pelo apoio na correcção da tese.
Ao Rui, pela ajuda nas microscopias e pela boa disposição. E ao João, pelas "conversas" e pela ajuda com os computadores....

Ao Professor Teixeira da Silva, por me ter ensinado a gostar da microscopia electrónica. Pelo apoio, interesse e incentivo.
Também à Paula Macedo pelas ajudas no microscópio electrónico, e pela contagiante boa disposição.

À Monica Castro, a minha ouvinte. Pela inesgotável paciência e grande amizade. À Sandra, por ser também uma grande amiga, sempre pronta nas horas em que mais se precisa.

Naturalmente, aos meus pais. È a eles a quem mais agradeço. E aos meus irmãos.

Finalmente, agradeço a apoio financeiro do programa PRAXIS XXI (BD/15725/98).

À minha mãe,
por me ajudar a sonhar....

Contents

Contents

Part III- Appendix

Abstract

Familial amyloidotic polyneuropathy (FAP) is an autosomal dominant disorder directly related to the presence of mutations in the transthyretin (TTR) protein. Pathologically, FAP is characterized by the extracellular deposition of insoluble TTR **-amyloid-** in several organs, with a special involvement of the peripheral nerve, leading to cell damage, organ dysfunction and finally, death. The mechanisms underlying TTR amyloid formation as well as other factors intervening in the amyloidogenic cascade are unknown. The only treatment for FAP that has proven successful is liver transplantation, though limited by the availability of livers for transplantation and the requirement for lifelong immune suppression. A therapy in which a small molecule drug inhibits TTR amyloid formation would be preferable.

Different markers have been used to identify amyloid throughout time. However, some of them are not appropriate for *in vivo* diagnosis and others imply very invasive methods. We studied the binding properties of a small protein, aprotinin, to different amyloid types and showed that this protease inhibitor binds insulin, TTR, β-amyloid peptide and immunoglobulin synthetic amyloid fibrils by a specific dot blot ligand binding assay. Aprotinin did not bind amorphous precipitates and/or the soluble fibril precursors. A Ka of 2.9 μM^{-1} for the binding of aprotinin to insulin amyloid fibrils was determined by Scatchard analysis. We suggest that aprotinin interacts with amyloid fibrils through pairing of β-sheets with exposed structures of the same type at the surface of amyloid deposits. Our results also indicate an electrostatic component in the binding of aprotinin to amyloid fibrils. We also tested binding of short peptides derived from aprotinin (APR1 and APR2) to different types of synthetic amyloid fibrils and showed that they are able to specifically bind to fibrils. In the future, aprotinin and particularly its peptides can be used not only to perform non-invasive diagnosis but also to follow up the progression of eventual treatments.

In an attempt to gain more insights into the ultrastructural organization and assembly of amyloid fibrils, we studied the time progression of TTR wild-type (WT) amyloid-like fibrils produced by acidification and of TTR Leu55Pro fibrils under physiological conditions, finding that they are dynamically very similar and present the same features and dimensions. The main species was an 8 nm wide fibril with a left-handed twist as shown by transmission electron microscopy (TEM) after metal shadowing, and atomic force microscopy (AFM). The preparations evolved from non-fibrillar aggregates to short fibrils elongating over time. These fibrils were also analysed by scanning transmission electron microscopy (STEM) and we clearly showed that the basic unit is an altered monomer. In relation to *ex vivo* fibrils, nerve amyloid fibrils from an FAP patient revealed dimensions similar to the *in vitro* ones, while vitreous fibrils were shown to be significantly larger. However, the latter seemed to result from the assembly of several 8 nm wide fibrils, suggesting that the wider structures can result from the lateral association of smaller fibrils. Mature fibrils, as the ones extracted from FAP patients, do not enable a dynamic study and thus, this problem as well as the identification of the building blocks in the *in vivo* or *ex vivo* fibrils should be addressed in the future.
The identification of different species present throughout the process of amyloid formation created the opportunity to evaluate the activity of different drugs interfering at different stages in the amyloidogenic cascade. A number of studies revealed that 4'-iodo-4'-deoxydoxorubicin (I-DOX) interact with amyloid fibrils. To ascertain the action on TTR amyloid-like fibrils, we performed a time and concentration study and concluded that I-DOX and I-DOX-like compounds tested do not inhibit formation of fibrils but rather disrupt

long fibrils, demonstrating the highest activity at 10^{-5} M/100 μg of fibrils, under the conditions tested. After assessing the toxicity of TTR Leu55Pro aggregates and fibrils at different stages, we concluded that only the initial aggregates are toxic; structures generated upon I-DOX treatment were also shown to be non-toxic. Further studies aiming at determining the toxicity associated with the treatment of other disrupters are required.

The transformation of tetrameric soluble TTR into insoluble aggregates (**priming** stage) was morphologically studied by TEM making use of TTR Tyr78Phe. Under physiological conditions (PBS, 37°C) the protein preparation starts with round particles resembling native TTR WT and evolves to oligomers, large aggregates and finally fibrils approximately 8 nm wide, identical to the TTR Leu55Pro and TTR WT fibrils. This mutant was further used to select drugs acting at the priming stage. TTR Leu55Pro, previously investigated as described above, was used to identify drugs interfering with fibril elongation (**extension** stage).

The screening methodology included an immunoassay with a monoclonal antibody (Mab15), which recognizes differentially amyloidogenic structures. Mab15 was previously demonstrated to recognize soluble TTR Tyr78Phe but our study revealed that once the amyloidogenic protein was incubated at 37°C for 48 hours, the reactivity lowered significantly. The antibody was also able to distinguish different TTR Leu55Pro species, reacting highly with the initial aggregates but not with amyloid-like fibrils.

Different groups of drugs were tested for their ability to affect TTR fibrillogenesis, either by inhibiting priming, extension or both. The compounds included benzofurans, non-steroid anti-inflammatory drugs, TTR stabilizers and/or thyroxine (T_4) competitors, extracellular matrix (ECM) components, a porphyrin, aprotinin, and an aprotinin peptide.

Among the compounds tested, benzofurans were the most effective, inhibiting both priming and extension, at approximately 60%. Ibuprofen showed intermediate activity against both stages; diflunisal and diclofenac, the two other compounds included in the non-steroid anti-inflammatory group, presented no inhibitory capacity. In the group of TTR stabilizers/T_4 competitors, diethylstilbestrol (DES) also showed a high degree of inhibition for both priming and extension (approximately 50%) whereas the remaining compounds in this group presented activity against only either priming or extension. Among the ECM components, laminin was the only molecule tested able to interfere with TTR fibrillogenesis and although it only inhibited extension, its activity was very high (70%). Hemin, the porphyrin included in this study, also showed to be an important inhibitor acting in both priming and extension (over 50% of inhibition). The results were confirmed by TEM.

Although the structural determinants responsible for the interactions between Mab15 and each one of the TTR species are not known nor the molecular mechanism behind the effects observed, results from TEM and the immunoassay seemed to correlate very well. In some cases, although some activity was observed by the immunoassay, visualization by TEM did not reveal important morphological differences implying that the sensitivity of the former method is higher. The selected drugs should be further tested in an amyloid animal model to establish dosage and related toxicity and finally to verify the *in vitro* results.

We also developed a cellular system by transfecting a Schwanoma cell line with different TTR constructs and demonstrated that TTR Leu55Pro aggregates extracellularly, after secretion, using a dot blot filter assay. Furthermore, Mab15 recognized TTR Val30Met and Leu55Pro while TTR WT was not detected in the immunoassay. This result suggests that although TTR Val30Met is not detected in the dot blot filter assay, the protein presents an altered conformation, which exposes amyloidogenic epitopes. Therefore, the cellular model might constitute a system to investigate drugs able to inhibit the very early conformational

changes prior to TTR dissociation and aggregation, occurring during TTR fibrillogenesis. The developed model will contribute to the study of cellular factors intervening in amyloid formation.

In conclusion, our studies provided new information on the ultrastructure of amyloid fibrils and important insights into the amyloidogenic pathway. The possibility of producing TTR fibrils under physiological conditions and the determination of the toxic species paved the way to search for molecules with therapeutic potential in FAP.

Sumário

A polineuropatia amiloidótica familiar (PAF) é uma doença directamente relacionada com a presença de mutações na proteína transtirretina (TTR). Patologicamente, a PAF é caracterizada por deposição extracelular de TTR insolúvel- **amilóide**- em vários orgãos, em especial no nervo periférico, resultando em danos celulares, disfunção orgânica e finalmente, em morte. O mecanismo responsável pela deposição de TTR, bem como outros factores intervenientes na cascata amiloidogénica, são desconhecidos. O transplante hepático é a única terapia aplicada à PAF com sucesso mas é limitado pela disponibilidade de orgãos e pela necessidade de realizar imunosupressão durante toda a vida. Métodos terapêuticos em que pequenas moléculas inibam a formação de amilóide são preferiveis.

Ao longo do tempo, diferentes marcadores têm sido usados para identificar amilóide. No entanto, alguns deles não são apropriados a diagnósticos *in vivo* e outros implicam técnicas muito invasivas. Nós estudámos as propriedades de ligação de uma pequena proteína, aprotinina, a diferentes tipos de amilóide e verificámos que este inibidor de proteases apresenta ligação específica a fibras de insulina, de péptido β e de uma imunoglobulina. A aprotinina não apresentou ligação a precipitados amorfos nem aos precursores solúveis das fibras. A metodologia usada baseou-se num ensaio de retenção em filtro em que a aprotinina ligada a fibras de amilóide é retida no filtro, enquanto que a livre ou não ligada é filtrada. Para fibras de insulina, a constante de ligação da aprotinina é de 2.9 μM^{-1}, determinada por análise Scatchard. Os resultados sugerem que a aprotinina interage com fibras de amilóide através do pareamento de folhas β com estruturas do mesmo tipo à superficie dos depósitos de amilóide. Dois pequenos péptidos derivados da aprotinina (APR1 e APR2) também foram testados e demonstrou-se que também eles ligam de forma específica a fibras de amilóide. No futuro, a aprotinina, e em particular os péptidos dela derivados, poderão ser utilizados não só para diagnosticar de forma não-invasiva doenças amiloidóticas mas também para seguir a progressão dos eventuais tratamentos.

Na tentativa de alargar o conhecimento sobre a organização ultra-estrutural e o processo de formação das fibras de amilóide, estudou-se a progressão no tempo de fibras produzidas por acidificação a partir de TTR selvagem (WT) e de fibras produzidas em condições fisiológicas a partir de uma variante de TTR (TTR Leu55Pro). Concluimos que estas fibras apresentam dinâmicas, caracteristicas morfológicas e dimensões semelhantes. A forma principal encontrada foi uma fibra de 8 nm de diâmetro, torcida para o lado esquerdo e com uma unidade de repetição de cerca de 17 nm. Esta última característica foi observada quer por microscopia electronica de transmissão (TEM) em amostras sombreadas metalicamente, quer por microscopia de força atómica (AFM). As preparacões de TTR WT e de Leu55Pro apresentam-se inicialmente como agregados não fibrilares e evoluem para fibras curtas que crescem ao longo do tempo. Uma outra técnica foi empregue para analisar estas fibras- microscopia electrónica de transmissão com varrimento (STEM)- permitindo concluir que as fibras amilóide de TTR são formadas a partir de monómeros de TTR, provavelmente com uma estrutura alterada. Neste trabalho, também foram analisadas fibras *ex vivo* de nervo e de vítreo de doentes PAF. Enquanto que as fibras de nervo apresentaram dimensões comparaveis às das fibras produzidas *in vitro*, as do vítreo revelaram diâmetros bastante superiores. No entanto, as fibras de vítreo pareciam resultar de associação lateral de várias fibras de 8 nm, sugerindo que as estruturas mais largas poderiam resultar da união de outras mais finas e de diâmetro semelhante ao das formadas *in vitro*. As fibras de amilóide maduras, como as que são extraidas dos doentes PAF não permitem o estudo da dinâmica

de formação das fibras. Por esta razão, esta questão bem como a identificação das unidades básicas de fibras *ex vivo* deve ser estudada no futuro.
A identificação de diferentes espécies durante o processo de formação de amilóide criou a oportunidade para avaliar a actividade de diferentes drogas que interferem na cascata amiloidogénica em diferente passos da mesma. Estudos anteriores indicaram que 4'-iodo-4'-deoxydoxorubicin (I-DOX) é capaz de interagir com fibras de amilóide. Para averiguar a acção deste composto nas fibras amilóide de TTR, fizemos um estudo de tempo e concentração e concluimos que o I-DOX e seus derivados não inibem a formação de fibras mas desagregam fibras longas originando pequenas particulas que se assemelham à proteína solúvel; o máximo de actividade foi observado para uma concentração de I-DOX de 10^{-5} M/100 μg nas condições testadas. Estudos de toxicidade realizados com as diferentes espécies detectadas durante a formação de fibras de TTR Leu55Pro demonstraram que os agregados não-fibrilares são as únicas espécies tóxicas. As estruturas resultantes da acção do I-DOX sobre as fibras de TTR Leu55Pro também se revelaram não tóxicas. Estudos respeitantes à toxicidade associada com o tratamento dos outros disruptores de fibras são necessários.

A transformação de TTR solúvel tetramérica em agregados insolúveis (estadio **priming**) foi estudada morfologicamente por TEM e fazendo uso da variante de TTR Tyr78Phe. Em condições fisiológicas (PBS, 37°C) a amostra apresenta-se inicialmente como particulas circulares em tudo semelhantes à proteína selvagem e evolui para oligómeros, grandes agregados e finalmente fibras com aproximadamente 8 nm de diâmetro. Esta variante de TTR foi utilizada para seleccionar drogas capazes de interferir com o estadio priming. A variante de TTR Leu55Pro, já estudada como descrito nesta secção, foi usada para identificar compostos que afectam o crescimento das fibras (estadio **extensão**).
A metodologia usada para o rastreio de compostos incluiu um ensaio imunológico com um anticorpo monoclonal (Mab15), o qual reconhece diferencialmente estruturas amiloidogénicas. Foi anteriormente demonstrado que este anticorpo reconhece TTR Tyr78Phe na sua forma solúvel. No entanto, o nosso estudo revelou que, após incubação a 37°C durante 48 horas, a reactividade baixa de forma muito significativa. Este anticorpo também é capaz de distinguir espécies de TTR Leu55Pro diferentes: reage fortemente com os agregados iniciais mas não com as fibras.
Várias classes de compostos foram testados com o intuito de avaliar as suas capacidades inibitórias, quer de priming quer de extensão. Nos testes foram incluidos benzofuranos, drogas não-esteróides anti-inflamatórias, estabilizadores tetraméricos de TTR ou que competem com a tiroxina (T_4), componentes da matrix extracelular, uma porfirina, aprotinina e um dos seus péptidos.
De entre os compostos avaliados, os benzofuranos foram os mais eficazes, inibindo quer o priming quer a extensão em cerca de 60%. O ibuprofeno demonstrou ter uma actividade intermedia nas duas fases amiloidogénicas; o diflunisal e o diclofenac, os outros dois compostos incluidos no grupo dos não-esteroides anti-inflamatórios, não revelaram qualquer actividade. No grupo dos estabilizadores tetraméricos/competidores de T_4, o dietilstilbestrol (DES) também apresentou um elevado grau de inibição quer do priming quer da extensão, enquanto que os restantes compostos deste grupo apenas apresentaram actividade inibitória numa das fases (priming ou extensão). De entre os componentes da matriz extracelular testados, a laminina foi a única capaz de interferir com a fibrilogénese da TTR e apesar de inibir apenas a extensão, a usa actividade foi muito elevada (70% de inibição). Quanto à hemina, a porfirina avaliada, também revelou ser um inibidor

importante, quer do priming quer da extensão, com cerca de 50% de inibição. Estes resultados foram confirmados por TEM.
Apesar dos determinantes estruturais responsáveis pelas interaccções entre o Mab15 e cada uma das espécies de TTR não serem conhecidos, bem como o mecanismo que explica os efeitos observados para cada uma das drogas testadas, os resultados obtidos por TEM e no ensaio imunológico com o Mab15 parecem ser concordantes. Em alguns casos, apesar de se observar alguma actividade no ensaio imunológico, o TEM não revelou alterações morfológicas importantes. Esta discrepância parece indicar que a sensibilidade do método imunológico é superior. As drogas seleccionadas devem ser posteriormente caracterizadas num modelo animal de amilóide para assim se estabelecerem critérios de dosagem, toxicidade e verificação dos resultados *in vitro*.
Neste trabalho também foi desenvolvido um sistema celular com uma linha celular de schanomas de rato transfectadas com diferentes cDNAs de TTR (TTR WT, Val30Met, Leu55Pro). Os resultados indicaram que a TTR Leu55Pro é capaz de formar agregados extracelularmente, depois da secreção da proteína. Além disso, o anticorpo Mab15 foi capaz de reconhecer quer a TTR Val30Met quer a Leu55Pro, enquanto que a TTR WT não apresentou qualquer reacção. Apesar da TTR Val30Met secretada pelas células não ser detectada no ensaio de retenção em filtro, indicando que não forma agregados, esta proteína deve, no entanto, possuir uma conformação alterada em relação à WT de forma que epitopos amiloidogénicos ficam expostos. Desta forma, este modelo celular poderá constituir um sistema para estudar drogas capazes de inibir alterações conformacionais que ocorrem no início da processo de agregaçao e que são anteriores à dissociação do tetrâmero da TTR. Este modelo tem ainda a vantagem de permitir o estudo de factores celulares envolvidos na amiloidogénese.

Em sumário, os nossos estudos forneceram novas informaçoões acerca da ultra-estrutura das fibras de amilóide e novos conhecimentos sobre o mecanismo amiloidogénico. A possibilidade de produzir fibras de TTR em condições fisiológicas, a determinação das espécies tóxicas e o desenvolvimento de um novo método (imunológico) facilitou a investigação de moléculas com potencial terapêutico em PAF.

Sommaire

La Polyneuropathie Amyloidotique Familiale (PAF) est une maladie genétique autosomale dominante directement liée à la présence de mutations de la protéine transthyrétine (TTR). La PAF est caractérisée par une déposition extracellulaire de TTR insoluble **-amyloïde-** dans plusieurs organes avec un engagement exceptionnel du nerf périphérique, conduisant à des pertubations cellulaires, un dysfunctionnement des organes et finalement à la mort. Les mécanismes de formation d`amyloïde de TTR ainsi que d'autres facteurs qui interviennent dans la cascade amyloïdeogénique sont inconnus. Actuellement, le seul moyen disponible pour traiter la PAF est la transplantation du foie. Cependant, ce traitement presente des limitations à savoir l'indisponibilité de cette organe et le risque d'immunosupression. Pour cela, une thérapie basée sur l'utilisation d'une drogue inhibitrice de la formation du TTR amyloïde serait profitable.

Plusieurs methodes ont été utilisées pour identifier la substance amyloïde. Cependant, certaines de ces methodes ne sont pas trés adaptées au diagnostique *in vivo* et d'autres provoquent des complications à risque. Nous avons étudié les propriétés de ligation de l'aprotinine, protéine de petite taille, à des différents amyloïdes. Nous avons montré par un dot blot ligand binding assay spécifique que cette protéine se lie aux fibres de l`insuline, de la TTR, de β-amyloïde et de l`amyloïde synthétique d`immunoglobuline. Cependant, l`aprotinine ne lie ni les précipités amorphes ni les précurseurs des fibres solubles. Un Ka de 2.9 μM^{-1} de la liaison de l`aprotinine à des fibres amyloïde d'insuline a été déterminé par l'analyse de Scatchard. Nos resultats suggérent que l`aprotinine intéragit avec les fibres d`amyloïde par l'intermediaire d'une interaction entre les feuillets beta de la proteine elle même et ceux des fibres d' amyloïde. Nos résultats indiquent également une liaison de type électrostatique entre l'aprotinine et les fibres d' amyloïde. Nous avons étudié la liaison de peptides dérivés de l`aprotinine (APR1 et APR2) à différents types de fibres d`amyloïde synthétique et nous avons montré qu'ils peuvent se lier aux fibres. L'ensemble de ces resultats laisse suggérer que l'aprotinine et particulièrement ses peptides derivés peuvent être utilisés non seulement dans le diagnostique non-invasif de la PAF mais également dans la progression d'éventuels traitements.

Afin d'obtenir plus d`information sur l'assemblage ultrastructurale de l`amyloïde, nous avons étudié la formation progressive des fibres de TTR WT produites par acidification ainsi que celle des fibres de TTR Leu55Pro produites sous conditions physiologiques. Le resultat de cette étude a montré que les fibres de TTR WT et TTR Leu55Pro sont dynamiquement similaires et qu`elles ont les mêmes caractéristiques et les même dimensions. La principale forme est une fibre de 8 nm de diamètre avec un gauche-handed twist comme a éte indiqué par la microscopie de transmission d`électrons (TEM) après ombrage métalique et par la microscopie de force atomique. Les préparations évoluaient de l`état non-fibrillaire à des petites fibres qui s´allongeaient au court du temps. L'analyse de ces fibres par microscopie scanning de transmission électronique (STEM) montre clairement que l'unité fondamentale de la fibre est un monomère altéré. Les fibres extraites apartir d'un nerf d'un malade de PAF ont révélé des dimensions similaires contrairement aux fibres du nerf vitreux qui sont significativement plus grandes. Ces dernières semblent être le resultat de l'assemblage de plusieurs fibres de 8 nm, suggérant que les structures plus

larges peuvent être le résultat d'une association latérale de plusieurs fibres de 8 nm. Fibres matures, comme celles extraitent des malades de PAF, ne permettent pas un étude dynamique. Ce problème ainsi que l'identification des constituants des fibres *in vivo* ou *ex vivo* doivent être adressés à l'avenir.

L'identification de formes différentes présentent au court de la formation d`amyloïde a incité l'évaluation de l'activité de différents médicaments qui interférent aux étapes différentes de la cascade de formation de l'amyloïde. Plusieurs études ont révélé que 4'-iodo-4'-deoxydoxorubicin (I-DOX) réagit avec les fibres d`amyloïde. Pour vérifier son action sur les fibres de TTR, nous avons effectué une étude au court du temps et à différentes concentrations. Cette étude a démontré que l`I-DOX et également les composés similaires à l`I-DOX n'inhibent pas la formation de fibres. Son effet passe essentiellement par une destruction des fibres avec une activité optimale de 10^{-5} M/100 µg de fibres. Après avoir evalué la toxicité de la TTR Leu55Pro et ses fibres à différentes étapes, nous avons conclu que seulement les agrégas initiales sont toxiques; les structures crées après le traitement avec I-DOX ont aussi démontré être non-toxique. Des études visant la détermination de la toxicité associé au traitement avec d'autres molecules ayant le même effet que I-DOX sont requises.

La transformation de la TTR soluble tétramérique en agrégas insolubles (l'étape d'**initiation**) a été morphologiquement étudié par le TEM utilisant TTR Tyr78Phe. Dans des conditions physiologiques (PBS, 37°C) la protéine forme des particules circulaires ressemblant à la TTR native et ensuite évolue en oligomères, grands agrégas et finalement en fibres d`approximativement 8 nm, identiques aux fibres de TTR WT et TTR Leu55Pro. Ce mutant a été également utilisé pour choisir des médicaments qui agissent à l'étape de d'initiation. TTR Leu55Pro, comme indiqué ci-dessous, a été utilisé pour identifier des médicaments qui interfèrent avec l'élongation de fibres (l'étape d'**extension**).

La méthodologie de triage est basée sur l'utilisation d'un immunoassay avec un anticorps monoclonal (Mab15), qui reconnaît différentiellement les structures d`amyloïde. Il a été démontré antérieurment que Mab15 est capable de reconnaître TTR Tyr78Phe soluble. Cependant, notre étude a révélé que l'incubation de la protéine amyloïdeogenique à 37°C durant 48 heures reduit significativement la réactivité avec Mab15. Cet anticorp est aussi capable de distinguer différentes formes de TTR Leu55Pro. Il réagit fortement avec les agrégas initiaux de TTR Leu55Pro mais pas avec ses fibres. Différent groupes de médicaments ont été étudiés afin de montrer leur capacité d`affecter la formation de fibres de TTR, d'inhiber le le processus d'intiation ou de l'extension ou les deux à la fois. Les produits étudiés sont: benzofurans, drogues non-steroïdes anti-inflammatoires, TTR stabilisateurs et/ou thyroxine (T_4) compétiteurs, composant de la matrice extracellulaire (ECM), une porphyrine, aprotinine, et un péptide d`aprotinine. L'évaluation des ces différentes molecules a montré que les benzofurans sont les plus efficaces . Ils inhibent 60% de la formation de fibres de TTR en agissant au niveau de l'initiation et l`extension. L'ibuprofen montre une activité intermédiaire au niveau de ces deux étapes. Le diflunisal et le diclofenac, deux autres composés du groupe non-steroïde anti-inflammatoire, ne présentent aucune capacité inhibitoire. Dans le groupe de TTR stabilizers/T_4 concurrents, le diethylstilbestrol (DES) a montré un haut degré d'inhibition pour l'initiation et l`extension (approximativement 50%) tandis que le autres composants de ce groupe ont un potentiel

inhibiteur soit de l'initiation soit de l'extention. Parmis les composants de l'ECM evalués, la laminine est la seule molécule capable d'interférer avec la formation de fibres de TTR, bien qu'elle agisse seulement dans le processus de l'extension avec une activité maximale de 70%. L'hemine, la porphyrine inclue dans cette étude, a également un effet inhibiteur important. Elle est capable d'agir dans les processus d'initiation et de l'extension (plus de 50% d'inhibition). Ces résultats ont été confirmés par le TEM.

Bien que les déterminants structuraux responsables des interactions entre Mab15 et chaqune des espèces de TTR ne soient pas connus ainsi que le méchanisme moléculaire responsable des effets observés, les résultats du TEM et de l'immunoassay sont en accord. Le fait que dans certains cas une activité a été observée par le test d'immunoassay , la visualisation par TEM n'a pas révélé d'importantes différences morphologiques suggérant que la sensibilité de la méthode antérieure est supérieur. Une étude *in vivo* utilisant un modèle animale amyloïde premetterait de verifier les résulats des études *in vitro* et également d'obtenir des informations concernant le dosage de ces drogues ainsi que leur toxicité.

Nous avons développé un système cellulaire par transfection d'une lignée cellulaire de Schwanoma avec différents constructions de TTR et nous avons démontré avec un dot blot filter assay que la TTR Leu55Pro forme des agrégas au niveau extracellulaire après secretion. De plus, Mab15 reconnait TTR Val30Met et Leu55Pro alors que TTR WT n'a pas été détecté dans l'immunoassay. Ce résultat suggère que malgré la non detection de TTR Val30Met par dot blot filter assay, la protéine présente un conformation altérée qui expose des épitopes amiloidogéniques. Pour cela, ce modèle cellulaire que nous avons mis au point pourrait être utilisé pour l'évaluation des médicaments qui ont le potentiel d'inhiber les altérations précoces de conformation qui se produisent avant la dissociation et l'agrégation de la TTR. Ce modèle cellulaire contribuera également à l'étude de facteurs cellulaires qui interviènnent dans la formation d'amyloïde.

En conclusion, nos études apportent une nouvelle information concerant l'ultrastructure des fibres d'amyloïde ainsi qu'une nouvelle perspective dans la cascade amyloïdeogenique. La possibilité de produire des fibres de TTR sous des conditions physiologique et la détermination des formes toxique offrent des facilités dans le domaine de recherche des molécules dotées d'un potentiel thérapeutique dans la maladie de PAF.

Part I

General Introduction

Part I- General introduction

Transthyretin (TTR) is the key protein in familial amyloidotic polyneuropathy (FAP). Our research project dealt with TTR deposition in this type of amyloidosis, which conveys us to knowledge on native transthyretin, protein destabilization and aggregation, amyloid deposition, fibril formation, biological ligands, inhibitory molecules, and others. From the gene to the protein, from health to disease, and from disease to therapy, we discuss here several concepts we find important to understand the experimental work presented in the next chapters.

1. TTR

Transthyretin (TTR), formerly called prealbumin due to its electrophoretic characteristics, located just in front of the albumin band, is a plasma protein secreted mainly by the liver and choroid plexus (Soprano *et al.*, 1985). The name "transthyretin" discloses its dual physiological role as a carrier for thyroid hormones (Woeber and Ingbar, 1968) and retinol, the latter through the binding to retinol-binding protein (RBP) (Goodman, 1987). TTR was first described in the cerebrospinal fluid (CSF) (Kabat *et al.*, 1942) and shortly after in the plasma (Seibert and Nelson, 1942).

1.1 TTR gene structure and expression

TTR is codified by a single copy gene localized in the long arm of chromosome 18 (Wallace *et al.*, 1985) and is codified by a single copy gene. The entire nucleotide sequence including the 5' (transcription initiating site) and the 3' (untranslated region) flanking regions was determined (Sasaki *et al.*, 1985; Tsuzuki *et al.*, 1985) and attributed to the region 18q11.2-q12.1 (Whitehead *et al.*, 1984). The full gene is 7.6 kilobase (kb) long comprising 4 exons and 3 introns (Sasaki *et al.*, 1985; Tsuzuki *et al.*, 1985). Exon 1 contains 95 baisepairs (bp), including 26 bp 5' untranslated and codes for a 20 aminoacid (aa) residue leader peptide and aa 1-3 of the mature protein; exon 2 (131 bp), 3 (136 bp),

and 4 (253 bp) hold the coding sequences for aa residues 4-47, 48-92 and 93-127, respectively.

The introns (A, B and C) are 934 bp, 2090 bp and 3308 bp long, respectively. Introns A and C contain two open reading frames (orf) of unknown significance (Tsuzuki *et al.*, 1985).

Several consensus sequences were found upstream the mRNA cap site: a TATA box at position –30 to –24 bp followed by a GC rich region of approximately 20 bp, a CAAT box at position –101 to –96 bp and overlapping sequences homologous to glucocorticoid responsive elements at positions –224 and –212 bp. A polyadenylation signal (AATAAA) was identified 123 bp downstream from the coding sequence (Sasaki *et al*, 1985).

The TTR mRNA spans ~0.7 kb and contains a 5'-untranslated region (26-27 nucleotides), a coding region (441 nucleotides), and a 3'-untranslated region (145-148 nucleotides) preceding the poly(A) tail (Mita *et al.*, 1984; Soprano *et al.* 1985). Human (Wallace *et al.*, 1985), rat (Sundelin *et al.*, 1985; Dickson *et al.*, 1985) and mouse (Costa *et al.*, 1986) coding regions exhibit a considerable degree of homology (~85%), suggesting a phylogenetically preserved modulating role in gene expression.

TTR is predominantly synthesized the by liver where more than 90% of the protein is produced. The remaining is produced in the choroid plexus and the retina. TTR is detected in the fetal blood very early during development, as soon as eight weeks after conception (Andreoli and Robbins, 1962). Fetal TTR is probably originated from 2 sources: one fraction seems to be inherited from the pregnant woman through transplacental filtration (Gitlin *et al.*, 1964); the other fraction results from fetal hepatic synthesis, as shown by the presence of considerable amounts of TTR mRNA early in development of this organ (Makover *et al.*, 1989).

TTR plasma concentration is age dependent and in healthy newborns it is about half of that in adults (Stabilini *et al.*, 1968; Vahlquist *et al.*, 1975). TTR values vary from 20 to 40 mg/ dL (Gittlin and Gittlin, 1975).

In addition to the liver, three other sites have been identified in mammals: visceral yolk sac endoderm (Sklan and Ross, 1986), retinal pigment epithelium (Martone *et al.*, 1988), and choroid plexus epithelium (Herbert *et al.*, 1986). For a long time, investigators supposed that the locally secreted TTR protein acted as a carrier of thyroid hormones between blood and brain, seeing that the blood brain barrier is not freely permeable to these molecules. TTR production within the central nervous system (CNS) was ascertained by immunochemical techniques demonstrating the participation of organelles involved in the

CSF secretory processes (Aleshire *et al.*, 1983). Animal experiments have shown considerable amounts of TTR mRNA in specific CNS regions, varying from 11 to 30% of the hepatic levels (Soprano *et al.*, 1985; Schreiber *et al.*, 1990). A different study revealed that the highest TTR mRNA concentration occurs in the epithelial cells lining the ventricular surface of the choroid plexus (Stauder *et al.*, 1986). In spite of the low TTR levels in CSF (~2 mg/ dL), the choroid plexus is presented as the major site of TTR expression, expressed as a ratio of tissue/ mass, corresponding to a ~30-fold higher than that found in plasma (Weisner and Roething, 1983). TTR represents 20% of the total CSF proteins (Weisner and Roething, 1983).

As for mammals, the major sites of TTR synthesis in birds are the liver and choroid plexus, but in reptiles TTR is synthesized only in the latter. This observation seems to imply that the philogenetic expression of TTR occurred first in the choroid plexus (Schreiber *et al.*, 1993). However, recent work (Santos and Power, 1999; Power *et al.*, 2000) reported the identification and cloning of TTR from the liver of amphibian and teleost fish, and its absence from the choroid plexus in both species, suggesting an alternative model for its evolution.

1.2- TTR structure

The TTR mRNA codifies for the TTR-monomer; the polypeptide of 147 aa residues whose N-terminal region is a hydrophobic signal peptide of 20 aa residues. The TTR monomer is subjected to a cleaving process during its migration through the endoplasmatic reticulum giving rise to the native TTR monomer after breaking of the signal peptide (Soprano *et al.*, 1985). Assembly of four identical subunits (13,745 Da) occurs yielding the mature tetrameric protein, with a molecular mass of 54,980 Daltons (Da) (Kanda *et al.*, 1974).

The tridimensional structure of TTR was made available at 1.8 Å resolution by X-ray diffraction studies on the crystallized protein (Blake *et al.*, 1978). A considerable amount of the aa residues in each monomer (55%) are implicated in the formation of β-sheet structure (Blake *et al.*, 1978). Each monomer contains two β-sheets formed by strands DAGH and CBEF (figure 1). All, except strands A and G, display an antiparallel orientation, and arranged in a topology similar to the classic greek key barrel. The strands are 7 to 8 residues long, except strand D, which, is only 3 residues in length.

Only about 5% of the aa residues are located in one segment of α-helix (Blake *et al.*, 1978) comprising residues 75 to 83 (Blake *et al.* 1978), at the end of strand E.

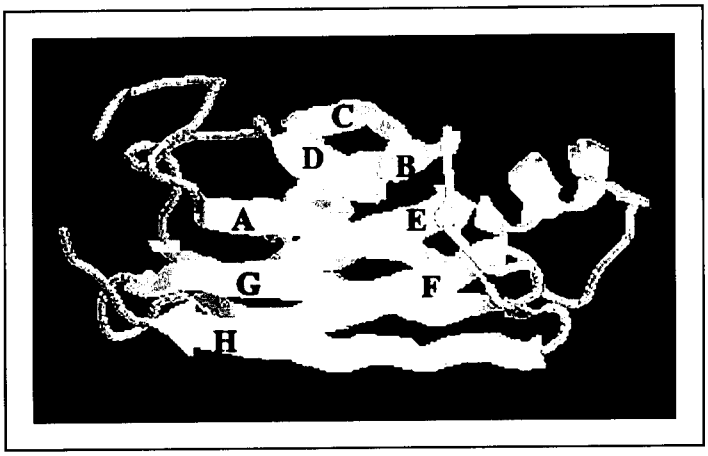

Figure 1- Schematic representation of the TTR monomer (PDB entry 1ETB; Hamilton *et al.*, 1993).

Two monomers associate forming the dimer by interactions between chains F and H of each monomer. Fixing the chains of one monomer as A-H and the ones of the other monomer as A'-H', the arrangement within a dimer is DAGHH'G'A'D' and CBEFF'E'B'C' (figure 2).

Figure 2- Representation of the TTR dimer. Each monomer contains two β-sheets composed of strands DAGH and CBEF, which extend to two 8-stranded β-sheets when two monomers associate forming a dimer (PDB entry 1ETB; Hamilton *et al.*, 1993).

The tetramer consists of two dimers with connecting edges occurring between the AB loop of one dimer with the H strand of the other dimer.

The quaternary structure of TTR has the shape of a globular protein with an overall size of 70 Å x 55 Å x 50 Å (Blake *et al.*, 1978). The two dimers are slightly rotated in relation to each other along the y axis (figure3).

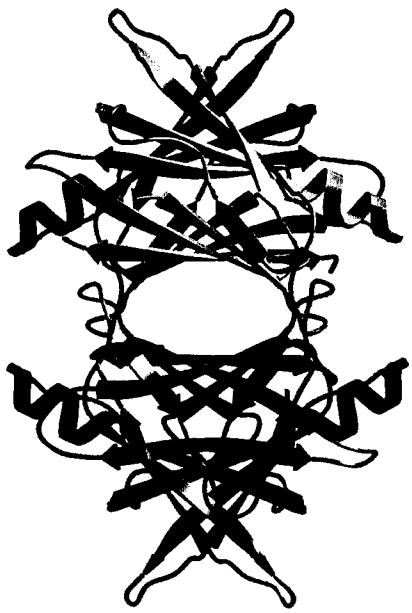

Figure 3- The human TTR tetramer (PDB entry 1ETB; Hamilton *et al.*, 1993).

1.3- Physiology and Metabolism

1.3.1- Transport of thyroxine (T_4)

Thyroxine (T_4) is the main secretory product of the thyroid gland. Triiodothyronine (T3) derives mostly from T_4 deiodination occurring in the peripheral tissues (Kohrle *et al.*, 1991). Thyroid hormones are transported in blood circulation and delivered in the target tissues. An incredible high amount of the hormones (99%) is bound to serum proteins. In human plasma, TTR, thyroxine-binding protein (TBG) and albumin are responsible for the delivery

of TTR into the target tissues (Robbins, 1991). Although TBG is much less concentrated in the plasma than TTR, it presents the highest affinity constant for T_4 (Ka = 1 x 10^{10} M^{-1}) and transports about 70% of the plasma T_4. TTR has an intermediate affinity for T4 is intermediate (Ka = 7 x 10^7 M^{-1}) and transports about 15% of the hormone, and ultimately, albumin presents the lowest binding affinity (Ka = 7 x 10^5 M^{-1}) (Robbins, 1991; Loun and Hage, 1992).

The four monomers within a TTR tetramer, demarcate through the molecule an open channel where two binding sites for thyroid hormones are located (Nilsson *et al.*, 1971; Blake *et al.*, 1978). These two binding sites present negative cooperativity (Ferguson *et al.*, 1975; Andrea *et al.*, 1980) implying that when the first thyroid hormone molecule occupies the first site, the affinity for the second molecule is highly reduced. As a result, the ka estimated for the two binding sites for T_4 are 1.05 x 10^8 M^{-1} and 9.55 x 10^5 M^{-1}, respectively (Andrea *et al.*, 1980); TTR also binds triiodothyronine (T_3) but with lower affinity.

T_4 transport into the brain is of particular interest and has raised much controversy. There are two possible mechanisms for thyroid hormones to reach the brain: partioning and diffusion through the lipid plasma membrane both at the choroid plexus epithelial cells and at the cerebral capillaries endothelial cells; and mediated by the TTR synthesized by the choroid plexus and secreted into the CSF. Several evidences suggested that TTR might have an essential role in thyroid hormone transport into and within the brain: TTR is the major T_4 binding protein in the cerebrospinal fluid (Hagen and Solberg, 1974). It has been shown that rat choroid plexus explants, *in vitro*, accumulate thyroid hormones from the surrounding media and that, when equilibrium is reached, the thyroid hormone intracellular/extracellular concentration ratio decreases when TTR media content is increased (Dickson *et al*, 1987). The same authors showed that after intravenous radioactive T_4 injection, the radioactivity first appears in the choroid plexus, followed later by the brain. It was then proposed that T4 is transported from the blood into the choroid plexus where by itself or bound to TTR it is secreted into the CSF. Some *in vitro* and *in vivo* studies by Schreiber *et al.* (1990), further supported this hypothesis.

In contrast, a study where ^{125}I-T_4 covalentely bound to TTR was intravenously injected in rats showed that the serum T_4 bound to TTR fraction is not transported into the CSF (Chanoine *et al*, 1992). The explanation is that given its high lipophylicity, thyroid hormones should be able to cross the membranes that constitute the blood-brain barrier

outside the choroid plexus without the need of any plasma transport protein.

Studies done in *ttr* knock-out mice (*ttr*-) (Episkopou *et al*, 1993) revealed that TTR is not essential for thyroxine to reach the brain and other tissues (Palha *et al*, 1997). In addition, measurement of several parameters of thyroid hormone function indicate that these mice are euthyroid despite strongly reduced total T_4 plasma levels (Palha *et al*, 1994). No other protein was found to replace TTR in the transport of T_4 in the CSF, and T_4 levels were normal in the cortex, cerebellum and hippocampus while strongly reduced in the choroid plexus of the *ttr*- mice (Palha *et al*, 2000a). Autoradiographic analysis of thyroid hormone distribution revealed that TTR is not required for the normal hormone distribution (Palha *et al., in press).*

Therefore, it was suggested that TTR might be a reservoir for T_4 both in the plasma and in the choroid plexus and CSF, which might become important under conditions of increased hormone demand.

1.3.2- Transport of vitamin A

TTR is also responsible for retinol transport through binding to retinol-binding protein (RBP) (Kanai *et al.*, 1968). RBP is a 21 kDa monomeric protein comprising 182 aa residues (Rask *et al.*, 1979). The conformational structure of RBP bound to retinol was determined by x-ray crystallography (Newcomer *et al.*, 1984). In most instances, RBP is transported in the bloodstream in the form of a saturated holo-RBP protein equimolarly attached to TTR (Goodman, 1984; Blaner, 1989).

Although TTR has four binding sites for RBP (Van Jaarsveld *et al.*, 1973; Kopelman *et al.*, 1976), under physiological conditions only one RBP molecule is bound to TTR due to the RBP limiting concentration.

In vitro TTR is able to bind two RBP molecules and this interaction occurs with only one of the dimers (Monaco *et al.*, 1995). The dissociation constants for the two RBP molecules are $1.9 \pm 1.0 \times 10^{-7}$ M for the first RBP molecule and 3.5×10^{-5} M for the second one. Each of the RBP molecules contacts with one of the remaining monomers and blocks the other RBP-binding sites in the tetramer molecule (figure 4).

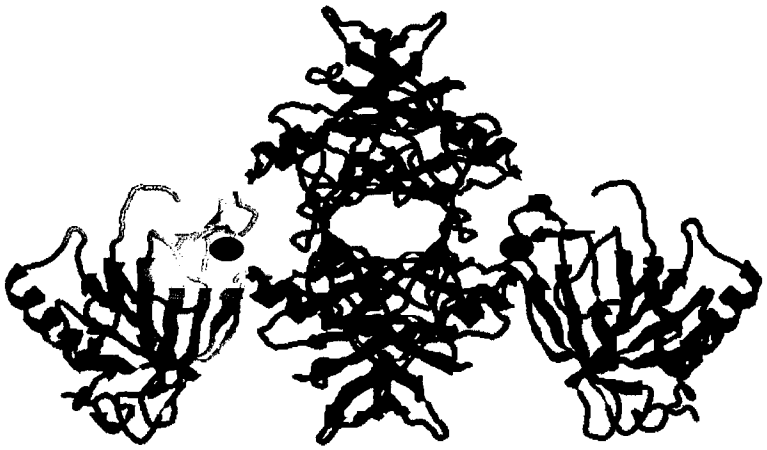

Figure 4- TTR complexed with RBP (PDB entry 1QAB; Naylor and Newcomer, 1999)

1.3.3- Other functions of TTR

TTR has been shown to interact with a variety of compounds. However, the relevance of these interactions, in most instances, is not known. These molecules include: noradrenaline oxidation products (de Vera *et al* 1988; Boomsma *et al*, 1991), pterins (Ernstrom *et al*, 1995), chicken lutein (Martone and Herbert, 1993; Martone *et al.*, 1993)), hemin and hemoglobin (Martone and Herbert, 1993; Martone *et al.*, 1993), polyhalogenated compounds (Brouwer, 1989; Cheek *et al*, 1999) and retinoic acid (Smith *et al*, 1994).

Other studies have shown that TTR can play a role in immunological processes by interfering with the secretion of interleukin I (Borish *et al*, 1992); a decapeptide corresponding to the first N-terminal aa residues of TTR has also been proposed to have thymic activity in thymectomized mice (Burton *et al* 1978; 1985; 1987).

Other *in vitro* work suggested that TTR can form stable complexes with amyloid β-peptide (Aβ) (Schwarzman *et al*, 1994), and prevent Aβ accumulation in cell culture experiments (Mazur-Kolecka *et al*, 1995) and in transgenic *Caenorhabditis elegans* (Linke, 1995). Studies on the interaction of TTR with Aβ suggest that, in the CSF, TTR plays a key role in the modulation of Aβ aggregation and prevents amyloid formation (Serot *et al*, 1997). In addition, TTR levels were reported to be significantly decreased in patients with Alzheimer`s disease (Riisoen, 1988; Serot *et al*, 1997; Merched *et al*, 1998) and depression (Sullivan *et al.*, 1999). These data raised the possibility that amyloid fibril formation could

be promoted in patients with late onset Alzheimer's disease by the lack of sufficient concentrations of TTR or by the presence of TTR variants. The absence of TTR mutations in patients with Alzheimer's disease argues against the latter hypothesis (Palha *et al*, 1996). TTR has also been found associated to lipoproteins: Tanaka *et al* (1995) reported the presence of TTR not only in isolated low density lipoproteins (LDL) but also in high density lipoproteins (HDL) from normal subjects and in Japanese patients with different TTR mutations associated with familial amyloidotic polyneuropathy (FAP) (namely TTR Val30Met, Glu89Gln, His56Pro and Arg34Thr). TTR was shown to associate with the HDL fraction to the same extent both in normal individuals and FAP patients, whereas the LDL fraction from the FAP patients showed higher amounts of TTR than normal individuals. Very recently, it has been shown that TTR also associates with HDL via apolipoprotein AI (apoAI) (Sousa *et al.*, 2000a).

1.3.4- TTR metabolism

The biological half-life of TTR is about 2-3 days in humans (Socolow *et al.*, 1965; Vahlquist *et al.*, 1973), 22-23 hours in monkeys (Vahlquist and Peterson, 1972) and 10-13 hours in rats (Peterson *et al.*, 1974). The major sites of TTR degradation in the rat are liver (36-38%), followed by the muscle (12-15%) and skin (8-10%) (Makover *et al.*, 1988). Tissues that are sites of 1-8% of body TTR degradation include the kidneys, adipose tissue, testes, and gastrointestinal tract. Less than 1% of total TTR degradation occurs in the other tissues examined. The mean fractional turnover of plasma TTR is 0.15/h, and that of the total body TTR 0.04/h.

A second study (Makover *et al*, 1988) was conducted in order to investigate the degradation of choroid plexus-derived TTR. The estimated turnover of cerebrospinal fluid TTR was in the order of 0.33/h. The major sites of degradation of labeled TTR injected in CSF or in plasma were approximately the same; almost identical tissue sites and quantitative patterns of TTR degradation were observed. Thus, for both routes of injection of labeled TTR, the liver was the major site of TTR degradation, followed by the muscle and skin. No specific transfer of plasma TTR to the nervous system or degradation of plasma TTR in the nervous system was observed.

The normal physiology of TTR is not completely understood, in particular, its cellular uptake. Nevertheless, several observations suggest that TTR internalization is receptor-mediated, both in human hepatoma cells (HepG2) (Divino and Schussler, 1990a, b) and in chicken oocytes (Vieira *et al.*, 1995). Recently, megalin, a receptor implicated in the renal re-uptake of plasma proteins carriers of lipophilic compounds, was shown to play a role in renal uptake of TTR (Sousa *et al.*, 2000b). Binding/uptake experiments performed with immortalized rat yolk sac cells expressing high levels of megalin and with radiolabelled TTR, free and complexed with T_4 or RBP, demonstrated that radiolabelled TTR (both free and T_4 complexed) was rapidly taken up by the cells. This uptake was strongly inhibited by a polyclonal megalin antibody and by the receptor-associated protein (RAP). Furthermore, different TTR mutations presented different levels of cell association and degradation, suggesting that the structure of TTR is important for megalin recognition. The same work shows that urine from patients with Dent's disease, a renal tubular disorder that alters receptor mediated endocytic reabsorption of proteins, presented high amounts of excreted TTR. Morover, immunohistochemical analysis of kidney sections of megalin-deficient mice, were negative for TTR in intracellular vesicles in the proximal tubule cells. This data strongly indicates that TTR represents a novel megalin ligand of importance in thyroid hormone homeostasis.

TTR internalization was further explored by studying TTR uptake using hepatomas and primary hepatocytes (Sousa and Saraiva, 2001). This work showed direct evidence for TTR internalization by a specific receptor, forming a ~90 kDa complex. TTR internalization was inhibited by RBP (70% decrease) and T_4 (20% decrease) and TTR mutants revealed differences in uptake, indicating again that the recognition by receptor is structure dependent. Internalization was also inhibited by lipoproteins and RAP, a ligand for all members of the low-density lipoprotein receptor family (LDLr). All together, these results suggest a common pathway for TTR and lipoprotein metabolism and the existence of a RAP-sensitive receptor for TTR internalization.

1.4- Molecular variants of TTR

Table 1 shows the TTR variants reported so far. Almost without exception, these mutations result from point mutations in the polypeptide chain. The exception is the case of a deletion of an aa residue. The majority of the TTR variants are amyloidogenic, mainly associated

with peripheral neuropathy but also with cardiomyopathy, carpal tunnel syndrome and vitreopathy.

Table 1- Amyloidogenic TTR mutations

Mutation	Codon change	Predominant Clinical Features	Origin
Cys10Arg	TGT CGT	PN, AN, Eye	Hungary
Leu12Pro	CTG CCG	LM, PN, AN	UK
Asp18Glu	GAT GAG	PN, AN	Columbia
Asp18Gly	GAT GGT	LM	Hungary
Val20Ile	GTC ATC	Heart	Germany
Ser23Asn	AGT AAT	Heart	Portugal
Pro24Ser	CCT TCT	Heart, CTS, PN	USA
Val28Met	GTG ATG	PN, AN	Portugal
Val30Met	GTG ATG	PN, AN, Eye	several
Val30Ala	GTG GCG	Heart, AN	Germany
Val30Leu	GTG CTG	PN, AN	Japan
Val30Gly	GTG GGG	LM, Eye	France
Phe33Ile	TTC ATC	PN, Eye	Poland
Phe33Leu	TTC CTC	PN, AN	Poland
Phe33Val	TTC GTC	PN, AN	UK
Arg34Thr	AGA ACA	PN, Heart	Italy
Lys35Asn	AAG AAC	PN, AN, Heart	France
Ala36Pro	GCT CCT	PN, Eye	Greece
Asp38Ala	GAT GCT	PN, Heart	Japan
Glu42Gly	GAG GGG	PN, AN	Japan
Glu42Asp	GAG GAT	Heart	France
Phe44Ser	TTT TCT	PN, AN, Heart	Ireland
Ala45Asp	GCC GAC	Heart	Italy
Ala45Ser	GCC UCC	Heart	Sweden
Ala45Thr	GCC ACC	Heart	Italy
Gly47Arg	GGG CGG	PN, AN	Japan
Gly47Ala	GGG GCG	Heart, PN, AN	Italy
Gly47Val	GGG GTG	PN, AN, Heart	Sri Lanka
Gly47Glu	GGG GAG	PN	Germany
Thr49Ala	ACC GCC	Heart, PN	Italy
Thr49Ile	ACC ATC	PN, Heart	Japan
Ser50Arg	AGT AGG	PN, AN	Japan
Ser50Ile	AGT ATT	Heart, PN, AN	Japan
Glu51Gly	GAG GGG	Heart	USA
Ser52Pro	TCT CCT	PN, AN, Heart	UK
Gly53Glu	GGA GAA	LM, Heart	France
Glu54Gly	GAG GGG	PN, AN	UK
Glu54Lys	GAG GAA	PN, AN, Heart	Japan
Leu55Arg	CTG CGG	LM, PN	Germany
Leu55Pro	CTG CCG	PN, Heart, AN	Taiwan
His56Arg	CAT CGT	Heart	USA
Leu58His	CTC CAC	CTS, Heart	Germany
Leu58Arg	CTC CGC	CTS, AN, Eye	Japan
Thr59Lys	ACA AAA	Heart, PN	Italy
Thr60Ala	ACT GCT	Heart, CTS	Ireland
Glu61Lys	GAG AAG	PN	Japan
Phe64Leu	TTT CTT	PN, CTS, Heart	Italy
Phe64Ser	TTT TCT	LM, PN, Eye	Italy
Ile68Leu	ATA TTA	Heart	Germany
Tyr69His	TAC CAC	Eye	Scotland
Lys70Asn	AAA AAC	CTS, PN, Eye	Germany
Val71Ala	GTG GCG	PN, Eye	Spain
Ile73Val	ATA GTA	PN, AN	Bangladesh
Ser77Phe	TCT TTT	PN	France
Tyr78Phe	TAC TTC	CPS, Heart	Italy
Ser77Tyr	TCT TAT	PN	Germany
Ile84Ser	ATC AGC	Heart, CTS, Eye	Switzerland
Ile84Asn	ATC AAC	Eye, Heart	Italy
Ile84Thr	ATC ACC	Heart, PN, AN	Germany
Glu89Gln	GAG CAG	PN, Heart	Italy
Glu89Lys	GAG AAG	PN, Heart	USA
Ala91Ser	GCA TCA	PN, CTS, Heart	France
Ala97Gly	GCC GGC	Heart, PN	Japan
Ala97Ser	GCC TCC	PN, Heart	France
Ile107Val	ATT GTT	Heart, CTS, PN	Germany
Ile107Met	ATT ATG	PN, Heart	Germany
Ala109Ser	GCC TCC	PN	Japan
Leu111Met	CTG ATG	Heart	Denmark
Ser112Ile	AGC ATC	PN, Heart	Italy
Tyr114Cys	TAC TGC	PN, AN, Eye	Japan
Tyr114His	TAC CAC	CTS	Japan
Tyr116Ser	TAT TCT	PN, CTS	France
Ala120Ser	GCT TCT	Heart, PN, AN	Africa
Val122Ile	GTC ATC	Heart	Africa
DelVal122	GTC loss	Heart, PN, CTS	Equador/Spain
Val122Ala	GTC GCC	Heart, Eye, PN	UK

AN - autonomic neuropathy; CTS - carpal tunnel syndrome; Eye - vitreous deposition

PN - peripheral neuropathy; LM - leptomeningeal amyloid; Heart - cardiomyopathy

(Taken from database www.ibmc.up.pt).

Several TTR mutations without pathogenic consequences have also been described and are presented in table 2. Additionally, several different compound heterozygotes, carriers of two different TTR mutations have been reported (table 2).

Table 2- Non-amyloidogenic TTR mutations and compound heterozygotes.

Mutation	Codon change	Frequency*
Gly6Ser	GGT AGT	33/558
Met13Ile	ATG ATC	nd
Asp74His	GAC CAC	nd
His90Asn	CAT AAT	16/12,400
Gly101Ser	GGC AGC	nd
Pro102Arg	CCC CGC	1/8,000
Arg104Cys	CGC TGC	nd
Arg104His	CGC CAC	nd
Ala108Ala**	GCC GCT	nd
Ala109Thr	GCC ACC	1/10,000
Ala109Val	GCC GTC	nd
Thr119Met	ACG ATG	35/10,000
Pro125Ser	CCC TCC	nd
Compound heterozygotes		
Gly6Ser/Val30Met		7/160
Gly6Ser Phe33Ile***		nd
Gly6Ser/Ala45Asp		nd
Gly6Ser/Ser77Tyr		nd
Gly6Ser/Tyr114Cys		nd
Gly6Ser/Thr119Met		nd
Gly6Ser/Val122Ala		nd
His90Asn/Val30Met		nd
His90Asn Glu42Gly***		nd
His90Asn/Thr119Met		nd
Arg104His/Val30Met		nd
Thr119Met/Val30Met		nd

* Refers to mutant allele frequency

** Silent mutation

*** Mutations on the same allele

(Taken from database www.ibmc.up.pt).

2- Amyloidosis and amyloid

The term amyloidosis comprises a large group of pathologies mainly characterized by the deposition of fibrillar proteins- **amyloid** – leading to cell damage, organ dysfunction and death.

Amyloid disorders are usually divided into two categories depending on the distribution of the amyloid deposits: localized and systemic amyloidosis.

2.1- Amyloid diseases

In localized amyloidosis, amyloid is restricted to a single tissue or organ, usually in the surroundings of the cells responsible for the synthesis of the precursor protein; in systemic amyloidosis, the amyloidogenic proteins are usually derived from circulating precursors that are either in excess, abnormal or both. Table 3 depicts the most common forms of amyloidosis.

Tabel 3- Amyloidosis in humans

Amyloid protein	Protein precursor	Amyloidosis	Syndrome and/ or involved tissues
Aβ	Aβ protein precursor (AβPP)	L	Alzheimer's disease Aging Familial (prototype Dutch)
$APrP^{sc}$	Prion protein	L	Spongiform encephalopathies
ACal	(Pro)calcitonin	L	C-cell thyroid hormones
AIAPP	Islet amyloid polypeptide	L	Islets of Langerhans Insulinomas
AANF	Atrial natriuretic factor	L	Cardiac atria
APro	Prolactin	L	Aging pituitary Prolactinomas
AIns	Insulin	L	Iatrogenic
ALac	Lactoferrin	L	Cornea
AMed	Lactadherin	L	Senile aortic
AKer	Kerato-epithelin	L	Cornea
AL	Immunoglobulin light chain	S, L	Primary Myeloma-associated
AH	Immunoglobulin heavy chain	S, L	Primary Myeloma-associated
ATTR	Tranthyretin	S	Familial Senile systemic
AA	(Apo) serum AA	S	Secondary, reactive
Aβ2M	β2-microglobulin	S	Chronic hemodialysis
AApoAI	Apolipoprotein AI	S	Familial
AApoAII	Apolipoprotein AII	S	Familial
AGel	Gelsolin	S	Familial (prototype Finnish)
ALys	Lysozyme	S	Familial
AFib	Fibrinogen α-chain	S	Familial
ACys	Cystatin C	S	Familial (prototype Iceland)
ABri	BRI gene product	S	Familial dementia, British

L- Localized; S- Systemic

Adapted from Westermark *et al.*, 1999.

2.1.1- Localized amyloidosis

2.1.1.1- β-peptide amyloidosis (Aβ)

Alzheimer's disease (AD) (acquired and familial) is the most common form of amyloidoisis and the major cause of dementia, affecting more than 5% of the population over the age of 65 years (Katzman, 1986; Ghiso *et al.*, 1994). AD in is mainly characterized by three different pathological changes:

- Intraneuronal deposits (neurofibrillar tangle, NFT) formed from the microtubule-associated protein tau
- Neuritic or senile plaques
- Cerebrovascular amyloidosis that affects small and medium vessels of the leptomeninges and cerebral cortex.

NFT deposits are localized mainly in pyramidal neurons of the neocortex, hippocampus, amygdala, and basal nuclei (Selkoe *et al.*, 1983). Neuritic or senile plaques are spherical lesions of variable size (10-200 μm) found in the cerebral cortex, especially in the associative areas of neocortex and limbic structures. A mature plaque is formed typically of a central amyloid core, dystrophic neuritis and glial cells (Merz *et al.*, 1983).

The major component of the amyloid deposits is a peptide, the amyloid β-peptide (Aβ). In neuritic plaques of AD patients this peptide is 42-43 aa residues long whereas in vascular amyloid it is 39-40 aa residues long (Glenner and Wong, 1984; Masters *et al.*, 1985).

The Aβ peptide is derived from the larger precursor protein (APP) as a normal cleavage product (Esch *et al.*, 1990; Haass *et al.*, 1992). APP is a transmembrane glycoprotein with a receptor-like structure composed of a large extracellular region (a cysteine-rich domain, an acidic fragment, and two putative Asn-glycosylation sites), a transmembrane domain and a C-terminus intracellular segment.

Fibrillization of Aβ appears to initiate a cascade of events producing neuronal death and resulting in the cognitive and behavioral decline characteristic of AD (Yankner, 1996).

2.1.1.2- Other localized amyloidosis

Several other common types of localized amyloidosis have been described, including amyloidosis restricted to certain tumors of endocrine glands. In medulary carcinoma of the thyroid, amyloid fibrils are composed of procalcitonin (Hill *et al.*, 1973; Sletten *et al.*, 1976), whereas in patients with islet cell tumors associated with diabetes mellitus type II, the amyloid subunit deposited is termed islet amyloid polypeptide or amylin (Westermark *et al.*, 1987; Johnson *et al.*, 1989).

Human amylin is a 3904 Da peptide hormone produced in the islet β-cells of the pancreas and usually co-secreted with insulin (Cooper, 1994). It has been proposed that amylin regulates glucose metabolism (Cooper, 1994; Young *et al.*, 1995). Amylin appears to be also involved in insulin resistance (Leighton and Cooper, 1988) and to play a role in the initiation and progression of diabetes type II (Cooper *et al.*, 1994; Verchere *et al.*, 1996). Synthetic amylin has a high tendency to aggregate producing amyloid-like fibrils; these fibrils present a polymorphic structure with a defined 5 nm protofilament, which can assemble into ribbon-like or into coiled fibrils (Goldsbury *et al.*, 1997) and grow bidirectionally (Goldsbury *et al.*, 1999).

Transmissible spongiforme encephalopathies in human (or prion diseases) are characterized by neuronal spongiform degeneration, astrocytic gliosis and parenchymal amyloid deposition in the form of amyloid plaques (Ghiso *et al.*, 1994)

Atrial amyloidosis is a form of senile cardiac amyloidosis restricted to the atria (Johansson *et al.*, 1987); in this condition, a 3 kDa fragment, α-atrial natriuretic peptide (AANP), is the main constituent of the amyloid deposits. It is derived from a larger precursor molecule (14 kDa) and has potent natriuretic and diuretic effects.

2.1.2- Systemic amyloidosis

2.1.2.1- Non hereditary amyloidosis

In humans, the most frequent forms of non hereditary systemic amyloidosis are amyloid A associated amyloidosis (AA) and light and heavy immnunoglobulin chains associated amyloidosis (AL and AH, respectively).

2.1.2.1.1- AA amyloidosis

AA, secondary or reactive amyloidosis, is a rare complication of common chronic infections, inflammatory disorders and certain neoplasms. The major constituent in AA amyloidosis is the protein AA (8.5 kDa), a 76 aa residue N-terminal fragment derived by proteolysis from serum amyloid A (SAA). SAA is a 12.5 kDa apolipoprotein synthesized in the liver that circulates as a high-density fraction (Levin *et al.*, 1972; Rosenthal *et al.*, 1976; Benditt and Erikssen, 1977).

AA is also the amyloid protein found in familial Mediterranean fever (FMF), an autosomal recessive disorder. In addition, AA is the main fibril constituent in experimentally induced and spontaneous amyloidosis in a number of animals (Ghiso *et al.*, 1994). The best studied AA animal model is the mouse, where amyloidosis can be induced with a variety of antigenic and inflammatory stimuli (Erikssen *et al.*, 1976; Skinner *et al.*, 1977; Benson *et al.*, 1985; DiBartola *et al.*, 1985).

AA fibrils *in situ* appear as straight rods approximately 10 nm wide and composed of a core covered by a sheet of 4.5-5 nm in width made up of heparan sulphate proteoglycan. HSPG. AA protein filaments are found associated in the outer surface of the fibrillar structure (Inoue *et al.*, 1998).

2.1.2.1.2- AL amyloidosis

AL amyloidosis is associated with amyloid deposits of a monoclonal B-cell-derived population that synthesizes amyloidogenic immunoglobulin light chains. No common structural motifs were found among the amyloidogenic light chains. However, comparison between the sequences available, demonstrated the existence of critical aminoacid positions possibly involved in amyloidogenesis (Stevens *et al.*, 1995). Although all light chains can originate amyloidosis, λ light chains are involved in disease two or three times more frequently than κ chains (Isobe and Osserman, 1974).

AL patients present amyloid deposits primarily distributed in the heart, skin, gastrointestinal tract, tongue, peripheral nerves and ligaments. Kidney, liver, spleen, and adrenal can also be affected (Kyle and Bayrd, 1975; Wright and Calkins, 1981; Kyle and Greipp, 1983; Browning *et al.*, 1985; Janssen *et al.*, 1986).

The amyloid subunit for AL was the first amyloid protein biochemically characterized (Glenner *et al.*, 1971). In almost all cases of AL amyloidosis, fibrils are composed of either N-terminal fragments of L-chain and intact L-chain (5-23 kDa) (Osserman *et al.*, 1987; Feiner, 1988; Finn and Gorevic, 1990; Castano and Frangione, 1988).

2.1.2.1.3- β_2-microglobulin related amyloidosis

β_2-microglobulin related amyloidosis constitutes a systemic form of disease with a preference for bone and synovium and appears in patients undergoing long-term hemodialysis. β_2-microglobulin accumulates in the plasma and undergoes extracellular amyloid deposition. Clinical features include carpal tunnel syndrome (Bardin *et al.*, 1985; Huaux *et al.*, 1985; Walts *et al.*, 1985), erosive arthropathy (Huaux *et al.*, 1985), lytic bone lesions, and pathologic fractures (Bardin *et al.*, 1985; Huaux *et al.*, 1985). Usually, after 5-6 years of hemodialysis the disease appears and after 20 years 80-100% of the patients are affected (Ghiso *et al.*, 1994).

β_2-microglobulin constitutes the light chain of the major histocompatibility complex of type I (MHCI) and the related amyloid fibrils consist of full-length β_2-microglobulin associated with fragments of various lengths (Linke, 1993). Like other amyloidogenic proteins, β_2-

microglobulin forms amyloid-like fibrils *in vitro* (Stoppini *et al.*, 1997). Fibrils extracted from the femoral head of a patient under chronic hemodialysis for 11 years, revealed β_2-microglobulin that was able to refold acquiring a tertiary structure identical to the native form (Bellotti *et al.*, 1998). These results suggest the possibility of refolding fibrillar proteins into globular proteins as a therapeutical goal. Renal transplantation showed, in some cases, to improve patient conditions leading to the reduction of the amyloid deposits (Nelson *et al.*, 1991). In other cases, amyloid deposits persisted even 11 years after renal transplantation (Bardin *et al.*, 1995).

2.1.2.2- Hereditary amyloidosis

The most common forms of this type of amyloidosis are related to six different proteins: TTR, apolipoprotein AI, apolipoprotein AII, lysozyme, gelsolin, cystatin C and fibrinogen.

TTR is associated with the most prevalent type of hereditary systemic amyloidosis. The pathologic conditions include familial amyloidotic polyneuropathy (FAP) and familial amyloidotic cardiomyopathy (FAC). A non hereditary condition is also related to TTR, systemic senile amyloidosis (SSA), and affects about 25% of people over 80 years of age. In SAA the deposits occur in the heart and are composed of wild-type TTR.

2.1.2.2.1- ApoAI and ApoAII

ApolipoproteinAI (apoAI) is a 28 kDa major apolipoprotein component of HDL and several amyloidogenic variants have been reported. Most of them result from point mutations in the gene (Nichols *et al*, 1990; Soutar *et al*, 1992; Vigushin *et al*, 1994; Booth *et al*, 1995; Asl *et al*, 1999; Hamidi *et al.*, 1999). Two variants involve deletions from the gene in exon 4 that produce a variant protein with either a deletion and insertion of two aa residues (Booth *et al*, 1996) or a deletion of three aa residues (Persey *et al*, 1998). The amyloid protein fraction was shown to be the amino terminal portion and fragments present variable lengths.
The mechanism behind apoAI deposition is not known and unlike other amyloid protein precursors, apoAI is not recognized as having β structure. The first mutation reported,

Gly26Arg, (Nichols *et al.*, 1988) is characterized by lower limb polyneuropathy, peptic ulcers, and nephrotic syndrome. Leu60Arg (Soutar *et al*, 1992) and Trp50Arg (Booth *et al*, 1995) have also renal involvement; and in the deletion variants (Booth *et al*, 1996; Persey *et al*, 1998), patients have both renal and cardiac amyloidosis. It was hypothesized that the electrostatic alteration caused by the extra positive charge could be responsible for amyloidogenecity. However, in 1999 a new mutation, Leu90Pro, was described (Asl *et al.*, 1999) arguing against the theory first raised as no change in charge is produced. This mutation results in cutaneous amyloid deposition and restrictive cardiomyopathy.

The deposition of N-terminal fragments of apoAI into amyloid was thougth to be caused by a local distortion caused by the mutation. As a result, it would affect lipid-apoAI interactions and/or expose sites for proteolytic cleavage and favoring the transition of α-helix into β-sheet. This hypothesis was contested by the discovery of an apoAI mutation located at the C-terminus of the protein, Arg173Pro (Hamidi *et al.*, 1999). Nevertheless, clinically this variant is associated with cardiac and cutaneous amyloidosis. Furthermore, the deposited fragments correspond to the N-terminal part of the protein. Recently, a new mutation at the C-terminal of apoAI was described (Leu174Ser) (Obici *et al.*, 1999). Interesting data arrived from the three-dimensional structure of free-lipid apoAI mutant, indicating that position 174 of one chain is located near position 93 of an adjacent chain; a new model was suggested proposing that the amino acid substitution at position 174 is permissive for a proteolytic cleavage at the N-terminal of Val93, releasing N-terminal fragments of the protein that, in turn, deposit as amyloid.

Very recently, a new C-terminal amyloidogenic variant of apoAI, Leu178His, was reported (Sousa *et al.*, 2000c), associated with cardiac and larynx amyloidosis and skin lesions with onset on the fourth decade. ApoAI and TTR co-localized in amyloid deposits and the amyloid deposits revealed both full-length and N-terminal fragments of ApoAI and normal TTR. Previous studies demonstrated that TTR is associated to HDL in plasma through apoAI (Sousa *et al.*, 2000a) and thus, TTR and apoAI interaction seems to be relevant not only in physiological conditions but also in amyloidosis.

In ApoAII amyloidosis, the protein suffers an extension at the C-terminus and it is thought that the added peptide is the direct cause of fibrillogenesis (Benson *et al.*, 2001). Although no direct evidences are available, it has been suggested that alterations in binding to HDL particles may be related to this amyloidosis. The patients present renal glomerular amyloid

deposition that causes death. Other organs, including adrenal glands, liver and spleen are also involved (Weiss and Page, 1973).

2.1.2.2.2- Other hereditary amyloidosis

Gelsolin is an actin-modulating protein that severs actin filaments, nucleates actin filament growth and caps barbed actin filaments ends (Stossel *et al.*, 1985). Gelsolin is associated with the Finnish type amyloidosis, an autosomal dominant form of systemic amyloidosis characterized by lattice corneal dystrophy, cranial neuropathy, and intermittent proteinuria (Meretoja, 1969). Amyloid deposits are found in kidney, muscle, nerves and cornea and fibrils are composed of gelsolin fragments (Haltia *et al.*, 1990; Maury *et al.*, 1990). The amyloidotic fraction starts at position 173 of the protein and contains one amino substitution at position 187 (Tyr187Asn). The same phenotype has also been described in Danish and Czech kindreds, but with the Tyr187 substituted by aspartic acid (de la Chapelle *et al.*, 1992).

In cystatin C related amyloidosis (ACys) amyloid deposition of a cystacin C fragment occurs in cerebral cortex and leptomeninges, walls of small arteries and arterioles, lymph nodes, spleen, adrenal gland, ovary, testis, appendix, peripheral nerves and skin (Benedikz *et al.*, 1990). The cystatin C fragment (12 kDa) contains one substitution at position 68 and misses 10 aa residues at the N-terminus (Barret *et al.*, 1984; Brzin *et al.*, 1984).

In 1993, amyloid fibrils from a transplanted kidney of a patient with hereditary renal amyloidosis were found to contain a fragment of fibrinogen Aα-chain with a substitution of Leu for Arg at position 554 (Benson *et al.*, 1993).
Two additional mutations in the fibrinogen Aα-chain were shown to be related to the disease. One of the mutations is a nucleotide deletion resulting in a frame shift and early termination of the fibrinogen Aα-chain after aa residue 547 (Uemichi *et al.*, 1996).

Lysozyme is associated with autosomal dominant hereditary non-neuropathic amyloidosis, caused by nucleotide base changes. The mutations occur in highly conserved residues as in the case of Ile56Thr and Asp67His (Pepys *et al.*, 1993) and the amyloid fibrils consist

exclusively of the variant protein (Booth *et al.*, 1997; Pepys *et al.*, 1993). Very recently, a new lysozyme mutation has been identified, Trp64Arg (Valleix *et al.*, 2002), associated with prominent nephropathy. Lysozyme is an ubiquitous bacteriolytic enzyme present in external secretions and in polymorphs and macrophages, but its physiological role is not clear.

2.1.2.2.3- Familial Amyloidotic Polyneuropathy (FAP)

Familial amyloidotic polyneuropathy (FAP) is related to a peculiar form of hereditary autosomal dominant polyneuropathy. Corino de Andrade first described the disease in 1952 (Andrade, 1952) in the Portuguese population mainly from the northern part of the country. Characterized by systemic deposition of amyloid and with a special involvement of the peripheral nerves, the age of onset of the disease is usually between 20 and 35 years of age, with a fast progression to death within 10 to 15 years.

Clinically, FAP is characterized by early impairment of temperature and pain sensation in the feet, and autonomic dysfunction leading to paresis, malabsorption and emaciation. Painless injury to the feet complicated by ulcers, celulitis, osteomyelitis and Charcots joints may also occur (Reilly *et al.*, 1993). Motor involvement occurs with disease development causing wasting and weakness and there is a progressive loss of reflexes. Upper limbs involvement may occur years after lower limb manifestations, progressing in a similar way.

The amyloid deposits (figure 5) can occur in any part of the peripheral nervous system, including the nerve trunks, plexus and sensory and autonomic ganglia. In the peripheral nerves, they affect the epineurium, perineurium and especially the endoneurium. In the endoneurium, deposits are usually closely opposed to Schwann cells or collagen fibrils.

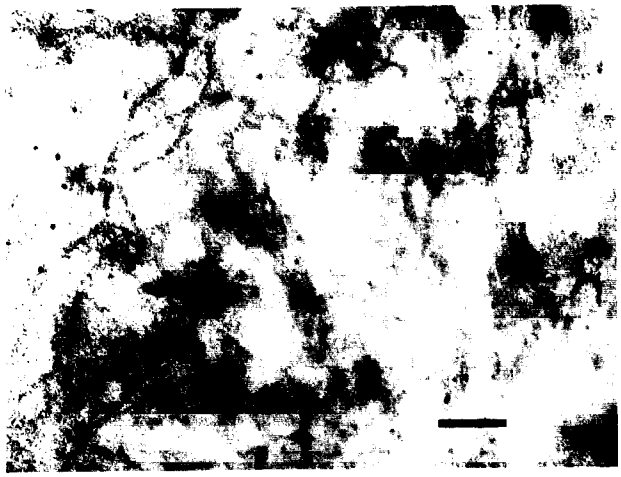

Figure 5– Amyloid fibrils from a FAP nerve section.
Scale bar = 100 nm (kindly provided by Rui Fernandes, Amyloid Unit, IBMC)

The other organ frequently involved in FAP, is the heart. Clinically, the cardiomyopathy may present as an arrhythmia, heart block or heat failure. Electrocardiographic abnormalities with Q-wave and T-wave repolarization changes and various conduction disturbances are some of the clinical features. Echocardiography shows a restrictive cardiomypathy with thickened interventricular septum and ventricular walls (Staunder, 1991), although changes consistent with a hypertrophic cardiomyopathy have also been described (Fonseca *et al.*, 1991).

In FAP the amyloid deposits are widely distributed and other clinical features additional to the main ones already described can occur: nephropathy and more rarely pulmonary (Diaz Lobato *et al.*, 1991) and bone involvement (Allard *et al.*, 1991).

The first report relating immunologically TTR as the main protein in FAP fibrils was in 1978 by Costa and colleagues. Six years latter, in 1984, Saraiva *et al* identified a Val30Met mutation in the protein isolated from Portuguese FAP patients. This variant was shown to be a biochemical marker for FAP (Saraiva *et al.*, 1985) that resulted from a point mutation in the exon 2 of the TTR gene (Maeda *et al.*, 1986).

Since the identification of the Val30Met variant, many others aa substitutions were identified in the TTR protein (table 1, page 11); these variants are associated with different

clinical phenotypes and a considerable number of non pathogenic TTR mutations have been identified (table 2, page 12).

For a long time it was thought that all the patients carrying the TTR Val30 Met mutation were Portuguese in origin and had a common founder. However, haplotype studies have shown at least three different haplotypes associated with this mutation (Yoshioka *et al.*, 1989; Almeida *et al.*, 1995).

2.1.2.2.3.1- Phenotypic diversity in TTR related amyloidosis

The Val30Met mutation is the most common among FAP patients of Portuguese origin (Saraiva *et al.*, 1984) but it has also been identified in patients of different origins: Sweden (Dwulet and Benson, 1984), Japan (Nakazato *et al.*, 1984), Cyprus (Holt *et al.*, 1989), Greece (Holt *et al.*, 1989), France (Bhatia *et al.*, 1993) and England (Bhatia *et al.*, 1993). Within these populations, there is some heterogeneity in FAP, both in age of onset and clinical presentation. Portuguese and Japanese Val30Met-related–FAP populations have a close median age of onset, 33.5 and 43.2, respectively (Sousa *et al.*, 1995; Ikegawa *et al.*, 1991), although cases of late onset in TTR Val30Met related FAP have been observed in Portuguese patients (Saraiva *et al.*, 1986; Sequeiros and Saraiva, 1987). For the Swedish kindred the average onset is at 56.7 years of age (Sousa *et al.*, 1995). Swedish patients also differ from Portuguese patients by presenting frequent vitreous opacities. An intermediate age of onset is found in Maiorca, at 49 years of age (Munar-Qués and *et al.*, 1990). Compounds heterozygous individuals carrying the Val30Met and the Thr119Met mutations present a late onset and a more benign clinical course of the disease (Coelho *et al.*, 1993). *In vitro* studies showed an increased T_4 binding affinity for TTR Thr119Met (Almeida *et al.*, 1997) and although there is no relationship between T_4 binding properties and amyloidogenecity, it is acceptable that both are related with structural alterations induced by the mutation. While TTR Val30Met is the most frequent and widespread variant, TTR Leu55Pro (Jacobson *et al.*, 1992) and TTR Leu12Pro (Brett *et al.*, 1999) are the most severe mutations.

Some TTR variants are associated predominantly with cardiomyopathy and absence of neuropathy. Familial cardiac amyloidosis (FAC) is related mainly to two TTR variants: TTR Val122Ile and TTR Leu111Met. TTR Val122Ile is the most common amyloidogenic

mutation producing FAC primarily in individuals of African descent (Jacobson, 1992). TTR Leu111Met has the earliest age of onset, around 40 years, with death occurring within 1-3 years (Ranlov *et al.*, 1992).

2.2- Amyloid - unifying features

The designation amyloid was introduced in 1854 by Virchow when studying cerebral samples with abnormal macroscopic appearance and describing a substance that stained blue pale with iodine, and violet after the addition of sulfuric acid. At the time, the tinctorial properties of amyloid were attributed to the presence of starch and thus, the name amyloid derives from the Latin amylum and the Greek amylon. A few years later, the presence of protein in the amyloid mass was demonstrated, shifting the study of amyloid first as a protein and later as a class of such.

Amyloid deposits show special tinctorial properties that for a long time were the only form diagnosis available. These include apple-green birefringence under polarized light after staining with Congo red (figure 6); staining with thioflavin S and thioflavine T, producing a yellow-green fluorescence (Vassar and Culling, 1959; Bennhold H., 1922); thioflavine T has also been shown to interact with amyloid in suspension producing a specific fluorescent signal with a new excitation maximum at 450 nm (LeVine III H, 1993, 1995).

Figure 6 – Amyloid deposit stained with Congo red and viewed under polarized light (from Sousa *et al.*, 2001a).

A century later after Friedreich and Kekule studies, electron microscopy observations revealed that the amyloid material was fibrillar (Cohen and Calkins, 1959). Methods to isolate and purify these deposits were developed and the capability to solubilize the fibrils (Pras *et al.*, 1868; Kaplan *et al.*, 1999) made possible the characterization of the protein constituents; in 1971 the first amyloid-related protein was sequenced and characterized (Glenner *et al.*, 1971), an immunoglobulin light chain. Since then, over 16 biochemically distinct amyloid-related proteins were identified.

2.2.1- The amyloid fibrils

Regardless the protein precursor involved in the amyloid disease, the properties associated to this condition are common to all forms. In addition to the tinctorial characteristics referred above, general structural features unify amyloid fibrils. Ultrastructurally, they appear as bundles of straight or coiled fibrils, non-branched, 7-10 nm wide and variable in length (Blanden *et al.*, 1966; Shirahama and Cohen., 1967; Glenner, 1980); in most cases they seem to be helically twisted. Amyloid fibrils present a high content in β-pleated sheet as demonstrated by x-ray diffraction analysis (Eanes and Glenner, 1968; Bonar *et al.*, 1969) and extensive antiparallel β-sheet strands with their axes running perpendicularly to the axis of the growing fibril (cross-β pattern), (figure 7) (Glenner, 1980 and 1981; Lansbury, 1992).

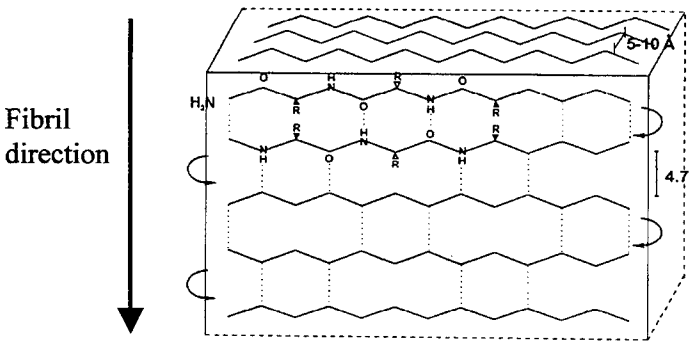

Figure 7 – Diagram of the antiparallel cross-β pattern present in amyloid fibrils. (Adapted from Spencer *et al.*, 1991).

2.2.2- Other components in amyloid deposits

Amyloid deposits are not entirely composed of the amyloid precursor protein. Several components have been found associated with all amyloid fibrils. These include: serum amyloid P component (SAP), sulphonated glycosaminoglycans (GAGs), apoliproteins E and J, α1-antichymiotrypsin, several basement membrane components such as fibronectin, laminin and collagen type IV, complement proteins, and metal ions.

In vivo amyloid formation may suffer the influence of other factors in addition to the fibrillar protein. Several components have been identified; some, implicated in amyloid inhibition acting as molecular chaperones (Wisniewski and Frangione, 1992); others inducing fibril formation or preventing amyloid degradation under normal conditions.

Serum amyloid protein (SAP), a decameric plasma glycoprotein, is found associated to all types of amyloid deposits (Coe *et al.*, 1981; Prelli *et al.*, 1985; Inoue and Kisilevsky, 2001) to which and it binds in a calcium–dependent manner. SAP contributes to amyloidogenesis, probably by stabilizing amyloid fibrils and retarding their clearance (Pepys, 2001). One possible way of contributing to persistence of amyloid *in vivo* is by protecting fibrils from proteolysis (Tennent *et al.*, 1997), as SAP is itself very resistant to proteolysis.

Other extracellular matrix components (ECM) including glycosaminoglycans (GAGs) and proteoglycans (PGs) have been demonstrated to be significant components of all amyloid deposits thus far analyzed. Their role is not clear and contradictory results have been reported.

Laminin, a major basement membrane glycoprotein, was found to interact with Aβ1-40 peptide by blocking fibril formation and even inducing depolymerization of preformed fibrils (Morgan and Inestrosa, 2001); aggregation of the Dutch Aβ1-40 variant, a peptide with a higher capacity to aggregate, was also inhibited by laminin (Bronfman *et al.*, 1998). Other studies reported a very high *in vitro* affinity between laminin and Alzheimer's amyloid precursors (AAPs), suggesting that very specific interactions normally occur between AAPs and the ECM (Narindrasorasak *et al.*, 1991, 1995).

It is thought that laminin interacts with Zn^{2+} and that the formed complex contributes to basement membrane cross-linking, which in turn is important for its assembly (Ancsin and Kisilevsky, 1996). Laminin contains 42 cysteine-rich repeats of which 12 contain nested zinc finger consensus sequences. The effect of several ions on laminin binding activity was evaluated and found that Zn^{2+} was the most effective at enhancing laminin-entactin and

laminin-collagen IV binding. Furthermore, apoSAA (the serum precursor of AA amyloid) also binds laminin, involving a single class of binding sites. The nature of this interaction is ionic and enhanced by Zn^{2+} (Ancsin and Kisilevsky, 1997), and probably mediated through Cys-rich zinc finger-like sequences. Further investigations, localized the laminin binding site on apoSAA (Ancsin and Kisilevsky, 1999) and the authors postulated that laminin facilitates AA amyloidosis by arresting apoAA. Collagen type IV also binds apoSAA but with lower affinity than laminin (Ancsin and Kisilevsky, 1997).

Interaction of Aβ with glycosaminoglycans significantly enhances fibril formation (Castillo *et al.*, 1997; Mclaurin *et al.*, 1999). The sulphate moiety of PG was proposed as being critical in this interaction. This hypothesis was confirmed when removal of all sulphates from heparin led to a complete loss in the Aβ fibrillogenesis.

Significant amounts of GAGs were detected in close association with purified myocardial amyloid fibrils (Magnus *et al.*, 1991). The GAGs were identified as 50% chondroitin sulphate, 33% heparin/ heparan sulphate and 17% hyaluronan. It is also suggested that the proportion of different GAGs in the amyloid deposits may depend both on the organ or tissues affected and the type of fibrils. TTR was also shown to interact with perlecan *in vitro* (Smeland *et al.*, 1997). It is clear that basement membrane and its constituents play a role in amyloidogenesis. Whether they enhance or inhibit fibrillogenesis is not clear.

Apolipoprotein E (Strittmatter *et al.*, 1993; Corder *et al.*, 1993; Wisniewski *et al.*, 1993) and apolipoprotein J (Ghiso *et al.*, 1993) have been shown to bind soluble Aβ. Immunoprecipitation with anti-ApoJ (Ghiso *et al.*, 1993) sequesters soluble Aβ from CSF, indicating that a complex is formed between them; α1-antichymotrypsin has been shown to influence fibril formation by Aβ synthetic peptides (Fraser *et al.*, 1993).

2.2.3- Amyloid ligands

Dyes as Congo red and thioflavin T are usually employed to identify *ex vivo* amyloid. For diagnostic purposes, these amyloid markers imply invasive methods, such as biopsy, to provide the sample to be analyzed. Conventional non-invasive diagnostic techniques, such as clinical evaluation, joint ultrasonography or X-ray, computed tomography or magnetic resonance imaging findings, as well as conventional bone scans, when available, suffer from relative non-specificity and/ or low sensitivity. In this regard, sensitive imaging

techniques have been developed in order to evaluate amyloid load and/ or treatment evolution.

In 1986, Baltz and colleagues (Baltz *et al.*, 1986) showed for the first time that the circulating SAP is the precursor of the amyloid P component in systemic amyloidosis. At the same time, this work provided a mean for selective targeting of diagnostic tracers and/ or effector agents to amyloid deposits *in vivo*. Labeled ^{123}I-SAP was shown to specifically bind amyloid deposits producing highly specific, high resolution scintigraphic images of amyloid in mice with experimentally induced amyloid A protein (Hawkins *et al.*, 1988a). Due to its ability to bind all known types of amyloid fibrils, SAP was further used to develop a new general diagnostic method for *in vivo* imaging of amyloid deposits (Hawkins *et al.*, 1988b; Hawkins, 1994). SAP was able to specifically bind AL, AA and β_2-microglobulin amyloid deposits. However, once localized to amyloid deposits, the ^{123}I-SAP persisted for long periods in contrast to its normal rapid degradation. Moreover, only a small part of the total injected dose became localized in the amyloid deposits (Hawkins *et al.*, 1988b; Baltz *et al.*, 1986), suggesting that SAP affinity might be reduced for certain organs. In fact, when used to evaluate amyloid deposition in patients with β_2-microglobulin-related amyloidosis, radiolabeled SAP failed to accumulate in some of the frequently involved sites, such as hips or shoulders (Floege *et al.*, 2000).

Small molecules such as (*trans,trans*)-1-bromo-2,5-bis-(3-hydroxycarbonyl-4-hydroxy)styrylbenzene (BSB) (Skovronsky *et al.*, 2000), a Congo red derivative, have been developed, especially directed to detection of amyloid in Alzheimer's disease. BSB sensitively labels senile plaques (SPs) in AD brain sections and is able to permeate living cells in culture, binding specifically to intracellular Aβ aggregates. In living transgenic mouse models of AD amyloidosis, BSB labels SPs composed of human Aβ and crosses the blood brain barrier (BBB), labeling numerous AD-like SPs throughout the brain of the transgenic mice after i.v. injection. BSB was also shown to bind diverse beta-pleated sheet structures in postmortem human neurodegenerative disease brains, including extracellular Aβ protein and intracellular lesions composed of abnormal tau and synuclein proteins (Schmidt *et al.*, 2001). These results suggest that radioiodinated BSB derivatives might be useful imaging agents to monitor different amyloids *in vivo*. X-34, another Congo red derivative, has also been proposed as an amyloid marker not only for Alzheimer's disease but for amyloidosis in general since it also binds AL and TTR amyloid (Link *et al.*, 2001; Styren *et al.*, 2000). Chrysamine G (CG) is a lipophilic Congo red derivative; it appears to

bind amyloid in the same way as Congo red- through a bidentate attachment spanning several amyloid peptide chains- and crosses the BBB. Furthermore, CG appears to have low toxicity (Klunk *et al.*, 1994) and binding of ^{14}C-CG correlated well with the number of SPs and neurofibrillar tangles (Klunk *et al.*, 1995) in mice models for AD. CG labeled with 99mTc (99mTc-MAMA-CG) was found to bind specifically to Aβ deposits (Dezutter *et al.*, 1999) and to amyloid in chickens with spontaneous joint amyloidoisis (Dezutter *et al.*, 2001a). This tracer agent was further tested in amyloid deposits types AA, Aγ and Aκ, suggesting it can be applicable for diagnostic purposes in clinical amyloidosis (Dezutter *et al.*, 2001b).

Lipophilic thioflavin derivatives (Mathis *et al.*, 2002; Klunk *et al.*, 2001) have also been described to bind amyloid deposits. These molecules are also capable of entering the brain and are proposed as promising candidates for *in vivo* amyloid imaging in Alzheimer's disease.

The antiprotease aprotinin, usually employed as a cortical renal tracer, was evaluated for the imaging of amyloid associated with AL deposition (Aprile *et al.*, 1995). Aprotinin labeled with technetium-99m (TcA) was shown to accumulate in organs known to have amyloid deposition, prompting this anti-serine protease as a low-cost available radiopharmaceutical for imaging in AL type amyloidosis.

3- Amyloid formation pathway

The mechanism that leads to amyloid formation is still poorly understood. It is believed that several factors take part in the process that culminates in fibril formation. A prominent agent is the amyloidogenic potential of the protein that can be enhanced or diminished by the presence of mutations; other intervening component is the presence of tissue and/or circulating factors that can contribute to the deposition of amyloid and may determine the specificity of localization; other factors, like environment and genetic background, have been proposed and could account for the differences in onset between individuals carrying the same mutation.

The large number of proteins associated to amyloidotic diseases together with their unrelated primary structure and lack of consensus sequences, suggest the presence of other particularities that may contribute to their tendency to self-aggregate. In this regard, the

high content in β-sheet structure, present in most amyloidogenic proteins, has been implicated as favoring fibril formation. This assumption is deduced from the cross-β pattern present in all amyloid fibrils and thus, proteins rich in β-sheet would be more prone to fibril formation. However, some proteins associated with amyloid disorders present predominantly α-helix in their secondary structure. It is the case of lysozyme that in its native form presents only a small amount of β-structure (Artymiuk and Blake, 1981) and of the prion protein; however, modifications, particularly changes in the β-content, lead to amyloid formation.

In vitro fibril formation has been a powerful tool in studying of mechanism that leads to amyloid formation. Theories for the events occurring *in vivo* have been proposed based on the knowledge of the *in vitro* results. Virtually all types of fibrils are produced *in vitro* from their normal precursors, suggesting that the amyloidogenic potential is determinant. Moreover, morphologically, synthetic fibrils (figure 8) are similar to those formed *in vivo*, suggesting a predominant role of the amyloidogenic potential of proteins in amyloid disorders.

Figure 8 – TTR fibrils formed *in vitro*. Scale bar = 100 nm (Amyloid unit, IBMC, Porto).

3.1- Hypotheses for amyloid formation

Different hypothesis have been raised to explain amyloid formation concerning the protein amyloidogenic potential. We next described some of the proposed theories.

3.1.1- Partial unfolding of globular proteins and partial folding of disordered proteins- the conformational hypothesis

Proteins like TTR, lysozyme and light-chain variable domain (V_L) adopt globular folds in their soluble states (Kelly, 1998, 1996). It is now currently accepted that these proteins must undergo destabilization into a partially unfolded state, in order to self-assemble into fibrils. Mutations seem to induce the structural conformations that favor the destabilization. In the case of TTR, the occurring mutations would favor the formation and/ or exposure of new structural motifs in the TTR molecule that would culminate with tetramer dissociation and formation of partially unfolded intermediates. TTR Val30Met crystal structure shows a higher spacing between DAGH and CBEF sheets in the monomer together with a movement of strand A exposing residue 10 to solvent (Terry *et al.*, 1993). For another variant, TTR Val122Ile, an increase in the length of the hydrogen bonds between dimers was reported (Damas *et al.*, 1996). Furthermore, the FG loop also differs in all amyloidogenic TTR variants while it is conserved in WT and non-amyloidogenic TTRs. The structural differences are thought to destabilize the tetrameric structure, the proposed initiation step in the amyloidogenic cascade.

Contrary to globular proteins, many amyloidogenic polypeptides consist primarily of random-coiled structure in their native states. Aβ and IAPP are examples. These proteins can, however, adopt a partially structured conformation that is stabilized by oligomerization (Ratnaswamy *et al.*, 1999). Kayed *et al.*, (1999) demonstrated that IAPP fibril formation involves a transient formation of a conformer with the characteristics of a molten globule, containing substantially more α-helix and β-sheet than the native state. When the fibrils are formed, the α-helix content decreases whereas the β-sheet contents increases even further. A similar process was observed for Aβ with a transient increase in α-helix during the conversion of largely unfolded low molecular Aβ to amyloid fibrils enriched in β-sheet (Walsh *et al.*, 1999).

3.1.2- Amyloid formation may require proteolysis- proteolytic hypothesis

Proteolysis has been viewed as an important event in most types of amyloidosis. Some amyloidogenic proteins are released from precursors by proteolysis. For example, Aβ is derived from the amyloid precursor protein by a combination of β- and γ- secretases cleavages (Teplow, 1998; Selkoe, 1999). Additional fibrillogenic fragments were identified in the recent past: the 34-residue Abri peptide, derived from a putative transmembrane precursor and found in plaques of British dementia (Vidal *et al.*, 1999; Lansbury and Kosik, 2000); the 50-residue medin peptide, derived from lactadherin and associated with aortic medial amyloid (Häggqvist *et al.*, 1999); an N-terminally cleaved fragment of lithostathine found in fibrillar aggregates of AD and chronic calcifying pancreatitis (Cerini *et al.*, 1999).
TTR peptides in addition to the intact protein, have been found in amyloid fibrils from SSA and some FAP patients, raising the hypothesis that proteolysis could trigger fibril formation by releasing amyloidogenic fragments (Saraiva and Costa, 1991). The fragments released result from cleavages that vary according to the TTR variant involved: in SSA fibrils, the fragments result from cleavage at positions 46, 49 and 52 (Cornwell III, 1988); TTR Val30Met (Wahlquist *et al.*, 1991), TTR Val122Ile (Gorevic *et al.*, 1989) and TTR Phe33Ile (Pras *et al.*, 1983; Nakazato *et al.*, 1984) fragments result from cleavage at position 49; TTR Leu111Met carriers showed amyloid fibrils containing TTR molecules cleaved at positions 46, 49 and 59 (Nordlie *et al.*, 1990; Hermansen *et al.*, 1995).
Several works were conducted in order to assess the capacity of TTR peptides to form amyloid fibrils. Most of the synthetic peptides that retain the ability to self-aggregate into fibrils represent β-strands in the tertiary structure of TTR and formed fibrils with the characteristic cross β-sheet arrangement (Gustavsson *et al.*, 1991). Nuclear magnetic ressonance (NMR) and circular dichroism (CD) studies using these peptides revealed that they are predominately comprised of random-coil structures but may also include a low percentage of turn or helical elements. The peptides displayed no predisposition to exclusively form β-strands structures in solution as supposed from the β-sheet based fibrils they form (Jarvis *et al.*, 1994).
However, in other samples of Val30Met TTR fibrils, no fragments are found (Saraiva *et al.*, 1984; Tawara *et al.*, 1983) and thus, the role of proteolysis in TTR amyloidosis is still unclear and evidences suggest that the release of peptides is not essential.

3.1.3- Nucleation and seeding

Several studies report that amyloid formation seems to occur via a nucleation dependent oligomerization (Harper and Lansbury, 1997; Lansbury, 1997) in which an ordered nucleus is formed after a lag phase. After nucleation, growth of the fibril occurs rapidly and follows an accumulation time course sigmoidal in shape (Kisilevsky, 2000). The development of animal models with accelerated AA amyloid and prion deposition are examples of fibril formation upon the supply of a template, usually employing isolated AA fibrils as amyloid enhancing factor (AEF) (Axelrad and Kisikevsky, 1980; Kisilevsky and Boudreau, 1983) and prions (Prusiner and Scott, 1997), respectively. Moreover, this nucleation event may be created using as nucleus heterologous fibrils. It is the case of *in vivo* murine AA amyloidosis, where fibrils derived from Aβ (Ganowiak *et al.*, 1994), TTR fragments (Johan *et al.*, 1998), IAPP or amylin (Johan *et al.*, 1998), and even modified silk fibrils (Kisilevsky *et al.*, 1999) may replace AEF.

TTR associated amyloidosis is thought to obey to this nucleation event. Although proteolysis is not absolutely necessary for TTR related fibril formation, the fragments originated in some cases, may provide a nidus for further and faster polymerization.

3.2 – Intermediate species in TTR amyloidogenesis

From the native form of the precursor to the mature fibril, several species appear as intermediates in the path that ends with the TTR mature fibril.

3.2.1- Monomeric intermediates

Fibril formation *in vitro* opened the possibility to study the process by which a native soluble protein loses its normal fold and aggregates into fibrils, paving the way for better understanding the mechanism that culminates in amyloid formation and to the design of drugs that interfere with such process. In 1991, Gustavsson and colleagues (Gustavsson *et al.*, 1991) first described the production of TTR amyloid-like fibrils when dissolving the protein in a 10% acetic acid solution, pH 2.3. Colon and Kelly (1992) further studied this

theme and showed that the rate of fibril formation is pH dependent with higher rates at pHs between 3.6-4.0 (Colon and Kelly, 1992). The accurate identification of the TTR denaturated intermediate was complicated by the fact that fibril formation occurs over a pH range that is close to the pH where a TTR tetramer to monomer transition is operating. The results were consistent with either a rearranged tetrameric or monomeric TTR denaturation intermediate. This work also hypothesized the lysosomal intervention in amyloid formation, supported by the range of pHs found to induce higher rates of fibril formation. However, *in vivo*, TTR amyloid deposits are extracellular arguing against this view.

Further work in 1996 by Lai *et al.*, suggested that tetrameric TTR dissociates to a monomer in a process that is dependent on both pH and concentration. The acid denaturation pathway of TTR involves the formation of several different intermediates having variable quaternary, tertiary and secondary structures. Moreover, the authors stated the dissociation of the TTR tetramer into monomers with a defined yet, non-native tertiary structure. The dissociation would involve rearrangement in the C-strand-loop-D-strand region in such a way that a monomeric β-sheet sandwich was afforded having the A, B, F, and H strands exposed allowing the self-assembly into amyloid.

Even though the use of low pH has been useful to study amyloid formation, physiological conditions were required to better understand the process that takes place *in vivo*. Others approaches under physiological conditions were performed. Quintas *et al.*, (1997) reported that TTR dissociates to a monomeric species at pH 7.0 and nearly physiological ionic strengths; the tetramer dissociation is apparently irreversible and the monomer is non-native (Quintas *et al.*, 1999). This monomeric species does not behave like a molten globule and leads to the formation of partially unfolded monomeric species and high molecular mass soluble aggregates (Quintas *et al.*, 1999). Based on aging experiments of tetrameric TTR, under physiological conditions, and protein unfolding experiments of the non-native monomeric forms, it has been shown that tetramer dissociation and partial unfolding of the monomer precedes amyloid fibril formation (Quintas *et al.*, 2001).

3.2.2- Dimeric intermediates

The structure of Val30Met reveals a movement of strand A exposing Cys10 to the solvent. This lead Terry *et al.* (1993) to consider that amyloidogenic fibrils could form after the

association of TTR molecules through disulphide bridges. However, this theory does not fit with the formation of fibrils by a TTR Cys10Arg variant.

Redondo *et al.*, (2000a) addressed the question of whether dimers are able to form amyloid fibrils; mutant dimmers covalently linked through disulphide bonds were unable to polymerize into amyloid while disruption of the S-S bridges by a reducing agent, lead to amyloid formation. These data implied the need of a monomeric entity prior to TTR fibril assembly.

In a recent work by Olofsson *et al.* (2001), the substitution of two aa in the hydrophobic core of TTR lead to a mutant very prone to form amyloid. Prior to fibril formation, a stable dimeric species was detected at low temperature. However, a small population of monomers was also observed. The data is in good agreement with the findings by Serag *et al.* (2001) that suggest that the native dimeric interactions are preserved within the amyloid fibril. The conclusions arrive from the ability of forming fibrils starting with cross-linked engineered TTR mutants with extra cysteins.

3.2.3- Tetrameric intermediates

In spite of the evidences supporting the involvement of monomeric species during TTR fibril assembly, several authors have questioned the monomer as the building block. Besides the dimeric block, a tetrameric structure has also been submitted for discussion.

Ferrão-Gonçalves *et al.*, (2000) proposed a hypothesis based on *in vitro* experiments under high pressure in which an altered tetramer could be responsible for TTR aggregation. However, the work did not present morphological evidence for fibril formation. This hypothesis may apply to very early events on fibril formation as the authors report the presence of a small population of monomers after treatment at high pressure. Moreover, the work was performed with TTR WT and did not include an equal treatment for TTR amyloidogenic variants.

Recently, the structure of the TTR synthetic variant, Gly53Ser, Glu54Asp, Leu55Ser, was resolved and an altered tetramer was suggested as the building block of TTR fibrils (Eneqvist *et al.*, 2000). This mutant, generated according to a predicted mutational hot spot region in the short D strand of the molecule (Serpell *et al.*, 1996), polymerizes at physiological conditions, originating high molecular weight aggregates with amyloid

characteristics (Goldsteins *et al.*, 1997). The crystal structure of this variant reveals a shift in the strand D that affects the positions of residues Ser-50-Glu-63, the β-slip, and the Leu58 is positioned at the site normally occupied by Leu55. New packing interactions include the BC loop, DE loop, FG loop and the area normally involved in complex formation with RBP. The proposed model does not imply tetramer dissociation into monomers for fibril formation. However, it should be noted that this is a non-natural TTR variant.

3.3- Structural amyloidogenic determinants in TTR

Two naturally occurring TTR mutations revealed to be very important in the study of the TTR aggregation pathway giving information on the structural determinants of intermediates: TTR Leu55Pro and Tyr78Phe.

3.3.1 - The Leu55Pro and the Tyr78Phe TTR variants

TTR Leu55Pro variant is associated with the one of the most aggressive forms of TTR-related amyloidosis, characterized by an early age of onset, between 15 to 20 years of age. The disease progresses very rapidly to death in 5 to 10 years (Jacobson *et al.*, 1992; Yamamoto *et al.*, 1994). Besides neuropathy, this variant is also associated with cardiomyopathy and vitreous opacities.

Biochemical studies reported lower tetramer stability towards acid denaturation for this variant when compared to the WT counterpart (McCutchen *et al.*, 1993; Lashuel *et al.*, 1998). Furthermore, TTR Leu55Pro was shown to form protofilaments *in vitro* at physiological pH (Lashuel *et al.*, 1999), indicating that this variant may represent an intermediate, involved in the events occurring *in vivo*. Thyroxine binding studies, used to assess structural modifications of TTR variants, showed a very low binding affinity for TTR Leu55Pro/TTR WT heterozygotic serum and inability to bind homozygotic recombinant protein (Almeida *et al.*, 1996).

To learn more about structure/ pathogenesis relationship in TTR variants, X-ray studies using recombinant TTR Leu55Pro were performed and results compared with the TTR WT

structure. Crystallographic works on other amyloidogenic variants, TTR Val30Met (Hamilton *et al.*, 1993; Terry *et al.*, 1993), TTR Val122Ile (Damas *et al.*, 1996), and TTR Ile84Ser (Hamilton *et al.*, 1996), revealed an overall structural homology with the WT protein. However, the crystal of TTR Leu55Pro showed the presence of eight monomers in the unit cell (Sebastião *et al.*, 1998) in contrast to the WT crystal that crystallizes with a dimer in the asymmetric unit (Blake *et al.*, 1978). In the mutant monomer, due to the disruption of hydrogen bonds between strands D and A, residues 54-56 are part of a long surface loop that connects strands C and E and thus, the TTR Leu55Pro monomer is organized in seven strands and one α-helix (figure 9), instead of the normal 8 strands that constitute the WT monomer. This loop is involved in the crystallographic packing observed in the crystal structure and contacts between CE loops are believed to be determinant in amyloid formation. Another element involved in the overall force in the assembly of units is the hydrogen bonding between the AB loop and the α-helix of the nearest neighbor.

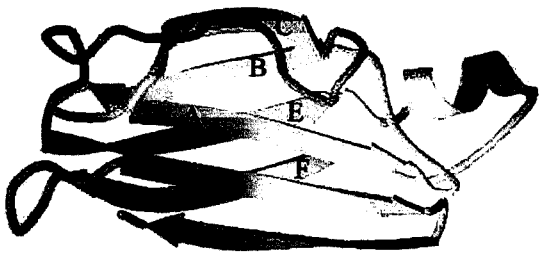

Figure 9– Representation of the TTR Leu55Pro monomer visualizing the long loop CE formed upon the disruption of H-bonds between strands D and A (PDB entry 5TTR; Sebastião *et al.*, 1998).

The topology presented by this mutant is similar to the classic β-barrel. Furthermore, the crystal packing shows several channels running parallel to each other, suggesting a tubular structure and the authors proposed that this variant can constitute an intermediate structure for TTR amyloid formation (figure 10) (Sebastião *et al.*, 1998).

Figure 10– TTR Leu55Pro crystal packing: several channels running parallel to each other, suggesting a tubular structure similar to the TTR amyloid fibril structure (Sebastião *et al.*, 1998).

The same authors re-enforce this view by showing that TTR Leu55Pro used for crystallization binds ThT, indicating the presence of an amyloid-like oligomeric structure (Sebastião *et al.*, 2000). Thus, changes in the D strand together with the contacts of the AB loop and the α-helix are pivotal in amyloid formation. Experiments performed with synthetic TTR mutants with a triple substitution or a triple deletion in the D strand (TTR 53, 54, 55) showed a high potential for amyloid formation even at physiological pH (Serpell *et al.*, 1996; Goldsteins *et al.*, 1997). Binding studies performed with an antibody raised against this mutant, demonstrated that the antibody displayed affinity to *ex vivo* TTR fibrils and TTR mutants with an amyloidogenic fold but not to TTR WT or mutants with the WT fold (Goldsteins *et al.*, 1999). Interestingly, in the TTR Leu55Pro crystal, the region corresponding to the D strand forms the outer part of the asymmetric units that assembles into the tubular structure (Sebastião *et al.*, 1998).

The data gathered so far on the described TTR variant, TTR Leu55Pro, clearly promotes this mutant to a high level in the study of amyloid formation.

Given the known crystallographic structure of TTR Leu55Pro (Sebastião *et al.*, 1998), and with the purpose of destabilizing the AB loop and thus the tetrameric fold, a TTR mutant with a Tyr residue at position 78 was generated (Redondo *et al.*, 2000b).

The resulting protein presents a soluble tetrameric form as shown by resistance to dissociation on native and SDS-PAGE electrophoretic studies and elution patterns on HPLC; the protein also retains the ability to bind T4 indicating a functional tetrameric folding. Interestingly, this variant is very prone to amyloid formation as observed by thioflavine T binding after acidification. Furthermore, the mutated protein is recognized by the monoclonal antibody known to react only with highly amyloidogenic mutant proteins and with amyloid fibrils and with similar binding properties as synthetic fibrils, as measured by surface plasmon resonance (SPR) spectroscopy. The authors propose that this variant may represent an early event in *in vitro* amyloidogenesis (Redondo *et al.*, 2000b). TTR Tyr78Phe was later observed in an Italian patient with TTR-related amyloidosis (Anesi *et al.*, 2001). The patient presented weight loss, chronic diarrhea, exertional dyspnea and distal muscle fatigue with walking difficulty. Physical examination revealed marked macroglossia with teeth indentation, peripheral edema and hepatomegaly. Echocardiography showed restrictive cardiomyopathy with a thickened interventricular septum of 14 mm and a conserved ejection fraction. Furthermore, bilateral carpal tunnel syndrome had been treated surgically 10 years earlier.

4- Proposed models for TTR amyloid

The question about the basic units that form an amyloid fibril is yet not answered. The problem is even more complicated for TTR related amyloid fibrils as the amyloidogenic protein involved presents itself as a tetramer. So far, we have discussed the intermediates that might be involved in the amyloidogenic pathway, apparently complex and difficult to unravel. Most of the times, authors propose the intermediate species as the building blocks. Altered dimers and/or tetramers of TTR may be captured when studying amyloid formation; that does not necessarily signify they are the building blocks of the fibrils but rather provide insights into the steps of fibril formation. Analyzing and resolving the structure of pre-formed fibrils is probably a better way to answer the question so many times asked. We next describe the available models based on the study of *ex vivo* fibrils from FAP patients.

4.1- Fibrils examined with high-resolution electron microscopy

Ultrastructure analysis of FAP TTR Val30Met fibrils from sural nerve biopsies was done by transmission electron microscopy (TEM) and immunolabelling. The FAP amyloid fibril seems to be formed by a core composed of a tight helix of 3 nm wide double tracks containing pentosomes (subunits of amyloid P component) at its center. Other type of double tracks 4.5-5 nm wide are observed made up of heparan sulphate proteoglycan (HSPG). Based on the observations a model was proposed (Inoue *et al.*, 1998) (figure 11), in which TTR appears as filaments 0.5-1 nm wide at the periphery of the core. The dimensions of the TTR filaments made the authors suggest that the TTR basic unit in the FAP fibrils is a modified monomer.

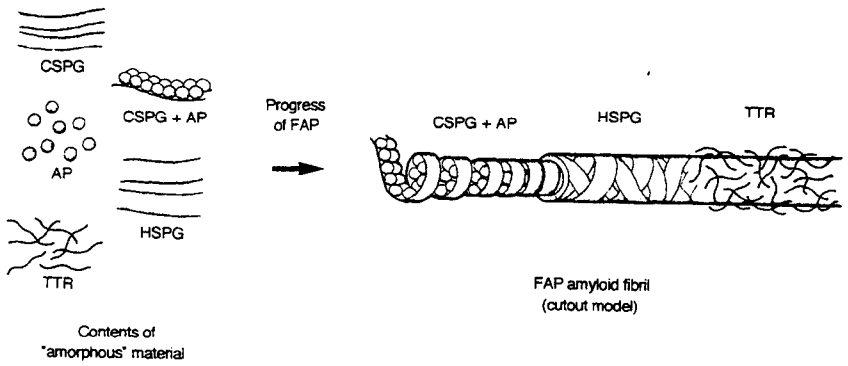

Figure 11– Schematic drawing of the formation of FAP amyloid fibrils (Inoue *et al.*, 1998).

4.2- Fibril analysis by reconstruction image

Reconstruction of TEM images was done on amyloid material obtained from the vitreous humor of patients homozygous for the TTR Val30Met mutation (figure 12).
Analysis showed that fibrils are about 130 Å in diameter and 4-fold symmetry with four protofilaments, each measuring 40 to 50 Å across, arranged around a central hollow core (Serpell *et al.*, 1995). This study did not allow determining the nature of the TTR component that makes up the protofilaments.

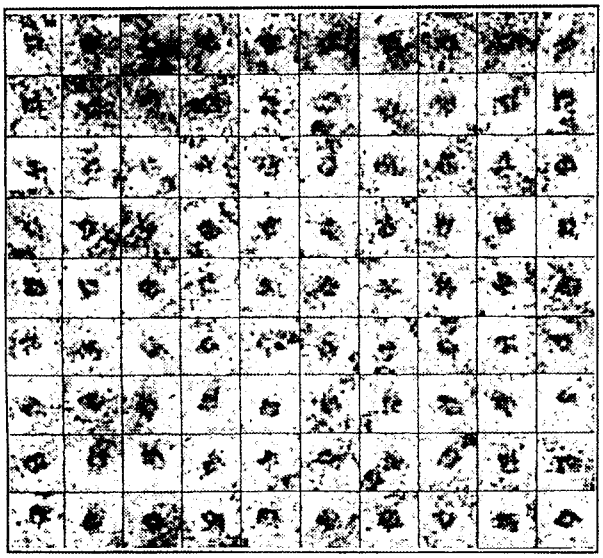

Figure 12- Isolated cross-section images used to study the structure and dimensions of the TTR amyloid fibril (from Serpell *et al.*, 1995).

4.3-X-ray fibril diffraction of *ex vivo* fibrils

Two main models have been proposed based on X-ray fiber diffraction studies. Although the source of FAP fibrils is the same in both cases, the results obtained are distinct.

4.3.1- Monomers are the building blocks of protofilaments

Based on X-ray diffraction studies on TTR amyloid fibrils isolated from biopsies of vitreous humor, a model was proposed in which the unit structure is similar to a monomer. The fibril is composed of a pair of β-sheets consisting of four hydrogen-bonded β-chains per sheet, with the β-chains oriented approximately perpendicular to the fibril axis (Inouye *et al.*, 1998). The altered monomers are stacked axially with a 29 Å- period, constituting the protofilament (figure 13). Furthermore, the dimensions of the fiber and the constituent protofilament are found to be 110-130 Å and 40-50 Å, respectively. The protofilaments within the fiber are not tightly packed, suggesting that components other than the full-length

TTR may fill the space between them. This probably accounts for the difference in size seen in the *in vitro* amyloid-like fibrils (60-100 Å) (Colon and Kelly, 1992; Gustavsson *et al.*, 1997).

When analyzing FAP fibrils, TTR fragments in addition to full-length TTR also appear to contribute to the fibrils (Westermak *et al.*, 1990; Cornwell III *et al.*, 1988). SDS-PAGE studies on vitreous FAP fibrils also show smaller bands apart from those corresponding to the monomer and dimer (Thylén *et al.*, 1993). One of these bands corresponds to a peptide starting at Thr49 and the other to a mixture of peptides starting at positions 1 and 3. The fact that the 29 Å-period lengths along the meridian are greater than the size measured for H-bonded β-chains, suggests that shorter TTR fragments may fill the space in between (Inouye *et al.*, 1998).

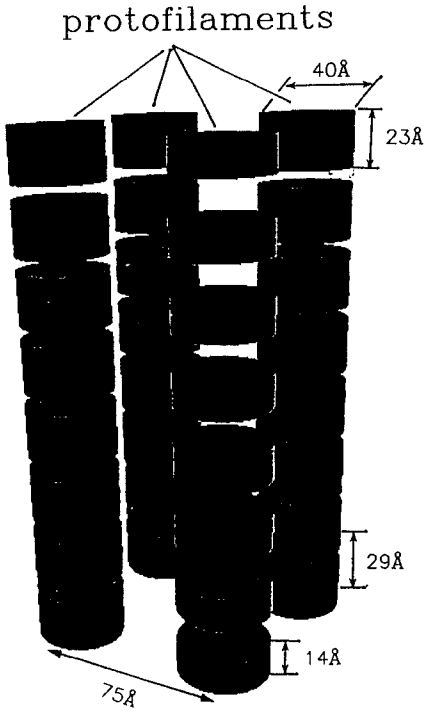

Figure 13– Schematic representation of the protofilament assembly for TTR amyloid (Inouye *et al.*, 1998).

4.3.2- Monomers or dimers are the building blocks

The other model suggests that amyloid fibrils consist of β-sheets extended in regular helical twists along the length of the fibril (Blake and Serpell, 1996). The polypeptide chains are hydrogen bonded together along the entire length of the fibril, contributing to the great stability of this structure. The suggested protofilament is composed of four β sheets related by a single helix axis coincident with the fibril axis. As in the previous model, the proposed structure for the FAP fibril requires a TTR building block structurally different from the native tetramer. However, the building block is not completely defined and the authors suggest it can be either a monomer or a dimer with reorganized or truncated β sheets. Moreover, amyloid formation would require significant structural change in precursor proteins, which contrasts with the previous model (figure14).

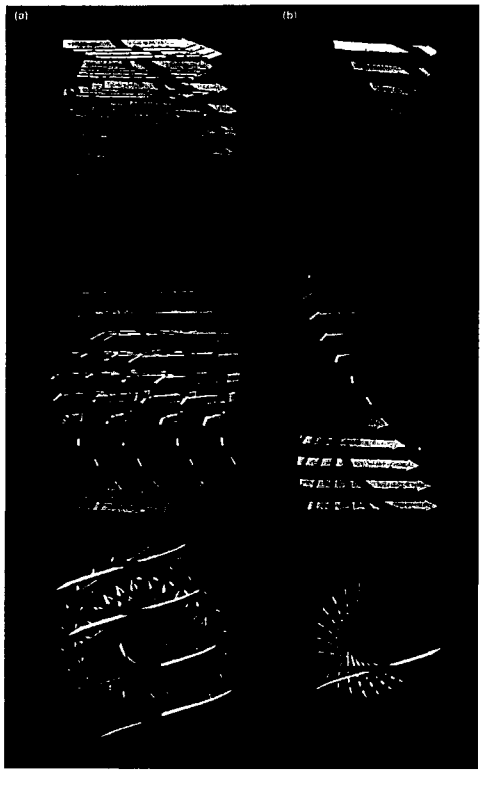

Figure 14– Model of the amyloid protofilament. **(a)** core structure of the amyloid protofilament viewed perpendicularly (top) and along (bellow) the filament axis. **(b)** an isolated β sheet; the strands in the four component sheets are parallel to one another. (From Blake and Serpell, 1996).

5- Animal models for FAP

Although *in vitro* studies have contributed to the knowledge of the amyloid formation mechanism, they tend to simplify the process and disregard a number of factors thought to play a role in pathogenesis. In order to acquire insights into amyloidogenesis occurring *in vivo*, several transgenic mice carrying the human TTR Val30Met gene were generated as models to study FAP. The homology between mouse and human TTR sequences is considerably high with only 25 out of 127 aa residues of the mature protein being replaced by different ones in the mouse. Almost all these substitutions (24 out of 25) are located in the outer surface of the protein, implying that the regions corresponding to functional domains of both proteins are highly conserved between the two species. Furthermore, the sequences of the 5'-flanking region are highly conserved and the homology from the putative TATA box to -189 region is 85% (Wakasugi *et al.*, 1986).
Microinjection of foreign DNA into the pronuclei of single cell ova and the subsequent implantation into pseudopregnant females has been the strategy used to produce transgenic animals.

5.1- Transgenic mice with inducible heterologous promoters

The first report of an FAP mice model occurred in 1986 by Sasaki and colleagues (Sasaki *et al.*, 1986). A DNA fragment containing the mouse metallothionein-I (MT) promoter fused to the structural gene coding for the human TTR Val30Met variant was microinjected into fertilized mouse eggs. Human TTR was inducible and secreted into serum but at low levels (2.5- 12 μg/ ml). In these animals TTR mRNA was present in the liver, kidney, intestine, spleen, brain, heart and testis. The testis showed constitutive mRNA synthesis, while all other tissues were zinc-inducible (Sasaki *et al.*, 1989). No amyloid deposition was observed (Sasaki *et al.*, 1989).
Shimada *et al.* (1989) reported the breeding of transgenic mice for TTR Val30Met in the background C57B1/6J. The structural portion of human ttr Met30 gene was associated to the mouse MT2 promoter (MT2-TTRMet30). In these animals TTR levels in serum were 10-60 μg/ml and amyloid deposits were found in the mucosa of small intestine after 6 months; after 12 months, the deposits extended to 10% of renal glomeruli, heart and thyroid

but no deposition was found in the brain, bone marrow, spleen, liver, lymph node, choroids plexus or peripheral nerves (Yi *et al.*, 1991; Araki *et al.*, 1994). The MT2-TTRMet30 gene was expressed in various tissues as liver, brain, heart, skeletal muscle, kidney and lung. However, mRNA expression was not found in the small intestine suggesting that the deposited human TTR in this organ originates from the serum.

5.2- Transgenic mice using homologous promoter regions

In 1987, Yamamura *et al.* (1987) produced transgenic mice using the entire human ttr Met30 structural gene with 600 bp of upstream sequence including the native promoter (0.6-TTRMet30). TTR mRNA was detected in liver and yolk sac but not in other tissues including brain. These animals showed low levels of human TTR mRNA being about one-tenth of those of mouse endogenous TTR mRNA. Analyses of serum TTR suggested that the human TTR was coupled with mouse TTR forming heterotetramers. Congo red staining indicated no amyloid deposition until 12-15 months of age (Shimada *et al.*, 1989).

A distant enhancer element was identified in the mouse ttr gene (Costa *et al.*, 1990) probably missing in the 0.6 kb sequence used to generate the transgenic mice above described. In cultured human hepathocytes, the mouse ttr gene expression is increased about 10 fold in the presence of the distant enhancer element. Thus, another DNA fragment containing about 6 kb of the upstream region and the entire human mutant ttr Met30 gene was used to produce transgenic animals (6-TTRMet30) (Yokoi *et al.*, 1996). The resulting mice have serum levels of human TTR varying from 0 to 170 μg/ml. Six months after birth, amyloid deposition starts in the gastrointestinal tract, cardiovascular system and kidneys and extends to other organs and tissues with advancing age (Nagata *et al.*, 1995; Takaoka *et al.*, 1997).

The 6-TTRMet30 transgenic mice also form hybrid TTR tetramers and this was one of the explanations raised for the lower and slower degree of amyloid deposition in transgenic mice. In 1993 the ttr knockout mice (ttr-) became available (Episkopou *et al.*, 1993) and crossed with the 6-TTRMet30 mice, generating animals lacking the endogenous ttr gene but carrying the human TTRVal30Met mutant (Maeda *et al.*, 1996; Yokoi *et al.*, 1996). Although the animals presented higher levels of circulating human TTR Val30Met than FAP patients, amyloid deposition was similar to the one observed for the 6-TTRMet

transgenics. Therefore, the presence of the mouse endogenous protein was not the factor leading to delayed amyloid deposition.

Transgenic animals carrying mutations other than the TTR Val30Met have been generated: TTR Leu55Pro (Teng *et al.*, 1995) and TTR Ile84Ser (Waits *et al.*, 1995). Surprisingly, no amyloid deposits were found in these animals. As TTRLeu55Pro is a very amyloidogenic mutation a new attempt to generate mice expressing this variant was performed (Sousa *et al.*, submitted). The transgene was expressed under the control of sheep metallothionein promotor and all the generated lines had the liver as the major site of TTR synthesis although other organs such as the intestine were shown to express the protein. Average plasma levels of TTR after one week of induction with $ZnSO_4$ were approximately 150 μg/ml. As for other transgenic animals, the formation of heterotetramers between mouse TTR and human TTR Leu55Pro was observed. Detection of mutant TTR-immunoreactive material occurred in several organs, particularly in the gastrointestinal tract starting at age of 3 months. Congo red staining was negative for this material.

To study the process of age-related fibrillogenesis, a feature of senile cardiac amyloidosis, transgenic mice overexpressing human wild-type TTR have been produced. Eighty-four percent of C57BI/6xDBA/2 mice older than 18 months developed TTR deposits primarily in the heart and kidney. In most animals, the deposits are non fibrillar and non congophilic (Teng *et al.*, 2001), however, 20% of the animals older than 18 months have TTR cardiac amyloid deposits identical to the lesions seen in SSA. Extraction of amyloid and nonamyloid deposits showed intact human TTR monomers with no evidence of proteolysis or deposition of murine TTR. This work first raised the hypothesis that the non-congophic material is either a pre-amyloid state or an alternate form of tissue deposition; the finding that older animals develop congophic amyloid deposits, suggests that non amyloid deposits occur prior to fibril formation.

The failure of many of the transgenic generated to develop amyloid raises the question of suitability of mice as animal models for FAP, especially because so far, no amyloid deposition in the peripheral nerve has been reported.

Table 4 summarizes the main transgenic mouse lines carrying human ttr sequences.

Transgenic strain	Genetic background	Promoter	[Human TTR] mg/dl	Tissue expression	Start age (months) /	organs affected	TTR amyloid deposition	References
MT1-TTR Met30	(C57BL/6xC3H)F1 x Balb C	Mouse metalothionein	0.25-1.4	Intestine, testis, brain, heart			negative	Sasaki *et al.*, 1986, 1989
MT2-TTR Met30	C57BL/6	Mouse metalothionein and h TTR promotor	1.0-4.8	Liver, brain, kidney, heart, lung, skeletal muscle	4/6		heart, GI tract, kidney, skin, thyroid, vesicular glands	Wakasugi *et al.*, 1987 Shimada *et al.*, 1989 Yi *et al.*, 1991
0.6-hTTR Met30	C57BL/6	0.6 kb hTTR regulatory regions	0.2-3.0	Liver, yolk sac	15		np	Yamamura *et al.*, 1987 Shimada *et al.*, 1989
6-hTTR Met30	C57BL/6	6 kb hTTR regulatory regions	0-17.1	Liver, yolk sac, choroids plexus, kidney	9		kidney, esophagus, heart, stomach, intestine, lung, spleen	Nagata *et al.*, 1995
6-hMet30 (knock-out for mTTR)	MF1x129/Sv/Ev	6 kb hTTR regulatory regions	20-60	Liver, yolk sac, choroids plexus, kidney	11		esophagus, stomach, heart, lung, liver, bladder, intestine, kidney, thyroid, spleen	Yokoi *et al.*, 1996 Episkopou *et al.*, 1993
TTR Ser84	C57BL/6xC3H	7 kb hTTR regulatory regions	25	Liver, yolk sac, choroids plexus			negative	Waits *et al.*, 1995
TTR Pro55	C57BL/6xDBA/2	All known hTTR regulatory regions	1-3	Liver, eye, brain			negative	Teng *et al.*, 2001
TTR Pro55	C57BL/6	Sheep metalothionein	20	Liver, intestine			negative	Sousa *et al.*, 2002 (s)
TTR Pro55 (knock-out for mTTR)	C57BL/6x129/SV/EV	Sheep metalothionein	5	Liver, intestine	4-8		skin, intestine	Sousa *et al.*, 2002 (s)
TTR WT	C57Bl/6xDBA/2	All known hTTR regulatory regions	100-350	Liver, eye, brain, kidney, heart, skeletal muscle, stomach	18		Heart, kidney	Teng *et al.*, 2001

Table 4- transgenic mouse lines carrying human ttr sequences

Np- not published; s- submitted

6- Therapeutical strategies in FAP

The knowledge acquired over time regarding not only the identification of the amyloidogenic proteins, their synthesis, metabolism and degradation but also the pathway for fibril formation with several intermediates involved, made several therapeutical strategies possible.

6.1- Liver transplantation

As TTR is mainly produced by the liver, strategies aiming at removing or reducing the amyloidogenic precursor pool, require liver transplantation (first strategy). This therapeutical approach abolishes the major site of synthesis of mutant TTR and replaces it with the normal protein. The first liver transplantation for an FAP patient occurred in 1990 in Sweden. The procedure is now used all over the world.

Liver transplantation seems to be the only method of slowing down the disease (Lewis *et al.*, 1994). Holmgren *et al.*, (1993) reported that amyloid deposits regressed after 1-2 years of transplantation. Stangou *et al.*, (1999) referred to liver transplantation as producing improvements in autonomic function, gut symptoms, nutritional state, and general well being. However, improvements are not always observed as recently reported for the progression of cardiomyopathy after liver transplantation in patients with FAP (Olofsson *et al.*, 2002). Moreover, the peripheral neuropathy seems to recover very slowly and this therapy is associated with considerable risks for the patients. Thus, other strategies aiming at reducing the amyloid deposits are necessary. They can be divided into three main categories: (II) tetrameric stabilizers; (III) fibril inhibitors and (IV) fibril disrupters (figure 15).

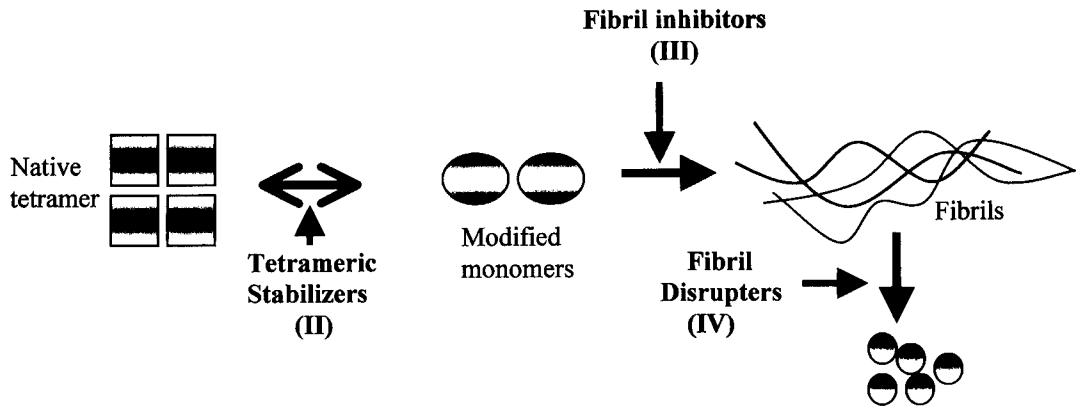

Figure 15- Amyloid fibril assembly (possible pathway). For each step the proposed strategy is indicated.

6.2- Preventing the formation of the amyloidogenic intermediate

The tetrameric nature of TTR implies that in FAP therapy the first step of the amyloidogenic cascade to be inhibited is protein dissociation (second strategy). The potential use of small molecules that bind in the TTR channel, stabilizing the native fold of the protein has been explored; molecules such as flufenamic acid and similar compounds inhibit the conformational changes leading to amyloid formation as assessed by its ability to inhibit the denaturation occurring at acidic pH (Peterson *et al.*, 1998; Baures *et al.*, 1998, 1999; Oza *et al.*, 1999; Klabunde *et al.*, 2000). Crystallographic studies indicate that flufenamic acid mediates intersubunit hydrophobic interactions and intersubunit hydrogen bonds that stabilize the normal tetrameric fold of TTR. The side chains of Ser117 and Thr119 rearrange to facilitate additional hydrogen bonding between the subunits of the tetramer. However, these compounds have not proved yet to be active against amyloid formation *in vivo*. Their use may be compromised by the presence of other proteins with higher binding affinity towards such molecules.

A different approach proposed was the intake of antioxidants to avoid oxidative stress. In this way, TTR monomers and tetramers would maintain the reduced state providing an increased stability to TTR molecule as assessed by isoelectric focusing (Altland and Winter, 1996). Further studies showed that oxidation of Cys10 (the only cysteine residue in TTR) by sulfite, produces more stable tetramer (Altland and Winter, 1999). The stabilizing effect of sulfite was further investigated *in vitro* and *in vivo* and showed to also increase the ratio tetramer/monomer (Altland and Winter, 1999). Facing these results, sulfite was proposed as a potential drug to delay the onset and progression of TTR related amyloidosis. However, *in vitro* studies by Kishikawa *et al.*, (1999), demonstrated that sulfonated TTR has an enhanced amyloidogenicity when compared to reduced or free TTR. Although different methodologies have been used, the different conclusions obtained from these experiments demonstrate the need for a full characterization and comprehension of the amyloid pathway in order to correctly interpret the results obtained.

6.3- Preventing fibril elongation

Inhibiting the formation of amyloidogenic intermediates from the soluble counterpart is expected to be a more specific reaction as amyloidogenic precursors are not structurally related and thus, molecules that inhibit TTR dissociation probably do not produce the same

effect in other amyloidogenic proteins. In contrast, drugs that inhibit elongation or disrupt a certain type of amyloid are most likely to have the same activity towards others amyloid types.

It is accepted that amyloid fibrils result from the assembly of intermediate species with amyloidogenic potential. In the case of FAP, an altered monomer seems to be in the base of such process. Therefore, one of the possible therapies in the treatment of amyloid diseases is to block the interaction and association of such structures into amyloid fibrils (third strategy).

This particular point of intervention has not been properly addressed due to the difficulty in identifying the species in question. In addition, amyloid formation seems to undergo a nucleation event with a rapid initial stage. Hence, the study of a single stage in the amyloidogenic cascade, such as fibril elongation, is most of the times difficult if not impossible. Moreover, studies aiming at studying and finding molecules capable of preventing TTR tetramer dissociation (second strategy) have been performed under acidic pH; under these conditions the dissociation process is very rapid and thus, it is possible that the results obtained also concern fibril elongation. In this view, experiments under physiological conditions that mimic the events occurring *in vivo* are necessary to conveniently distinguish intermediate formation from elongation. Such discrimination will allow testing the potential use of different drugs.

For example, in Alzheimer's disease, a considerable effort has been made in the search of therapeutic drugs inhibiting polymerization. Molecules of structurally diverse types such as cyclodextrins (Camilleri *et al.*, 1994), hemin (Howlett *et al.*, 1997) and benzofurans (Howlett *et al.*, 1999a) are able to prevent the formation of a biologically active form of Aβ. Carbazole-type compounds were also investigated as inhibitors of Alzheimer β-amyloid fibril formation; a number of common structural features seemed to be associated with their inhibitory properties (Howlett *et al.*, 1999b). Rifampicins were shown to inhibit *in vitro* Aβ aggregation and to prevent its toxic effects in cultured rat PC12 cells (Tomiyama *et al.*, 1994); hexadecyl-N-piperidinium bromide was reported to specifically inhibit Aβ(1-40) aggregation *in vitro* but not TTR or IAPP (Wood *et al.*, 1996). Finally, antibodies have also been investigated and shown to reduce pathology in a mouse model of Alzheimer's disease (Bard *et al.*, 2000).

6.4- Disaggregation of amyloid fibrils

Therapeutic strategies can also aim at dissolving/disrupting mature amyloid fibrils (fourth strategy). 4'-deoxy-4'-iododoxorubicin (I-DOX) is an example of a drug fitting in this category. Recently, I-DOX has been proven useful as a tool for disrupting TTR amyloid fibrils (Palha *et al.*, 2000b); it strongly interacts with TTR amyloid fibrils and is able of disrupting the characteristic fibrillar structure of amyloid into amorphous material.

I-DOX has been previously shown to induce amyloid resorption in patients with AL amyloidosis (Gianni *et al.*, 1995); nevertheless, in clinical trials not all AL patients responded to treatment (Merlini *et al.*, 1999; Gertz *et al.*, 2002). The activity of this drug was also tested against prion disease producing the delay of the clinical signs and the extension of survival time in an animal model (Tagliavini *et al.*, 1997). *In vitro* experiments demonstrated that I-DOX interacts with different types of amyloid fibrils besides TTR and AL, including insulin, β2-microglobulin, Aβ (Merlini *et al.*, 1995) suggesting that the drug recognizes a motif common to all amyloid fibrils. Modeling studies using TTR Leu55Pro crystals, which represent an amyloid-like oligomer, indicated that the I-DOX iodine atom is trapped in a pocket located between the two β-sheets of the TTR monomer and with the aromatic-moiety long axis nearly perpendicular to the direction of the β-sheets (Sebastião *et al.*, 2000). I-DOX cardiotoxicity is, however, a drawback for its use and efforts are under way to design non toxic analogues.

Other compounds have been tested and shown to possess a disrupter activity. *In vitro*, anthracyclines were shown to affect Aβ fibril formation leading to the disassembly of pre-formed fibrils (Forloni *et al.*, 2001; Howlett *et al.*, 1999b). In addition, Aβ aggregation was also inhibited. Tetracyclines contain an extended hydrophobic core formed by aromatic moieties, allowing interactions with lipophilic residues of Aβ. Tetracycline and its derivatives also contain a variety of polar substituents that can form hydrogen bonds with specific residues of Aβ (Forloni *et al.*, 2001). It is conceivable that some of these motifs are still exposed in Aβ fibrils and common to all type of fibrils, constituting the basis of these drug activity. Supporting this hypothesis is the work describing the ability of tetracyclines to prevent and reverse the prion protein (Tagliavini *et al.*, 2000), indicating that the anti-amyloidogenic capacity of tetracyclines is not exclusive of Aβ.

Suggestions that hydrophobic interactions mediated by the C-terminal portion of Aβ are important for fibril stability lead to the hypothesis that small hydrophobic compounds might be able to interfere with the stability of the fibrils. In this view, nitrophenols were tested and

shown to disaggregate previously formed Aβ fibrils (De Felice *et al.*, 2001). In addition, they were also able to prevent Aβ aggregation.

7- Concluding remarks

The process leading to TTR amyloid formation is not fully understood and although a common mechanism is thought to underline all types of amyloid, it is expected that some differences occur between them. In spite of the possibility of generating TTR fibrils *in vitro*, their particular morphological features, kinetics and species present have not been subjected to an exhaustive study. Furthermore, the building blocks making up TTR fibrils remain to be elucidated. In FAP, TTR mature fibrils have been described as the causative agent of disease but the toxicity of amyloidogenic species generated throughout the different stages of amyloid formation is unknown.

Among the key therapeutic steps, inhibiting tetramer denaturation/ intermediates formation and fibril elongation are presented as decisive concerning FAP treatment. However, the identification of drugs affecting these stages has been limited by the characterization of the structural determinants in TTR amyloidogenic species. TTR Leu55Pro crystal suggests that this natural mutant is an amyloidogenic intermediate presenting a tubular structure that might be similar to the TTR amyloid fibril structure. Another naturally occurring variant, TTR Tyr78Phe, was also shown to possess amyloid-like properties. The subsequent characterization of these two mutants concerning the formation of amyloid-like fibrils will be of great importance on the investigation of drugs affecting the amyloidogenic cascade. In addition, disaggregation of amyloid fibrils is also a possibility in FAP treatment.

The present study addresses some of these unsolved questions.

Part II

Research Project

Objectives

1- Objectives

The present project aimed at investigating aspects concerning amyloid structure and the mechanism of TTR amyloid formation, particularly the basic units that constitute the related fibrils and the characterization of the stages occurring from the native protein to the mature fibrils, and respective intermediary species. Another major proposal was the search for drugs affecting the amyloidogenic cascade.

The delineated experiments had the following goals:

A. Characterize the binding properties of a new amyloid fibril ligand (aprotinin).

B. Characterize the assembly progression of TTR Leu55Pro fibrils formed under physiological conditions and determine the building blocks of TTR fibrils.

C. Search for TTR amyloid fibrils disrupters and assess the toxicity of different TTR species.

D. Characterize the early events in the amyloidogenic cascade and search for compounds inhibiting them. Develop a method for detecting TTR subtle conformational alterations during denaturation and aggregation.

Experimental Work

Chapter I

Aprotinin binding to amyloid fibrils

Aprotinin binding to amyloid fibrils

Isabel Cardoso[1,3], Pedro José Barbosa Pereira[4], Ana Margarida Damas[2,3] and Maria João M. Saraiva[1,3]

Amyloid[1] and Molecular Structure[2] Units, Instituto de Biologia Molecular e Celular and Instituto de Ciências Biomédicas Abel Salazar[3], Universidade do Porto, Porto, Portugal
Abteilung für Strukturforschung[4], Max-Planck-Institut für Biochemie, Martinsried, Germany.

Running title: Binding of aprotinin to amyloid fibrils

Correspondence to M. J. Saraiva, Amyloid Unit, IBMC, Rua do Campo Alegre, 823, P-4150 PORTO, Portugal; Tel. +351-22-6074900; Fax +351-22-6099157; E-mail mjsaraiv@ibmc.up.pt; WWW http://www.ibmc.up.pt/~mjsaraiv/home.htm

Summary

Different low molecular weight ligands have been used to identify amyloid deposits. Among these markers, the dyes Thioflavin T and Congo red interact specifically with the β-sheet structure arranged in a cross-β conformation, which is characteristic of amyloid. However, the molecular details of this interaction remain unknown. When labeled with Technetium-99m, the proteinase inhibitor aprotinin has been shown to represent a very important radiopharmaceutical agent for *in vivo* imaging of extra-abdominal deposition of amyloid in amyloidosis of the immunoglobulin type. However, no information is available whether aprotinin binds other types of amyloid fibrils and on the nature and characteristics of the interaction. The present work shows aprotinin binding to insulin, transthyretin, β-amyloid peptide and immunoglobulin synthetic amyloid fibrils by a specific dot blot ligand binding assay. Aprotinin did not bind amorphous precipitates and/or the soluble fibril precursors. A Ka of 2.9 μM^{-1} for the binding of aprotinin to insulin amyloid fibrils was determined by Scatchard analysis. In competition experiments, analogues such as an aprotinin variant, a spermadhesin and the soybean trypsin inhibitor were tested and results suggest that both aprotinin and the spermadhesin interact with amyloid fibrils through pairing of β-sheets of the ligands with exposed structures of the same type at the surface of amyloid deposits. An electrostatic component may also be involved in the binding of aprotinin to amyloid fibrils since important differences in binding constants are observed when substitutions Lys15Val, Arg17Leu, Met52Glu are introduced in aprotinin and β-sheet containing acidic proteins, like the soybean trypsin inhibitor (STI), are unable to bind amyloid fibrils. We also tested binding of short peptides derived from aprotinin (APR1 and APR2) to different types of synthetic amyloid fibrils and showed specific binding to insulin, TTR Leu55Pro and Aβ amyloid fibrils; no binding was observed with the soluble counterpart or amorphous precipitates. On competition assays, the two peptides were shown to bind insulin fibrils with similar strengths and a Ka of 1.7 μM^{-1} was determined for APR2 by Scatchard analysis. Together with aprotinin, these peptides can contribute to the development of future peptide radiopharmaceuticals for diagnosis of amyloidosis.

Keywords: aprotinin, transthyretin, amyloid fibrils, spermadhesin

Introduction

The term amyloidosis designates a group of clinically and biochemically diverse diseases mainly characterized by the extracellular deposition of insoluble fibrilar protein, leading to organ dysfunction and cell death. All the deposits bind the dye Congo red resulting in a very characteristic positive green birefringence when viewed under polarized light and yellow-green fluorescence upon staining with Thioflavin S. Thioflavin T (Th T) interacts specifically with amyloid fibrils generating a characteristic fluorescent signal. The ultrastructural morphology of amyloid deposits is characteristically fibrilar, with unbranched appearance, consisting of a number of filaments aggregated side-by-side, forming fibers 75-100Å in diameter and with variable length. There is a predominant β-pleated sheet structure and extensive antiparallel strands with their axes arranged perpendicular to the longitudinal axes of the fiber. Efforts are being developed to understand the detailed molecular organization of amyloid fibrils (for a review see Teplow *et al.*, 1998).

Antiproteases, together with several other elements, are known to be present in certain types of amyloid deposits (Campistol *et al.*, 1992). Recently, the serine proteinase inhibitor aprotinin (a.k.a. bovine basic pancreatic trypsin inhibitor (BPTI), Trasylol®) has been successfully used for *in vivo* imaging of extra-abdominal light chain type amyloid (AL) (Aprile *et al.*, 1995) allowing ascertainment of organ involvement with no need for biopsy procedures. This low molecular weight polypeptide (6,500Da) is composed of 58 amino acid residues arranged in a single chain and is selectively and stably accumulated in the kidney, being for that reason usually employed as a cortical renal tracer (Bianchi *et al.*, 1984). No information is available on the significance of antiprotease accumulation in amyloid deposits, whether aprotinin binds other types of amyloid and if so, what is the nature of this interaction. The purpose of the present study was to characterize binding of aprotinin and aprotinin peptides to synthetic amyloid fibrils, contributing to the comprehension of the nature of the amyloid-aprotinin/peptide interaction and to establish a sensitive binding assay for amyloid detection *in vitro*. For this purpose we used synthetic insulin fibrils, which are easily obtained and widely used in *in vitro* studies, synthetic fibrils from two transthyretin (TTR) mutants (TTR Val30Met and Leu55Pro), Aβ(1-42) fibrils and fibrils derived from a Bence Jones protein (BJP).

Binding of aprotinin to amyloid fibrils

Experimental procedures

Isolation and purification of TTR

Mutant TTR Val30Met and Leu55Pro proteins were produced in an *E. coil* expression system, isolated and purified as described elsewhere (Furuya *et al.*, 1991).

Preparation of amyloid fibrils

Mutant TTR Val30Met (2mg/ml) was incubated with 0.05M sodium acetate/0.1M KCl pH 3.6 for 48 hours at 25°C to form amyloid fibrils (Colon and Kelly, 1992).

Bovine insulin (Sigma) dissolved at 10mg/ml in 0.5% acetic acid, pH 2 (with HCl) was incubated at 85°C for about 2 hours and then alternately frozen at –80°C and heated at 50°C to form amyloid fibrils (Bourke and Rougvie, 1972). After 5 freeze/thaw cycles, the fibrils were sedimented by centrifugation at 15,000g for 30 minutes in a microfuge and the pellet resuspended in water.

Mutant TTR Leu55Pro protein was dialysed against water and concentrated to 5 mg/ml. After centrifugation at 15,000g for 30 minutes at 4°C this preparation produced a pellet, which was resuspended in PBS and incubated at 37°C overnight to produce amyloid fibrils.

Aβ-peptide amyloid fibrils were prepared by dissolving Aβ(1-42) (Sigma) in 50% acetonitrile, 0,1% trifluoroacetic acid and water at 1mg/ml. Immediately after dissolution the preparation was lyophilized. After lyophilization, Aβ(1-42) was dissolved in PBS at 0.5mg/ml and incubated at 37°C for 3 days.

One Bence Jones protein (λ-BJP ZIM) (Eulitz *et al.*, 1987) was digested with pepsin (Boehringer Mannheim) in 0.1M sodium acetate buffer pH 3.5 to produce amyloid fibrils. The enzyme to protein ratio used was 1:1000 and the digestion was conducted at 37°C for 10 hours. The fibrils were sedimented by centrifugation at 15,000g at 4°C for 30 minutes.

All types of amyloid fibrils were tested for Th T fluorescence: Excitation spectra were recorded on a Jasco FP-770 spectrofluorometer at 25°C with 30μM Th T (Fluka) in 50mM Glycine-NaOH buffer, pH 9.0 in 1ml assay volume. Preparations showing the characteristic novel excitation maxima at 450nm upon Th T binding were used in binding experiments.

Aprotinin-peptide synthesis

Aprotinin peptides were synthesized by Q-BIOgene yielding 95% pure peptide. The peptides, APR1 and APR2, comprised aa residues 16-37 with a few modifications.

Labeling with ^{125}Iodine and with Biotin

Aprotinin (bovine lung, Sigma) and aprotinin peptides (APR1 and APR2) were radiolabeled with ^{125}I (Amersham) by the iodogen method, following the instructions of the supplier, which gave specific radioactivities of ~48,000 and ~25,000 cpm/ng protein, respectively. Aprotinin was biotinylated by incubating 2mg aprotinin with 1.5mg biotinyl-ε-aminocaproic acid N-hydroxysuccinimide (Pierce) in 2ml sodium phosphate buffer, pH 7.4, for 2 hours at 4°C with constant stirring, followed by exhaustive dialysis (Bilingsley *et al.*, 1985). APR2 peptide was biotinylated by incubating 0.5 mg of peptide with 20 μg of biotinyl-ε-aminocaproic acid N-hydroxysuccinimide (Pierce) in 2ml sodium phosphate buffer, pH7.4, for 2 hours at 4°C with constant stirring. The biotinylated peptide was purified in a Bio- Gel P2 column with PBS (BioRad).

Dot Blot assay for aprotinin and APR2 binding

Soluble protein, fibrils and trichloroacetic acid (TCA) precipitates of insulin and TTR Val30Met, Aβ(1-42) and fibrils derived from λ-BJP ZIM were immobilized onto a nitrocellulose membrane (Hybond^{TM}-C pure, Amersham). The membrane was then blocked with 5% powdered milk at room temperature for 1 hour, washed with phosphate buffered saline-Tween 20 solution (PBST) and incubated with 500,000 cpm ^{125}I-aprotinin. Finally, the membrane was washed with PBST and processed for autoradiography. Alternatively, the samples were immobilized onto the nitrocellulose membrane, blocked and then incubated with biotinylated aprotinin for 1 hour at 37°C. Bound aprotinin was visualized by streptavidin-biotinylated horseradish peroxidase complexes (Amersham).

Other soluble proteins tested included: β2-microglobulin (human urine, Calbiochem) and four different BJPs (Eulitz *et al.*, 1987; Eulitz *et al.*, 1982).

To study APR2 ability to bind other types of amyloid fibrils, soluble protein, fibrils and trichloroacetic acid precipitates of insulin, Aβ(1-42), and TTR Pro55 were tested following the procedures described above.

Binding of aprotinin to amyloid fibrils

Reduction and alkylation of aprotinin

2mg of lyophilised wild type aprotinin were dissolved in 10ml 0.1M Tris/HCl pH 8.0, 5% (v/v) 2-mercaptoethanol and incubated at room temperature, in the dark. After 16h, 5% (v/v) 4-vinylpyridine was added and the incubation proceeded for 45 minutes. The sample was then loaded onto a reverse-phase HPLC column (Bio-Sil 318-10, 250x4.6mm, BioRad) and eluted with a 15 minutes linear gradient from 15 to 60% (v/v) acetonitrile in 0.1% (v/v) trifluoroacetic acid at a flow rate of 1ml/min. The degree of S-pyridylethylation of the eluted fractions was determined by MALDI-MS analysis. The fractions containing fully modified aprotinin were dried and used for further experiments.

Amyloid fibril – Aprotinin/APR competition binding assay

64μg of insulin of fibrils were incubated with 100μl of cold aprotinin or APR solutions of variable concentrations ranging from 0 to 75μM containing a constant amount of labeled ^{125}I-aprotinin or APR (~50,000 cpm) in a final volume of 400μl. This mixture was incubated for 1 hour at 37°C and then applied onto a 0.2μm pore cellulose acetate membrane filter (Schleicher & Schuell) using a manifold system (Gibco BRL) under vacuum to separate fibril-aprotinin/APR complex from free aprotinin or APR. The filter was washed 3 times with PBST and counted. Bound aprotinin or APR was expressed as a percentage of the total amount added. Each sample was tested in triplicate and each binding assay was performed at least twice. The binding data was analyzed using the GraphPad Prism computer version (version 2.01). The equilibrium constant was determined by Scatchard analysis. In the case of aprotinin, competitive assays were also performed in the presence of Congo Red, Thioflavin T (concentrations ranging from 0 to 150μM), soybean trypsin inhibitor (Type I-S, Sigma), aprotinin variant Lys15Val, Arg17Leu, Met52Glu, spermadhesin PSP-II (Calvete *et al.*, 1995; Varela *et al.*, 1997), Lysozyme (chicken egg white, Sigma), cytochrome C (bovine heart, Sigma) and histones (calf thymus, Sigma) at concentrations ranging from 0 to 75μM.

Protein concentration

Protein concentrations were determined spectrophotometrically at 280 nm, using an extinction coefficient of $7.76 \times 10^4\ M^{-1}cm^{-1}$ based on a 55 kDa molecular weight for TTR (Van Jaarsveld *et al.*, 1973), 5480 $M^{-1}cm^{-1}$ for aprotinin (wild-type and variant Lys15Val, Arg17Leu, Met52Glu), 3400 $M^{-1}cm^{-1}$ for soybean trypsin inhibitor (type-I, Sigma) and 14890 $M^{-1}cm^{-1}$ for spermadhesin PSP-II. The extinction coefficients used for aprotinin, soybean trypsin inhibitor

and PSP-II were calculated with the program PeptideSort from the Wisconsin Package (version 9.0 Genetics Computer group (GCG), Madison, Wisconsin). Thioflavin and Congo red (Aldrich) concentrations were determined spectrophotometrically at 411nm using an extinction coefficient of 2.2×10^4 $M^{-1}cm^{-1}$ and at 488nm using an extinction coefficient of 595 $g^{-1}dm^3cm^{-1}$ (as referred to in Merck Index), respectively.

Results

Dot blot assay for binding of aprotinin to amyloid fibrils:

In order to investigate the binding of aprotinin to different amyloid fibrils, a dot blot binding assay was set up. For that purpose, variable amounts of protein fibrils were immobilized on a nitrocellulose membrane, and as negative controls the soluble proteins and the same amount of protein precipitated with trichloroacetic acid (TCA) were used.

Four different proteins were assayed: insulin, TTR Val30Met, Aβ-(1-42) and one BJP (λ-BJP ZIM). Figure 1 documents specific binding of aprotinin to amyloid fibrils: insulin (top row, a to d), TTR Val30Met (middle row), λ-BJP ZIM and Aβ(1-42) in the bottom row. No binding was observed with all the four soluble proteins or amorphous materials.

Other soluble proteins with high β-sheet content were also used as negative controls: human β2-microglobulin and four different BJP (κ-BJP MEV, λ-BJP ZIM, λ-BJP HEN and κ-BJP GRI) and they showed no binding to aprotinin (data not shown).

Identical results were obtained when using biotinylated aprotinin (data not shown).

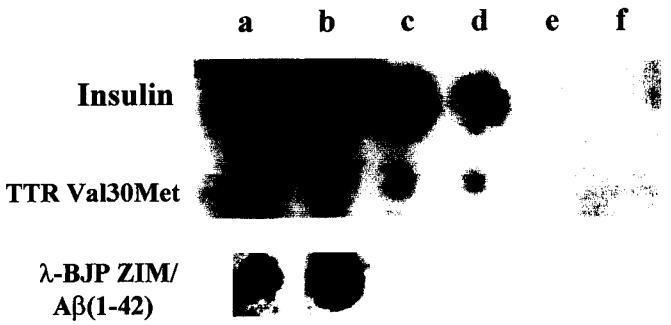

Figure 1- Dot blot binding assay using ^{125}I-aprotinin.

Top row- insulin fibrils (100, 50, 25, 10μg from a to d, respectively), 100μg of soluble (e) and TCA precipitated (f) insulin. **Middle Row**- TTR Val30Met fibrils (100, 50, 25, 10μg from a to d, respectively), 100μg of soluble (e) and TCA precipitated (f) TTR Val30Met. **Bottom Row**- 100μg of amyloid fibrils derived from λ-BJP ZIM. (a), 100μg of Aβ(1-42) fibrils (b).

Characterization of Aprotinin binding

Specific binding of aprotinin

Aprotinin has three disulfide bonds, which are determinant for the maintenance of its three-dimensional structure (Fritz *et al.*, 1983). To further substantiate the specificity of aprotinin binding to amyloid fibrils, the capacity of fully reduced aprotinin to bind synthetic insulin fibrils was tested. Insulin fibrils (64μg) were incubated for 1 hour at 37°C with 50,000 cpm ^{125}I-aprotinin in the presence of increasing concentrations (0-75μM) of cold aprotinin or cold fully reduced and S-pyridylethylated aprotinin and then processed as described in material and methods. Specific binding of aprotinin to insulin fibrils was observed as cold aprotinin completely abolished binding of the radioligand (figure 2A). Reduced and S-pyridylethylated aprotinin failed to bind insulin fibrils (data not shown).

Competitive binding with Th T and Congo red

Competitive assays using increasing concentrations (0-150μM) of Th T or Congo red and ^{125}I-aprotinin as the displaceable radioligand were also performed. No competition was observed between the dyes and aprotinin, indicating they bind differently to amyloid fibrils (data not shown).

Characterization of the binding site of aprotinin

In order to investigate whether aprotinin binding to amyloid fibrils involved the binding loop of the inhibitor, a competitive binding assay was performed in the presence of Soybean trypsin inhibitor (STI). No competition for binding was observed (data not shown).

To further characterize the aprotinin-amyloid fibril interaction, an aprotinin variant (Lys15Val, Arg17Leu, Met52Glu) and a spermadhesin (PSP-II) were also tested for their ability to bind amyloid fibrils. The results obtained for the competition assays were plotted against increasing concentrations of cold aprotinin, aprotinin variant or PSP-II, as competitor. The results are shown in figure 2A and each curve represents the mean values obtained for 3 replicates. Both aprotinin variant and PSP-II bind insulin fibrils in a saturable manner, but with a lower potency than aprotinin (IC_{50} = 10820.0nM, 690.0nM and 391.2nM, respectively). Figure 2B represents the Scatchard analysis for aprotinin and a Ka value of $2.9 \pm 0.37 \mu M^{-1}$ was determinated for the fibril-aprotinin interaction.

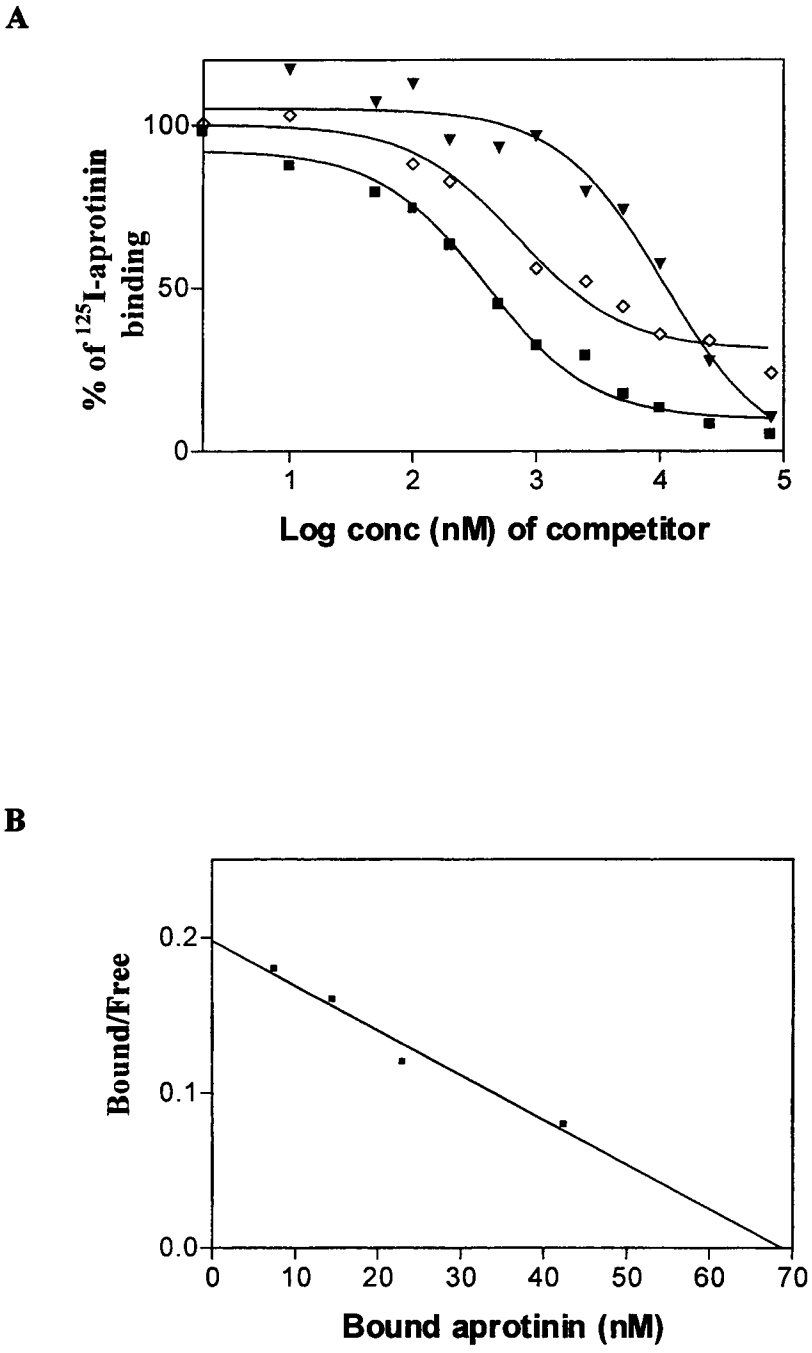

Figure 2- Aprotinin binding to insulin fibrils.

(A) competition curves. The symbols are: (■) aprotinin; (▲) aprotinin variant Lys15Val, Arg17Leu, Met52Glu; (□) spermadhesin PSP-II. **(B)** Scatchard analysis for aprotinin. A Ka value of 2.9 ± 0.37μM^{-1} was determined.

The aprotinin peptides APR1 and APR2 were tested for insulin fibrils binding. On competition assays, APR1 and APR2 were shown to bind insulin fibrils with similar strengths (figure 3).

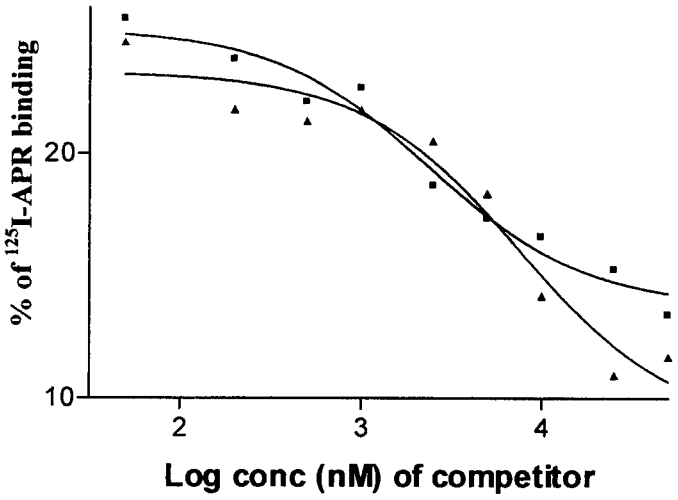

Figure 3- Binding of APR1 and APR2 to insulin fibrils. Competition assay.

(■) APR1

(▲) APR2

Binding of aprotinin to amyloid fibrils

We determined the affinity constant for APR2 binding to insulin fibrils and found a Ka = 1.7 μM^{-1} (figure 4A and B).

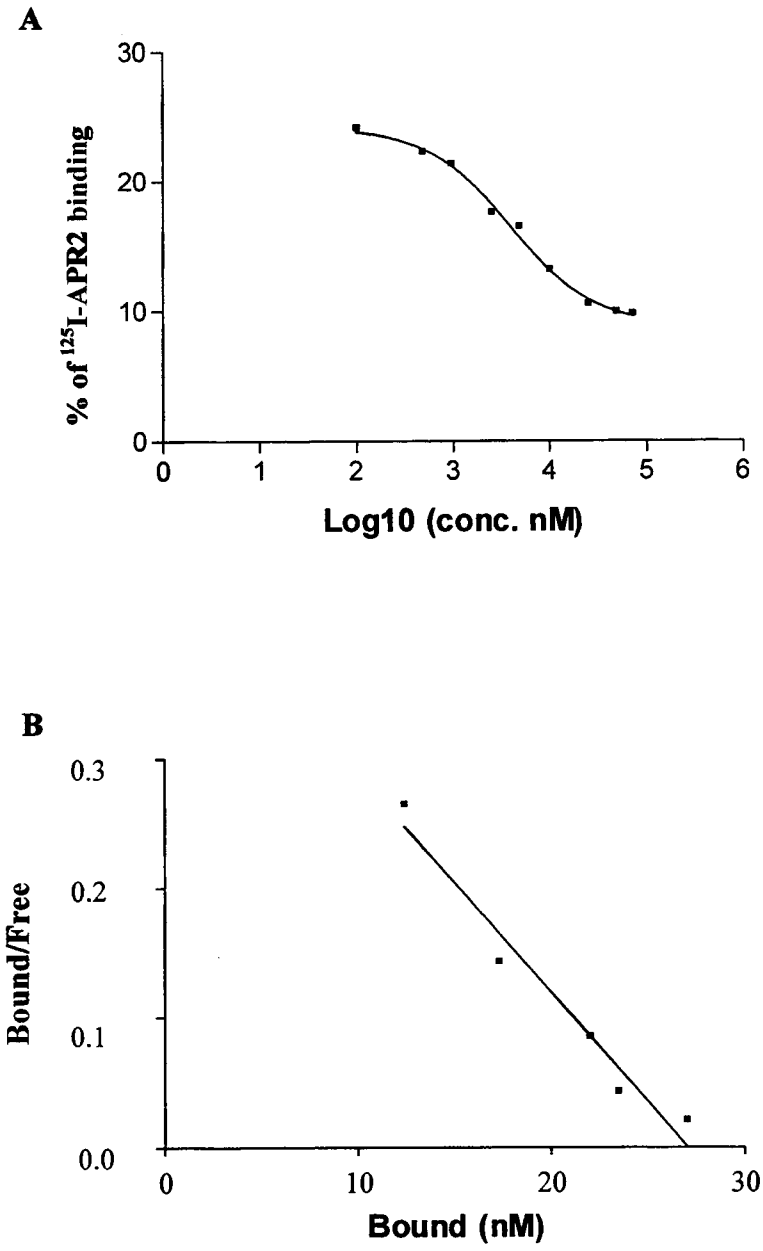

Figure 4- APR2 binding to insulin fibrils.

(A) Competition curve. **(B)** Scatchard analysis: a Ka value of 1.7 μM^{-1} was determined.

A dot blot assay using either ^{125}I- or biotinylated APR2 showed specificity for amyloid since no binding was observed for soluble precursors or for amorphous precipitates of both insulin and TTR. Additionally, APR2 also bound β-peptide (1-42) fibrils- Figure 5A and 5B.

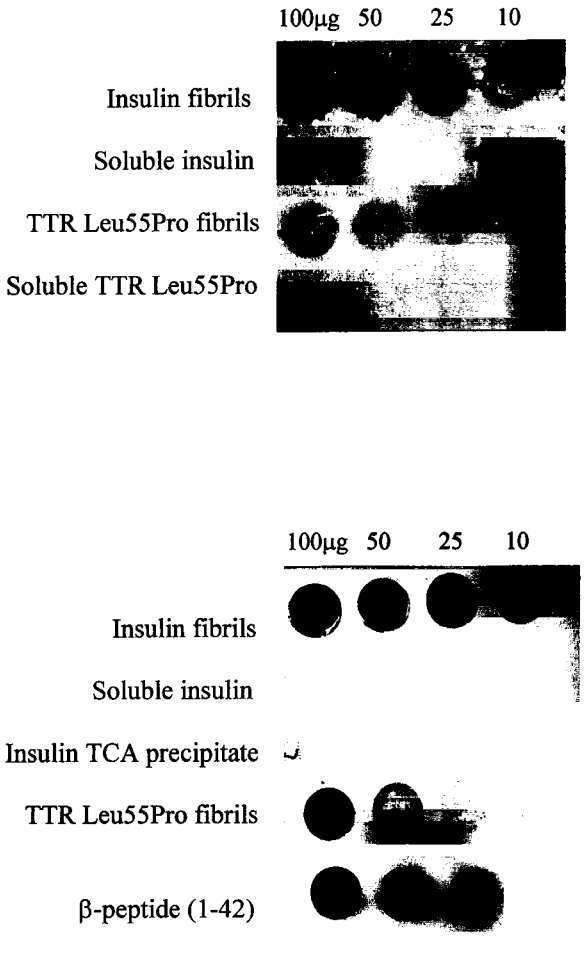

Figure 5- Dot blot binding assay using APR2.
(A)- Dot blot using ^{125}I-APR2. **(B)** Dot blot using biotinylated APR2. Specific binding of APR2 to insulin, TTR Leu55Pro and Aβ fibrils was observed; No binding was detected to soluble insulin, TTR Leu55Pro and insulin TCA precipitates.

Discussion

The process by which certain soluble proteins aggregate to form amyloid fibrilar structures is at present the subject of intense research. Amyloid fibrils can be produced *in vitro* from different protein precursors indicating that they have an intrinsic amyloidogenic potential. *Ex vivo* amyloid fibrils have other proteins associated, such as particular basement membrane components. These common components might recognize structural features shared by different amyloid proteins. In this context, molecular studies on the interaction of amyloid fibrils with different ligands are important to reveal commonalities among amyloid structures and subunit assembly pathways.

Here we reported aprotinin binding to insulin, TTR, Aβ(1-42) and immunoglobulin synthetic fibrils and investigated biochemical and structural features of the aprotinin-amyloid interaction. Due to its size and availability for clinical use, aprotinin constitutes an ideal tracer for amyloid imaging purposes. Our results showed that aprotinin is very specific for the four types of amyloid fibrils tested since no interaction with soluble or TCA precipitates of amyloid precursor proteins were observed.

Aprotinin interacted more strongly with amyloid fibrils formed from insulin than from TTR (data not shown). The same trend is observed for the relative interaction between Thioflavin T and insulin and TTR fibrils (LeVine, 1995). This may be the result of structural differences in fibrils from different precursors, most likely a different accessibility of the structures recognized by aprotinin and thioflavin or small differences in the aminoacid sequence present in the binding region of the amyloid proteins. Alternatively, it may be the result of different ratios fibrils/amorphous precipitates present in the sample. In fact, it is known that the efficiency of fibril formation *in vitro* is much higher for insulin (with almost 100% yield) than for TTR, making insulin fibrils an optimal tool to test amyloid binding reagents.

The specific binding to amyloid deposits displayed by aprotinin has been previously observed for certain organic dyes such as Thioflavin and Congo red. These compounds are proposed to interact with the β-sheet structure characteristic of amyloid. However, Thioflavin T and Congo red did not compete with aprotinin for binding to amyloid fibrils. This suggests that the interactions amyloid-aprotinin and amyloid-organic dyes are essentially different in nature.

Soybean trypsin inhibitor (STI) is, like aprotinin, a proteinaceous inhibitor of serine proteinases. Both inhibitors display canonical proteinase-binding loops, and they do inhibit similar proteinases. Competition binding assays with STI and aprotinin revealed no competition for binding to amyloid fibrils. This rules out the possibility that the rather strong binding of aprotinin to amyloid deposits occurs through the proteinase binding loop of the inhibitor and/or is an interaction of the proteinase: inhibitor type.

As aprotinin has a strong basic character (pI=9.1), while TTR, insulin, Aβ-peptide and immunoglobulins (and presumably also their fibrils) are acidic, the interaction we observed could be simply electrostatic. To rule out this possibility, the interaction of several proteins, both basic and acidic, with amyloid fibrils was tested. We observed that the aprotinin mutant Lys15Val, Arg17Leu, Met52Glu displays a lower affinity towards amyloid fibrils than the wild-type molecule. Since this mutant is a proteinase inhibitor as active as the wild-type molecule, albeit of a different specificity, we assume that its three-dimensional structure is unchanged. However, as a result of the triple mutation the electrostatic potential at the surface of the protein is certainly altered, resulting in a less basic molecule (pI=8.2). Other basic proteins were tested for fibrils binding, with varying results. STI (pI=4.7) did not bind at all, while PSP-II (pI=8.9; IC_{50}=690nM), hen egg while lysozyme (pI=9.2; IC_{50}=2580.5nM), horse heart cytochrome C (pI=10.4; IC_{50}=905.7nM) and bovine histone (pI=11-12; IC_{50}=601.8nM) did. It must be noted that all the basic proteins tested bound amyloid fibrils with different affinities that do not correlate directly with their basicity. Thus, PSP-II, the most acidic protein in the experiment, binds more strongly than the hen egg white lysozyme and horse heart cytochrome C; on the other hand, the highly basic bovine histones are only slighter better amyloid fibrils ligands than PSP-II, despite having a 2 to 3 full units higher pI. In our opinion, this completely rules out the hypothesis of pure electrostatic binding in the amyloid-aprotinin complex, suggesting other type of forces involved in the interaction.

In aprotinin, a central anti-parallel two-stranded β-sheet and a C-terminal α-helix form the core of the molecule to which the proteinase-binding loop is attached. The central β-sheet constitutes the most prominent secondary structure element of aprotinin (figure 3). Upon reduction and modification of the three disulfide bonds of aprotinin with 4-vinylpyridine the inhibitor fails to bind to amyloid deposits. This is mostly likely due to the alteration of the three-dimensional structure of aprotinin induced by reduction and S-pyridylethylation.

Analysis of X-ray diffraction patterns from amyloid fibrils reveals a cross-β conformation and it has been suggested that interactions between β-sheets of adjacent molecules are involved in amyloid formation (Blake and Serpell, 1996; Sebastião *et al.*, 1998; Inoue *et al.*, 1998; Lansbury *et al.*, 1995) (see figure 3). Based on the above observations, we propose a similar mechanism for the interaction of aprotinin with amyloid fibrils, through pairing of β-sheets of the ligands with exposed structures of the same type at the surface of amyloid deposits. This is supported by the fact that the proteins found to bind more efficiently to amyloid fibrils (aprotinin and PSP-II) are those that possess secondary β-structure, while in egg hen white lysozyme, horse heart cytochrome C and bovine histones are completely devoid of these.

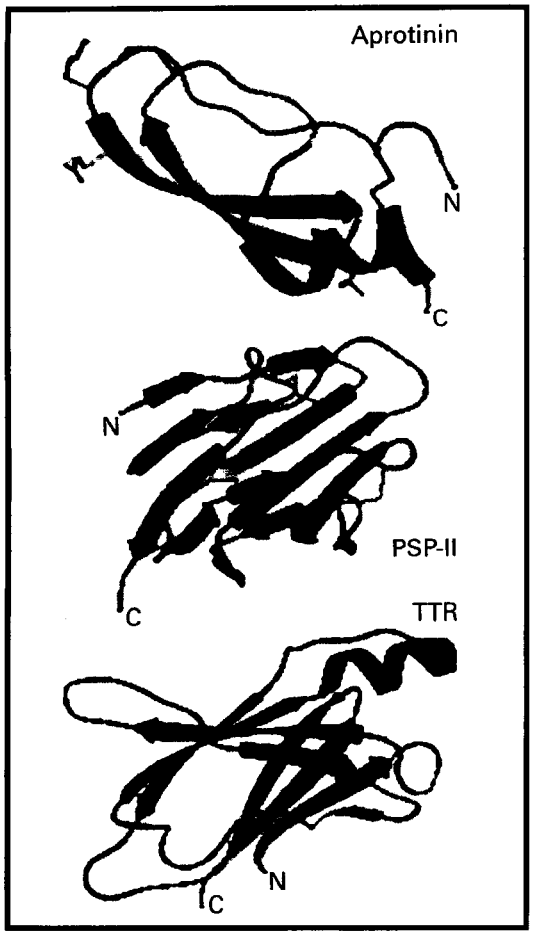

Figure 3- Schematic representation of the three-dimensional structure of aprotinin (PBD entry 5PT1), porcine spermadhesin II (PSP-II; PDB entry 1SPP), and transthyretin (TTR; PDB entry 2PAB). The secondary structure elements are shown. The location of the aprotinin residues mutated in the variant used is also indicated. Figure produced with SETOR (Evans, 1993).

The aprotinin peptides tested were also shown to bind amyloid fibrils derived from insulin, TTR Leu55Pro and β-peptide. The peptides bound insulin fibrils with similar strengths and

with the same magnitude as aprotinin. Although we cannot predict the structure of these peptides, we have calculated the theoretical pI (http://us.expasy.org/tools/pi_tool.html) resulting in 9.31 for APR1 and 9.99 for APR2. Therefore, the electrostatic effect is still present and probably partially responsible for the binding to amyloid fibrils.

In summary, binding of aprotinin and related structures to amyloid is proposed to have two major components, namely interactions between β-structure elements of both fibrils and ligands and an electrostatic effect. The first component is suggested by the observed impairment of aprotinin binding upon disruption of its three-dimensional structure and by the significantly weaker binding of exclusively α-helical proteins. Important differences in binding constants when substitutions Lys15Val, Arg17Leu, Met52Glu are introduced in aprotinin, a general binding observed for basic proteins, and the inability of β-sheet containing acidic proteins (e.g. STI) to bind amyloid fibrils, are in favor of an electrostatic component in the mechanism of binding. Molecular modeling and crystallographic studies, together with site-directed mutagenesis of amyloidogenic proteins are underway in order to fully characterize the interaction of this proteinase inhibitor with amyloid fibrils.

Acknowledgments

We thank Paul Moreira for excellent technical assistance in the preparation of recombinant TTR Val30Met. Aprotinin variant Lys15Val, Arg17Leu, Met52Glu was a generous gift of Dr. Ennes Auerswald (LMU, Munich, Germany), PSP-II and BJPs were kindly provided by Dr. Juan J. Calvete (Instituto de Biomedicina, C.S.I.C., Valencia, Spain) and Dr. Reinhold P. Linke (Max-Planck-Institut für Biochemie, Martinsried, Germany), respectively. This work was supported in part by a grant (SAU/1290/95) and PhD scholarships (BD/15725/98 to I. C. and BD/9782/96 to P. J. B. P.) from Fundação para a Ciência e a Tecnologia, Portugal. P. J. B. P. is a Programa Gulbenkian de Doutoramento em Biologia e Medicina fellow.

Chapter II

Transthyretin fibrillogenesis entails the assembly of monomers: a molecular model for *in vitro* assembled transthyretin amyloid-like fibrils

Transthyretin fibrillogenesis entails the assembly of monomers: A molecular model for *in vitro* assembled transthyretin amyloid-like fibrils

Cardoso, I.[1, 2], Goldsbury, C., S.[3], Müller, S. A.[3], Olivieri, V.[3], Wirtz, S.[3], Damas, A. M.[2, 4], Aebi, U.[3], and Saraiva M. J.[1, 2]

[1] Amyloid and [4] Molecular Structure Units, Institute for Molecular and Cell Biology, [2] Institute for Biomedical Sciences of Abel Salazar, Porto University, Porto, Portugal and [3] M. E. Mueller Institute for Structural Biology, Biozentrum, University of Basel, Switzerland

Running title: Dynamics of transthyretin fibril assembly

Correspondence to: M. J. Saraiva, Amyloid Unit, IBMC, Rua do Campo Alegre, 823, P-4150-180 Porto, Portugal. Fax: +351 22 609 9157, Tel.: +351 22 607 4900, E-mail: mjsaraiv@ibmc.up.pt

Abstract

Extracellular accumulation of transthyretin (TTR) variants in the form of fibrillar amyloid deposits is the pathological hallmark of Familial Amyloidotic Polyneuropathy (FAP). The TTR Leu55Pro variant occurs in the most aggressive forms of this disease. Inhibition of TTR wild-type (WT) and particularly TTR Leu55Pro fibril formation is of interest as a potential therapeutic strategy and requires a thorough understanding of the fibril assembly mechanism. To this end, we report on the *in vitro* assembly properties as observed by transmission electron microscopy (TEM), atomic force microscopy (AFM) and quantitative scanning transmission electron microscopy (STEM) for both TTR WT fibrils produced by acidification, and TTR Leu55Pro fibrils assembled at physiological pH. The morphological features and dimensions of TTR WT and TTR Leu55Pro fibrils were similar, with up to 300 nm long, 8 nm wide fibrils being the most prominent species in both cases. Other species were also evident; 4 – 5 nm wide fibrils, 9 - 10 nm wide fibrils and oligomers of various sizes. STEM mass-per-length (MPL) measurements revealed discrete fibril types with masses of 9.5 and 14.0 ± 1.4 kDa/nm for TTR WT fibrils and 13.7, 18.5 and 23.2 ± 1.5 kDa/nm for TTR Leu55Pro fibrils. These MPL values are consistent with a model in which fibrillar TTR structures are composed of 2, 3, 4 or 5 elementary protofilaments, with each protofilament being a vertical stack of structurally modified TTR monomers assembled with the 2.9 nm axial monomer-monomer spacing indicated by X-ray fibre diffraction data. *Ex vivo* TTR amyloid fibrils were also examined. From their morphological appearance compared to these, the *in vitro* assembled TTR WT and Leu55Pro fibrils examined may represent immature fibrillar species. The *in vitro* system operating at physiological pH for TTR Leu55Pro and the model presented for the molecular arrangement of TTR monomers within fibrils may, therefore, describe early fibril assembly events *in vivo*.

Keywords: AFM, atomic force microscopy/ amyloid fibrils/ TEM, transmission electron microscopy/ TTR, transthyretin/ STEM, scanning transmission electron microscopy

Introduction

Familial amyloidotic polyneuropathy (FAP) is an autosomal dominant disorder characterised by the extracellular deposition of fibrillar protein (amyloid) with special involvement of the peripheral nerve. The major protein component of the amyloid deposits in FAP is a transthyretin (TTR) variant. To date, about 80 different TTR mutations related to amyloid deposition, and 10 non-pathogenic mutations have been described (Saraiva, 2001). TTR is a 55-kDa tetrameric serum protein involved in the transport of thyroid hormones and vitamin A. Each 14-kDa monomer within the functional tetramer contains a small helical segment and two beta-sheets composed of the strands DAGH and CBEF (Blake *et al.*, 1978). The most pathogenic FAP variant known, Leu55Pro, causes a very aggressive form of the disease (Jacobson *et al.*, 1992). Biochemical studies indicate lower tetramer stability for this variant compared to the wild-type (WT), as measured by a lower activation barrier for tetramer dissociation (Lashuel *et al.*, 1998). The recent finding that TTR Leu55Pro crystallises with different packing contacts compared to TTR WT is in agreement with this observation; while the unit cell of TTR WT crystals contains a single TTR dimer (Blake *et al.*, 1978), the unit cell of TTR Leu55Pro crystals contains eight monomers (Sebastião *et al.*, 1998). The dissociation of tetramers into monomers is thought to mediate TTR fibril formation (Lashuel *et al.*, 1998). Indeed, the fact that TTR Leu55Pro crystals are able to bind thioflavin-T, an amyloid binding dye, suggests that they may already have fibril-like properties (Sebastião *et al.*, 2000). The leucine substitution at residue 55 disrupts the hydrogen bonds between beta-sheet strands D and A, exposing new surfaces which are involved in aggregation. The consequent ready formation of fibrils by TTR Leu55Pro *in vitro* under physiological conditions makes this variant an important tool in the study of amyloidogenesis and fibril structure.

As revealed by electron microscopy, amyloid deposits generally consist of straight or coiled fibrils, 7.5 to 10 nm in width and up to several microns in length. The morphology of *ex vivo* TTR fibrils appears to depend on the tissue localization as well as to some degree on the extraction technique employed and the presence of other non-TTR components. The deposits are characterised by certain tinctorial properties such as a green birefringence under polarised light after staining with Congo red, and by a "cross-beta" X-ray fibre diffraction pattern (Eanes and Glenner, 1968). Although the cross-beta model has long been accepted as the consensus structure for all forms of amyloid, the details of the molecular subunit

packing for each respective form are still not fully understood. Early electron microscopy investigations of isolated amyloid revealed the existence of a hierarchical assembly system (Shirahama and Cohen, 1967). Accordingly, elementary sub-fibres associate to form higher order fibrils. These sub-fibres and fibrils have been given a variety of names in the literature: "filament", "fibril", "sub-protofibril", "protofibril", "protofilament". For simplicity, we reduce to two terms and herein define the smallest sub-fibres of TTR "fibrils" as "elementary protofilaments". In combination with Eanes and Glenner's cross-beta structural model, this concept of an amyloid protofilament first proposed by Shirahama and Cohen, has led to recent attempts at molecular modelling of amyloid fibrils (Blake and Serpell, 1996; Lazo and Downing, 1998; Chaney *et al.*, 1998; Malinchik *et al.*, 1998; Inouye *et al.*, 1998).

There are conflicting molecular definitions of the elementary protofilament in the TTR literature. X-ray fibre diffraction studies of vitreous FAP TTR (Val30Met variant) amyloid fibrils using synchrotron radiation, have lead to two interpretations of the structure both consistent with the cross-beta model. According to Blake and Serpell (Blake and Serpell, 1996) the protofilament core is a continuous beta-sheet helix composed of four parallel, twisted beta-sheets resulting in an elemantary protofilament 5 to 6 nm wide with a helical repeat of 11.5 nm. Considerable structural reorganization of the TTR molecule from its native tetrameric state must occur to form this protofilament "building block" that is not only either monomeric or dimeric but also has an altered beta-sheet structure. Four of the elementary protofilaments are considered to associate around a central hollow core to form the four-fold symmetric fibrils observed by electron microscopy (Serpell *et al.*, 1995). An alternative interpretation of the same data has been proposed by Inouye *et al.* (1998). In this model, each TTR protofilament is composed of a single chain of axially aligned TTR monomers. Although there are also four protofilaments in the mature TTR fibril in this scenario each protofilament contains just two twisted beta-sheets. Other models suggest the formation of TTR amyloid fibrils from different building blocks: The beta-slip concept proposes a tetrameric subunit that is distorted but intact (Eneqvist *et al.*, 2000) and Serag *et al.* (2001) suggest that TTR amyloid fibrils assemble from dimeric subunits or a multiple of such, rather than from rearranged monomers. These models are conflicting. The precise nature of the building block (tetrameric, dimeric or monomeric) and its arrangement within the architecture of the fibril remain to be defined.

The mechanism that leads to TTR amyloid fibril formation is also poorly understood. In

most cases the assembly process has been studied under acidic rather than physiological conditions. Kelly and co-workers have suggested that *in vivo* fibril formation takes place at a low pH like that found in the lysosome (McCutchen *et al.*, 1993). They report that *in vitro* the variant Leu55Pro forms "protofilaments" at physiological pH but not mature fibrils (Lashuel *et al.*, 1999) and consider the TTR WT fibrils produced by acidification to be mature. Thus, the universal definition of the elementary TTR protofilament and how it relates to mature fibrils remains unclear. We seek to clarify these issues and present an ultrastructural characterization of *in vitro* assembled TTR WT and TTR Leu55Pro fibrils.

In the detailed electron microscopy study outlined in this report, including mass-per-length (MPL) measurements of *in vitro* assembled TTR fibrils, we clearly show these to be polymorphic, and propose that they are composed of 2, 3, 4 and 5 elementary protofilaments. Furthermore, consistent with our data and that of others (Inouye *et al.*, 1998; Quintas *et al.*, 2001) we propose that each protofilament contains two twisted beta-sheets and is a single vertical stack of structurally modified TTR monomers.

Materials and Methods

Isolation and purification of TTR

TTR WT and mutant TTR Leu55Pro proteins were produced in an *E. coli* expression system (Furuya *et al.*, 1991), isolated and purified as previously described (Almeida *et al.*, 1997). Briefly, after growing the bacteria, the protein was isolated and purified by preparative gel electrophoresis after ion exchange chromatography. Protein concentration was determined using the Lowry method (Lowry *et al.*, 1951).

Preparation of amyloid fibrils

To initiate amyloid fibril formation, TTR WT (2 mg/ml) was incubated in 0.05 M sodium acetate pH 3.6, for 72 hours at room temperature (Colon and Kelly, 1992). The sample was then centrifuged at 15,000 g for 30 minutes at 4°C and the pellet obtained was washed and re-suspended in MilliQ water and incubated at 37°C.

TTR Leu55Pro was dialysed against water pH ~ 7.0 and concentrated to 5 mg/ml. At this point the preparation was centrifuged at 15,000 g for 30 minutes at 4°C. The pellet was then washed and re-suspended in phosphate buffer pH 7.4 (PBS) at 2 mg/ml and incubated at 37°C.

At given time points, the samples were visualised for the presence of amyloid fibrils by TEM and/or AFM. The fibril concentrations were assessed by the Lowry method (Lowry *et al.*, 1951).

Native TTR amyloid vitreous fibrils were obtained from a FAP patient expressing the TTR Val30Met mutant, who had been subjected to vitreoctomy. The sample was negatively stained for TEM observation.

A peripheral nerve biopsy obtained from a FAP TTR Val30Met patient was fixed in 2.5% glutaraldehyde for 3 hours at room temperature, rinsed in PBS and postfixed with 1% osmium tetroxide for 1.5 hours at 4 °C. The specimen was then cut into 3-mm^3 fragments, which were subsequently dehydrated in a graded series of ethanol/water mixtures (70% to 100 % ethanol) and embedded in Epon. Polymerisation was carried out at 50°C overnight.

Transmission electron microscopy (TEM)

For visualization by TEM aliquots of the recombinant protein samples were diluted (1:50) with water (TTR WT) or PBS buffer (TTR Leu55Pro) and immediately adsorbed to glow-

discharged carbon-coated collodion film supported on 200-mesh copper grids. The vitreous sample was used without dilution. For negative staining, the grids were then washed with deionised water and stained with 0.75% uranyl formate. For metal shadowing, freeze-dried specimens were first uni-directionally shadowed with tungsten at an elevation angle of 25° and then uniformly coated with a thin layer of carbon evaporated from above using a Balzers machine (BAF 301). In both cases the grids were visualised at a defined orientation relative to the electron beam in order to determine the direction of fibril coiling. A Hitachi 7000, 100kV was employed. Measurements of the fibril widths and lengths were made from enlarged prints of the electron micrographs using a magnifying glass with a built-in calibrated ruler.

Ultra-thin (450 nm) sections of the peripheral nerve fragments were collected on carbon coated nickel grids (Agar) and the indirect immunogold technique was applied. Once on the grids, the Epon sections were exposed to a saturated aqueous solution of sodium metaperiodate for 1 hour. Next, they were floated on the surface of a drop of 1% bovine serum albumin (BSA, Sigma) in PBS followed by diluted (1:50, 1% BSA in PBS) rabbit anti-human transthyretin antibody (Dako) for 1 hour at room temperature. The grids were washed in PBS and exposed to goat anti-rabbit immunoglobulins (1:15, 1% BSA in PBS) that had been coupled to 5-nm gold particles (Amersham). They were washed again in PBS and Tris-HCl buffer, pH 7.6 and counterstained with uranyl acetate for 4 minutes followed by lead citrate for 15 seconds. The grids were examined in a JEOL 100 CX II electron microscope operated at an acceleration voltage of 60 KV.

Atomic force microscopy (AFM)

All AFM images were recorded in liquid. A diluted aliquot (50 µl, 1:500 dilution in water for TTR WT and PBS for TTR Leu55Pro fibrils) of the TTR fibril preparation was adsorbed to a freshly cleaved mica substrate for 15 minutes. The substrate was then rinsed with the sample buffer (but not dried) and transferred to the fluid cell of the AFM (Nanoscope III multimode AFM equipped with a J- or E- scanner, Digital Instruments). Imaging was carried out in water (TTR WT) or PBS buffer (TTR Leu55Pro). Tapping mode images (512 x 512 pixels) were obtained using 100 µm oxide sharpened cantilevers with a nominal spring constant of 0.38 N/m (Digital Instruments). A scan speed of 2 Hz, drive amplitude of 160-200 mV and resonant frequency of 8.7-9.5 Hz were employed. The scan sizes ranged between 0.5µm and 5.0 µm.

Scanning transmission electron microscopy (STEM)

In the dedicated scanning transmission electron microscope a small electron beam is raster scanned over the specimen. The electrons elastically scattered from each point (pixel) of the scan are collected by an annular dark-field detector capable of single electron counting. In a calibrated instrument, knowledge of the incident electron dose and the collection efficiency allows the mass irradiated to be calculated. A Vaccuum Generators HB5 STEM interfaced to a modular computer system (Tietz Video and Image Processing systems) and calibrated to measure the mass of protein samples (Engel, 1978; Müller *et al.*, 1992) was employed in the present experiments. The microscope was operated at an acceleration voltage of 80 kV.

For mass measurement, 7-µl aliquots of the TTR WT and TTR Leu55Pro samples were diluted with water and PBS, respectively, and adsorbed for 1 min to glow discharged, thin (approximately 3 nm) carbon films which spanned a thick fenestrated carbon layer covering 200-mesh/inch, gold plated copper grids. The grids were then blotted, washed with 5 drops of water to remove buffer salts and freeze-dried at -80°C and $5x10^{-8}$ Torr, overnight in the microscope. Isolated tobacco mosaic virus particles (kindly provided by Dr. Ruben Diaz-Avalos, Institute of Molecular Biophysics, Florida State University, USA) adsorbed in the same way to a separate grid, washed on 5 drops of 0.01M ammonium acetate and air-dried, served as an instrument control for each experiment.

Low dose, 512x512 pixel, digital dark-field images were recorded from the unstained samples at a nominal magnification of 200 000x. The images were evaluated using the program package IMPSYS as outlined by Mueller *et al.* (Müller *et al.*, 1992). Accordingly, fibril segments suitable for mass-per-length (MPL) measurement were selected in square boxes, tracked and their length calculated. The total scattering within an integration box matched to their width was then calculated, the background scattering of the carbon support film subtracted and the average MPL determined. The corresponding mass profile was displayed for each fibril stretch and the width at half maximum height of the mass profile (termed the full width half maximum, FWHM) assessed. The accuracy of the FWHM measurement was limited by the pixel size at the magnification used, ~ 0.9 nm.

In addition, beam induced mass-loss was experimentally determined for the TTR Leu55Pro sample by repeatedly scanning the same region and monitoring the change in fibril MPL (Müller *et al.*, 1992). The relationship obtained, $y = 100 - 0.01613\ x$, where y is the residual mass percent and x the incident electron dose in electrons/nm^2, was assumed to hold for all samples. The recording doses were 356 ± 24 electrons/nm^2 and 369 ± 24 electrons/nm^2 for

the two TTR WT samples and 353 ± 32 electrons/nm^2 for the TTR Leu55Pro sample. In each case, making the correction increased the MPL values by almost 6%. The resulting absolute values were displayed in histograms and described by Gauss curves.

Finally an error assessment was made considering both the standard error (SE) of each MPL measurement and the 5% uncertainty in the STEM calibration (CU). The SE was estimated for each peak according to the equation, $SE = SD/(\sqrt{n})$, where n is the number of segments included in the peak and SD is the standard deviation of the results. The SE and CU were combined by calculating the square root of the sum of the squares.

Results

Assembly of TTR WT fibrils

Solutions of recombinant TTR WT were prepared at acidic pH and incubated at 37 °C for 11 weeks. Fibrils readily formed during this time. Their assembly dynamics and structure was studied by withdrawing aliquots of the solution at various stages and examining them by negative stain transmission electron microscopy (TEM) (Figures 1A-C). The protein remained non-fibrillar in control experiments made at physiological pH; even after 4 weeks incubation at 37° only very small recombinant TTR WT oligomers (probably tetramers) were observed on the microscopy grids (Figure 1D).

The fibrillar structures formed at acidic pH were polymorphic (Figures 1A, B and C). Prominent among them were 8 nm wide fibrils, which lengthened with time becoming up to 300 nm long (arrow, Figure 1A; white arrow, Figure 1E). At least three other structures were also present during the first 6 weeks: 9-10 nm wide fibrils (arrowhead, Figure 1B; black arrow, Figure 1E); 4 - 5 nm wide fibrils (arrow, Figure 1B; white arrowhead, Figure 1E); and oligomers with diameters of approximately 5 or 8 nm (arrowheads, Figure 1A, black arrowheads Figure 1E). As shown in Figure 1F, occasionally the lateral association and coiling together of 4 – 5 nm wide fibrils was observed. Freeze-drying followed by unidirectional metal shadowing and TEM (Figure 1G), and atomic force microscopy (AFM) (Figure1H), both revealed small subsets of 8 nm wide fibrils twisted in a left-handed sense with an axial substructure of 17 nm. A longer twist appeared in figure 1F, which probably does not represent an end point of fibril coiling. After approximately 6 weeks incubation, the fibrils started to aggregate by lateral association forming bundles (Figure 1 C). This was frequently accompanied by additional intertwining giving rise to tangles. Fibril bundles had widths of up to 20 nm; length measurements were not possible due to their tangled nature.

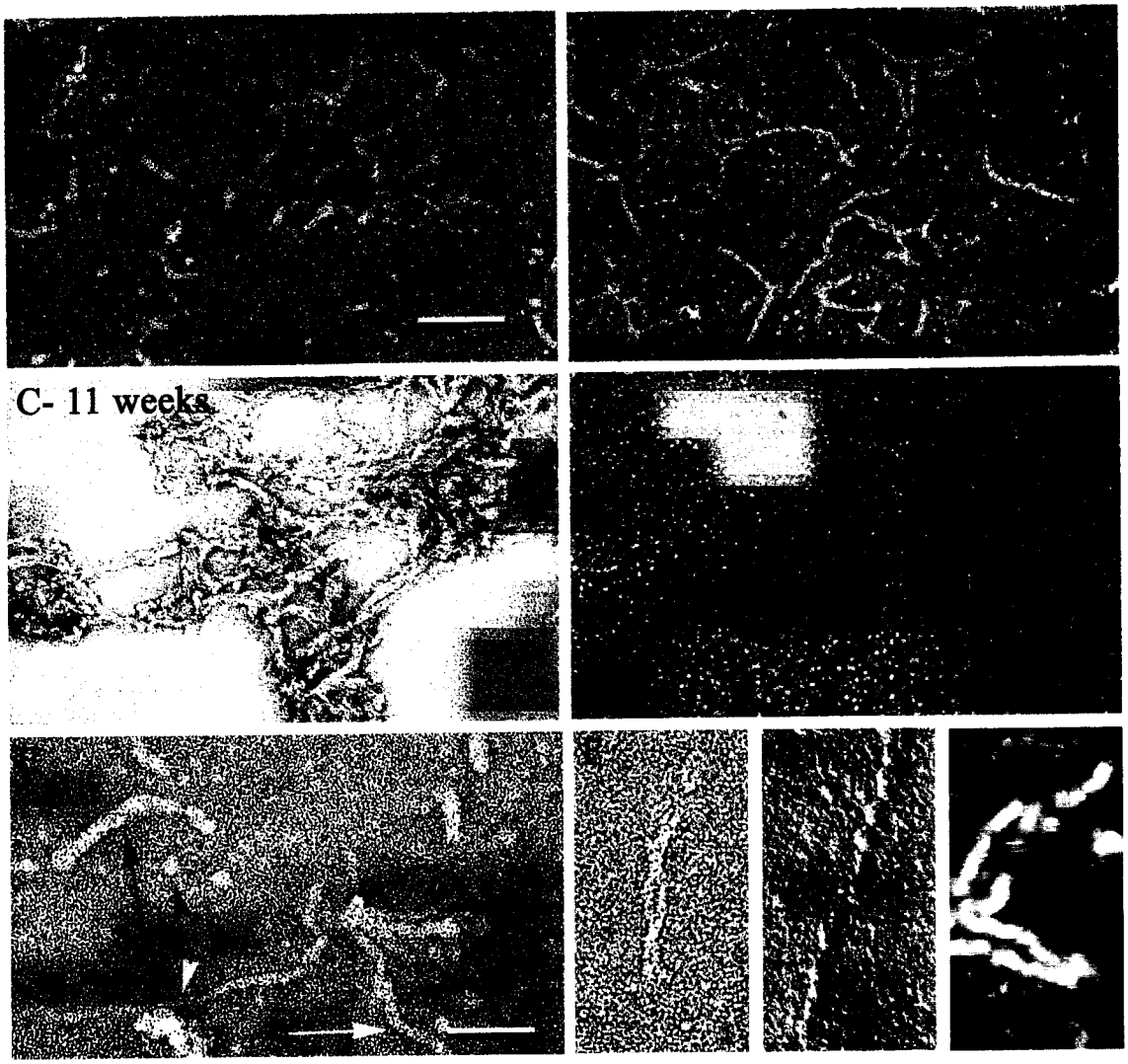

Figure 1- Assembly of TTR WT fibrils produced by acidification.

(A-C) Negative stain TEM images documenting the polymorphism observed over an 11-week period of TTR WT fibril assembly at acidic pH and 37°C: 8 nm wide fibril **(arrow, panel A)**, oligomers approximately 5 or 8 nm wide **(arrowheads, panel A)**, a 4 nm wide fibril **(arrow, panel B)** and a thicker fibril 9 - 10 nm wide **(arrowhead, panel B)**. **(D)** TTR WT after incubation at physiological pH and 37°C for 4 weeks. Scale bar (A-D) = 100 nm. **(E)** Image showing the different species present in the acidified TTR WT fibril sample at higher magnification: Oligomers of different size **(black arrowheads)**, an 8 nm wide fibril **(white arrow)**, a 4 nm wide fibril **(white arrowhead)** and a thicker fibril 9-10 nm wide **(black arrow)**. **(F)** Two 4 - 5 nm wide fibrils present after approximately 7 weeks incubation, associating laterally and coiling together. The end-point of fibril coiling has probably not yet been attained. **(G)** TEM image of a TTR WT fibril formed after 6 weeks incubation, which has been freeze-dried and unidirectional shadowed with tungsten. A 17-nm left-handed axial substructure is clearly visible. **(H)** Tapping mode AFM image of the TTR WT fibrils formed after 6 weeks incubation. The fibrils were adsorbed to a mica surface and imaged in water. Again a 17-nm left-handed axial substructure is clearly visible. Scale bar (E- H) = 50 nm.

Assembly of TTR Leu55Pro fibrils

An analogous morphological study was carried out at physiological pH for the TTR Leu55Pro variant. Figure 2 is representative of the assembly progression occurring over 11-weeks. The morphological development was similar to that followed by the TTR WT preparation on acidification, starting with abundant short fibrils and oligomers (Figure 2A and B) and evolving to longer fibrils (Figure 2C, D and E). Although there was substantially more tangling, after 11 weeks incubation the assembly of new fibrils appeared to have reached a steady state (compare Figures 2D, E and F). Eight nanometer wide fibrils were again the most prominent species throughout (Figure 2B and C, arrow). Interestingly, at equivalent time points the relative abundance of the various fibril species was different in the TTR Leu55Pro and TTR WT preparations. In particular, 4 - 5 nm wide fibrils were rarely detected on the TTR Leu55Pro grids. Furthermore, after extended incubation periods the TTR Leu55Pro fibrils produced at physiological pH (Figure 2F) appeared to undergo a lower degree of bundling than the TTR WT fibrils formed by acidification (Figure 1C).

As revealed by unidirectional metal shadowing (Figures 2G and H, arrow), like TTR WT fibrils TTR Leu55Pro fibrils also occasionally exhibited a 17 nm axial sub-structure with a left-handed twist. TTR Leu55Pro fibrils adsorbed to mica and imaged in buffer solution by AFM had similar lengths to those imaged by TEM, but were slightly wider (Figure 2 I). This apparent width difference may be explained by the dependence of the width measured by AFM on the size and shape of the scanning tip used for imaging, which in this case did not allow the visualization of any axial substructure.

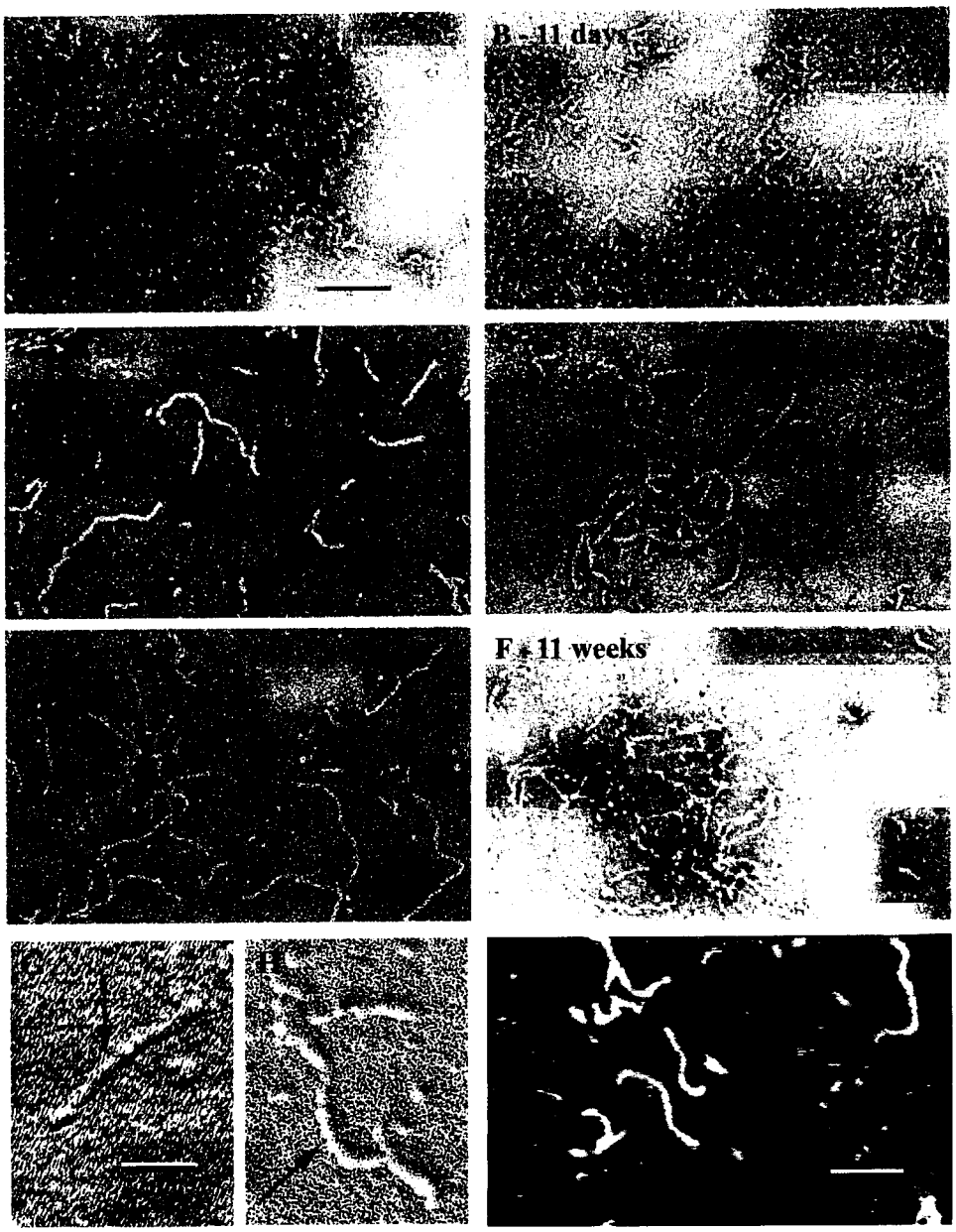

Figure 2- Assembly of TTR Leu55Pro fibrils produced at physiological pH.

(A – F) Negative stain TEM images documenting the polymorphism observed over an 11-week period of TTR Leu55Pro fibril assembly at physiological pH and 37°C: 8 nm wide fibril **(arrow, panels B and C)**, oligomers approximately 5 or 8 nm wide **(panel B)**, a 4 nm wide fibril **(arrowhead, panel B)**. Scale bar (A- F) = 100 nm. **(G, H)** TEM image of a TTR Leu55Pro preparation after freeze-drying and unidirectional metal (tungsten) shadowing. A left-handed substructure can be distinguished on some fibrils **(arrow)**. Scale bar (G, H) = 50 nm. **(I)** Tapping mode AFM image of TTR Leu55Pro fibrils after 6 weeks incubation. The fibrils were adsorbed to a mica surface and imaged in PBS buffer. No substructure was resolved. Scale bar (I) = 100 nm.

Dynamics of transthyretin fibril assembly

A more detailed analysis of the *in vitro* fibril growth rate was made since TTR Leu55Pro is of particular interest, occurring in the most aggressive forms of FAP, and it is possible to follow the assembly at physiological pH. The frequency distribution of TTR Leu55Pro fibril length is shown in Figure 3. The measurements were made at the time points examined by TEM in Figure 2A-E; 100 fibrils were measured in each case. The average fibril length versus incubation time is plotted in Figure 3F. This graph illustrates that TTR Leu55Pro fibril growth was sigmoidal in character and that the fastest rate of fibril growth occurred between 11 and 18 days corresponding to an elongation rate of 9.2 nm/day. Unfortunately the need for acidification prohibited the same experiment for TTR WT.

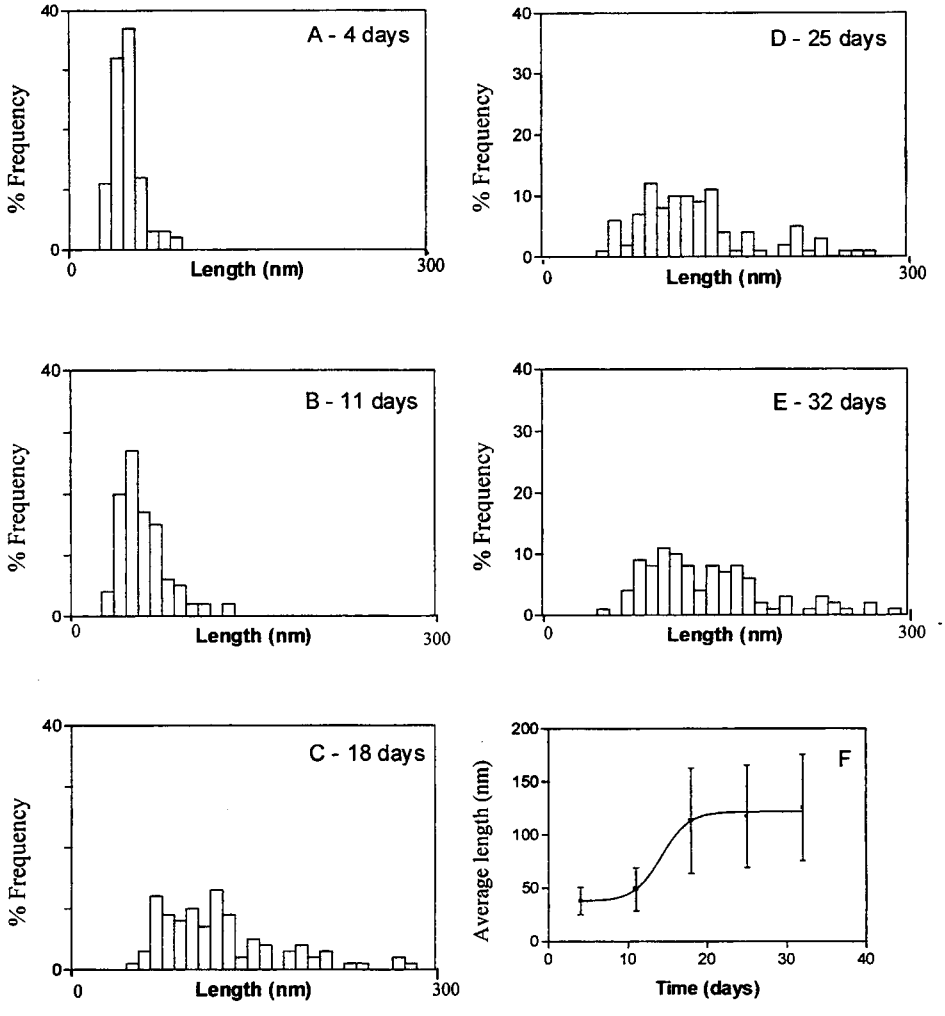

Figure 3- Fibril elongation.

Frequency distribution of fibril length **(graphs A-E)** and growth rate **(F)** of TTR Leu55Pro fibrils followed over a 32-day period. The fastest rate occurred between days 11 and 18 corresponding to an elongation of 9.2 nm/day.

Mass-per-length analysis

To estimate the arrangement of TTR molecules within the fibrils, their mass-per-length (MPL) was measured by quantitative scanning transmission electron microscopy (STEM). For this purpose, TTR WT fibrils formed under acidic conditions and TTR Leu55Pro fibrils formed under physiological conditions, were incubated for approximately 6 weeks at 37°C, adsorbed to thin carbon films, freeze-dried and imaged. As in negative stain TEM, tangling of the assembled fibrils to form clusters was frequently observed on the STEM images of both variants. The resulting overcrowding meant that these regions, which usually included fibrils of various widths (Figure 4A, bottom left), could not be employed for MPL measurement. Accordingly, for each variant over 300 fibril segments of various lengths were selected on well-separated individual fibrils or where these extended from tangles, and analysed. After correction for beam induced mass-loss (see Materials and Methods), corresponding data sets were pooled, displayed in histograms and fitted with Gauss curves.

Typical images of the freeze-dried, unstained TTR WT fibrils analysed are shown in Figure 4A. Comparison of their MPLs (indicated for the regions marked by square boxes; units, kDa/nm) documents the sample heterogeneity. This heterogeneity was quantitatively assessed by pooling the MPL data from 358 TTR WT segments (Figure 4B). The peaks at 9.5 and 14.0 ± 1.4 kDa/nm (number of segments, n ~ 195 and 125, respectively; Figure 4B) indicate the presence of two major fibril types. In addition, there are two very minor fibril populations with average MPLs of 19.9 ± 1.4 kDa/nm (n = 23) and 25.8 ± 1.3 kDa/nm (n = 11). As detailed in Table 1A the overall uncertainty in the major peak positions was < 1 kDa/nm. An estimate of the fibril widths was obtained from the corresponding mass profiles. The full-width-half-maximum (FWHM; see Materials and Methods) values documented the absence of the 4 - 5 nm wide fibrils detected by negative stain TEM at earlier time points (data not shown). Interestingly, fibrils giving rise to the 9.5 and 14.0 kDa/nm peaks had very similar FWHM values (~7 nm). As the FWHM is an underestimate of the actual width, these fibrils probably correspond to the 8 nm wide fibrils that predominated at most of the time points examined by TEM.

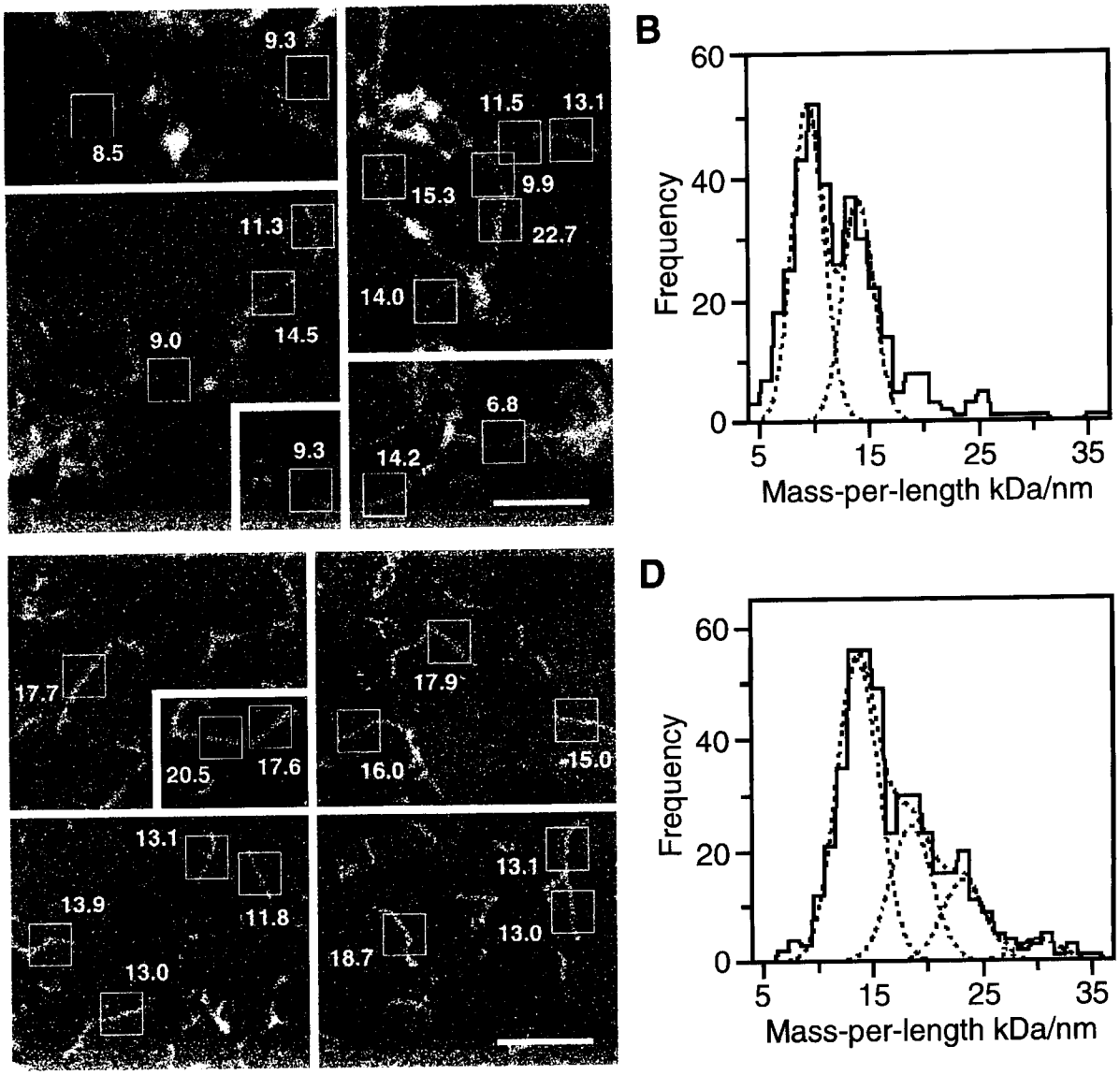

Figure 4- MPL analysis of TTR WT and TTR Leu55Pro fibrils after approximately 6 weeks incubation at 37°C.

STEM dark-field images of unstained TTR WT fibrils produced by acidification **(A)** and TTR Leu55Pro fibrils formed at physiological pH **(C)**. The absolute MPLs of the segments are cited in white (units: kDa/nm). Scale bar = 100 nm.

Histogram for the TTR WT samples **(B)** displaying the absolute MPL values of 358 fibril segments with an average length of 35.1 ± 7.7 nm and for the TTR Leu55Pro samples **(D)** displaying the absolute MPL values of 441 fibril segments with an average length of 30.03 ± 9.54 nm.

Representative images recorded from freeze-dried, unstained Leu55Pro fibril samples are shown in Figure 4C. Again, comparison of the MPL values (evaluated for the regions marked by square boxes; units, kDa/nm) documents considerable sample heterogeneity, which was in this case quantitatively assessed by pooling the MPL data from 441 fibril segments (Figure 4D). As shown in Figure 4D, three major species were present in the TTR Leu55Pro samples. These had MPLs of 13.7, 18.5 and 23.2 ± 1.9 kDa/nm (n ~ 250, 105 and 65, respectively). The few remaining segments had MPLs in the range of 30.1 ± 1.9 kDa/nm (n ~ 19). The MPL peak at 9.5 kDa/nm found for the TTR WT fibrils was not present on the TTR Leu55Pro histogram instead there were two additional, well defined peaks at higher mass, implying that this variant forms a larger percentage of higher-order structures than TTR WT after 6 weeks of incubation. The overall uncertainty in the peak positions is detailed in Table 1B and was < 1 kDa/nm for the two lowest peaks. The fibrils giving rise to the peaks at 13.7 and 18.5 kDa/nm had very similar FWHMs (6 to 7 nm in both cases) while the FWHM of those with a MPL of 23.2 kDa/nm was somewhat larger (8 to 9 nm). Again, as documented by the FWHM values, 4 - 5 nm wide fibrils were absent from these samples.

Table 1 Error assessment for the MPL measurements

A. TTR WT

Peak	Standard deviation	approx. n	Standard error	5% Calibration uncertainty	Overall uncertainty
9.5	1.4	195	0.1	0.5	0.5
14.0	1.4	125	0.1	0.7	0.7
19.9	1.4	23	0.3	1.0	1.0
25.8	1.3	11	0.4	1.3	1.4

The smallest segment evaluated was only 14.9 nm long while the longest segment evaluated was 46.9 nm long; their mass-per-length values were weighted equally in the histograms.

B. TTR Leu55Pro

Peak	Standard deviation	approx. n	Standard error	5% Calibration uncertainty	Overall uncertainty
13.7	1.9	250	0.1	0.7	0.7
18.5	1.9	105	0.2	0.9	0.9
23.6	1.9	65	0.2	1.2	1.2
30.1	1.9	19	0.4	1.5	1.6

The three smallest segments evaluated were only 8.1±0.1nm long while the two longest segments evaluated were 46.9±0.4nm long; their mass-per-length values were weighted equally in the histograms.

The STEM data confirm and quantitatively characterize the fibril polymorphism observed by TEM and AFM. Within experimental uncertainties, the increment between the MPL peaks is the same for both isoforms (4.5 - 4.8 kDa/nm; average value, 4.7 ± 0.1 kDa/nm).

FAP *ex vivo* fibrils - a comparison

The data presented so far refers exclusively to *in vitro* TTR fibril assembly from recombinant TTR. For a structural comparison, we also analysed TTR Val30Met *ex vivo* fibrils from two different sources, the vitreous of the eye and the peripheral nerve. Negative staining of the vitreous *ex vivo* preparation is presented in Figures 5A and 5B. The fibrils were several microns long, 15 - 20 nm wide (Figure 5A) and exhibited longitudinal stripes implying the presence of multiple strands; in support of the latter, a few fibril fragments appeared to be a bundle of 8 nm wide strands associated laterally (Figure 5B, arrow). A transverse banding pattern that had an approximate repeat of 20-25 nm, but was not always periodically spaced along the fibril axis, was also distinguishable (Figure 5A). These features are identical to those reported for TTR fibrils isolated from the vitreous and analysed by image reconstruction from electron micrographs by Serpell *et al.* (Serpell *et al.*, 1995).

Finally, we examined *in situ* TTR Val30Met amyloid deposits found in a biopsy of the peripheral nerve of a FAP patient. Figure 5C shows the result of ultrastructural immunogold labelling for TTR. Interestingly, these fibrils, seen in cross section, were much narrower (7-10 nm wide) than the fibrils extracted from the vitreous (15-20 nm wide) even though the same mutant was present. This suggests that polymorphism of TTR fibrillar assemblies also occurs *in vivo*.

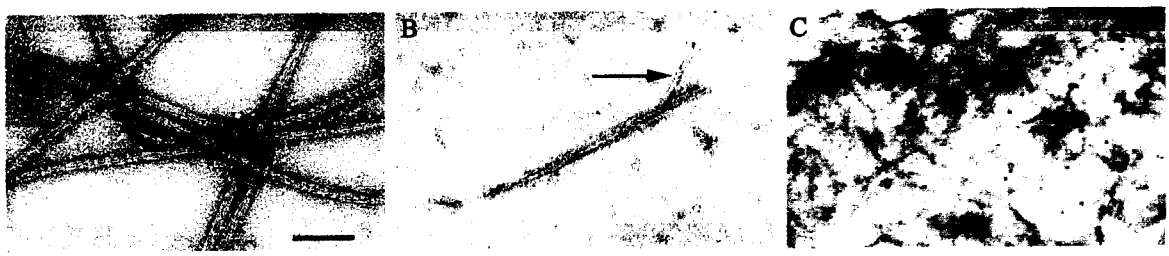

Figure 5- TTR *ex-vivo* fibrils analysed by TEM.

(A and B) TEM images of a negatively stained *ex vivo* vitreous sample, that was obtained from a FAP TTR Val30Met patient. The fibrils were several microns long and exhibited longitudinal striations implying the presence of multiple strands **(panel A)**. A transverse banding with an approximate repeat of 20-25 nm could also be distinguished. However, this was not always periodically spaced along the fibril axis. A fragmented fibril suggests the presence of a bundle of laterally associated 8 nm wide strands **(arrow, panel B)**. **(C)** Cross-section of a peripheral nerve biopsy from a FAP TTR Val30Met patient after labelling with anti-TTR. The fibrils are much narrower (7 - 10 nm wide) than those extracted from the vitreous of the eye **(panels A and B)** even though the same mutant was analysed. Scale bar for (A-C) = 100 nm.

Discussion

Mutations in the TTR protein cause FAP, a hereditary amyloidosis disease affecting predominantly and at high frequency, populations in northern Portugal, northern Sweden and Japan. The TTR Leu55Pro variant gives rise to a very aggressive form of FAP disease and the recombinant protein has a correspondingly high fibril forming capacity *in vitro*. Accordingly, strategies to inhibit TTR amyloid fibril formation would be promising as therapeutic interventions. Their development requires an understanding of the mechanism of fibril assembly and the molecular arrangement of the elementary subunits. Since fewer parameters are involved in *in vitro* systems, allowing the conditions to be precisely controlled, we used recombinant TTR, to investigate the assembly of TTR amyloid-like fibrils. Our major goals were to define the elementary protofilament subunits and their arrangement within the fibrils and to compare the *in vitro* assembled structures with *ex vivo* TTR fibrils derived from diseased organs.

In the early stages of polymerisation (Figures 1A and 2A) recombinant TTR WT and TTR Leu55Pro samples contained abundant oligomers 5 or 8 nm in diameter. Fewer oligomers were observed at latter time points, suggesting that they are used up on fibril formation. The assembled TTR fibrils were polymorphic. In TTR WT samples, the most predominant fibrils had widths of 8 nm, lengths of up to 300 nm and sometimes exhibited a 17 nm axial sub-structure. Fibrils with widths of 9 - 10 nm or 4 - 5 nm were also observed. Given their small dimensions, the 4 - 5 nm wide fibrils probably represent single elementary protofilaments. All these species were also present in TTR Leu55Pro samples but both negative stain microscopy and STEM mass measurements indicated that the assembly kinetics were faster for this variant, particularly since the 4 –5 nm wide fibrils were only rarely observed.

Mass measurement by STEM allowed the morphological polymorphism of both variants revealed by TEM and AFM (Figures 1 and 2) to be more precisely characterized. Within experimental uncertainties (Table 1), the increments between the major MPL peaks at 9.5 and 14.0 kDa/nm for TTR WT and at 13.7, 18.5 and 23.2 kDa/nm for TTR Leu55Pro (Figure 4) are identical (4.5 - 4.8 kDa/nm; average value, 4.7 ± 0.1 kDa/nm), suggesting that this reflects the MPL of the elementary protofilament and that the protofilaments of both variants have the same architecture. Given the molecular weight of a TTR monomer (14 kDa), a MPL of 4.8 kDa/nm would be expected for a vertical stack of monomers with the

monomer-monomer spacing of 2.9 nm predicted by X-ray fibre diffraction data (Inouye *et al.*, 1998). Therefore, the MPL increment, 4.7 ± 0.1 kDa/nm, supports the hypothesis that this is the architecture of the elementary protofilament and prompts the assembly model presented in Figure 6A. The 8 nm wide fibril, with a MPL of 9.5 kDa/nm, formed by two protofilaments strands with a left-handed twist has an axial crossover repeat of 17 nm, for both TTR WT and Leu55Pro, as assessed by unidirectional metal shadowing and AFM. Since each TTR monomer is 14 kDa, these results imply that a total of 6 monomers are present per crossover repeat with a twist of 30° between neighbouring monomers (figure 6B).

Here, the monomeric subunits are proposed to have a modified structure similar to that found in the TTR Leu55Pro crystal. Based on this model, in the case of TTR WT the major MPL peaks arise from fibrils containing 2 and 3 elementary protofilaments, and in the case of TTR Leu55Pro 3, 4 and 5 elementary protofilaments, respectively. Further, the two very minor TTR WT populations with higher MPLs represent fibrils containing 4 and 5 elementary protofilaments. All of these higher order fibrils could either form by the lateral association of two or more elementary protofilaments or nucleate and elongate separately but maintain a common protofilament substructure. In either case intertwining of their elementary protofilaments would giving rise to the 17nm axial repeat occasionally observed. It should be noted that none of the MPL data are compatible with an elementary protofilament formed by the stacking of 55-kDa TTR tetramers with dimensions similar to those revealed by X-ray crystallography (Blake *et al.*, 1978)(7.0x5.5x5.0 nm). In this case, higher MPL increments would be expected (minimum value 7.9 kDa/nm, maximum value 11.0 kDa/nm depending on how the tetramers stack).

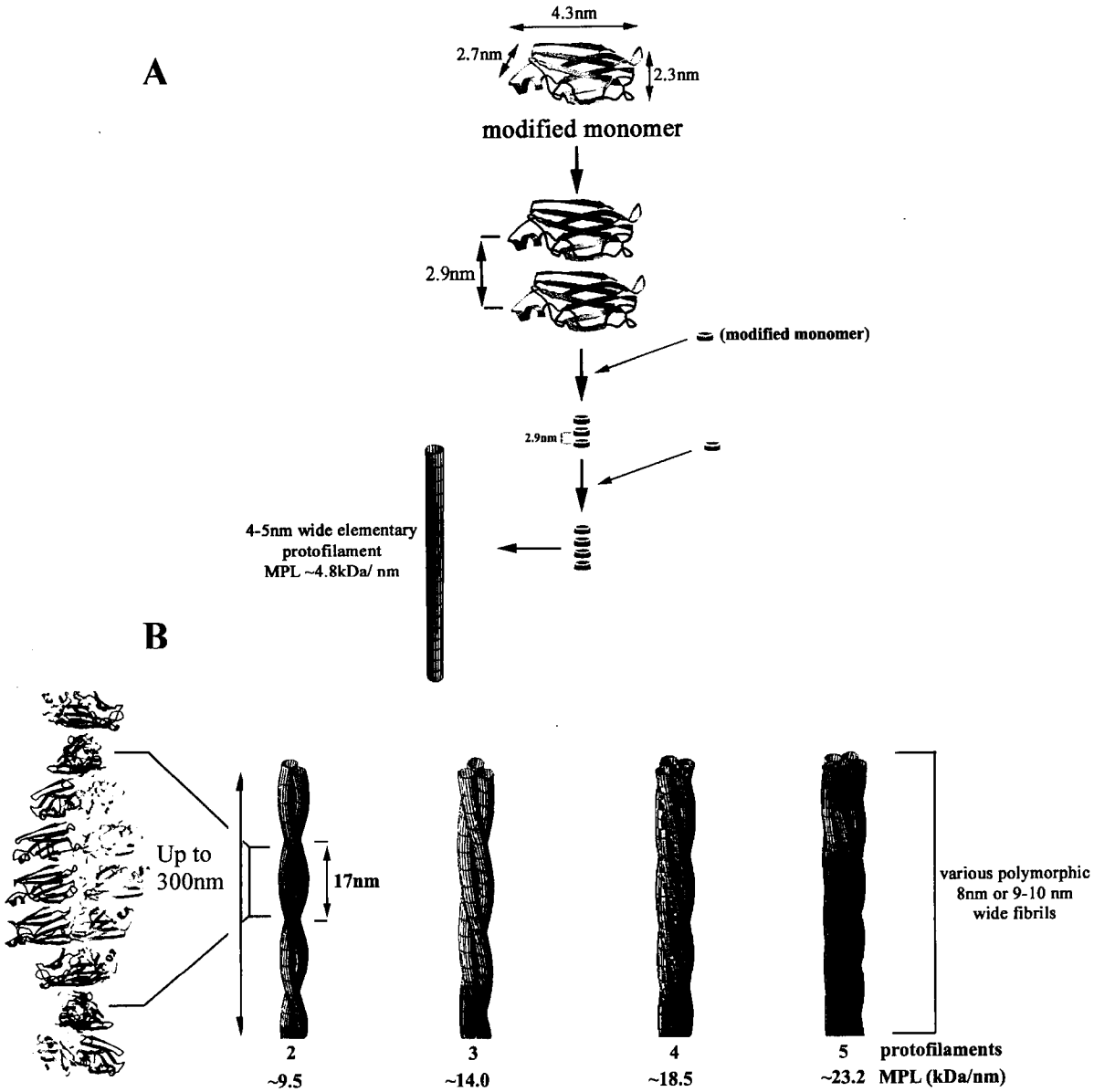

Figure 6- Structural model describing the observed *in vitro* TTR fibril assembly.

(A) Structurally modified monomers (discs) stack vertically with the 2.9 nm monomer-monomer spacing indicated by X-ray diffraction data (Inouye *et al.*, 1998). to form the smallest filamentous structure, a 4 - 5 nm wide elementary protofilament which has a MPL of 4.8 kDa/nm. **(B)** Fibrils with the distinct MPLs measured by STEM. The indicated intertwining of their elementary protofilaments would give rise to the 17nm axial repeat observed for some 8nm fibrils. These fibrils either form by the lateral association of 2, 3, 4 or more of elementary protofilaments or nucleate and elongate separately but maintain a common protofilament substructure. Intertwining of their elementary protofilaments may be a relatively rare event. The 9.5 kDa/nm fibril presenting the 17nm crossover repeat has a total of 6 monomers/crossover/strand with a twist of 30° between neighbouring monomers. This model is also proposed to describe the early stages of *in vivo* fibril formation, the immature fibril types considered being precursors of the much longer, rigid mature fibrils with distinct axial substructure that are isolated from *in vivo* sources. The structure of the monomer was taken from the database bank (PDB entry 5TTR).

Interestingly, the FWHM values corresponding to all of the major MPL peaks except that at 23.2 kDa/nm (TTR Leu55Pro variant), were essentially equivalent (~7 nm; an underestimate of the width dependent on the mass profile shape), implying that all of these fibril types might have been classified as 8 nm wide fibrils by TEM. The peak at 23.2 kDa/nm arose from fibrils with somewhat larger FWHM values (8 to 10 nm). Thus, the 8-nm fibrils observed by negative stain TEM were probably heterogeneous comprising at least two morphologically distinct species for both the TTR WT and the TTR Leu55Pro samples. In addition as detailed above, the number of elementary protofilaments making up the major fibrillar species was different for TTR WT (2 and 3 protofilaments) compared to TTR Leu55Pro (3, 4 and 5 protofilaments).

In the TTR Leu55Pro variant crystal the three-dimensional structure of the monomers is changed compared to TTR WT by the disruption of beta-sheet strand D, which becomes a long loop connecting beta strands C and E. This variant packs into a tubular crystal formed by monomers with several channels running parallel to each other. Given the binding propensity of the crystals to the amyloid dye thioflavin T, the packing interactions occurring within them could be significant for amyloidogenesis (Sebastião *et al.*, 1998). It is conceivable that the monomers of adjacent elementary protofilaments within TTR fibrils interact via their CE loops in a similar manner. Such lateral protofilament interactions might be highly favoured during the *in vitro* assembly of TTR Leu55Pro, which would explain both why single 4 - 5 nm wide protofilaments were only rarely seen and the formation of higher order fibrillar species at earlier time points than the WT (Figure 4). However, although fibril assembly was faster for TTR Leu55Pro, as illustrated by comparing Figures 1C and 2F, after reaching a certain size the TTR WT fibrils showed a higher tendency to bundle.

The work of Redondo *et al.* (Redondo *et al.*, 2000a) is in agreement with the model outlined in Figure 6. The recombinant TTR variants they produced existed as tetramers, formed by the association of dimers that were stabilised by disulphide bridges between their monomers. These recombinant proteins were unable to form fibrils. However, amyloid-like fibrils assembled upon the release of monomeric units by reduction. Studies made on other specially engineered TTR variants not found in nature have led to alternative hypotheses. Eneqvist *et al.* (Eneqvist *et al.*, 2000) suggest that conformational rearrangement but not tetramer dissociation is required for fibril formation. Similarly, Ferrão-Gonçalves *et al.* (Ferrão-Gonzales *et al.*, 2000) suggest that an altered tetramer could be responsible for TTR

aggregation, although it should be noted that a detailed structural analysis of the fibrils was not made. This hypothesis may apply to very early events on fibril formation as the latter authors reported the presence of a small population of monomers after treatment at high pressure (Ferrão-Gonzales *et al.*, 2000).

The TTR WT and TTR Leu55Pro fibrils assembled during out *in vitro* experiments were relatively short (up to 300 nm in length), flexible and in most cases did not exhibit any clear axial substructure such as helical twisting, transverse banding or periodic coiling (Figures 1 and 2). This suggests that they are probably immature fibril types and precursors of the much longer (several microns), rigid mature fibrils exhibiting distinct axial substructure, isolated from *in vivo* sources such as the vitreous of the eye or the peripheral nerve (Figure 5). Consequently, our *in vitro* system may be detecting early events relevant to fibril assembly *in vivo* making it particularly interesting for therapeutic studies. The model presented in Figure 6 is accordingly proposed to also describe the early stages of *in vivo* fibril formation.

We found distinct differences in the dimensions and morphology of the *ex vivo* fibrils obtained from two different sources. Although both fibril types reached lengths of several microns, the fibrils were 7 - 10 nm wide in the peripheral nerve and 15 - 20 nm wide in the vitreous. These observations indicate that after a certain stage amyloid formation may follow different pathways and involve different non-TTR components in the various organs. It also prompts the hypothesis that after this point the presence of such non-TTR components is essential for further assembly, and that it is these that control the formation of the organ-specific amyloid species. The two molecular models present in the literature for the structure of *ex vivo* vitreous amyloid (Blake and Serpell, 1996; Inouye *et al.*, 1998) are conflicting in their definition of the elementary protofilament. One proposes a protofilament formed from a single vertical-stack of monomers i.e., two beta-sheets per building-block (Inouye *et al.*, 1998), while the other proposes four beta-sheets related by a single helix axis arising from two monomers or a dimer as the repeating unit (Blake and Serpell, 1996). MPL measurements of the *ex vivo* vitreous amyloid samples after the removal of non-TTR components would allow these two X-ray models to be differentiated.

To conclude, the *in vitro* systems examined have provided invaluable information, revealing the large degree of polymorphism that occurs during TTR amyloid fibril formation. The structural model proposed for the *in vitro* fibrils is based on the results of quantitative STEM and defines the elementary protofilament as a vertical stack of structurally modified

TTR monomers. Further experiments are now required to determine which of the *ex vivo* models is correct and to show exactly how the very short, flexible *in vitro* assembled fibrils are related to the long, rigid fibrils found *in vivo*. Accordingly, the role of non-TTR components must be elucidated.

Acknowledgements

This work was supported in part by a grant (35785/99) and a PhD scholarship (BD/15725/98 to Isabel Cardoso) from Fundação para a Ciência e Tecnologia, Portugal, by the Swiss National Foundation (grant number 3159 415.99) and by the M. E. Müller Foundation of Switzerland. We thank Paul Moreira for his excellent technical assistance in the preparation of recombinant TTR WT and Leu55Pro, Rui Fernandes for the electron immunocytochemical analysis, Prof. Andreas Engel for helpful discussions and Jaime Cardoso and Jorge Cardoso for their collaboration on preparing figure 6.

Chapter III

4'-iodo-4'-Deoxydoxorubicin disrupts transthyretin amyloid fibrils *in vitro* producing non-cytotoxic species. Screening for transthyretin fibril disrupters

4'-iodo-4'-Deoxydoxorubicin disrupts transthyretin amyloid fibrils *in vitro* producing non- cytotoxic species. Screening for transthyretin fibril disrupters.

Cardoso I.[1,2], Saraiva, M. J.[1,2]

[1] Amyloid Unit, Institute for Molecular and Cell Biology and [2] Institute for Biomedical Sciences of Abel Salazar, Porto University, Porto, Portugal.

Running title: IDOX disrupts TTR Leu55Pro fibrils *in vitro*

Correspondence to: M. J. Saraiva, Amyloid Unit, IBMC, Rua do Campo Alegre, 823, P-4150-180 Porto, Portugal. Fax: +351 22 609 9157, Tel.: +351 22 607 4900, E-mail: mjsaraiv@ibmc.up.pt

I-DOX disrupts TTR Leu55Pro fibrils *in vitro*

Abstract

Familial Amyloidotic Polyneuropathy (FAP) is an autosomal dominant disorder characterized by extracellular deposition of fibrillar amyloid protein- transthyretin (TTR)- with special involvement of the peripheral nerve. A large number of TTR variants are associated with this disease. TTR Leu55Pro is one of the most aggressive forms known and has the ability of forming fibrils *in vitro* under physiological conditions (PBS, pH 7.4).

We studied by transmission electron microscopy (TEM) the effect of the drug 4'-iodo-4'-Deoxydoxorubicin (I-DOX) on the *in vitro* assembly of TTR Leu55Pro fibrils, by following the fibril growth over a 15 day period. Our results showed that I-DOX at a concentration of 10^{-5} M/100 μg fibrils does not inhibit fibril formation up to 10 days since fibrils of approximately 7- 8 nm wide, identical to the fibrils present in the non-treated sample were observed. However, after 15 days of I-DOX treatment, only round particles approximately 5- 6 nm wide, resembling soluble native TTR were observed. We also tested the ability of a series of compounds to interfere with amyloid fibril formation. These included ten I-DOX analogues, tetracyclines, and nitrophenols and found that they all act as fibril disrupters. The group of compounds tested showed fibril disruption activity to different extents and some of them resulted in the complete disaggregation of fibrils.

In addition, the species generated upon I-DOX treatment are non-toxic, as revealed by the lack of significant caspase-3 activation on a Schwanoma cell line. This result suggests that I-DOX is a potential therapeutic drug in TTR related amyloidosis.

Keywords: familial amyloidotic polyneuropathy, transthyretin, I-DOX, amyloid disruption, caspase-3.

Introduction

Familial Amyloidotic Polyneuropathy (FAP) is an autosomal dominant disorder characterized by extracellular deposition of fibrillar amyloid protein with special involvement of the peripheral nerve (Coimbra and Andrade, 1971). The major component of the amyloid deposits in FAP is a variant transthyretin (TTR). To date, about 80 different TTR mutations related to amyloid deposition, and 10 non-pathogenic mutations have been described (Saraiva, 2001).

TTR is a tetrameric serum protein composed of four identical 127-residue subunits (Blake and Swan, 1972). Each 14 kDa monomer within the functional tetramer contains two-beta-sheets composed of strands DAGH and CBEF, as well as a small helical segment (Blake *et al.*, 1978). TTR Leu55Pro is one of the most pathogenic FAP variants known (Jacobson *et al.*, 1992) and has been implicated as the causative agent in early-onset FAP. X-ray studies on this mutant showed the disruption of hydrogen bonds between strands D and A leading to the formation of a long loop between strands C and E. It is believed that interactions between CE loops of neighboring monomers are very important in the amyloidogenic process.

Amyloid fibrils are characterized by certain tinctorial properties such as birefringence under polarized light after staining with the dye Congo red and binding to thioflavin T (Th T). The fibrils are straight or coiled, non-branched, 7.5 to 10 nm in diameter and several microns in length. X-ray studies revealed a cross-β pattern with the β-sheets running perpendicular to the axis of the growing fibril. Several other components are associated with amyloid deposits, including a non-fibrillar glycoprotein, the P component, and a variety of mucopolysacharides and other plasma and tissue proteins (Staunter *et al.*, 1991).

In vitro fibril formation has been a powerful tool in the study of the mechanism that leads to amyloid formation. Theories for the events occurring *in vivo* have been proposed based on *in vitro* results. *In vitro* screening of drugs that reverse or avoid the amyloidogenic process is necessary to prevent or treat the disease. Therefore, it is very important to elucidate the dynamics of amyloid fibril formation to prevent disease: different drugs may act on different species present at different stages on the amyloidogenic pathway, and this knowledge enables us to search for specific drugs for each step of the process.

In this work we investigated the action at different time points of TTR fibril formation, of a class of compounds known to disrupt amyloid fibrils. The drugs tested included 4'- Deoxy-4'- iododoxorubicin (I-DOX) (Gianni *et al.*, 1995; Merlini *et al*, 1995; Palha *et al.*, 2000b),

tetracycline derivates (Howlett *et al.*, 1999b; Forloni *et al.*, 2001; Tagliavini *et al.*, 2000) and nitrophenols (De Felice *et al.*, 2001).

Whether this drug produces toxic intermediate species has not been addressed. Specifically, we investigated the nature and toxicity of the intermediate species formed by the action of these drugs on TTR amyloid.

Materials and methods

Isolation and purification of TTR

TTR proteins were produced in an *E. coli* expression system (Furuya *et al.*, 1991), isolated and purified as previously described (Almeida *et al.*, 1997). Briefly, after growing the bacteria, the protein was isolated and purified by preparative gel electrophoresis after ion exchange chromatography. Protein concentration was determined using the Lowry method (Lowry *et al.*, 1951).

Preparation of amyloid fibrils

TTR Val30Met (2 mg/ml) was incubated in 0.05 M sodium acetate pH 3.6, for 72 hours at room temperature (Colon and Kelly, 1992). The sample was then centrifuged at 15,000 g for 30 minutes at 4°C; the pellet obtained was washed and re-suspended in MilliQ water and incubated at 37°C.

TTR Leu55Pro was dialyzed against water pH ~ 7.0 and concentrated to 5 mg/ml. The preparation was centrifuged at 15,000 g for 30 minutes at 4°C and the pellet was then washed and re-suspended in phosphate buffered saline (PBS) or 0.9% NaCl, at 2 mg/ml and incubated at 37°C.

Fibril concentrations were assessed by the Lowry method (Lowry *et al.*, 1951).

Filter assays

To investigate whether I-DOX was able to dissolve amyloid fibrils, 100 μg of TTR synthetic fibrils (obtained by acidification) or soluble TTR were incubated with 10^{-5} M I-DOX in 0.9% NaCl added freshly everyday for 7 days, at room temperature in the dark. The samples were applied to SPINE-X (Costar) centrifuge filter units, centrifuged, and washed with 0.9%NaCl. Protein concentration of the filtered material was determined using the Bio-Rad protein Assay (Bio-Rad) and albumin as standard.

IDOX effect on TTR fibrils

IDOX (kindly provided by Pharmacia and Upjohn) was dissolved in 0.9% NaCl and filtered through a 0.2 μm filter (Schleicher & Schuell). IDOX concentration was determined spectrophotometrically at 478 nm, using an extinction coefficient of 13300 $M^{-1}cm^{-1}$ based on a 631 Da molecular weight. Stock solutions were prepared at approximately 10^{-3} M.

I-DOX disrupts TTR Leu55Pro fibrils *in vitro*

Aliquots of TTR Leu55Pro (100 μg), prepared as described above and resuspended in 0.9% NaCl or PBS, were incubated at 37°C in the dark alone or in the presence IDOX 10^{-5} M. The same amount of IDOX was added everyday for 15 days. In one aliquot IDOX was added only once in the first day.

At given time points, the samples were visualized by TEM for the presence of amyloid fibrils.

In a different set of experiments TTR Leu55Pro prepared as above and resuspended in 0.9% NaCL, was allowed to grow into fibrils for 10 days at 37°C and then I-DOX was added in concentrations ranging from 10^{-4} to 10^{-7} M. After five more days at 37°C in the dark, the samples were analyzed by TEM.

Transmission electron microscopy (TEM)

For visualization by TEM, samples aliquots were diluted (1:50) with NaCl 0.15 M and immediately adsorbed to glow-discharged carbon-coated collodion film supported on 200-mesh copper grids. For negative staining, the grids were washed with deionized water and stained with 1% uranyl acetate. The grids were visualized with a Zeiss microscope, operated at 60kV. Measurements of the fibril widths and lengths were made from enlarged prints of the electron micrographs using a magnifying glass with a built-in calibrated ruler.

Screening for TTR fibril disrupters

A series of compounds were tested for their ability to interfere with TTR amyloid fibril formation or to disrupt mature fibrils. These included: (i) I-DOX analogues (1-10), kindly provided by the MD Anderson Cancer Center (University of Texas, USA); (ii) the tetracycline derivatives rolitetracycline and doxycycline, a kind gift of the Department of Neuroscience, SmithKline Beecham-Pharmaceuticals, UK; (iii) and tetracycline, 2,4-dinitrophenol (DNP) and 3-nitrophenol (NP) were purchased from Sigma.

I-DOX analogues (1-10) were dissolved in methanol (Merck) at a concentration of approximately 10^{-3} M. 100 μg of fibrillar TTR Leu55Pro (2 mg/ml, 0.9% NaCl) were incubated with each one of the analogues at a concentration of 10^{-5} M added freshly everyday for 15 days.

Tetracycline, rolitetracycline, doxycycline, DNP and NP were prepared in dimethylsulfoxide (DMSO) at 10 mg/ml. 100μg of fibrillar TTR Leu55Pro prepared as described (2 mg/ml, PBS) was incubated with a single dose of each of the compounds at 360 μM.

Controls (TTR Leu55Pro alone and TTR Leu55Pro with equal amounts of methanol or DMSO) and compound-added aliquots were analyzed by TEM at different time points.

Caspase-3 assay

RN22 cells (rat Schwanoma cell line) were propagated in 25 cm^2 flasks and maintained at 37°C in a humidified atmosphere of 95% and 5% CO_2. Cells were grown in Dulbecco's minimal essential medium (DMEM) supplemented with 10% fetal bovine serum (FBS) (Life Technologies).

TTR Leu55Pro fibrillar material (500 μg) was treated with I-DOX added freshly everyday for 3 or 15 days (10^{-5} M I-DOX/100 μg fibrils). The sample was then centrifuged at 14,000 rpm, washed 3 times with 0.9% NaCl to remove IDOX in excess and resuspended again in 0.9% NaCl. Toxicity of I-DOX treated fibrils was evaluated by activation of caspase-3, measured using the CaspACE colorimetric 96 well plate assay system (Promega), following the manufacturer's instructions. Briefly, 80% confluent RN22 cells in DMEM in 1% FBS were exposed for 48 hrs to 2 μM TTR (either soluble, fibrillar TTR Leu55Pro alone or I-DOX treated). Subsequently, each well was trypsinized and the cell pellet was lysed in 100 μl hypotonic lysis buffer (Promega) by 5 cycles of freeze/ thawing. 40 μl of each cell lysate was used in duplicates for determination of caspase-3 activation. The remaining cell lysate was used to measure total cellular protein concentration using the BIO-RAD protein assay kit (Bio-Rad), using BSA as standard. Values shown are the mean of duplicates and the experiment was performed twice.

I-DOX disrupts TTR Leu55Pro fibrils *in vitro*

Results

Effect of the drug I-DOX on the *in vitro* assembly of TTR Leu55Pro fibrils

TTR Leu55Pro is a TTR variant associated with a very aggressive form of FAP disease and X-ray data on this mutant revealed important conformational changes suggesting this variant as a representative of amyloid precursors forms (Sebastião *et al.*, 1998). This variant constitutes thus, an important tool to follow and study fibrillogenesis.

We studied the effect of I-DOX (figure 1) on the *in vitro* assembly of TTR Leu55Pro fibrils by following the morphological properties over a 15 days period by EM, and comparing with the characteristics of the sample incubated in the absence of the drug.

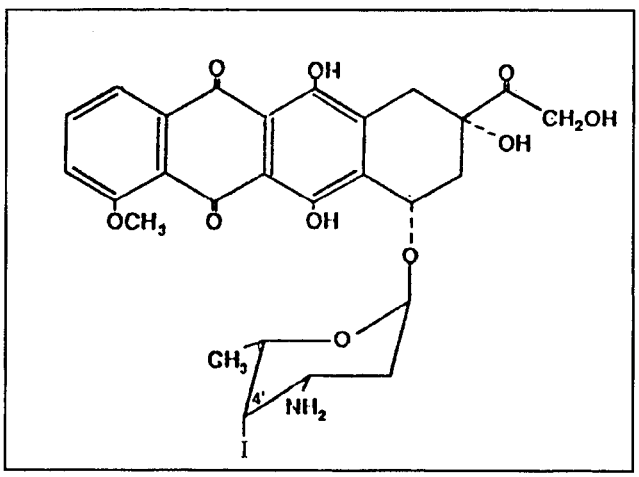

Figure 1- 4'-iodo-4'-deoxydoxorubicin (I-DOX)

In the following described experiments both TTR Leu55Pro fibrils and I-DOX were prepared in 0.9% saline as the drug is not active in PBS (results not shown).

I-DOX was co-incubated at 37°C with the TTR Leu55Pro preparation and after 6 days we observed fibrils identical to the ones in the non-treated sample (figure2). Up to 10 days it was still possible to observe fibrils in the treated sample (figure2). The continuous addition of the drug to the preparation up to 15 days lead to the disruption of the fibrillar material (figure 2, lower panel) into round particles, that resembled soluble protein.

We next investigated whether these round particles, in fact, represented soluble protein. Specifically, incubating synthetic mature fibrils TTR fibrils with I-DOX for periods up to 7

days, we checked for the presence of soluble TTR after filtration. While soluble TTR (in the absence or presence of I-DOX) was completely filtered, TTR fibrils or amorphous precipitate (resultant from I-DOX treatment) were completely retained (not filtered) when applied on SPIN-X centrifuge filter units. Since no protein is detected in the filtrate upon fibril incubation with I-DOX, and given the formation of amorphous material, we concluded that I-DOX is able to disrupt but not dissolve the TTR fibrils.

I-DOX disrupts TTR Leu55Pro fibrils *in vitro*

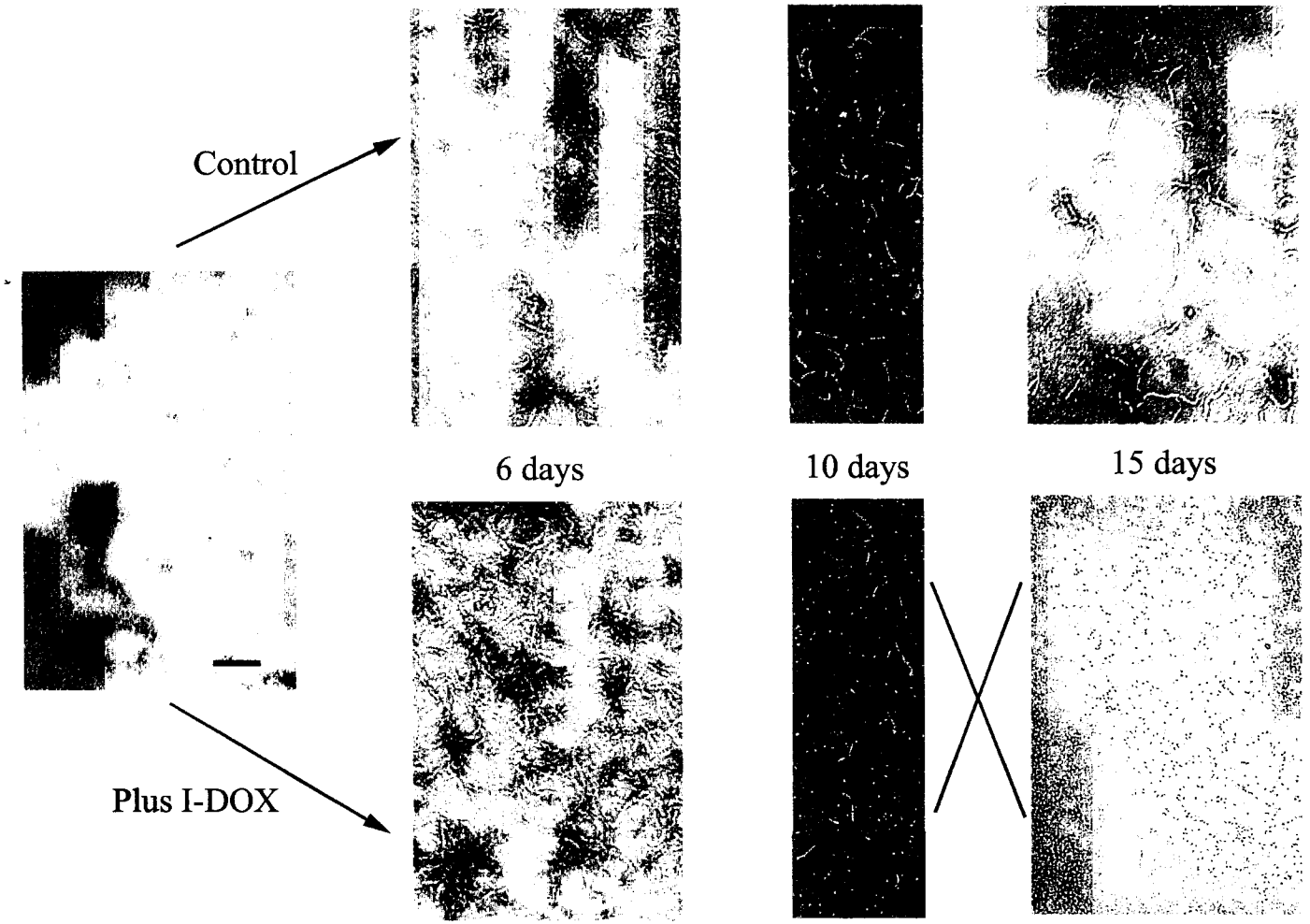

Figure 2- Effect of I-DOX on the *in vitro* assembly of TTR Leu55Pro fibrils as followed by TEM. In the control situation, after incubation for 6 days at 37°C, TTR Leu55Pro initial aggregates organized into short fibrils, which elongated after 10 and 15 days **(upper panels)**. When I-DOX is added daily to the TTR Leu55Pro initial aggregates at a concentration of 10^{-5} M, similar short fibrils are observed up to 10 days of incubation at 37°C; after 15 days the fibrils are disrupted producing small round particles **(lower panels)**. Scale bar = 100 nm.

I-DOX stability

Previous work with *ex vivo* and *in vitro* amyloid fibrils defined the necessity of I-DOX to be freshly added everyday (Merlini *et al.*, 1995). In fact, when a single dose of I-DOX 10^{-5} M was added on day one to TTR Leu55Pro initial aggregates, and the sample was further incubated at 37°C for 14 days, observation by TEM revealed the presence of fibrillar structures; these fibrils appeared shorter in length when compared to the non-treated sample and a mixture of round particles and short pre-fibrillar elements were visible (figure 3). In contrast, when the drug is added daily, round particles were observed (see figure 2), which suggests that the drug is inactive after some time, probably due to a destabilization process, and loses its activity as a fibril disrupter.

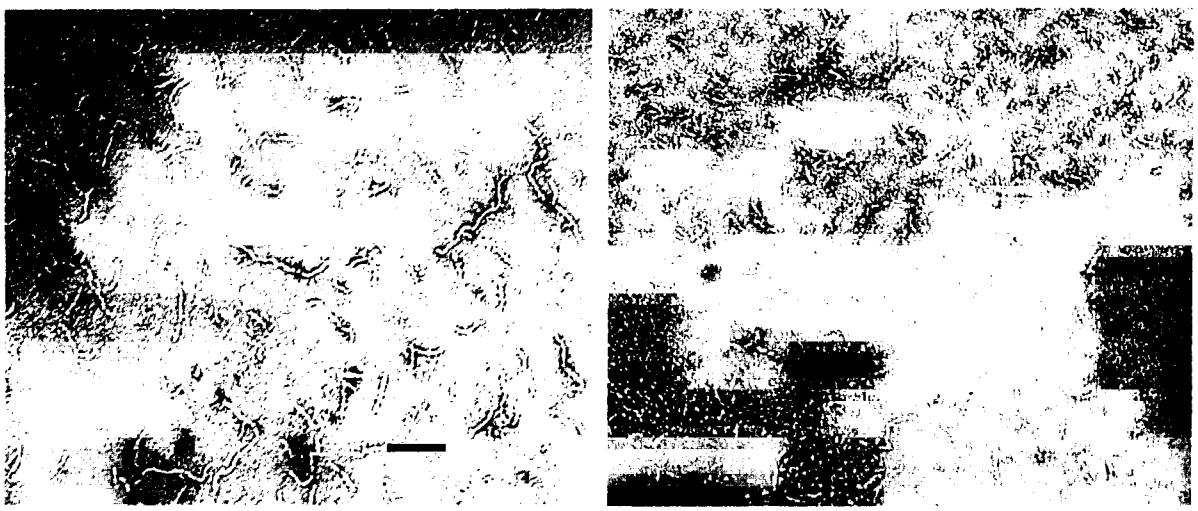

Figure 3- TTR Leu55Pro incubated for 15 days at 37°C in the absence **(right panel)** or in the presence of I-DOX 10^{-5} M added solely once on day 1 **(left panel)** in the dark. Scale bar = 100 nm.

I-DOX concentration effect

I-DOX ability to interact with amyloid fibrils has been preferentially studied in AL-related amyloidosis and used in concentrations ranging from 10^{-6} to 10^{-5} M (Merlini *et al.*, 1995).
To determine the optimal concentration at which I-DOX acts on TTR Leu55Pro fibrils, TTR Leu55Pro initial aggregates were incubated at 37°C and allowed to grow into fibrils for 10 days. After this period of time, aliquots of 100 μg were separated and incubated with one single dose of I-DOX at 10^{-4}, 10^{-5}, 10^{-6} or 10^{-7} M. The samples were further incubated at 37°C for 5 more days in the dark and then analyzed by TEM.

I-DOX disrupts TTR Leu55Pro fibrils *in vitro*

Negatively stained samples were observed by electron microscopy and revealed that at I-DOX 10^{-7} and 10^{-6} M did not disrupt completely the TTR Leu55Pro fibrils formed at 10 days (figure 4, top panels). In contrast, the drug added at 10^{-5} M, it completely disrupted the fibrils previously produced (figure 4, bottom panel). I-DOX at 10^{-4} M showed the same effectiveness as at 10^{-5} M generating only round particles (data not shown).

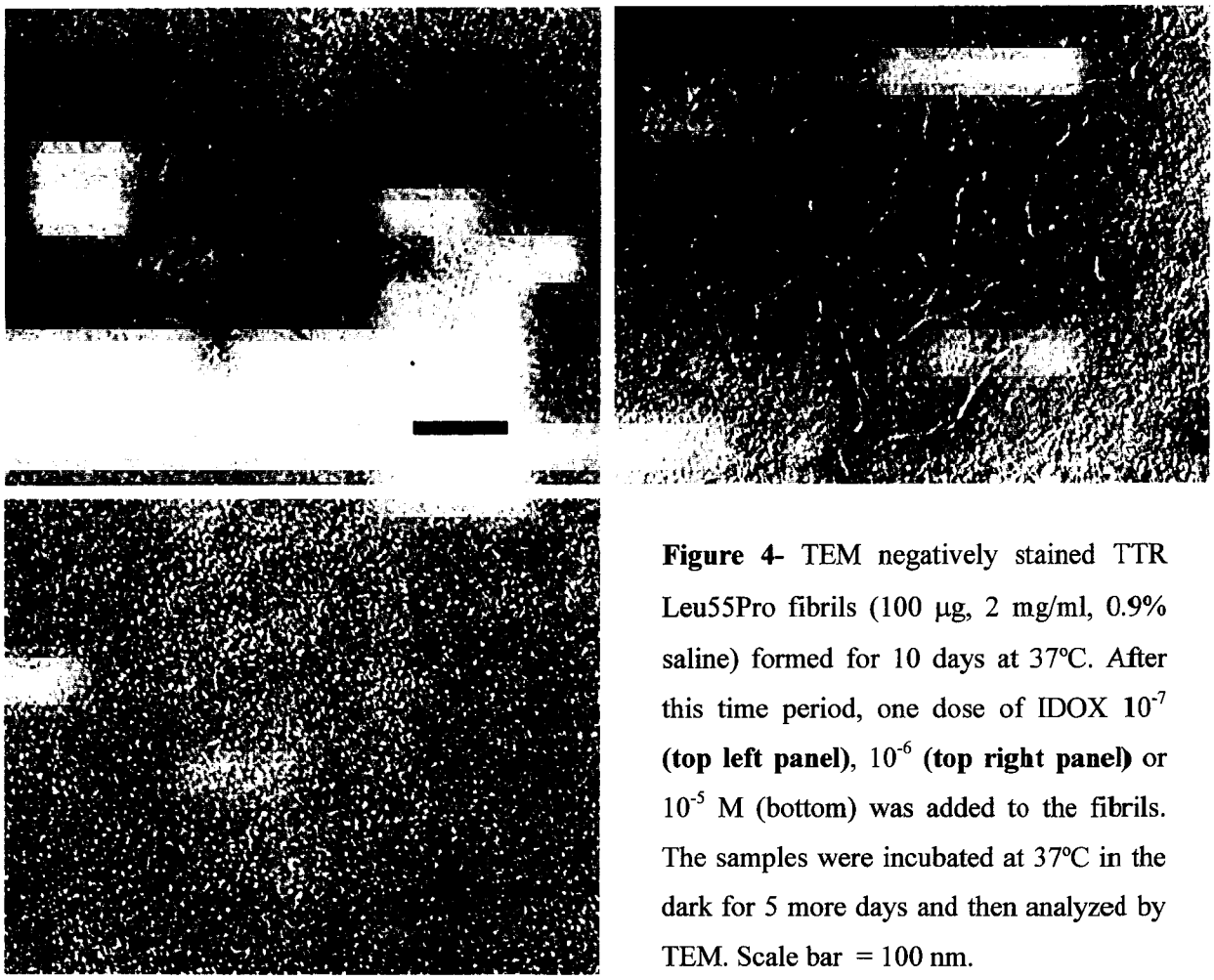

Figure 4- TEM negatively stained TTR Leu55Pro fibrils (100 μg, 2 mg/ml, 0.9% saline) formed for 10 days at 37°C. After this time period, one dose of IDOX 10^{-7} **(top left panel)**, 10^{-6} **(top right panel)** or 10^{-5} M (bottom) was added to the fibrils. The samples were incubated at 37°C in the dark for 5 more days and then analyzed by TEM. Scale bar = 100 nm.

The latter experiment, using a single dose of I-DOX on pre-formed fibrils grown for 10 days, allowed the assessment of the optimal concentration for I-DOX performance at 10^{-5} M/100μg fibrils. In addition, it corroborated the finding that I-DOX disrupts TTR Leu55Pro fibrils *in vitro*. Furthermore, it guaranteed that the effect observed when I-DOX was added everyday for 15 days to TTR Leu55Pro initial aggregates was not due to a cumulative concentration effect of the drug.

In addition the data showed, for the first time, at which stage of fibril formation is I-DOX interfering with the amyloidogenic cascade.

Study of TTR fibril disrupters

1. I-DOX analogues

The results described above, indicate I-DOX as a good candidate to treat advanced cases of amyloid deposition. However, I-DOX cardiotoxicity is a limitation for its wide use and that lead us to search for similar non-toxic compounds with the ability to disrupt amyloid fibrils. A series of drugs synthesized based on I-DOX structure were tested. The structures of some of the compounds are represented on figure 5.

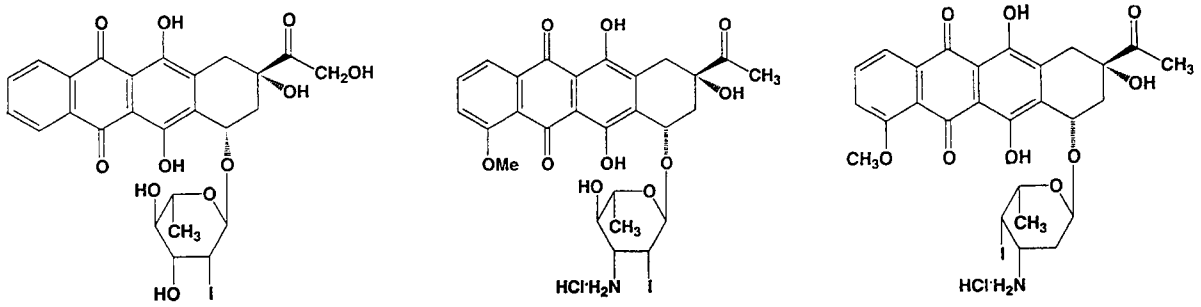

Figure 5- Structures of three I-DOX-related compounds tested.

The experiments were performed by incubating TTR Leu55Pro initial aggregates (100 μg, 2 mg/ml, 0.9% saline) with 10^{-5} M of 10 different compounds, at 37°C in the dark. The observation that some variability concerning fibrils formation occurred between protein batches, leads us to include in the experiment the drug I-DOX as a control. The compounds were added freshly everyday and shown to act only as disrupters. Two out of 10 compounds

tested exhibited a complete disrupter activity whereas the remaining had intermediate activities resulting in a mixture of fibrils of different lengths, short non-fibrillar structures and round particles. Figure 6 shows the results obtained with two of the compounds tested and that are representative of two distinct groups; in one group, 2 compounds presented full disrupting activity whereas another group reflected partial disrupting activity.

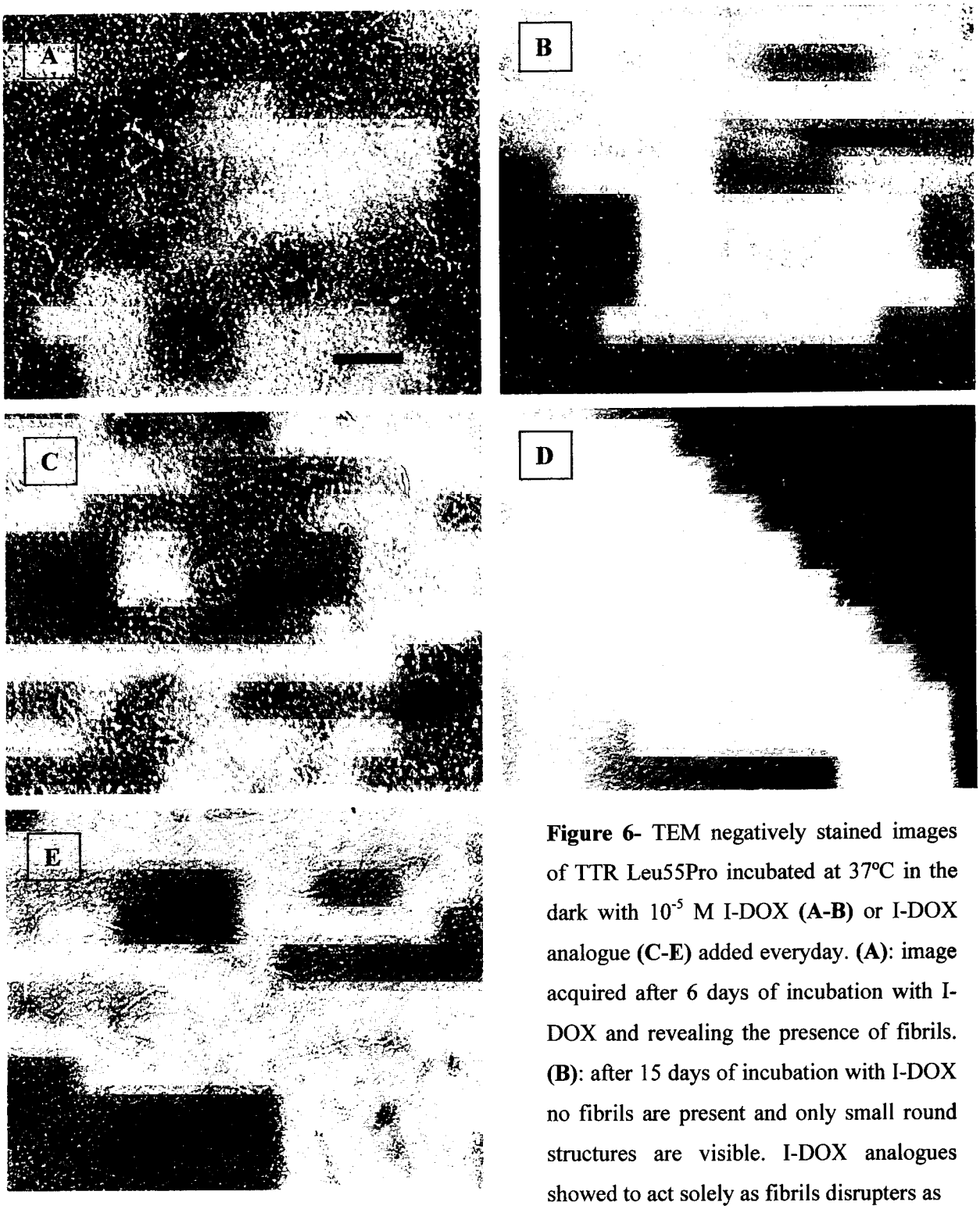

Figure 6- TEM negatively stained images of TTR Leu55Pro incubated at 37°C in the dark with 10^{-5} M I-DOX **(A-B)** or I-DOX analogue **(C-E)** added everyday. **(A)**: image acquired after 6 days of incubation with I-DOX and revealing the presence of fibrils. **(B)**: after 15 days of incubation with I-DOX no fibrils are present and only small round structures are visible. I-DOX analogues showed to act solely as fibrils disrupters as fibrils are observed after 6 days at 37°C **(C)**; The continuous addition of two of the compounds resulted in the complete disaggregation of fibrils after 15 days **(D)**. The other group of the compounds tested revealed partial disruption activity, resulting in the presence of a mixture of fibrils and round particles **(E)**. Scale bar = 100 nm.

TEM analysis at day 6 showed fibrils, supporting the idea that this group of compounds acts only as disrupters but does not inhibit fibril formation.

2. Tetracyclines

It has been reported that tetracyclines exhibit anti-amyloidogenic properties towards Aβ-amyloid, not only by inhibiting β-amyloid aggregates formation but also by disaggregating pre-formed fibrils (Forloni *et al.*, 2001). This class of antibiotics presents a safe toxicological profile and thus, is a good candidate for treatment of amyloid related diseases.

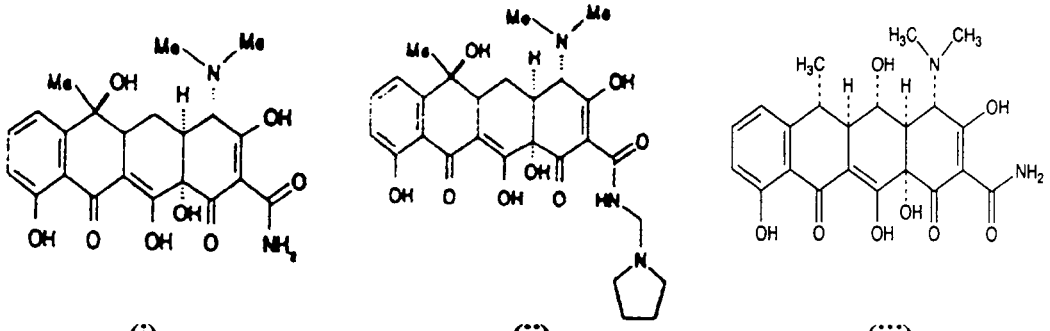

(i) **(ii)** **(iii)**

Figure 7 – Structures of **(i)** tetracycline, **(ii)** rolitetracycline and **(iii)** doxycycline.

We tested tetracycline and two tetracycline derivates, rolitetracycline and doxycycline (figure 7) for their competence to interfere in the process of TTR amyloid formation and assessed their capacity to inhibit fibril formation and/ or disrupt TTR fibrils. Up to 17 days this capacity was determined by exposing TTR Leu55Pro initial aggregates to the drugs followed by TEM analysis.

Our results showed that the antibiotics tested act primarily as fibril disrupters since fibrils were observed in intermediate time points (data not shown), before 17 days. After 17 days of incubation at 37°C with tetracycline, the sample clearly shows small round particles very abundante, when compared to the control situation. However, a small portion of fibrils with apparent similar lengths to the control are also observed (figure 8, right upper panel),

implying that although tetracycline behaves as a disrupter, it does not fully disaggregate TTR Leu55Pro fibrils *in vitro* under the tested concentrations. Rolitetracycline showed lower disrupting activity than tetracycline since a large amount of fibrils were still visible after 17 days of incubation at 37°C (figure 8, left lower panel). Nevertheless, in average, the fibrils appeared shorter than in the control with slightly more abundant short particles. Finally, doxycycline revealed as the most effective of the three compounds of this class tested: no fibrils were visible after incubation (figure 8, right lower panel). Doxycycline is, therefore, a good candidate in therapeutic approaches in TTR related amyloidosis.

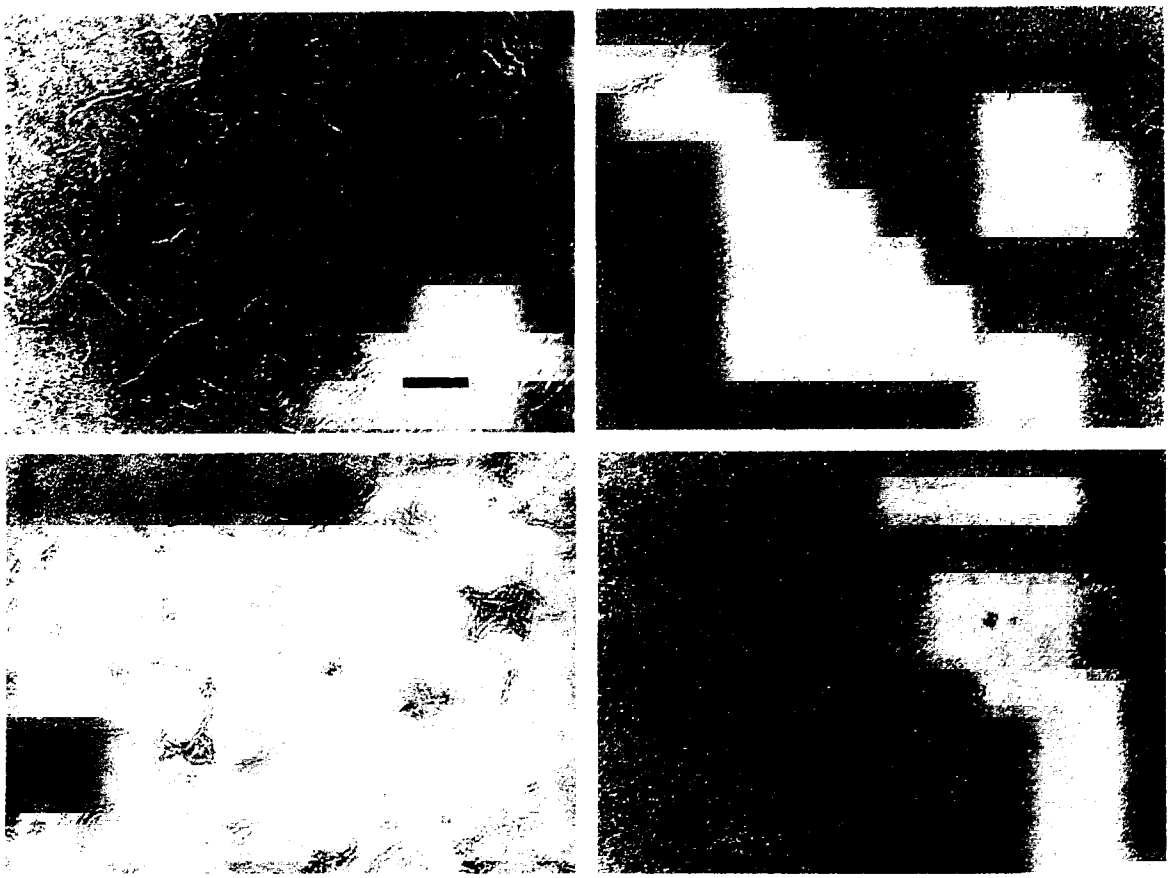

Figure 8- Effect of tetracyclines on TTR Leu55Pro fibril assembly *in vitro*. After 17 days at 37°C fibrils formed in the absence of drug were visualized by TEM **(left upper panel)** whereas **incubation** with drugs **(i)** tetracycline **(right upper panel)**, **(ii)** rolitetracycline **(left lower panel)** and doxycycline **(right lower panel)** resulted in various degrees of fibril disruption.
Scale bar = 100 nm.

3. Nitrophenols

Another group of compounds tested for their capacity to obstruct TTR fibril formation included 2,4-dinitrophenol (DNP) and 3-nitrophenol (NP) (figure 9).

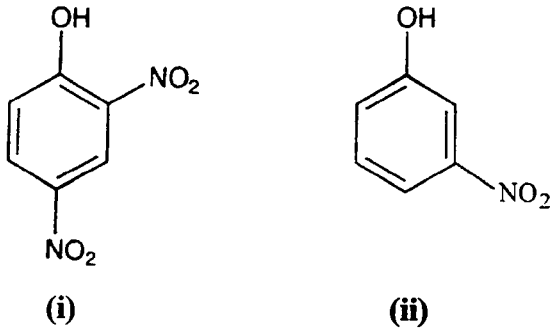

(i) (ii)

Figure 9 – Structure of **(i)** 2,4-nitrophenol and **(ii)** m-nitrophenol.

Figure 10 shows that both DNP and NP disrupt TTR Leu55Pro fibrils. NP resulted in partial disaggregation of the fibrils whereas DNP activity resulted in complete disruption.

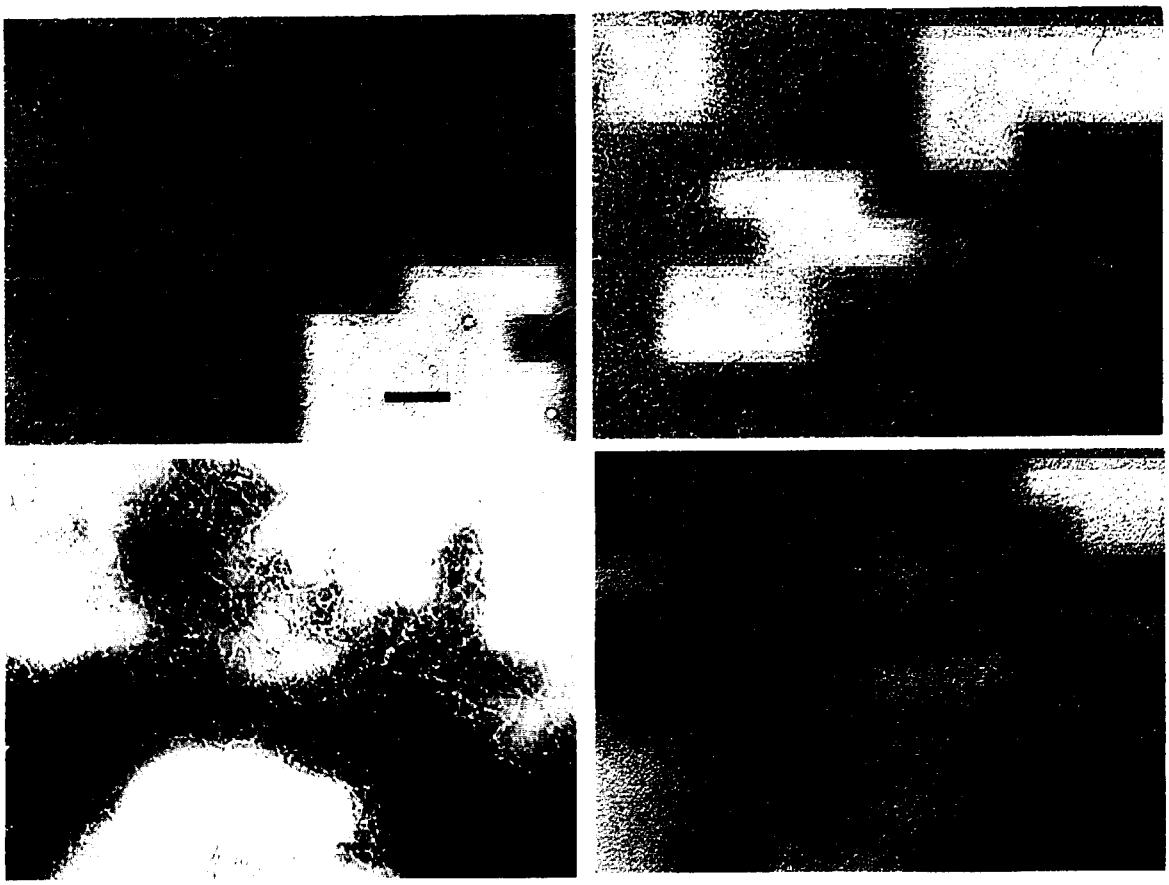

Figure 10- Effect of nitrophenols on TTR Leu55Pro assembly *in vitro.* Incubation for 17days in **the** absence of compound **(left upper panel)** and with NP **(right upper panel)** showing partial disruption of the fibrils after 17 days; DNP disruption activity is revealed by the presence of fibrils after 5 days of incubation **(left lower panel)** which are completely disrupted upon 17 days of incubation at 37°C **(right lower panel)**. Scale bar = 100 nm.

Cytotoxicity of non-fibrillar and fibrillar TTR in cell culture

In vitro and under physiological conditions (PBS, pH 7.4), TTR Leu55Pro preparations start to form non-fibrillar aggregates and very short pre-fibrillar structures (figure 11A, top right panel) that evolve to short fibrils (figure 11A, bottom left panel), which elongated over time into fibrils approximately 8 nm wide and with variable length (figure 11A, bottom right panel). Soluble protein (figure 11A, top left panel) appears as round particles of 5- 6 nm of diameter.

Toxicity of the different species observed during the TTR Leu55Pro fibril assembly process, including the initial aggregated non-fibrillar form of TTR (1 day incubation), and

fibrillar forms of different lengths (6- and 15- days incubation) was assessed by caspase-3 activation on a Schwanoma cell line. Caspase-3 activation was observed only with the initial aggregates, whereas the soluble counterpart and the longer fibrils did not produce statistically significant caspase-3 activation (Figure 11B).

A

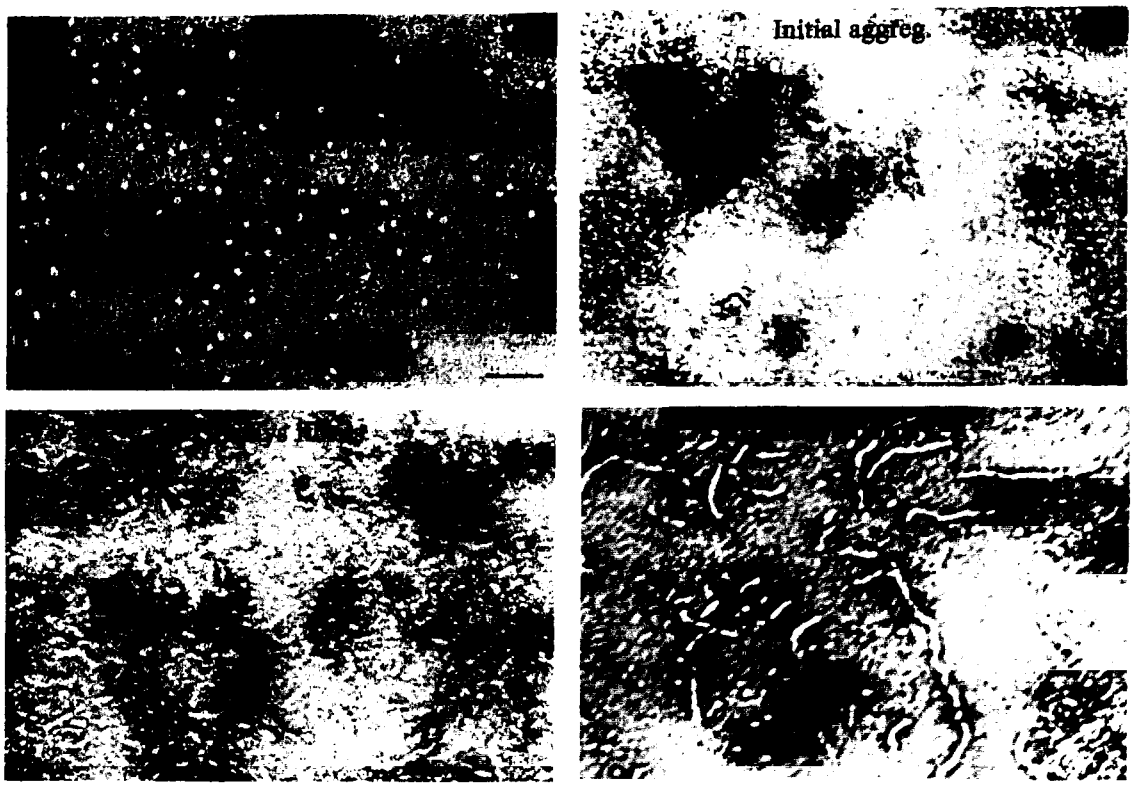

B

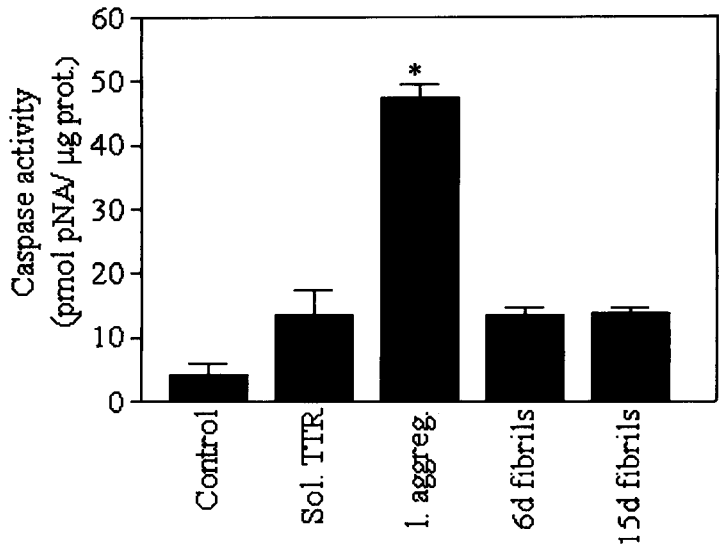

Figure 11- A: TEM of negatively stained TTR Leu55Pro: soluble, initial aggregates, 6- and 15-days fibrils. Scale bar = 100 nm. **B**: Activation of caspase-3 in RN22 cells exposed for 48 hours to 2 µM of the different species shown in **A**: soluble TTR **(sol. TTR)**, initial aggregates **(I. Aggreg.)**, 6-day fibrils **(6d fibrils)**, and 15-day fibrils **(15d fibrils)**. * $p < 0.003$.

These results show that non-fibrillar TTR constitute the most toxic species and that mature amyloid fibrils are not toxic for the cell line used.

Cytotoxicity of the species resulting from the action of I-DOX

Since I-DOX has the ability to interact only with fibrils formed for approximately 11-15 days and thus, these are the most interesting species to study, in which concerns cytotoxicity.

The toxicity of the species generated upon treatment with I-DOX after 15 days compared to different species present during the TTR Leu55Pro fibril assembly process, including the initial aggregates and fibrils assembled for 15 days, was assessed by caspase-3 activation on an Schwanoma cell line. Figure 12A depicts the results obtained showing that I-DOX treatment for 15 days did not produce toxic species as compared with the toxic initial aggregates.

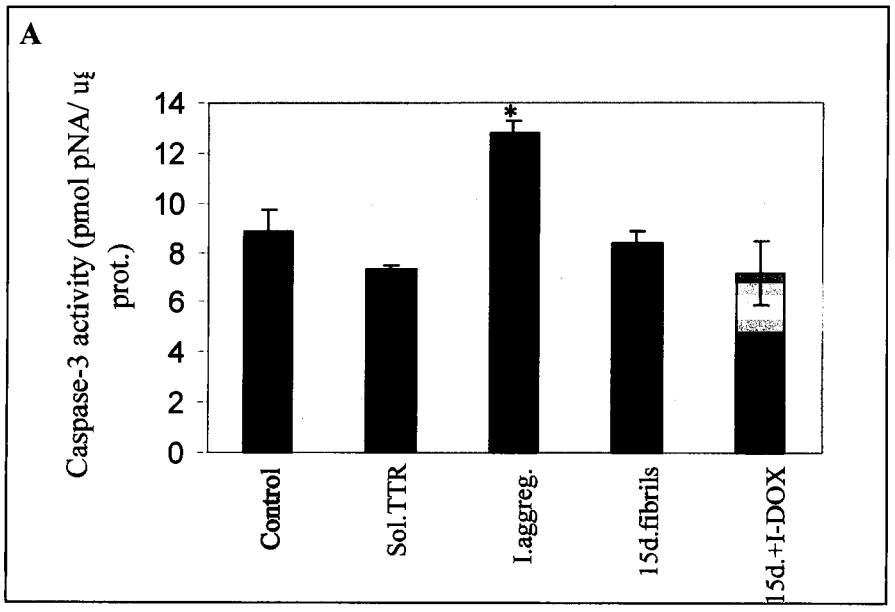

Figure 12A- Activation of caspase-3 in RN22 cells exposed for 48 hours to 2 μM of different species observed throughout TTR Leu55Pro formation and after I-DOX action. * $p < 0.04$.

However, at early time points, specially until 3 days, the species present both in control and I-DOX treated samples are small, non-fibrillar structures. Ascertaining for drug activity at this point is, thus, difficult. Nevertheless, it is important to assess for cytotoxicity of the related drug treated structures.

Figure 12B is representative of caspase-3 activation, showing that a TTR Leu55Pro preparation treated with I-DOX for 3 days still retains the toxicity associated with the initial aggregates. This finding supports our previous observation that I-DOX has no action until a certain fibril length is reached, since species resulting from I-DOX action are non-toxic to the cell line used.

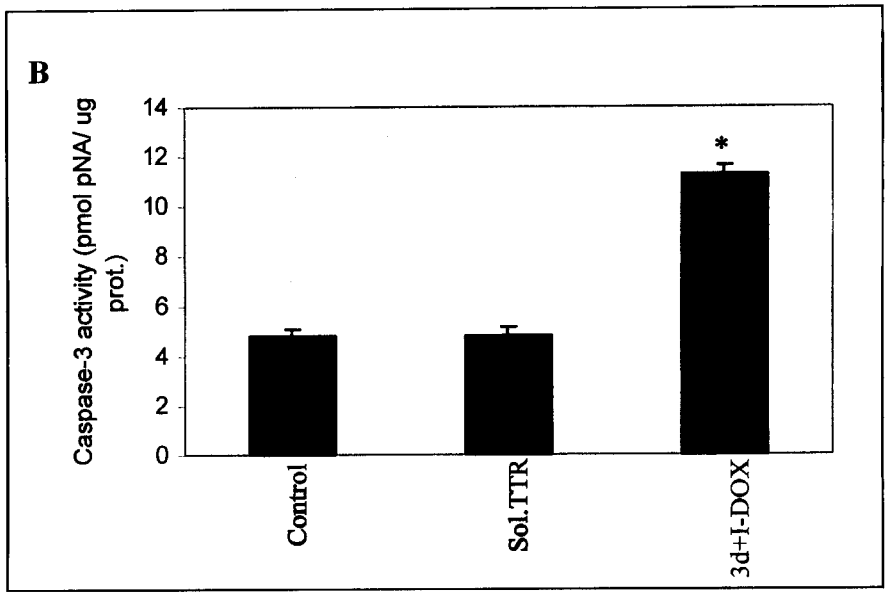

Figure 12B- Activation of caspase-3 in RN22 cells exposed for 48 hours to 2 μM of the different species. * $p < 0.002$.

Discussion

The only therapy presently available for FAP is liver transplantation and although the amyloidogenic precursor protein is eliminated from blood, clinical improvement is not observed in all patients. Alternative therapies should therefore be considered. One possible route for treatment is to inhibit amyloid deposition and /or to disrupt already formed fibrils. In the present work we tested different classes of compounds for their ability to inhibit fibril elongation and/ or to disrupt TTR fibrils.

The data presented in this study clearly showed that I-DOX disrupts *in vitro* pre-formed amyloid fibrils assembled for 15 days but does not inhibit fibril formation until a certain fibril length. TTR Leu55Pro fibril elongation pattern was previous ascertained (refer to chapter II) and shown to be sigmoidal in character. Furthermore, the fastest rate of fibril growth occurred between days 11 and 18, corresponding to an elongation rate of 9.2 nm/day. The observation that I-DOX exerts its effect within this time interval suggests that the drug has an important action on fibril elongation and raises the question for the need of a structural motif that allows the drug to bind to fibrils and disrupt them. In fact, I-DOX was shown to very rapidly destroy TTR Leu55Pro crystals presenting an oligomeric-like structure, while TTR WT crystals were quite stable, under the same conditions (Sebastião *et al.*, 2000). Molecular modeling studies were performed and the results suggested that I-DOX binding site to TTR Leu55Pro crystals corresponds to a region of interaction between monomers. In this variant structure, the main crystal-packing interactions are loops CE, loop AB-α-helix and loops FG; these interactions are disturbed by I-DOX, leading to the disruption of the amyloid-like oligomer. Although the structures of TTR Leu55Pro intermediate and fibrils are different, it is conceivable that in TTR amyloid fibrils the interactions described above also occur and that I-DOX acts in a similar mode.

The concentration study revealed that I-DOX holds its maximum activity towards fibrils disruption at 10^{-5} M/100 μg fibrils, which is within the range of concentrations regularly used in amyloid related studies. Anthracyclines are a well-known category of compounds used in clinical practice and constitute a promising group of drugs to be used in treatment of amyloidosis. A recent clinical trial work reports the study of I-DOX dosage in patients with AL amyloidosis (Gertz *et al.*, 2002). Patients received I-DOX at a dose of 15 mg per m^2 once a week for 4 consecutive weeks, repeated every 3 months up to 4 times. The study aimed at developing a dosing schedule to confirm previous reports (Gianni *et al.*, 1995)

where higher doses were used (up to 30 mg per m^2). The work by Gertz and colleagues (2002) reveals improvement of symptoms in a small number of patients but concludes that it failed regarding the decision of the dosage criteria. Nevertheless, the toxicity was minimal and future investigations concerning pharmacokinetic studies are planed. The results obtained infer the need for optimization of the conditions in each particular situation.

I-DOX belongs to a class of chemotherapeutic agents presenting cardiotoxicity as the most important side effect. Nevertheless, this compound is clearly less cardiotoxic than the parental drug, doxorubicin (DOX) both in animal models (Podesta *et al.*, 1994; Villani *et al.*, 1988; Danesi *et al.*, 1990) and in humans (Mross *et al.*, 1990; Villani *et al.*, 1991). However, and due to its cardiotoxicity, I-DOX use has been limited to AL-related amyloidosis, caused by a neoplastic plasma cell population in the bone marrow. Efforts should be made to find other I-DOX related compounds with anti-amyloidogenic activity but producing fewer side effects. We tested a group of compounds I-DOX related and demonstrated that they all behave like I-DOX, i.e. disrupters. Two of those compounds showed fibril disruption ability comparable to I-DOX (100% fibrils disruption) by generating round particles similar to the native protein. For the same concentrations, the other compounds tested partially disrupted the fibrils formed for 15 days upon incubation, resulting in a mixture of fibrils of various lengths, short non-fibrillar particles and round structures. However, these drugs may play an important role for structural comparative studies and thus, further studies must be conducted.

Screening for compounds capable of inhibiting and /or disrupting amyloid fibrils must pay great attention not only to the compound toxicity but also to the toxicity of the structures resulting from the action of these drugs. The toxicity associated with Aβ species has been generally determined based on the 3-(4,5-dimethyl-2-thiazolyl)-2,5-diphenyl-2H-tetrazolium bromide (MTT) reduction assay as a measure of apoptosis. However, the nature of the biological activity assessed by this method is unknown. Apoptosis involves the activation of a proteolytic cascade where caspases have a determinant role (Hengartner, 2000). Among the caspases, caspase-3 has been shown to play an imperative role, as it is activated late in apoptosis. We first studied the toxicity associated with the different species formed during TTR Leu55Pro fibril *in* vitro assembly and demonstrated that non-fibrillar initial aggregates are toxic to a Schwanoma cell line, as measured by caspase-3 activation. In contrast, soluble protein and long fibrils did not produce significant caspase-3 activation.

This data is in line with other observations reported: in Alzheimer's disease, the mean level of soluble Aβ is increased and correlates very well with disease severity (McLean *et al.*, 1999; Naslund *et al.*, 2000); the SH3 domain from bovine phosphatidyl-inositol-3'-kinase (PI3-SH3) and the amino terminal domain of the *Escherichia coli* HypF protein (HypF-N) have been shown to form fibrils *in vitro* under appropriate conditions (Guijarro *et al.*, 1998; Chiti *et al.*, 2001). Very recently, it has been demonstrated that species formed very early in the aggregation process of these proteins are highly toxic to a fibroblast cell line while the related fibrillar structures do not produce significant effect (Bucciantini *et al.*, 2002). We also determined the toxicity of the species generated upon I-DOX treatment again by assessing caspase-3 activation in the same Schwanoma cell line. TTR Leu55Pro initial aggregates treated with I-DOX for 3 days retained cytotoxicity whereas the round particles resembling soluble TTR produced after 15 days of incubation with I-DOX produced non significant caspase-3 activation. However, a filter assay revealed that these species are not soluble. Consequently, different studies must be conducted to study how the tissue processes the generated insoluble material. It as been shown that the receptor for advanced glycation end products (RAGE) interacts with TTR fibrils triggering the activation of nuclear transcription factor kB (NF-KB) (Sousa *et al.*, 2000d). Using the RN22 cell line, anti-RAGE abolished caspase-3 activation induced by TTR fibrils suggesting toxicity of TTR fibrils to be a RAGE mediated process (Sousa *et al.*, 2001b). *In vivo* it was observed that RAGE expression is increased in FAP tissues overlapping with TTR deposition and increased with the progression of the disease. Therefore, future *in vivo* studies using I-DOX are necessary to quantify RAGE, inflammatory and oxidative stress gene expression in FAP tissues.

Several other compounds have been reported as amyloid inhibitors, in particular in Alzheimer's disease. Some, like laminin, were found to inhibit the fibrillogenesis (Monji *et al.*, 1998) and even depolymerize pre-formed fibrils (Morgan and Inestrosa, 2001); however, the result of this interaction on laminin is not known, and it is possible that it may disrupt laminin normal function, including its role on neuronal survival. Others, like short synthetic peptides, showed the capacity of both inhibiting and disaggregating amyloid fibrils (Soto *et al.*, 1998) but they are not suitable for clinical use and several chemical modifications of their structure are necessary. Antibodies have also been subject of studies with the aim at interfering with amyloid formation (Frenkel and Solomon, 2001; Heiser *et al.*, 2000).

A group of tetracyclines based on structural analogies with Congo red and I-DOX were experimentally tested and shown not only to inhibit Aβ self-aggregation but also to disrupt pre-formed Aβ-amyloid aggregates (Forloni *et al.*, 2001). Tetracycline also affects the properties of synthetic prion protein (PrP) aggregation by disrupting the fibrils and reverts the protease-resistence of PrP^{Sc} from Creutzfeldt-Jakob disease (CJD) patients (Tagliavini *et al.*, 2000). Doxycycline, a tetracycline derivate, is readily accessible to the central nervous system (CNS) (Yrjanheikki *et al.*, 1998) and thus, makes it particularly interesting, especially for amyloid diseases with involvement of the central nervous system. It has been recently shown that another derivate of tetracycline, minocycline, exerts a neuroprotective effect in a transgenic model of Huntington disease (Chen *et al.*, 2000). In this process, inhibition of caspase-1 and –3 has been proposed as a potential mechanism responsible for this drug effect. However, there are no reports on minocycline action on amyloid fibrils and other effects such as neuroprotection besides the anti-amiloidogenicity of the others tetracyclines mentioned is not known. Thus, tetracycline and derivatives needed further testing for their ability to prevent amyloid deposition (either by inhibiting or disrupting fibrils) and neuroprotection through caspase inhibition. Compounds showing both effects would constitute an added value in the study of amyloidosis.

Our results suggested tetracyclines as TTR fibril disrupters but not as inhibitors. Doxycicline was able to completely destroy TTR fibrils, while rolitetracycline displayed partial activity. The finding that tetracyclines do not inhibit TTR fibril formation in contrast to the inhibition provoked in Aβ aggregation, probably reflects structural differences between TTR and Aβ unfolded intermediates. The disruption ability of this class of antibiotics is present towards both amyloid fibrils implying the recognition of a common motif present in amyloid fibrils.

It has been hypothesized that hydrophobic interactions mediated by the C-terminal portion of Aβ are important for fibril stability (De Felice *et al.*, 2001), leading to the investigation of hydrophobic compounds effective in destabilizing and disaggregating amyloid fibrils. The results showed that 2,4-dinitrophenol (DNP) and 3-nitrophenol (NP), the two compounds tested, possessed both inhibitory and disrupter activities. Our data supports only the latter, and DNP was shown the most active. Thus, DNP might additionally recognize a common amyloid fibril motif.

The work here described provides a strategy for studying compounds affecting the amyloidogenic cascade, allowing both the assessment of the stage affected and the relevance of the results by determining the toxicity of the generated species.

Acknowledgments

This work was supported in part by a grant (35785/99) and a PhD scholarship (BD/15725/98 to Isabel Cardoso) from Fundação para a Ciência e Tecnologia, Portugal. We thank Paul Moreira for his excellent technical assistance in the preparation and purification of recombinant TTR Leu55Pro.

Chapter IV

Screening for compounds affecting transthyretin fibrillogenesis

Screening for compounds affecting Transthyretin amyloidogenesis

Cardoso, I.[1, 2] and Saraiva, MJ[1, 2]

[1] Amyloid Unit, Institute for Molecular and Cell Biology and [2] Institute for Biomedical Sciences of Abel Salazar, Porto University, Porto, Portugal.

Running title: Screening for TTR inhibitors

Correspondence to: M. J. Saraiva, Amyloid Unit, IBMC, Rua do Campo Alegre, 823, P-4150-180 Porto, Portugal. Fax: +351 22 609 9157, Tel.: +351 22 607 4900, E-mail: mjsaraiv@ibmc.up.pt

Abstract

It is believed destabilizing the tetrameric fold is the basis of a series of events that lead to the formation of transthyretin (TTR) amyloid. Subtle structural changes are likely to occur, favoring tetramer denaturation and initiating the amyloid cascade. TTR mutations seem to destabilize the tetramer and therefore, increase the amyloidogenic potential of the protein. In order to address amyloidogenesis several engineered variants have been constructed.

We evaluated the possibility of using the TTR Tyr78Phe and Leu55Pro variants to study inhibition of early events in TTR amyloidogenesis. We first characterized, by transmission electron microscopy (TEM), the time course process of TTR Tyr78Phe fibril assembly, starting from the soluble tetramer under physiological conditions (PBS, pH 7.4; 37°C) and showed that this variant evolves from round particles identical to TTR WT to soluble oligomers within 48 hours and slowly aggregate; after 15 days discrete fibrils of approximately 8 nm are clearly visible. This variant was selected to study compounds able to inhibit tetramer destabilization and formation of soluble oligomers (priming).

TTR Leu55Pro was chosen to test drugs that interfere with fibril extension as its kinetic fibril assembly process during that step was previously ascertained.

In order to screen a large number of compounds, we set up an immunoreactivity assay using a monoclonal antibody (Mab15). This antibody detects subtle conformational alterations occurring in the process of priming and extension. The drugs tested included benzofurans, non-steroids anti-inflammatory molecules, tetrameric stabilizers, extracellular matrix (ECM) components, a porphyrin and aprotinin, among others. The results indicated that benzofurans are good candidates as inhibitors for both priming and extension, ranging from approximately 57% to 64% of inhibition; ibuprofen displayed intermediate strength for inhibiting priming and extension, with 20% and 37% of inhibition, respectively; with respect to the tetrameric stabilizers tested included diethylstilbestrol (DES), sulphite, a diflunisal derivative, a flufenamic acid derivative, a xanthone, and a pyridine derivative. DES presented activity against both stages inhibiting the process in about 50% whereas the flufenamic acid derivative presented about 50% inhibition but only against extension; 1, 3-diidroxixanthone and a pyridine derivative interfered with priming, inhibiting it by approximately 30%. Among the ECM components, laminin showed the highest activity of all compounds but only concerning the extension stage, with 70% inhibition; hemin produced over 50% inhibition in both stages and aprotinin caused 34% of inhibition of

priming. For some of the compounds the results were confirmed by TEM and seemed to correlate well.

In addition, we generated an *in vitro* cellular system for TTR intermediate/aggregate formation and for screening for inhibitors in cell culture. Constructs carrying the TTR WT, Val30Met or Leu55Pro cDNA were transfected into a rat Schwanoma cell line and studied for the ability to form aggregates by a dot blot filter assay followed by immnunodetection. The results showed that TTR Leu55Pro forms aggregates after 24 hours whereas no aggregation was detected for TTR WT and Val30Met up to 72 hrs. The formation of aggregates by TTR Leu55Pro was not lysosome dependent and seemed to occur extracellularly. Moreover, TTR Val30Met and Leu55Pro reacted with Mab15 prompting this cellular model as a potential tool in the study of conformational changes occurring very early and prior to TTR dissociation and aggregation.

Keywords: Transthyretin; amyloid; priming; fibril extension; intermediate species.

Screening for TTR inhibitors

Introduction

The knowledge acquired in the last years on structural and biochemical features characteristic of amyloidogenic intermediates, paved the way for the investigation of drugs capable of interfering early on the amyloidogenic pathway. For TTR related amyloidosis, the first step of intervention is to obstruct tetramer dissociation and thus, prevent potential species from being generated (hereafter designated as **priming**). A second target is to inhibit the association between intermediate species that lead to fibril elongation (hereafter designated as **extension**). Several authors have reported the identification of compounds capable of inhibiting TTR fibril formation (Klabunde *et al.*, 2000; Oza *et al.*, 1999; Baures *et al.*, 1998; Baures *et al.*, 1999). However, most of these studies were performed under non-physiological acidic conditions, which are believed to induce rapid conformational changes and no specific distinction is made regarding the species affected by those drugs. In these studies, the methodology used consisted in measuring the turbidimetry of the samples in the presence of absence of inhibitors and thus, polymerazation into soluble oligomeric species might have gone undetected.

Other tools need to be developed to assess TTR fibrillogenesis under physiological conditions, namely to detect early subtle conformational changes. In this regard, an engineered TTR variant, TTR Tyr78Phe has recently been proposed as an early intermediate in the amyloidogenic cascade. This mutant is recognized by a monoclonal antibody raised against an engineered synthetic TTR with a triple substitution at positions 53, 54 and 55 (Gly53Ser, Glu54Asp, Leu55Ser) (Goldsteins *et al.*, 1999). The observation that Mab15 reacts with sera of patients with different TTR mutations, but not with sera of normal individuals, further suggests the presence of modified circulating soluble TTR species in FAP patients (Palha *et al.*, 2001), and increases the significance of the Mab15 antibody in recognizing conformational intermediates.

In the present study we used this antibody to investigate the ability to recognize intermediary species in fibrillogenesis. Therefore, studying the reactivity of this antibody towards different species formed *in vitro* was applied as mean for screening compounds able to inhibit subtle TTR *in vitro* conformational changes.

Cellular systems, not yet available for TTR, represent a more physiological approach to study inhibitors of amyloidogenesis *in vitro*. Such systems do not require isolation of the target protein, enable to follow up of the complete amyloidogenic process, and include

modulating factors such as chaperones and the eventual cellular processing of the formed fibrillar structures. We developed a cellular system to study the kinetics and dynamics of TTR amyloid formation.

Screening for TTR inhibitors

Materials and Methods

Isolation and purification of TTR

TTR proteins were produced in an *E. coli* expression system (Furuya *et al.*, 1991), isolated and purified as previously described (Almeida *et al.*, 1997). Briefly, after growing the bacteria, the protein was isolated and purified by preparative gel electrophoresis after ion exchange chromatography. Protein concentration was determined using the Lowry method (Lowry *et al.*, 1951).

Preparation of amyloid fibrils

TTR Tyr78Phe was dialyzed against phosphate buffered saline (PBS) and incubated at 37°C at 2 mg/ml.

TTR Leu55Pro was dialyzed against water pH ~ 7.0 and concentrated to 5 mg/ml. At this point the preparation was centrifuged at 15,000 g for 30 minutes at 4°C. The pellet was then washed and re-suspended in PBS, at 2 mg/ml and incubated at 37°C.

Fibril concentrations were assessed by the Lowry method (Lowry *et al.*, 1951).

At given time points, samples were analyzed by transmission electron microscopy (TEM).

Transmission electron microscopy (TEM)

For visualization by TEM, sample aliquots were diluted (1:50) in PBS and immediately adsorbed to glow-discharged carbon-coated collodion film supported on 200-mesh copper grids. For negative staining, grids were washed with deionized water and stained with 1% uranyl acetate. The grids were visualized with a Zeiss microscope, operated at 60kV. Measurements of fibril widths and lengths were made from enlarged prints of the electron micrographs using a magnifying glass with a built-in calibrated ruler.

Screening for compounds

A series of compounds were tested for the ability to inhibit TTR priming and/or extension. The different drugs were included into 6 groups:

Group 1 (control)- compounds able to disrupt amyloid fibrils, enabling priming and extension, as previously described (chapter III): tetracycline (Sigma); tetracycline derivatives rolitetracycline and doxycycline (a kind gift of the Department of Neuroscience, SmithKline Beecham_Pharmaceuticals, UK); 2,4-dinitrophenol (DNP) and 3-nitrophenol

(NP) (Sigma).

Group 2- six benzofuran compounds (a kind gift of the Department of Neuroscience, SmithKline Beecham Pharmaceuticals, UK), previously shown to inhibit Aβ fibrillogenesis.

Group 3- (non-steroid anti-inflammatory drugs)- diflunisal, ibuprofen, and diclofenac, purchased from Sigma.

Group 4- (tetrameric stabilizers/T_4 competitors)- diethylstilbestrol (DES) (Sigma), sulphite (Merck), modified diflunisal and modified flufenamic acid (provided by the Centro de Investigacion y Desarrolo, Barcelona), one xanthone, 1,3-diidroxixanthone (a generous gift of Dr. Madalena Pinto), and pyridine derivative, 2-amino-7-bromo-5-oxo-5H[1]benzopyrano[2,3-b]pyridine-3-carbonitrile (Aldrich). All compounds were shown to compete with T_4 by ^{125}I-T_4 competition binding assays; sulphite and modified diflunisal were also shown to stabilize the tetramer by isoelectric focusing, by Drs. Rosário Almeida and Bárbara Macedo; the methodology has been previously described (Almeida *et al.*, 2000).

Group 5- (ECM compounds)- heparin, dextran sulphate, heparan sulphate, laminin, fibronectin and matrix gel (Sigma).

Group 6- (others)- Hemin (a porphyrin kindly provided by the Department of Neuroscience, SmithKline Beecham Pharmaceuticals, UK), aprotinin (Sigma) and aprotinin peptide (APR2, residues 16-37).

The compounds were weighted and dissolved at approximately 10 mg/ml in dimethylsulphoxide (DMSO), with the exception of sulphite, aprotinin, aprotinin peptide and the ECM components that were dissolved in water. Soluble TTR Tyr78Phe and Leu55Pro aggregates prepared were incubated with or without each one of the compounds above described at a molar ratio 1:10 for 48 hours at 37°C. Control samples were incubated with DMSO or water alone.

Anti-fibrillogenic activity was tested by immunoassay and/or TEM.

Immunoassay for priming/ extension

96 well plates (Maxisorp-Nunc) were coated for 1 hour at 37°C with 1:500 diluted polyclonal rabbit anti-human TTR (Dako) and blocked overnight at 4°C with 5% skim milk in PBS. Soluble TTR WT, soluble TTR Tyr78Phe, and Leu55Pro initial aggregates, with or without drugs, were applied to the wells (2 μg/100 μl) for 1 hour at 37°C, followed by incubation with Mab15 (1:10 in PBS) for another hour. Peroxidase conjugated anti-mouse

Screening for TTR inhibitors

IgG (Amersham) 1:5000 was used as secondary antibody and development was performed with 2,2`-azino-bis (3-ethylbenzthiazoline-6-sulfonic acid) (ABTS, Sigma) / H_2O_2 (Merck). For each compound a minimum of two independent experiments, each of which analyzed in duplicate, were performed.

Vector constructions

Vectors p169ZT carrying human wt TTR (p169ZT-hTTRwt) and p169ZT carrying human TTR Leu55Pro (p169ZT-hTTR55) (figure 1) were available in the laboratory (Sousa *et al.*, submitted). These constructs were obtained as follows: pBluescript II KS (pKSII) (Stratagene) carrying the sheep methalothionein promoter-1 (SMT-1) between *Eco*RI and *Bam*HI sites (this vector was termed p169 and was kindly provided by Dr Kevin Ward, Commonwealth Scientific and Industrial Research Organization, Australia) was cut with *Sac*I, blunted with T_4 DNA polymerase by standard procedures, and subsequently digested with *Bam*HI. All the restrictions were made following the manufacturer's instructions for each enzyme. The β-globin splice site (β-SS) and the SV40 poly A tail (pA) were excised from pZT (a generous gift of Dr. José Belo, IGC Portugal) with *Kpn*I and *Bam*HI. The *Kpn*I site of the above excised insert was blunted with T_4 DNA polymerase I and the insert was subcloned in *Sac*I blunted- *Bam*HI sites of p169. The vector so generated, carrying SMT-I, β-SS and pA was termed p169ZT (Figure 1a). Both the splice site and the polyA tail were used to ensure a correct transcription and mRNA processing since this vector was used to subclone TTR cDNA and not a genomic clone. Human WT TTR full-length cDNA, available in the laboratory, was excised from pKSII with *Eco*RV and *Not*I. The TTR insert was cloned in *Nhe*I blunted (using Klenow fragment of DNA polymerase I by standard procedures) site of p169ZT (Figure 1b). The Leu55Pro mutation was inserted by site-directed mutagenesis using the Quickchange mutagenesis kit (Stratagene) following the manufacturer's instructions and the appropriate primers: 5`-TCTGGAGAGCCGCATGGGCT-3` and 5`-AGCCCATGCGGCTCTCCAGA-3`. We further generated the construct carrying the Val30Met TTR mutation by site directed mutagenesis as described above and using the following primers: 5'-AATGTGGCCATGCATGTGTTC-3' and 5'-GAACACATGCATGGCCACATT-3'.

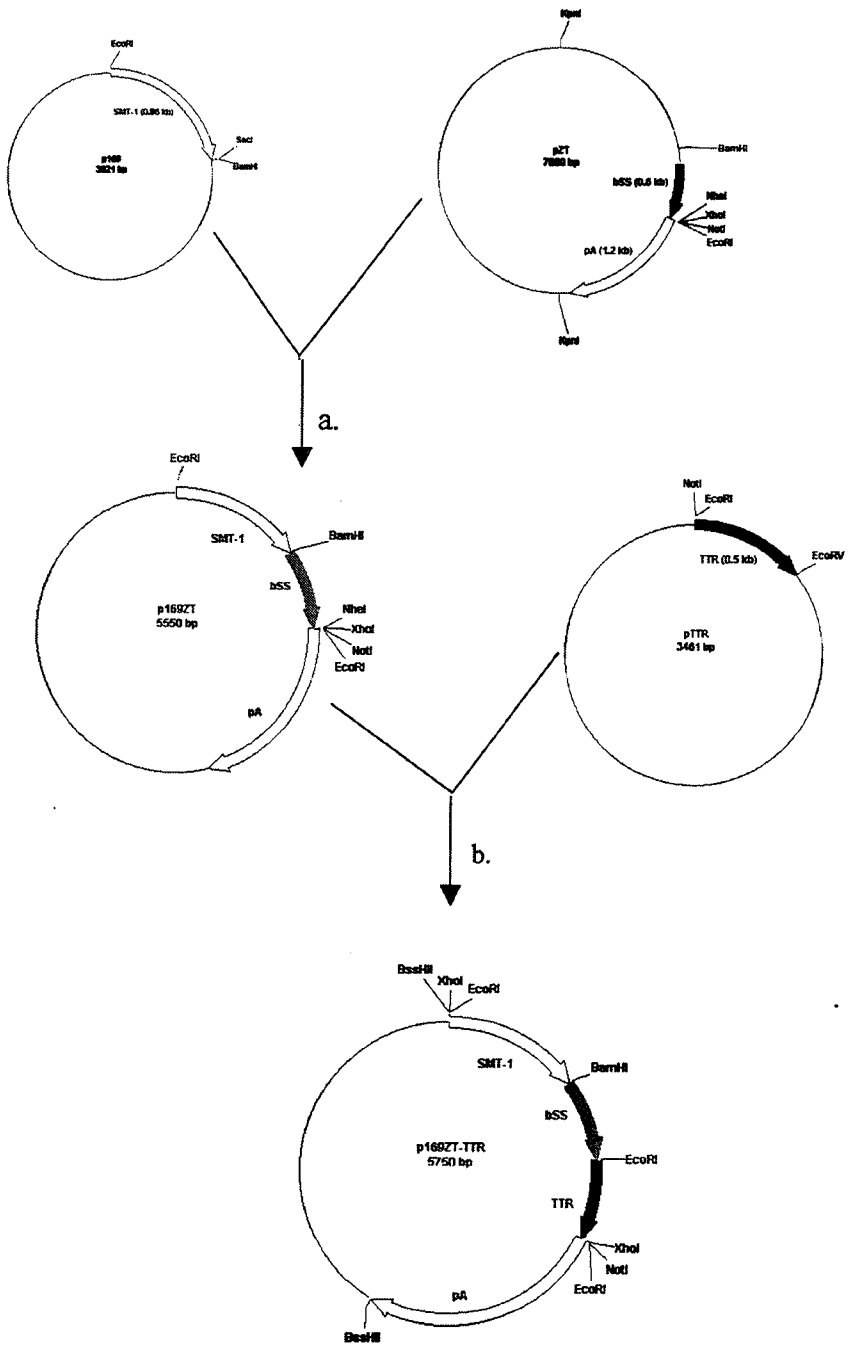

Figure 1- Schematic representation of p169ZT-TTR vector construction.

In this figure, TTR can either represent human TTR WT, Val30Met or Leu55Pro.

Screening for TTR inhibitors

Transfection and TTR expression in cell culture

Rat Schwanomas (RN22) (American Type Cell Collection) were stably co-transfected with each of the constructs carrying the TTR cDNA (WT, Val30Met or Leu55Pro) plus a plasmid with resistance to neomycin (pLNeo, kindly provided by Dr. Paulo Vieira, IGC, Portugal), following the $CaPO_4$-DNA precipitate method (Sambrook *et al.*, 1989). Briefly, cells were grown to approximately 30-50% confluence in 10 cm dishes (Costar). 25 μg of the appropriate plasmid carrying the TTR cDNA plus 5 μg of pLNeo purified using QUIAGEN columns were ressuspended in 500 μl of 250 mM $CaCl_2$ and diluted with 500 μl 2X Hepes-buffered saline (2X HeBS). The $CaPO_4$-DNA precipitate was allowed to form by standing the mixture 20 min at room temperature and was subsequently added to the cells. After 5 hours incubation, cells were washed twice with phosphate-buffered saline (PBS) and fed with 10 mL complete medium. 24 hours later, transfection medium was replaced by complete medium supplemented with G418 (1 mg/mL). Resistant colonies arose approximately after 7 days of selection and were isolated and separated over the course of the following weeks.

Quantification of TTR

The presence of TTR in conditioned media of cells transfected with constructs bearing human TTR (p169ZT-hTTRWT, Met30 and Pro55) was tested by quantitative enzyme linked immunoreactive assay (ELISA) (Sousa *et al.*, 2000a): 96 well plates (Maxisorp-Nunc) were coated overnight at 4°C with 1:500 diluted polyclonal rabbit anti-human TTR (DAKO) and blocked with 5% skim milk in PBS; each sample, diluted in PBS, was applied to the wells for 1 h at room temperature; as secondary antibody, peroxidase conjugated anti-human TTR (The Binding Site) 1:500 diluted in PBS-0.05% Tween 20 (PBS-T) was used. Development was performed with ABTS (Sigma) / H_2O_2 (Merck).

For all constructs, experiments were performed both in the absence and presence of 100 μM $ZnSO_4$ in the cell culture media in order to test activation of the sheep MT-1 promoter.

Immunoprecipitation

Selected cells expressing TTR and induced with 100 μM $ZnSO_4$ were grown to approximately 100% confluence in complete medium. Complete medium was then replaced by ^{14}C-Leucine containing medium, which was subsequently collected 4 hours later. Cells were harvested and then lysed with 1 ml of lysis solution (30 mM Tris pH 7.5, 300 mM

NaCl, 1% triton x-100, 10 μM PMSF), centrifuged 30 minutes at 14,000 rpm. The pellet was discarded and the supernatant collected.

Both medium and cell supernatant were incubated with rabbit anti-human TTR 1:20 (Dako) overnight at 4°C with agitation. Next, 150 μl of protein A sepharose (62.5 μg/μl in 30 mM Tris pH 7.5) (CL-4B, Pharmacia) were added and allowed to incubate for 1 hour at room temperature with agitation. The immunoprecipitated complex was washed 3 times with washing solution (30 mM Tris pH7.5, 300 mM NaCl, 1% triton x-100) and the complex eluted with SDS loading buffer. Finally, samples were separated on a 15% polyacrylamide gel under denaturing conditions (SDS-PAGE) and processed for autoradiography.

Dot blot filter assay for aggregate detection

Cells expressing TTR as well as non-transfected RN22 induced with $ZnSO_4$ for 3 days were grown to about 80% confluence and then incubated with serum-free medium for different periods of time. In one set of experiments cells were also incubated with chloroquine 10 μM in serum-free medium for 24 hours.

TTR in the medium was quantified by ELISA as described above, and 500 ng were applied onto a 0.2 μm pore cellulose acetate membrane filter (Schleicher & Schuell) using a manifold system (Gibco BRL) under vacuum to separate soluble proteins from aggregates. The filter was washed 3 times with PBST and processed for TTR immunodetection. Briefly, the membrane was blocked with 5% skim milk in PBS for 1 hour at room temperature, and then incubated with 1:500 rabbit anti-human TTR (Dako) for another hour; anti-rabbit HRP 1:500 was used as secondary antibody. Detection was performed with enhanced chemiluminescence (ECL, Amersham).

Western blotting

Alternatively, after applying the medium on the membrane filter, the area of each dot was cut and boiled with SDS loading buffer. The material removed was run on a 15% denaturing acrylamide gel and then transferred to a nitrocellulose membrane (Amersham). The membrane was blocked with 5% skim milk in PBS for 1 hour at room temperature and then incubated with 1:500 rabbit anti-human TTR (Dako) for another hour at room temperature; as secondary antibody, 1:5000 peroxidase-conjugated anti-rabbit IgG (Amersham) was used. Development was performed with 3', 3'-diaminobenzidine (DAB) (Sigma).

Screening for TTR inhibitors

Immunoassay for conformational changes in TTR in cell culture

Transfected cells were grown and induced to express TTR as previously described. Serum-free media was collected at different time points and TTR quantified by ELISA, as already described. The reactivity with Mab15 antibody was assessed using the same amount of mutant or WT TTR in each well, following the conditions described for the immunoassay of priming and extension.

Results

1- Priming – morphological characterization

TTR Tyr78Phe variant was designed with the purpose of destabilizing the AB loop (Redondo *et al.*, 2000b) thought to be involved in amyloidogenesis. The resulting mutated protein revealed to be very prone to fibril formation under acidic conditions as assessed by thioflavin T binding.

We investigated the capacity of TTR Tyr78Phe to aggregate and form amyloid-like fibrils under physiological conditions (PBS pH 7.4, 37°C). Morphologically, soluble TTR Tyr78Phe appears as rounds particles identical to native TTR WT. After 24 hours at 37°C, no alterations were visible under the electron microscope (figure 2A). The protein started to aggregate and within 48 hours, oligomeric species were clearly visible (figure 2B), increasing after 4 days (figure 2C). Further incubation extended the degree of aggregation and at 8 days large clusters of aggregated protein as well as short pre-fibrillar structures were visualized (figure 2D). This material organized into well-defined amyloid-like fibrils after 15 days (figure 2E).

The morphological data presented here reinforces the biochemical evidences suggesting that this variant possesses a high amyloidogenic potential. Moreover, the morphological characterization of TTR Tyr78Phe aggregation pathway from the soluble counterpart enables us to test compounds that may inhibit fibril formation. In particular, the changes taking place within 48 hours, most probably corresponding to early tetrameric dissociation and unfolding events provide an opportunity to screen for compounds that inhibit the priming stage.

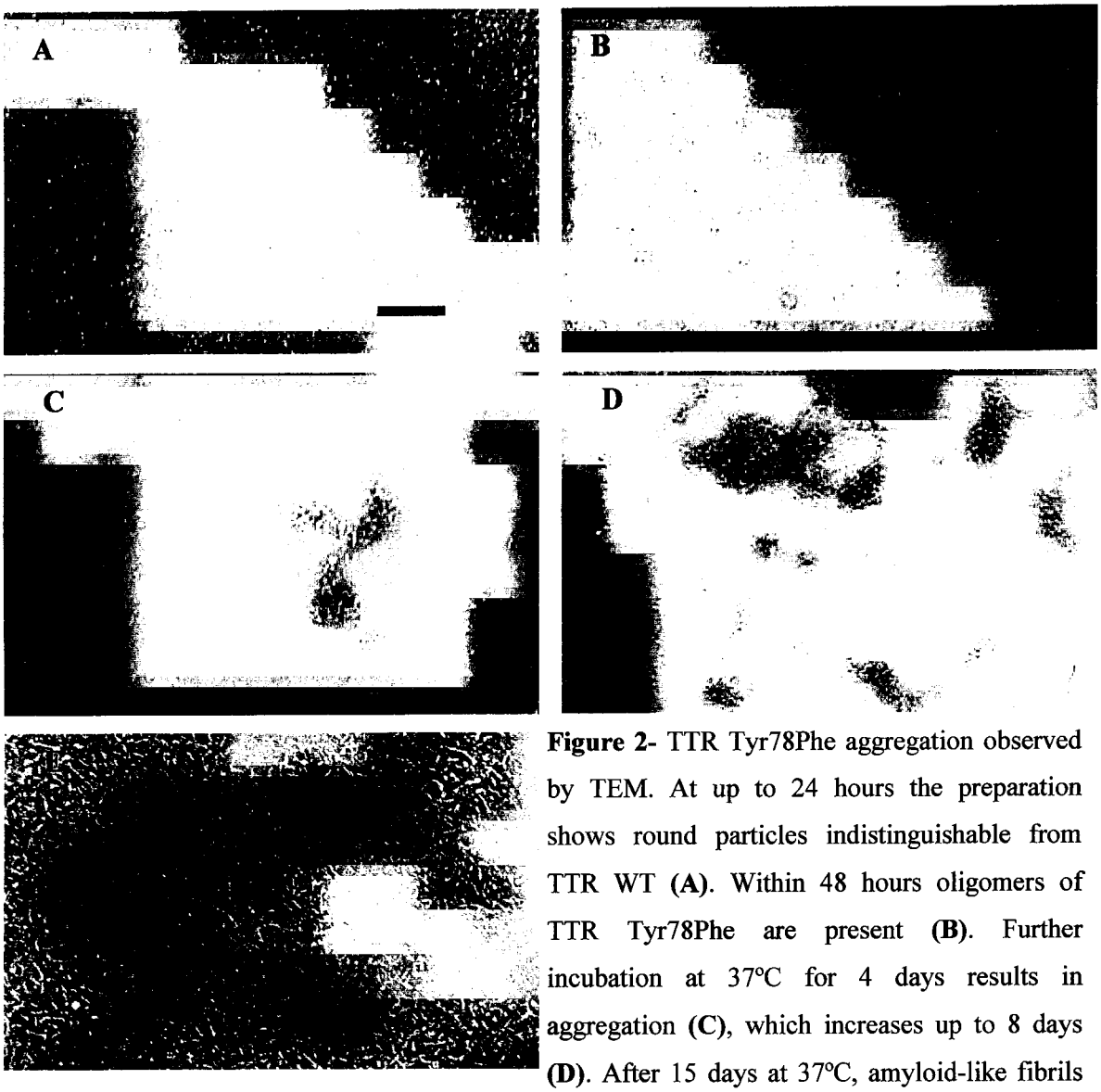

Figure 2- TTR Tyr78Phe aggregation observed by TEM. At up to 24 hours the preparation shows round particles indistinguishable from TTR WT **(A)**. Within 48 hours oligomers of TTR Tyr78Phe are present **(B)**. Further incubation at 37°C for 4 days results in aggregation **(C)**, which increases up to 8 days **(D)**. After 15 days at 37°C, amyloid-like fibrils are observed **(E)**. Scale bar (A-F) = 100 nm.

2- Extension- morphological characterization

The extension stage refers to the association of potential amyloidogenic species generated during the priming period; it also relates to fibril elongation.

We previously characterized this phase in chapter II using the TTR Leu55Pro variant; in the extension reaction we used TTR Leu55Pro initial aggregates instead of soluble TTR Leu55Pro.

3- Immunoassay

Although transmission electron microscopy allowed the ultrastructural characterization of fibril assembly and the identification of several different species present throughout the process, this method, apart from being time consuming, does not enable the detection of subtle structural modifications or their quantification. Aiming at screening a considerable amount of drugs, we therefore investigated the possibility of studying the progress of fibrillogenesis by immunoreactivity with the specific monoclonal antibody Mab15 that recognizes cryptic epitopes of TTR amyloid and modified soluble TTR.

3.1- Immunoassay for priming

A previous work demonstrated that Mab15 reacts with soluble TTR Tyr78Phe in the sandwich ELISA (as described in Material and Methods) (Redondo *et al.*, 2000b) but does not recognize TTR WT or Leu55Pro under the same conditions. Here we investigated the immunoreactivity of the species generated upon incubation of TTR Tyr78Phe at 37°C for 48 hours under the same conditions.

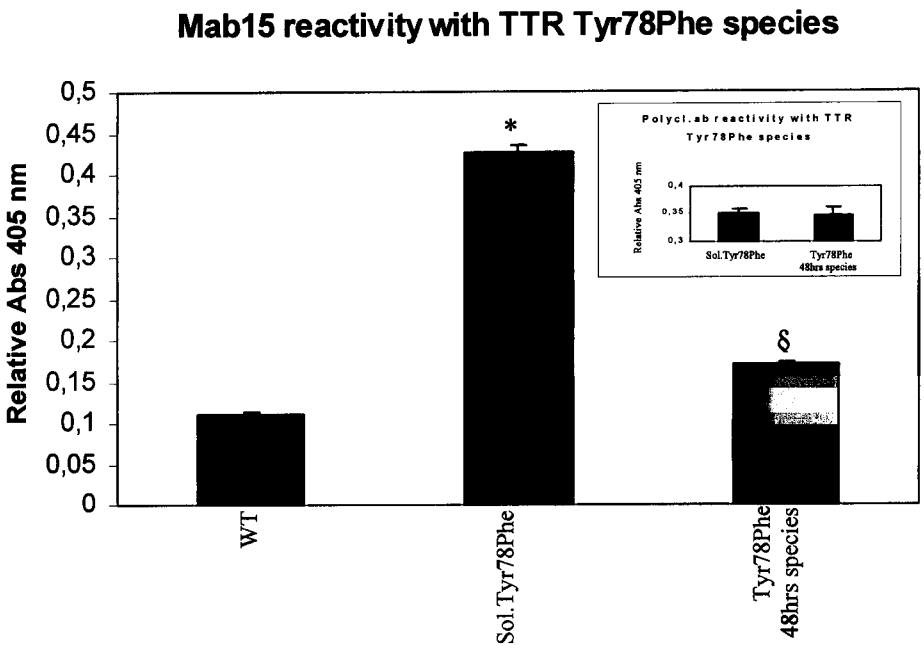

Figure 3- Mab15 reactivity towards TTR Tyr78Phe species. Soluble TTR WT (Sol.WT) does not react with this antibody while soluble TTR Tyr78Phe (Sol.Tyr78Phe) is recognized. Immunoreactivity against TTR Tyr78Phe species decreases upon incubation for 48 hours at 37°C (Tyr78Phe 48hrs species). (* $p < 0.0005$; § $p < 0.004$). **Inset:** soluble TTR Tyr78Phe and TTR Tyr78Phe 48 hours species tested with an anti-human TTR polyclonal antibody showed no differences in affinity.

While Mab15 does not recognize WT, soluble TTR Tyr78Phe strongly reacts with the antibody (figure 3). However, after 48 hours of incubation the reactivity is 2.5-fold decreased compared to the soluble TTR Tyr78Phe (figure 3), suggesting that conformational changes occurred upon incubation, leading to a decrease of the specific epitopes available for antibody recognition. These conformational changes are most probably related to aggregation, which occurs readily with this variant.

The ability provided by Mab15 in discriminating between native TTR Tyr78Phe and species lacking the tetrameric fold, constitutes an opportunity to identify drugs inhibiting the priming stage.

To ensure that the observed distinction of species by Mab15 was not a consequence of different affinities towards those species by the polyclonal antibody used in coating, an

immunoassay for TTR quantification (see Material and Methods) was performed using an anti-human TTR HRP antibody as secondary antibody. In this case, soluble TTR Tyr78Phe and species formed upon incubation at 37°C for 48 hours presented identical reactivity (figure 3, inset), further supporting that the differences previously detected were due to differential interaction with Mab15.

3.2- Immunoassay for extension

We also tested whether Mab15 could distinguish species formed during the extension step, using TTR Leu55Pro aggregates as the starting material.

The reactivity of this antibody was high for the initial aggregates but decreased as fibrils assembled under physiological conditions (PBS, pH 7.4, 37°C) for 5 and 15 days (figure 4). As expected soluble TTR Leu55Pro did not significantly react with Mab15. We attributed this result to lower epitope accessibility in the fibril. The different species of TTR Leu55Pro presented identical affinity to the polyclonal antibody used (figure 4, inset) and thus, the ability of Mab15 to discriminate early aggregates from fibrils enables the screen of drugs inhibitory of extension.

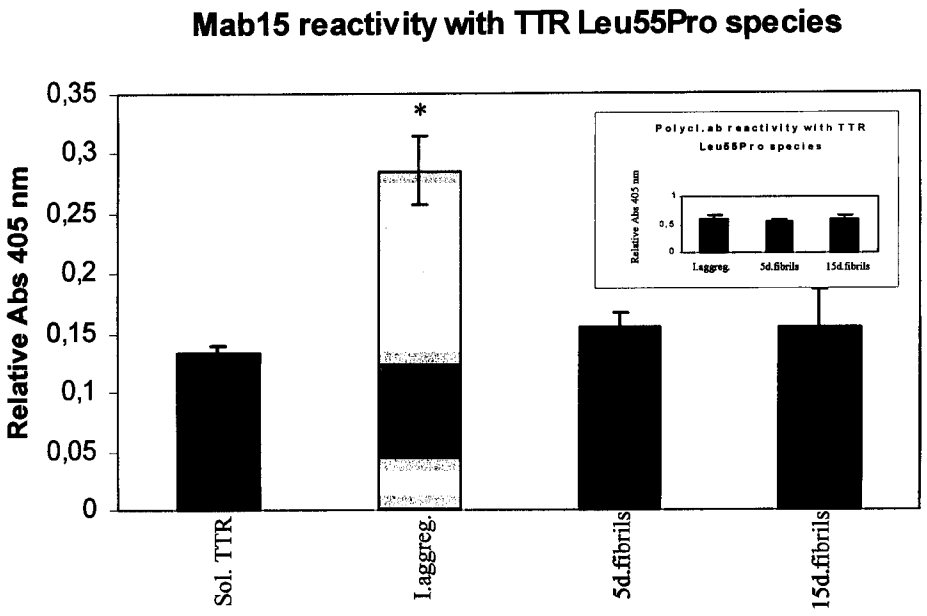

Figure 4- Mab 15 Immunoassay for different species of TTR Leu55Pro.

Reactivity of recombinant TTR Leu55Pro (Sol.TTR), TTR Pro55 initial aggregates (I.Aggreg.) (24 hours), and fibrils assembled for 5 (5d.fibrils) and 15 days (15d.fibrils) at 37°C, respectively. Mab15 reactivity is significantly decreased as TTR Leu55Pro fibrils assembled for 5 and 15 days; * $p < 0.02$. **Inset:** TTR Leu55Pro initial aggregates, 5 and 15 days fibrils, tested with an anti-human TTR polyclonal antibody, revealed identical affinity.

4- Screening of compounds interfering with TTR amyloidogenecity

A series of compounds were tested for their ability to interfere with TTR priming and/or extension and thus, to affect the reactivity of TTR species with Mab15. The drugs studied were grouped according to their structure and/or biological activity.

Table 1 discriminates the drugs tested, and figure 5 displays the structures of some of these drugs.

Table 1- Compounds tested for inhibition of priming and extension.

Compound group	Compound number	Compound name
Group 1 Control	1	tetracycline
	2	rolitetracycline
	3	doxycycline
	4	2,4-dinitrophenol
	5	3-nitrophenol
Group 2 Benzofurans	6	SKF 99130
	7	SKF 73033
	8	SKF 64346
	9	SKF79313
	10	SKF74652
	11	SB205550
Group 3 Non-steroid anti-inflammatory	12	diflunisal
	13	ibuprofen
	14	Diclofenac
Group 4 Tetrameric Stabilizers and/or T_4 competitors	15	DES
	16	sulphite
	17	modified diflunisal
	18	modified flufenamic acid
	19	1,3-diidroxixanthone
	20	2-amino-7-bromo-5-oxo-5H[1]benzopyrano[2,3-b]pyridine-3-carbonitrile
Group 5 ECM components	21	heparin
	22	dextran sulphate
	23	heparan sulphate
	24	laminin
	25	fibronectin
	26	matrix gel
Group 6 Others	27	hemin
	28	aprotinin
	29	aprotinin peptide

Screening for TTR inhibitors

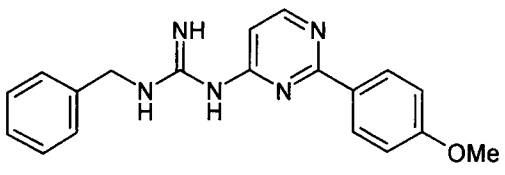

SKF 99130

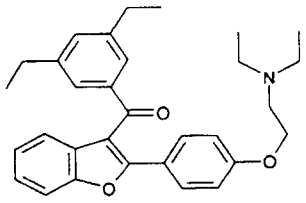

SKF 73033

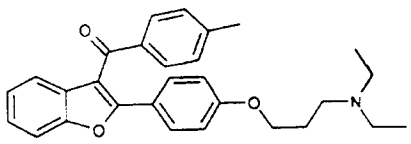

SKF 64346

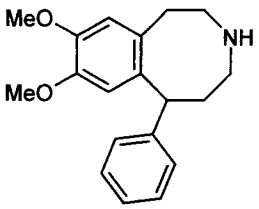

SKF 79313

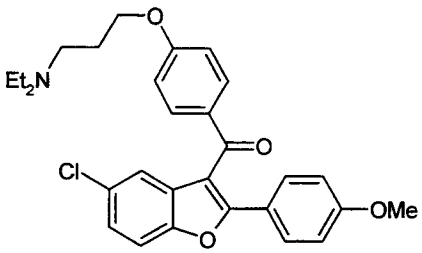

SKF 74652

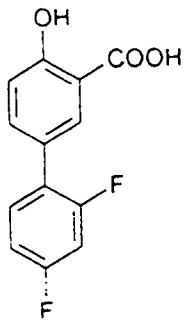

Diflunisal

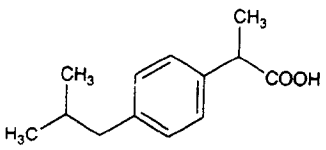

Ibuprofen

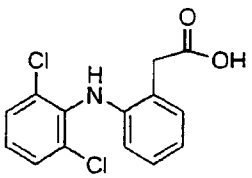

Diclofenac

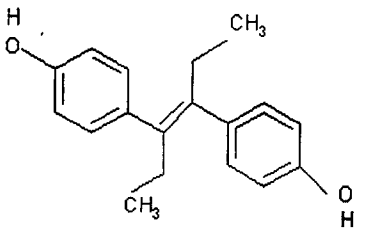

DES

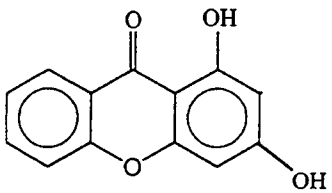

1,3-diidroxixanthone

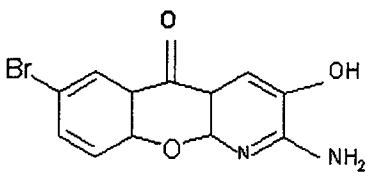

2-amino-7-bromo-5-oxo-5H[1]benzopyrano[2,3-b]pyridine-3-carbonitrile

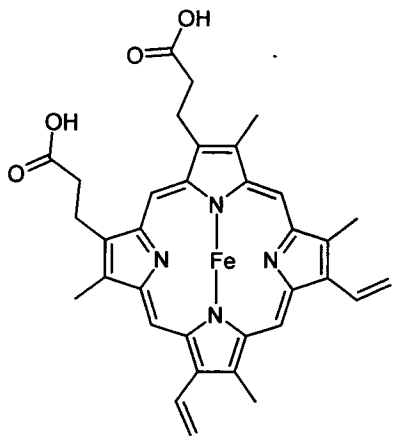

Hemin

Figure 5- Structures of some of the drugs tested for inhibition of priming and extension.

4.1- Selection of priming inhibitors- immunoassay

To select for compounds that inhibit priming, soluble TTR Tyr78Phe was incubated with or without different compounds for 48 hours at 37°C, and then tested for Mab15 reactivity (see Materials and Methods). An aliquot of TTR Tyr78Phe alone was kept at –20°C and used as control. The percentage of inhibition was calculated as follows:

% inhibition = [(Abs 405 nm (sample with inhibitor) – Abs 405 nm (sample without inhibitor)) * 100]/ [Abs 405 nm (Soluble TTR Tyr78Phe) – Abs 405 nm (sample without inhibitor)]

Figure 6 depicts the results obtained, showing the percentage of priming inhibition by each compound.

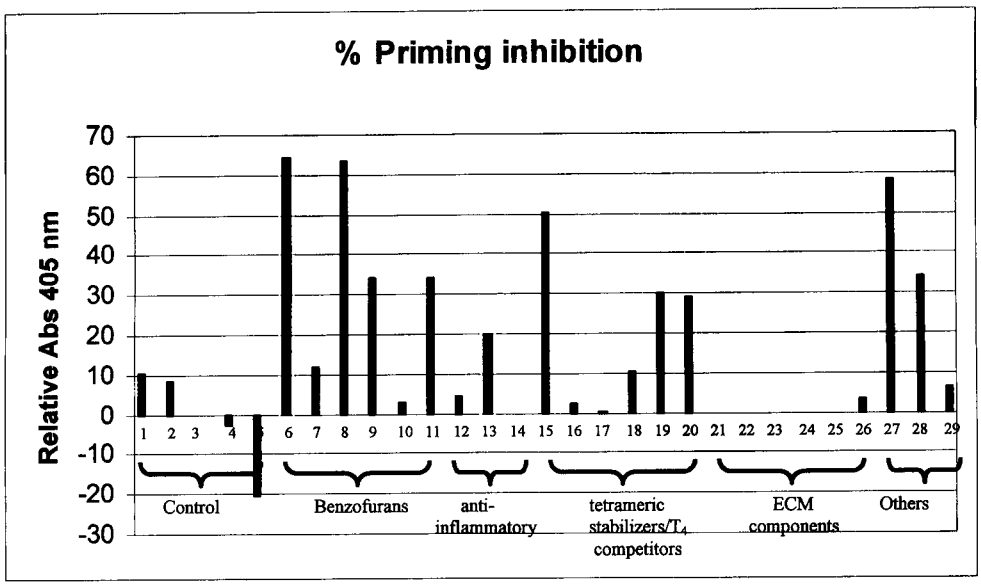

Figure 6 – Mab15 reactivity with TTR Tyr78Phe species after incubation of soluble Tyr78Phe with different drugs for 48 hours at 37°C (refer to table 1 for compound identity).

Screening for TTR inhibitors

Control samples of TTR Tyr78Phe containing the same percentage of DMSO, as the resulting from the addition of compounds, were prepared; DMSO revealed no influence in Mab15 reactivity. Control tests in which each compound was added to the TTR Tyr78Phe protein at time t = 0 were also performed and showed no influence on the reaction with Mab15 (data not shown).

Tetracycline and its derivatives and nitrophenols were used as control since they were previously shown to act primarily as fibril disrupters. The immunoassay also showed that these compounds had no inhibitory effect on both priming and extension and thus, validated this new method.

Results showed that benzofurans compounds (group 2) were among the most effective on inhibition of priming; SKF 99130 and 64346 had inhibitory capacities above 50%, while SKF 79313 and SB 205550 inhibited approximately 35% of priming; SKF 73033 and 74652 failed to efficiently inhibit TTR fibrillogenesis at this stage. Non-steroid molecules did not present important inhibitory abilities (group 3) and among the three drugs tested only ibuprofen showed some capacity, though intermediate, with 20% of priming inhibition. The 4^{th} group of compounds studied included tetrameric stabilizers and compounds that compete with T_4 for TTR binding. Inhibition of priming by these drugs varied from approximately 50% (DES) to intermediate values of approximately 30% (compound 19 and 20). Modified diflunisal and modified flufenamic acid had no activity. The group composed of ECM components presented no activity regarding inhibition of priming. Finally, the porphyrin hemin revealed about 58% of priming inhibition; aprotinin presented mild activity, with 34% whereas the peptide derived from this anti-protease showed no activity. Compounds with less than 20% inhibitory effect were not considered relevant.

4.2- Selection of inhibitors of extension- immunoassay

The same approach and the variant TTR Leu55Pro were used to screen for compounds affecting extension, using the variant TTR Leu55Pro. The percentage of inhibition was calculated as before as well as the control experiments. Figure 7 depicts the results obtained.

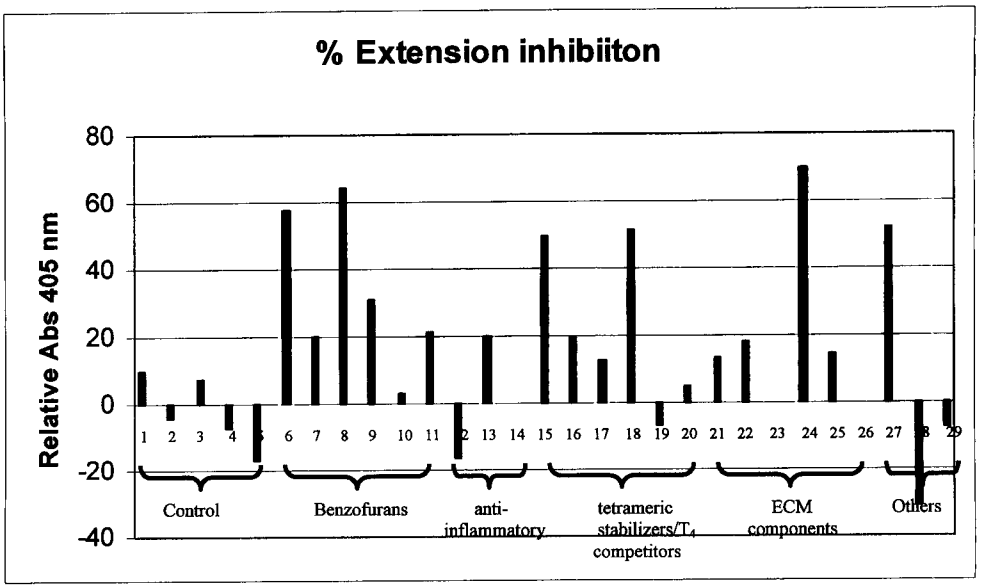

Figure 7– Mab15 reactivity with TTR Leu55Pro species after incubation of Leu55Pro initial aggregates with a series of drugs for 48 hours at 37°C.

The same group of control compounds, i.e., fibril disrupters, was used in this experiment, revealing no inhibition against TTR extension. Among the benzofurans, SKF 99130 and 64346 were the compounds with the highest inhibitory effect on TTR extension, with approximately 57% and 64% inhibition, respectively; SKF 73033, 79313 and SB 205550 showed intermediate activities and SKF 74652 had no significant effect. In the group of non-steroid anti-inflammatory drugs, only ibuprofen showed expressive inhibition (37%); in the group of the tetrameric stabilizers/T_4 competitors, DES and modified flufenamic acid were able of inhibiting extension almost by 50% whereas the remaining drugs in that group did not significantly affect extension. ECM components also did not interfere with TTR extension, with the exception of laminin, which showed the highest inhibitory effect of all

compounds tested. In the last group, only hemin presented expressive inhibition of extension with 52%.

Table 2 summarizes the results obtained for both priming and extension.

Table 2- Inhibition of TTR fibril priming and extension by different classes of compounds.

Compound group	Compound number	Compound name	% inhibition **Priming**/TTR Tyr78Phe Method- Mab15 reactivity	% inhibition **Extension**/TTR Leu55Pro Method- Mab15 reactivity
Group 1 Control	1	tetracycline	10.5	10.0
	2	rolitetracyc.	8.5	-
	3	doxycycline	-	7.5
	4	DNP	-	-
	5	NP	-	-
Group 2 Benzofurans	6	SKF 99130	64.5	57.3
	7	SKF 73033	11.7	20.0
	8	SKF 64346	63.2	64.1
	9	SKF79313	34.0	31.2
	10	SKF74652	3.0	3.0
	11	SB205550	34.1	21.5
Group 3 Non-steroid anti-inflammatory	12	diflunisal	4.5	-
	13	ibuprofen	20.0	37.0
	14	Diclofenac	-	-
Group 4 Tetrameric Stabilizers/T_4 competitors	15	DES	50.2	49.6
	16	sulphite	2.3	19.5
	17	Modified diflunisal	0.5	12.8
	18	Modified flufenamic acid	10.5	51.2
	19	1,3diidroxixanthone	30.0	-
	20	2-amino-7-bromo-5-oxo-5H[1]benzopyrano[2,3-b]pyridine-3-carbonitrile	29.0	4.9
Group 5 ECM components	21	heparin	-	13.5
	22	dextran sulphate	-	18.0
	23	heparan sulphate	-	-
	24	laminin	-	70.0
	25	fibronectin	-	14.4
	26	Matrix gel	3.4	-
Group 6 Others	27	hemin	58.3	52.0
	28	aprotinin	34.0	-
	29	Aprotinin peptide	6.4	-

4.3- Electron microscopy

To ascertain the reliability of the previous method, we investigated the influence of some of the compounds on priming and extension by TEM. Drugs with high, intermediate or no inhibitory capacity, as assessed by immunoreactivity, were tested. Due to certain batch variability, in each experiment a control preparation was included.

4.3.1- Electron microscopy- Priming inhibition

Concerning priming inhibition, after incubating soluble TTR Tyr78Phe at 37ºC for 48 hours, substantial aggregates are visible in the control preparation (figure 8, no drug). When pre-incubated with SKF 99130, no large aggregates were visible (figure 8, plus SKF 99130) and only a few oligomers were identified (figure 8, plus SKF 99130, arrow), which supports the results obtained by immunoassay (64.5% inhibition). In the presence of SKF 64346, a higher amount of oligomers and small aggregates (figure 8, plus SKF 64346, arrow) were present in the preparation when compared to the aliquot with SKF 99130, although similar results were obtained by antibody recognition (63.2% inhibition). Round particles were also present (figure 8, plus SKF 64346, arrowhead). Ibuprofen was shown to inhibit priming only by 20% by immunoassay; in fact, although the aggregates observed are not as large and numerous as in the control (figure 8, plus ibuprofen), they represent a significant portion of the material present in the respective preparation. Pre-incubation with modified diflunisal did not avoid the formation of very large aggregates after 48 hours (plus modified diflunisal) as observed in the control situation (no drug added), strengthening the results obtained by immunoassay which suggested that this compound did not inhibit TTR Tyr78Phe priming. The same results were obtained for diclofenac (data not shown).

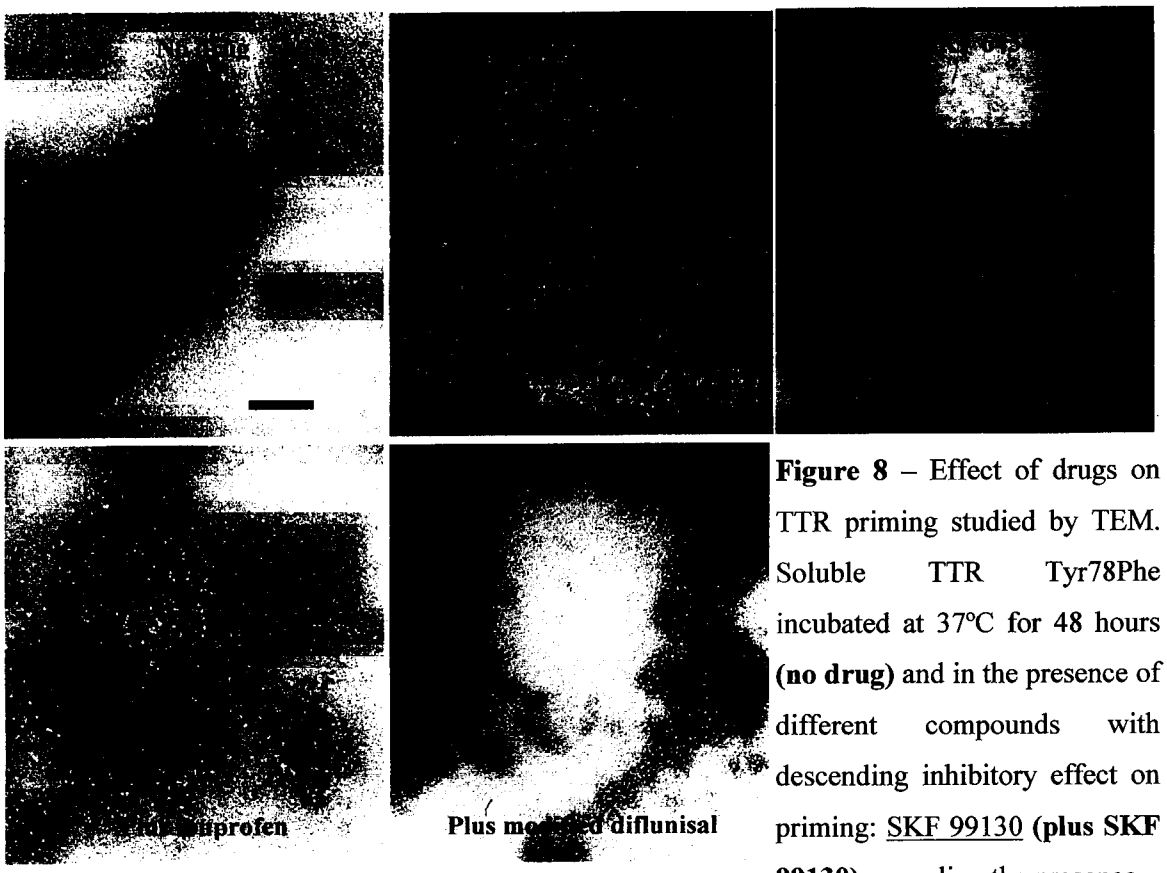

Figure 8 – Effect of drugs on TTR priming studied by TEM. Soluble TTR Tyr78Phe incubated at 37°C for 48 hours **(no drug)** and in the presence of different compounds with descending inhibitory effect on priming: SKF 99130 **(plus SKF 99130)**, revealing the presence of round particles and a few oligomers **(arrow)**; SKF 64346 **(plus SKF 64346)**, showing oligomers and small aggregates **(arrow)** and round particles **(arrowhead)**; ibuprofen **(plus ibuprofen)** and modified diflunisal **(plus modified diflunisal)**. Scale bar = 100 nm.

4.3.2- Electron microscopy- Extension inhibition

Some of the compounds were also tested by TEM for their ability to inhibit TTR Leu55Pro extension, and results are shown in figure 9.

SKF 99130 was very active at inhibiting TTR extension resulting mostly in round particles; a few short fibrils were also observed (figure 9D). SKF 64346 seemed even more active and no fibrillar structures were visible (figure 9C). The presence of round species resembling soluble protein suggests that both SFKs, in addition to inhibiting extension, also have the ability to disaggregate the initial aggregates (compare figure 9A and C). Pre-incubation with SKF 73033 also inhibited the extension stage but not as strongly as the previous compounds since fibrils were occasionally observed (figure 9E). The results obtained with hemin

suggest that it has the capacity of inhibiting extension as no fibrils like those observed in the absence of drug (figure 9B) were visualized. However, it is unable to disaggregate the initial aggregates (figure 9F), as the resulting material was very similar to the initial preparation used in this experiment (figure 9A). These results are in good agreement with those obtained by the Mab15 immunoassay. By TEM only SB205550 did not show inhibitory activity against TTR Leu55Pro extension, although the immnunoassay indicated 21,5% inhibition.

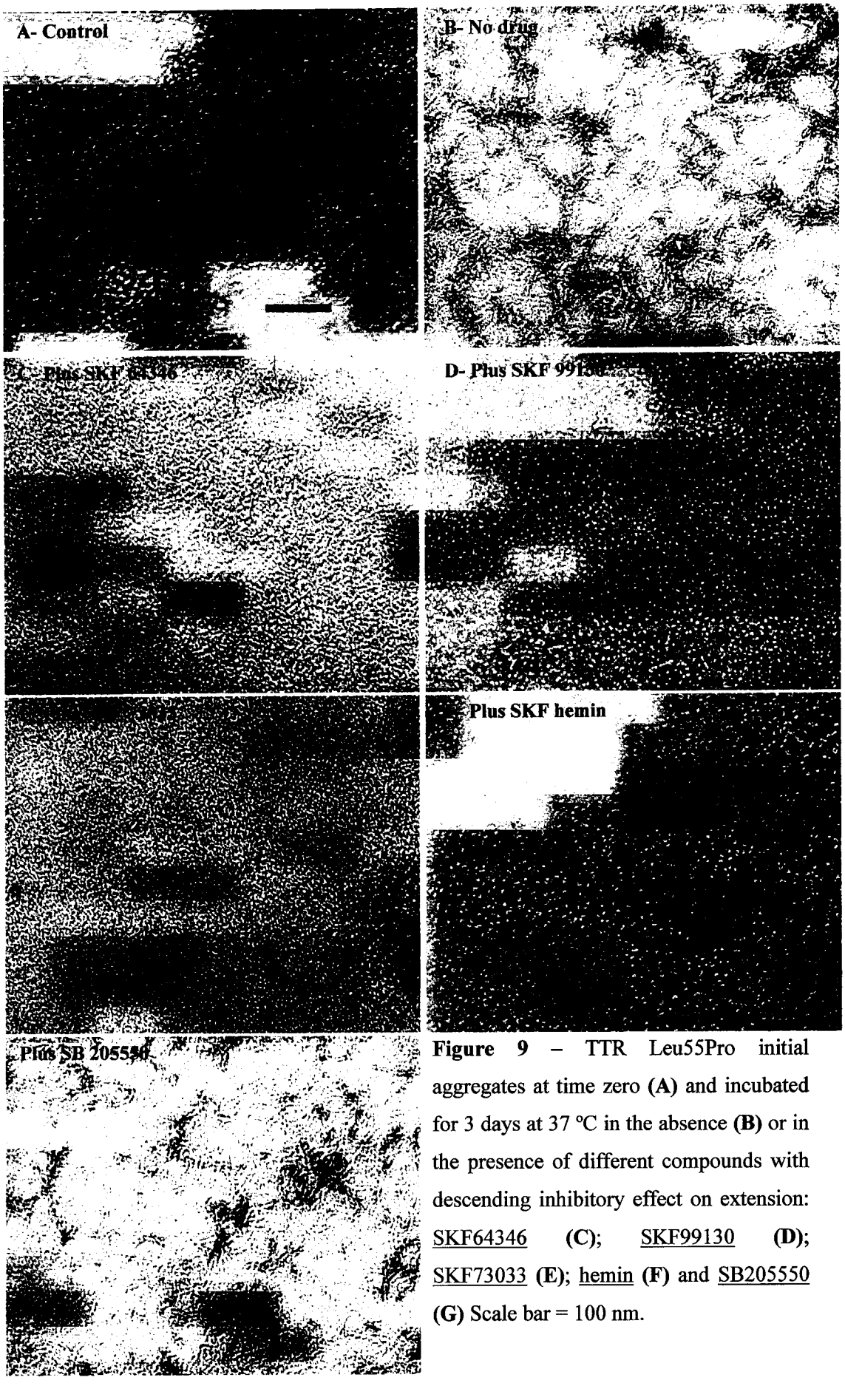

Figure 9 – TTR Leu55Pro initial aggregates at time zero **(A)** and incubated for 3 days at 37 °C in the absence **(B)** or in the presence of different compounds with descending inhibitory effect on extension: SKF64346 **(C)**; SKF99130 **(D)**; SKF73033 **(E)**; hemin **(F)** and SB205550 **(G)** Scale bar = 100 nm.

However, further incubation with SB 205550 for 17 days, showed a mixture of fibrils and round particles (figure 10, right panel) suggesting that this particular compound acts primarily as a fibril disrupter. When compared to the preparation control (in the absence of drug, figure 10, left panel), it is clear that SB 205550 originated a large amount of round species.

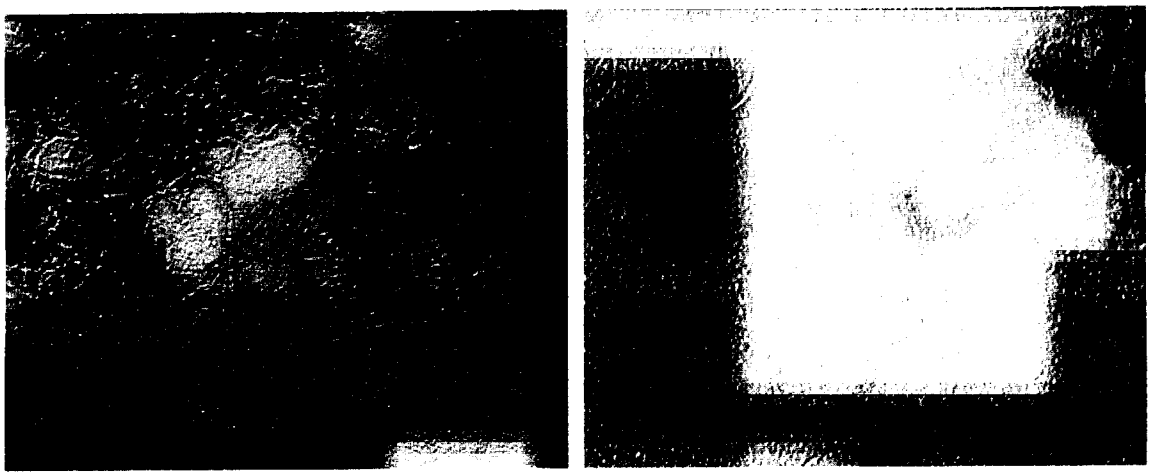

Figure 10 – TTR Leu55Pro incubated for 17 days at 37°C in the absence **(left panel)** or in the presence of SB20550 **(right panel)**. Scale bar = 100 nm.

Screening for TTR inhibitors

When analyzed by TEM, the anti-inflammatory compounds ibuprofen, modified iododiflunisal and diclofenac did not show significant effect on extension (data not shown), as fibrils similar to the ones observed in the absence of drug were detected (see figure 9B). While the results of modified diflunisal and diclofenac are in agreement with those obtained in the immunoassay the same is not the case for ibuprofen since it revealed 37% inhibitory effect in the immunoassay. It is possible that further incubation times are needed to see the effect of ibuprofen by TEM as was shown for SB 205550 (figure 10, right panel). This might also reflect different sensitivities of the two methodologies and it is possible that the inhibitory effects of ibuprofen are detected by TEM at higher concentrations of the compound.

5- The cellular system

To set up a cellular system for the production of TTR aggregates, cells were transfected with TTR human constructs (p169ZT-hTTRWT, p169ZT-hTTRMet30, and p169ZT-hTTRPro55). Demonstration of TTR production was performed by quantitative ELISA, in conditioned media of 24 hours under serum-free conditions. Cells were previously induced with 10 μM $ZnSO_4$ for 3 days and showed different levels of expression. Table 3 depicts the interval range of TTR expression for each construct.

Table 3- TTR secreted into the medium by RN22 transfected cells.

Transfected RN22/ Construct	**TTR expression (ng/ml)/10^6cells/24 hours)**
p169ZT-hTTRWT	100-300
p169ZT-hTTRMet30	350-1000
p169ZT-hTTRPro55	300-900

Protein expression and degradation was also assessed by immunoprecipitation on both media and cell lysate. Figure 12 shows TTR from media (M) and cell lysate (P), separated under denaturing conditions (SDS-PAGE) after immunoprecipitation with anti-human TTR antibody and reveals that most of the protein produced is secreted into the medium. No degradation is observed.

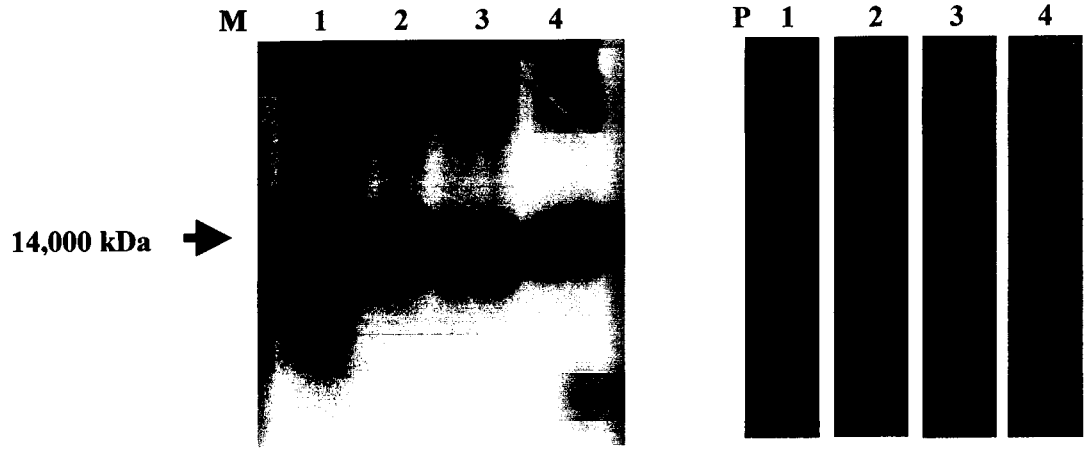

Figure 12– Immunoprecipitation analysis of RN22 cells medium (M) and pellet (P).
(1) RN22 non-transfected; **(2)** RN22 p169ZT-hTTRWT; (3) RN22 p169ZT-hTTRMet30; and **(4)** RN22 p169ZT-hTTRPro55.

We investigated the ability of the different constructs to induce the production of amyloidogenic species. Cells were grown in serum free medium for 24, 48 and 72 hours and then analyzed for the presence of oligomers retained by a 0.2 μm filter in a dot blot assay. While TTR produced by cells transfected with constructs carrying the TTRWT or TTR Val30Met cDNA was not retained in the filter even after 72 hours, TTR Leu55Pro protein was partially retained by the membrane filter as soon as 24 hours (figure 13A), suggesting the formation of oligomers or aggregates.

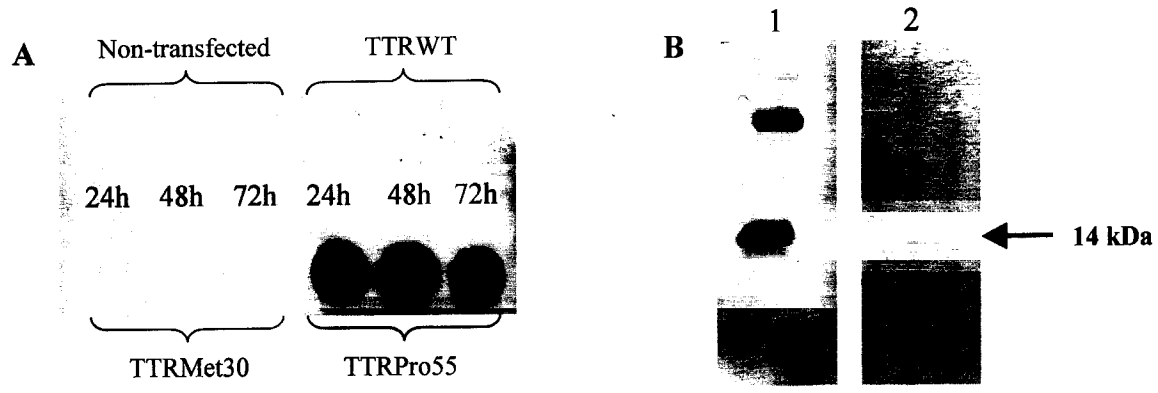

Figure 13– Dot blot filter assay.

A: RN22 cells non-transfected or transfected with plasmid p169ZT carrying different TTR variants (WT, Met30 and Pro55). TTR was quantified in the medium by ELISA and 500 ng were applied in the filter, followed by TTR immunodetection.

B: Western blotting of the material retained on the membrane filter, revealing the presence of TTR **(lane 2);** TTR standard **(lane 1)**.

To confirm the presence of TTR in the material retained on the filter, the doted area was cut, boiled with denaturing loading buffer and run on a SDS-PAGE gel. The proteins were then transferred to a nitrocellulose membrane followed by immunodetection against TTR (figure13B), revealing the intact TTR monomer; under these conditions we did not have evidence for aggregate formation since SDS probably disrupted those aggregates. Our assumption of aggregate formation is thus solely based on the retention filter assay.

We further investigated the nature of the secreted and aged TTR species by immunoassay with Mab15. The cell medium of RN22 TTR WT, RN22 TTR Val30Met and RN22 TTR Leu55Pro was collected at different time points and TTR quantified by ELISA. Using equal amounts of TTR protein, as measured by the polyclonal antibody that recognizes equally all TTR variants, Mab15 immunoassay was performed showing that TTR WT was not recognized by this antibody up to 72 hours (data not shown). In contrast, TTR Val30Met and Leu55Pro were recognized as early as 18 hours (figure 14) with a maximum reactivity

at 24 hours. TTR Leu55Pro expressed protein showed a higher reactivity when compared to the TTR Val30Met counterpart.

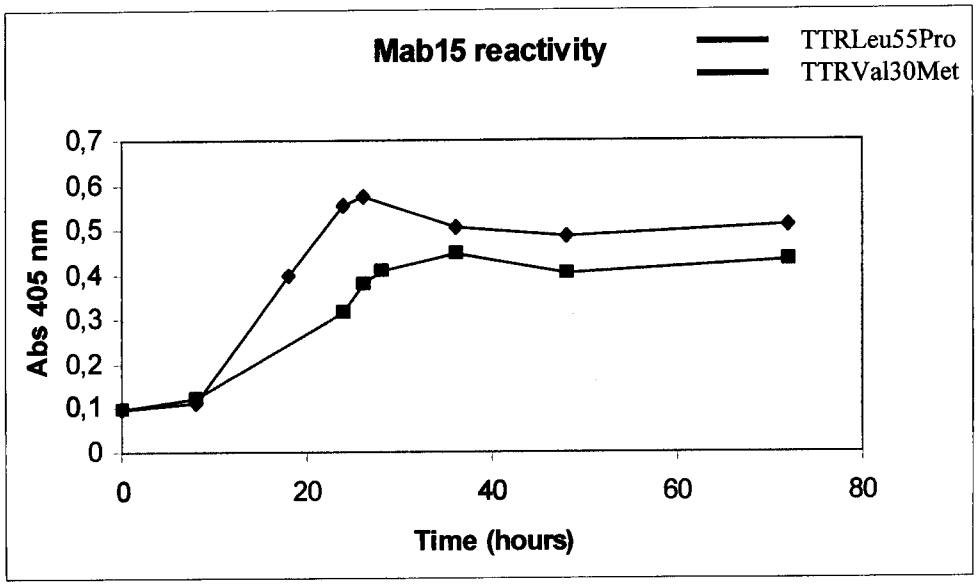

Figure 14– Mab15 reactivity towards TTR Val30Met and Leu55Pro variants expressed and secreted into the medium by RN22 transfected cells.

In this system, Mab15 recognizes TTR Val30Met and Leu55Pro, probably in a similar way to what happens in the serum of FAP patients. However, for the time points analyzed TTR Val30Met does not aggregate whereas TTR Leu55Pro does, as demonstrated by dot blot filter assay.

The ability of producing TTR amyloid-like fibrils by lowering the pH *in vitro* lead to the hypothesis that the lysosomal acidic environment might play a major role in TTR fibril formation (Colon and Kelly, 1992), although no intracellular deposits have ever been observed in FAP patients. We investigated the participation of these organeles in the formation of the TTR Leu55Pro aggregated species by inhibiting lysosomal activity with chloroquine (figure 15) and results showed that TTR Leu55Pro is still retained in the filter in the presence of this lysosomal inhibitor.

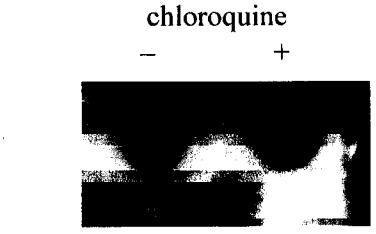

Figure 15– Dot blot filter assay. Lysosomal influence on the formation of TTR Pro55 aggregates. RN22 cells medium expressing TTR Pro55 protein for 24 hours **(-)** and in the presence of chloroquine 10 μM **(+)**.

These data suggest that the species retained in the filter and recognized by Mab15 are formed independently of lysosomal activity and are probably generated extracellularly in the medium, after secretion.

Discussion

The process that converts a soluble protein into amyloid is complex and not fully understood. In the literature, TTR amyloid deposits are indicated as the causative agent of FAP. However, the finding that asymptomatic individuals carrying the TTR Val30Met mutation show a positive reaction for inflammatory markers and present non fibrillar TTR deposits in the nerve, raised the possibility that others species besides mature fibrils could be involved in disease (Sousa *et al.*, 2001a). In fact, *in vitro* studies showed that TTR Leu55Pro initial aggregates are toxic to a Schwanoma cell line, inducing caspase-3 activation, while long fibrils do produce significant caspase-3 activation (chapter III). These observations suggest that a major target on FAP therapy is to inhibit the formation of intermediate species and that the study of how native TTR converts into toxic species is of major importance.

We used TTR Tyr78Phe to follow fibril formation progress by TEM and observed the morphological changes for up to 15 days. The initial round particles (native protein) lead to oligomers and after further incubation produced large aggregates and finally fibrils. So far, the data available on this variant consisted on biochemical properties, namely that this variant possesses an amyloid-like fold in its soluble form, as judged by its reactivity with Mab15 (Redondo *et al.*, 2000b). The work by Anesi and co-workers (Anesi *et al.*, 2001) showed TTR Tyr78Phe *ex* vivo amyloid fibrils by TEM; however, no kinetic characterization was performed. We presented here a morphological characterization and time progression evaluation for TTR Tyr78Phe under physiological conditions. In particular, the changes observed within 48 hours may mimic very early events occurring *in vivo* and therefore, this variant was selected to study the influence of several compounds on TTR priming, the first stage of the amyloidogenic cascade. Since we had previously characterized the second amyloidogenic stage (extension) we used TTR Leu55Pro to search for compounds affecting this step.

Using the above TTR mutants, we studied the possibility of screening drugs affecting TTR priming and/ or extension by using a monoclonal antibody (Mab15) known to distinguish between amyloidogenic and non-amyloidogenic structures. Although Mab15 reacts with TTR Tyr78Phe, 48 hours after incubation at 37°C, by the time TTR Tyr78Phe produces oligomers, the reactivity decreases about 2.5 times, suggesting that the epitopes necessary for recognition are no longer accessible available upon polymerization. The decrease in

Mab15 reactivity was also observed when TTR Leu55Pro maturated from non-fibrillar aggregates and oligomers into short fibrils; moreover, Mab15 detected changes associated with oligomers formation since soluble TTR Leu55Pro is not immunoreactive.

It is possible that the conformational changes that occur during fibrillogenesis differ between TTR Tyr78Phe and Leu55Pro. The kinetics of polymerization seems also to be different: macroscopically, no precipitation is observed in the TTR Tyr78Phe sample until 8-10 days; in contrast, the TTR Leu55Pro initial aggregates are isolated by centrifugation (see Materials and Methods). This type of aggregate might also be present during TTR Tyr78Phe fibrillogenesis but at a different time. Further structural studies are necessary to clearly identify the motifs recognized by Mab15 in these TTR species. It is also important to determine the three-dimensional structure of TTR Tyr78Phe in order to ascertain the differences between the two mutants. Nevertheless, within each step of fibrillogenesis of the two tested variants a consistent conformational behavior is observed making this methodology adequate for testing compounds inhibiting priming and/or extension of TTR amyloid fibrils.

A panel of compounds belonging to different structural classes was tested (see table 1) using the Mab15 immunoassay. Tetracyclines and nitrophenols have been shown to act primarily as fibril disrupters by TEM (chapter III) and thus, they were used as negative controls in this new method. Mab15 detected no priming or extension inhibition by these compounds, which confirmed the TEM results.

Benzofurans have been shown to inhibit Aβ fibril formation (Howlett *et al.*, 1999a). The effectiveness of these compounds in preventing the formation of a fibrillar Aβ form seemed to involve the binding of benzofuran to soluble peptide. Among the benzofurans tested for inhibition of TTR fibril priming and extension, SKF 99130 and SKF 64346 were the most effective while SKF 73033, SKF 79313 and SB 205550 were considerably less effective; SKF 74652 revealed no inhibitory activity under the conditions tested. Similar results were found for the degree of inhibition of SKF 64346 and 73033 against Aβ fibrillogenesis (Howlett *et al.*, 1999a), and an explanation advanced for the distinct two activities was the positioning of the bulky 3,5-diethyl-substituted phenyl ring in relation to the basic ethanolamine side chain. SKF 99130 was also shown to be a major inhibitor of Aβ fibrillogenesis (Howlett, 2001). The main differences towards inhibition of fibrillogenesis of TTR and Aβ were for SKF 79313, SB 205550 and SKF 74652; SKF 79313 and SB

205550 showed only intermediate inhibitory capacity towards TTR priming and extension while they were highly effective against Aβ (Howlett, 2001); SKF 74652 was completely unable to inhibit both TTR priming and extension, whereas it was a major inhibitor against Aβ fibrillogenesis (Howlett *et al.*, 1999a). Thus, although some structural motifs might be common for Aβ and TTR oligomers and protofibrils, others certainly differ.

Non-steroid anti-inflammatory compounds, including flufenamic acid, diflunisal and diclofenac have been investigated and shown to inhibit TTR fibrillogenesis under acidic conditions. Flufenamic acid was shown to inhibit the conformational changes of TTR associated with amyloid formation under acidic conditions, using both TTR WT and Leu55Pro (Peterson *et al.*, 1998). Sedimentation velocity and sedimentation equilibrium ultracentrifugation studies showed that in the presence of flufenamic acid on acidic environment, TTR adopts its normal tetrameric conformation (Peterson *et al.*, 1998). Under these conditions and in the absence of drug, it would normally result in the dissociation of the TTR tetramer and in conformational changes leading to amyloid formation (Miroy *et al.*, 1996). The crystal structure of TTR complexed with flufenamic acid indicated that this drug mediates intersubunit hydrophobic interactions and intersubunit hydrogen bonds, promoting the normal tetrameric fold of TTR (Peterson *et al.*, 1998). Rational drug design centered on the identification of important substructures of flufenamic acid, lead to the selection of diflunisal as a potent fibril inhibitor (Baures *et al.*, 1998; 1999). Diclofenac (Baures *et al.*, 1999) and its derivatives (Oza *et al.*, 2002) were also reported to strongly inhibit TTR fibril formation, under acidic conditions. Under physiological conditions and using the immunoassay here described, no inhibitory activity was detected for diflunisal or diclofenac, either for priming or extension. In the case of diclofenac, TEM studies revealed discrete fibrils approximately 7 nm wide that constituted the great majority of the preparation. Thus, we showed, by making use of two different methodologies under physiological conditions, that diflunisal and diclofenac are not sufficiently strong (adequate) to stabilize the tetrameric fold of TTR (priming) or to inhibit the polymerization reaction (extension).

We also selected ibuprofen, another non-steroid anti-inflammatory drug, that has been tested preferentially in studies related to Alzheimer's disease and associated with inhibition of toxicity of Aβ aggregates (Lim *et al.*, 2000; Frautschy *et al.*, 2001; Lim *et al.*, 2001; Blasko *et al.*, 2001). The mechanism behind ibuprofen action is not known and weather it acts directly on the amyloid precursor/ intermediates or indirectly affects amyloid

deposition is yet to be determined. This drug was shown to cause modest reductions in Aβ load but not in Congo red staining leading the authors to suggest that the effects of ibuprofen were restricted primarily to non-fibrillar deposits (Jantzen *et al.*, 2002). In our study, ibuprofen showed intermediate inhibitory effects against both TTR priming and extension. Further studies on FAP animal models, namely the effect on oxidative stress as performed in Alzheimer's, should be done to assess the usefulness of this compound in FAP therapy.

We assessed a group of compounds including DES, sulphite, modified diflunisal, modified flufenamic acid, one xanthone and a pyridine derivative, with stabilizing effects on soluble tetrameric TTR as ascertained by isoelectric focusing and/or competition with T_4 for TTR binding. In this group, DES presented high inhibitory capacity for both priming and extension (approximately 50%), whereas the others had effect only either on priming or on extension. These results are unexpected, as tetrameric stabilizers should also inhibit priming. One possible explanation for these apparently discrepant results might be the different TTR variants used in the different methodologies: while the stabilizing studies by isoelectric focusing were performed with TTR Val30Met, the assessment of inhibitory effects on priming were done with TTR Tyr78Phe. In contrast with TTR Val30Met, TTR Tyr78Phe possesses amyloid-like properties in its soluble form and thus, some tetrameric stabilizer compounds might not be able to bind to already amyloidogenic conformations. Further binding studies of these class of compounds to TTR Tyr78Phe might clarify this issue. Tetrameric stabilizers should also be able to inhibit extension when starting with soluble protein. However, in our study, potential inhibitors of extension were tested using TTR Leu55Pro initial aggregates, implying that intermediate species were already formed and soluble tetrameric TTR was no longer available.

In this study we also included a group of ECM components, thought to play a role in amyloidogenesis. No important inhibitory competences were found, except for laminin, which presented the highest percentage of inhibition of extension (70%) among all the compounds tested. Similarly to the other ECM components tested, laminin did not affect priming. In the literature, a large number of reports describe the influence of laminin on Aβ aggregation. Different authors refer to the anti-amyloidogenic properties of laminin both by inhibiting fibril formation (Monji *et al.*, 1998a; Monji *et al.*, 1998b; Monji *et al.*, 1999; Bronfman *et al.*, 1998) and disaggregating pre-formed fibrils (Morgan and Inestrosa, 2001; Castillo *et al.*, 2000). Laminin is also able to reverse the toxic effects of Aβ aggregates on

cultured cells (Drouet *et al.*, 1999). Castillo and co-workers (Castillo *et al.*, 2000) studied the effect of several ECM components, including laminin, perlecan, type IV collagen and fibronectin, on Aβ fibrillogenesis and concluded that laminin had the greatest inhibitory effect. In our work we demonstrated, by immunoreactivity with Mab15, that laminin inhibits TTR extension. However, structural studies are necessary to confirm this result. Also, at this point, we have no indication if laminin acts as TTR fibril disrupter and thus, different amyloidogenic assays should be performed addressing this issue.

Hemin and other heme-containing compounds were found to prevent Aβ fibril formation (Howlett *et al.*, 1997). The mechanism underlying this process is not known. Free iron has been reported to promote β-amyloid aggregation (Mantyh *et al.*, 1993) whereas iron chelation was protective (Schubert and Chevion, 1995). Evidences point out that APP level shows a direct relationship with free iron levels and indirect relationship with hemin and iron chelators (Bodovitz *et al.*, 1995). Furthermore, hemin prevents the formation of toxic Aβ species as measured by MTT assays (Howlett *et al.*, 1997). Our data suggests that hemin prevents both TTR priming and extension in about 50%. In the case of extension, we also analyzed the effect of hemin by TEM and although it prevented fibril elongation, unlike other compounds such as the SKF series, hemin was not able of disaggregate the TTR Leu55Pro aggregates as the resulting species were morphologically similar to the starting material.

Aprotinin and aprotinin peptide were shown to bind amyloid fibrils (chapter I) and were presented as possible markers in the diagnosis of TTR related amyloid. Aprotinin was found to inhibit priming (34%) while the respective peptide (aa residues 16-37) did not show any activity for either priming or extension, suggesting that more organized structural motifs, probably absent in the peptide, are necessary to interfere with fibrillogenesis.

We intend to perform further studies to establish the binding sites of the tested molecules to soluble and aggregated TTR. Furthermore, cytotoxic studies should be developed in order to determine the usefulness of these compounds. In this regard the cellular model we developed is an important tool to be used. Different cellular models have been generated in order to study amyloidogenesis. A cell culture system for generation of AA amyloid was established using mice peritoneal macrophages that had received repeated injections of Hammersten casein (Palm *et al.*, 1997). Staining with Congo red, thioflavin T, and anti-AA revealed amyloid-like structures associated with macrophage clusters. Such systems can be

useful in studies of the influence of chaperone molecules and other factors on the formation and degradation of amyloid fibrils. Transfected cells with the presenilin 2 (PS2) gene were used to examine the processing and degradation pathways of PS2 (Kim *et al.*, 1997). Mutations in the presenilin genes (PS1 and PS2) are related to familial Alzheimer's disease although the reasons are not known. Results suggested that PS2 normally undergoes endoproteolytic cleavage and is degraded via the proteasome pathway.

A major question concerning amyloid formation is whether deposits are formed extra or intracellularly. In Aβ fibrillogenesis, it has been proposed that oligomers formation might first form intracellularly. Studies revealed the presence of SDS-stable Aβ dimers in the CSF from patients suffering from Alzheimer's disease and in the conditioned medium from CHO transfected cells expressing mutated APP (Val717Phe, associated with familial AD); incubation of these samples at 37°C did not lead to new oligomer formation (Walsh *et al.*, 2000). In a different study, cells transfected with the APP gene, carrying the same mutation as above, were treated with cysteine protease inhibitors and shown to accumulate a novel 22 kDa carboxyl-terminal fragment; treatment with chloroquine, a lysosomal inhibitor, completely blocked the generation of this fragment (Knops *et al.*, 1992). The authors suggested that the results revealed a non-secretory pathway for APP degradation mediated by cysteine proteases in an intracellular acidic compartment; inefficient degradation of the 22 kDa intermediate might lead to the formation of aggregating β-peptide. A different cellular model was created for AL-amyloid formation using mesangial cells exposed to amyloidogenic light chains (Isaac *et al.*, 1998); in this system treatment with chloroquine significantly attenuated amyloid formation, suggesting that AL-amyloid formation may begin intracellularly, in the lysosome. In our system, the event leading to the generation of oligomers or aggregates is probably occurring extracellularly, in the medium, as lysosomal inhibition did not avoid their formation. Our result is in agreement with the *in vivo* observations since, so far, no intracellular deposits were detected in patients.

TTR Leu55Pro protein secreted in our culture system was shown to form species that were retained by a filter. Mab15 also reacted with the material secreted by cells expressing the Leu55Pro and the Val30Met variants, although the last was not retained on the membrane filter. This observation might imply that although TTR Val30Met does not aggregate, it undergoes conformational changes determinant for Mab15 recognition, probably mimicking the events occurring with serum from FAP patients, which also react with this monoclonal antibody. Such model can provide the means to study compounds affecting events prior to

Screening for TTR inhibitors

TTR aggregation avoiding species with an altered tetrameric fold. Although TTR Tyr78Phe is produced as a tetramer in its soluble form, probably the transformations leading to aggregate formation, upon incubation at 37°C, occur very fast due to the *in vitro* conditions. The generated cellular model constitutes an opportunity to study compounds classified as tetrameric stabilizers that failed to inhibit priming and/ or extension.

The proposed system needs further assessment, including the morphological characterization of the species present. The lower amount of protein secreted by the cells may constitute a draw back in this study, as amyloidogenesis is concentration-dependent. Although this is not an *in vivo* model, it has the advantage of reuniting a number of biological factors absent in the other *in vitro* systems used (TEM and immunoassay).

In summary: we developed an immunoassay based on the different reactivity of intermediary TTR species during fibrillogenesis with the monoclonal antibody Mab15, and applied it to test different compounds for their ability to interfere with the progression of aggregate growth. The immunoassay permits screening of compounds and overcomes difficulties that are usually present in assays with colored or fluorogenic markers.

Although at this point TEM analysis does not allow quantification of compound activity, the morphological results seem to be in good agreement with the specific immunoassay, thus, validating the latter.

We suggest that during the study and screening of compounds for therapeutic use in FAP, several steps should be followed:

1- For compounds with high activity on priming and extension proceed with cell assays to assess toxicity of the compound *per se*, and of the species generated by its action (activation of caspase-3 assays-chapter III), followed by animal studies for the non-toxic drugs and structural analysis to design non-toxic compounds.

2- Compounds with intermediate activity on priming and/or extension should be further characterized, especially if the drug has anti-inflammatory properties. Such characterization encompasses TEM analysis with different concentrations, cell toxicity as above, and tests of inhibition of aggregate formation by filter assays and ELISA in the cellular system here described.

   Animal studies and structural analysis for design of derivatives should follow.

3- Compounds with no activity should go for TEM analysis to assess disrupting activity; drugs with high disrupting activity need to go through toxicity assays before animal and structural studies.

In the future, modeling studies may contribute to determine common structural motifs in amyloid fibrils and in drugs with disrupting activity, reducing the number of compounds that need to be studied by TEM.

Acknowledgements

This work was supported by grants (POCTI/35785/99 and 35201/99) and a PhD scholarship (BD/15725/98 to Isabel Cardoso) from Fundação para a Ciência e Tecnologia, Portugal. We thank Paul Moreira for his excellent technical assistance in the preparation of recombinant TTRs.

Conclusions and Perspectives

3- Conclusions and Perspectives

Non-invasive procedures for whole body imaging amyloid are crucial not only for diagnostic purposes but also for follow up of therapies aiming at reducing the amyloid load in organs and tissues. The available methodology for imaging amyloid deposition in systemic amyloidosis uses human serum amyloid P component - SAP- a component that binds all types of amyloid, but that has limitations related to risks of viral contamination, and reduced affinity for certain tissues. We investigated aprotinin as a marker for several types of amyloid. Two aprotinin peptides were designed and shown to bind specifically to different types of amyloid and not the soluble protein precursor. This opens perspectives for their use in imaging amyloid deposits, including systemic and cerebral forms (Alzheimer's disease) of amyloidosis.

The ability to study the pathogenic mechanisms associated with FAP and in particular the amyloid deposits, implies the fully characterization of the dynamics of fibril formation, the identification and structural characterization of the different species generated in the course of such process, and the assessment of toxicity associated with them.

We studied the fibril assembly progression of the TTR variants TTR Tyr78Phe and Leu55Pro, under physiological conditions, corresponding to two different stages in amyloidogenesis, priming and extension, respectively. The building blocks of TTR amyloid fibrils have been the subject of controversy. We showed by STEM that both TTR Leu55Pro fibrils under physiological conditions and TTR WT fibrils produced by acidification are assembled from TTR monomers, probably with an altered structure.

The toxicity of the species generated, including initial aggregates, short and long fibrils, was investigated: we demonstrated that the toxic species are the initial aggregates while fibrils did not significantly produce toxic effects on the cell line used. Although non-fibrillar TTR aggregates are observed in the pre-clinical phase of asymptomatic carriers of mutant TTR, no direct evidence exist that *in vivo* mature amyloid fibrils are originated from non-fibrillar deposited TTR. Further studies are necessary to establish a relation between the non-fibrillar deposits and the disease. The possibility of extracting these aggregates should also be considered in future work, creating the opportunity for studying the assembly of *ex vivo* fibrils and determining the basic units constituting them. With this respect, the available animal models might prove important tools.

Conclusions and Perspectives

Based on the gained knowledge, several drugs have been tested for their ability to interfere with TTR amyloidogenic cascade at different stages. Those compounds included anthracyclines, tetracyclines, nitrophenols, benzofurans, non-steroid anti-inflammatory molecules, ECM components, and a few others.

In the present work we tested I-DOX and a group of I-DOX derivatives and showed that they act as disrupters and not as inhibitors of the amyloidogenic process. The species generated by I-DOX 15 days after addition of the drug were non-toxic, raising in possibility to use this drug or its derivatives in FAP treatment. A group of three tetracyclines and two nitrophenols also revealed to act primarily as TTR fibril disrupters. Similar studies should be conducted in order to assess the toxicity of the species generated by I-DOX derivatives and the other classes of disrupters.

An extended group of drugs was investigated for the ability of interfering with both priming and extension of TTR amyloid. Benzofurans and anti-inflammatory compounds were among the most effective, inhibiting both stages. Studies in a cell culture system using a Schwannoma cell line and caspase assays, are necessary to evaluate toxicity and further use in *in vivo* studies.

We also generated a cellular model capable of producing TTR Leu55Pro aggregates. Further investigation is necessary to determine the morphological, conformational and toxic characteristics of the secreted TTR. This system can provide the means to evaluate the cellular events underlying amyloid formation and the mechanisms responsible for inhibitory effects of therapeutic drugs.

In the future, investigation should be conducted to assess toxicity *in vivo* and maximal dose allowance as well as pharmacokinetics of the different compounds selected in this work. Studies on selected non-toxic and stable compounds should then be conducted in animals presenting TTR deposition to evaluate subsequent protocols of drug administration and to compare pharmacokinetics. The effects of the different drugs on TTR deposition need to be evaluated on transgenic animal models generated in our laboratory (Sousa *et al.*, submitted). These models present TTR deposition as oligomeric species between 3 and 6 months of age and as amyloid fibrils after 9 months of age. Thus, administration of the selected drugs could take place at different times ranging from 1 to 3 months for inhibitors of priming and extension, from 3 to 6 months for inhibitors of extension and after 6 months for amyloid disrupters. The effect of the drugs on the different stages of animal amyloidogenesis (early, central, late) can be evaluated histologically, by quantitative image analysis (Sousa *et al.*,

2001). Different regimens of drug application, i.e., mixed regimens of priming and extension inhibition and disruption, at different time intervals on the same animal have to be tested. Additional studies concerning reduction of inflammatory and apoptotic effects resulting from the administration of the selected drugs need to be conducted since tissue stress markers increase with age and deposition load in these animal models as our laboratory as recently demonstrated (*Sousa et al.*, submitted).
Drugs with evident *in vivo* activity on TTR deposition and/or disrupting activity will set-up the stage for future clinical application.

In summary, the work presented in this thesis provided new information on the amyloidogenic cascade and contributed to the methodology for selection of drugs with potential therapeutic use in FAP.

Part III

Appendix

Abbreviations

Abbreviations

0.6-TTRMet30: transgenic mouse containing the entire human TTR Val30Met gene with 600 bp of upstream sequence including the native promoter.

6-TTRMet30: transgenic mouse containing entire human Val30Met gene with about 6 kb of the upstream region.

Aβ(1-42): amyloid derived from β-peptide residues 1-42

Aβ(1-40): amyloid derived from β-peptide residues 1-40

Aβ: amyloid β-peptide (Aβ) or β-peptide amyloidosis

aa: aminoacids

AA: amyloid A associated amyloidosis

AANF: ANF amyloidosis

AANP: α-atrial natriuretic peptide

ABTS: 3-ethylbenzethiazoline-6-sulfonic acid

ACalc: Calc amyloidosis

Acys: cystatin C related amyloidosis

AD: Alzheimer's disease

AEF: amyloid enhancer facctor

AFM: atomic force microscopy

AGel: gelsolin related amyloidosis

AH: heavy immunoglobulin chains associated amyloidosis

AIns: insulin related amyloidosis

AL: light chain type amyloidosis

ALac: lactoferrin related amyloidosis

ANF: atrial natriuretic factor

ApoAI, ApoAII, ApoE, ApoJ: apolipoproteins AI, AII, E and J, respectively

ApoSAA: serum precursor of AA amyloid

APP: amyloid precursor protein

APro: prolactin related amyloidosis

aprotinin Lys15Val, Arg17Leu, Met52Glu: valine for lysine exchange at residue 15, leucine for arginine exchange at residue 17 and glutamate for methionine exchange at residue 52 of aprotinin

APrP: prion protein diseases

Abbreviations

BBB: brain blood barrier

BJP: Bence Jones Proteins

bp: basepairs

BPTI: bovine basic pancreatic trypsin inhibitor or aprotinin

BSA: bovine serum albumin

BSB: (*trans,trans*)-1-bromo-2,5-bis-(3-hydroxycarbonyl-4-hydroxy)styrylbenzene

Calc: calcitonin

CD: circular dichroism

CG: chrysamine G

CJD: Creutzfeldt-Jakob disease

CNS: central nervous system

CSF: cerebrospinal fluid

CU: calibration uncertainty

Da: dalton

DES: diethylstilbestrol

DMEM: Dulbeco's minimal essential medium

DMSO: dimethylsulphoxide

DNA: desoxiribonucleic acid

DNP: dinitrophenol

DOX: doxorubicin

ECL: enhanced chemiluminescence

ECM: extracellular matrix

ELISA: enzyme linked immunoreactive assay

FAC: familial amyloidotic cardiomyopathy

FAO: rat hepatomas

FAP: Familial amyloidotic polyneuropathy

FBS: fetal bovine serum

FCS: fetal calf serum

FMF: familial Mediterranean fever

FWHM: full-width-half-maximum

GAG: glycosaminoglycan

HBSS: Hank´s balanced salt solution

HDL: high density lipoproteins

HeBS: HEPES buffered saline

HepG2: human hepatoma cells

HSPG: heparan sulphate proteoglycans

hTTR55- transgenic mouse containing the entire human Leu55Pro TTR cDNA

hTTRwt- transgenic mouse containing the entire human wt TTR cDNA

HypF-N: amino terminal domain of the *Escherichia coli* HypF protein

IAPP: islet amyloid polypeptide derived amyloidosis

I-DOX: 4'-iodo-4'-deoxydoxorubicin

Ka: binding affinity constant

kb: kilobase

kDa: kilodalton

LDL: low density lipoprotein

LDLr: low-density lipoprotein receptor

MHCI: major histocompatibility complex of type I

MPL: mass-per-length

mRNA: messenger RNA

MT: metallothionein promoter

MT1-TTRMet30, MT2-TTRMet30: transgenic mouse containing the mouse MT fused to a human ttr gene containing the Val30Met mutation

MTT: 3-(4,5-dimethyl-2-thiazolyl)-2,5-diphenyl-2H-tetrazolium bromide

n: number of segments included PBS

NF-kB: nuclear transcription factor kB

NFT: neurofibrillar tangle

NMR: nuclear magnetic ressonance

NP: nitrophenol

orf: open reading frames

pA: SV40 poly-A tail

PAGE: polyacrylamide gel electrophoresis

PBS: phosphate-buffered saline

PBST: phosphate-buffered saline with 0.05% tween20

PDB: protein data bank

PG: proteoglycan

pI: point isoelectric

Abbreviations

PI3-SH3: SH3 domain from bovine phosphatidyl-inositol-3'-kinase

PLNeo: plasmid with resistance to neomycin

PrP: prion protein

PS: presenilin gene

PSP-II: spermadhesin

RAGE: receptor for advanced glycation end products

RAP: receptor-associated protein

RBP: retinol-binding protein

RNA: ribonucleic acid

sAβ: soluble β-peptide

SAA: serum amyloid A

SAP: serum amyloid P component

SD: standard deviation

SDS: sodium dodecyl sulphate

SE: standard error

SMT-1: sheep MT-1 promoter

SP: senile plaques

SPR: surface plasmon resonance

sRAGE: soluble RAGE

SSA: systemic senile amyloidosis

STEM: scanning transmission electron microscopy

STI: soybean trypsin inhibitor

sTTR: soluble TTR

T_3: triiodothyronine

T_4: thyroxine

TBG: thyroxine binding glubulin

TcA: technetium-99m

TCA: trichloroacetic acid

TEM: transmission electron microscopy

TFA: trifluoroacetic acid

Th T: thioflavin T

TTR Leu55Pro: leucine for proline exchange at position 55 of transthyretin.

TTR Tyr78Phe: tyrosine for phenylalaline exchange at position 78 of Transthyretin

TTR Val30Met: valine for methionine exchange at residue 30 of transthyretin

TTR: transthyretin

ttr: transthyretin gene

TTR: transthyretin;

ttr-: *ttr* knock-out mice

VHDL: very high density lipoproteins

$\mathbf{V_L}$: light-chain variable domain

VLDL: very low density lipoproteins

VLDLr: VLDL receptor

WT: wild-type

β-ss: β-globin splicing site

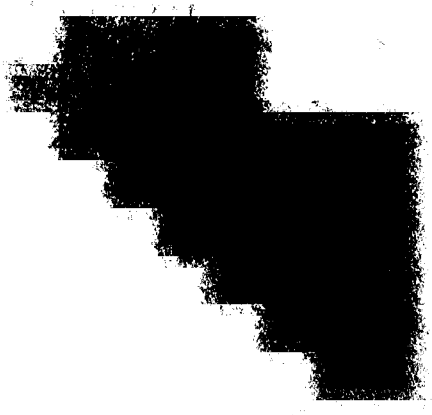

References

References

Aleshire SL, Bradley CA, Richardson LD and Parl FF (1983). Localization of human prealbumin in choroid plexus epithelium. *J Histochem Cytochem* **31**: 608-12.

Allard SA, King RH, Thomas PK, Bourke BE (1991). Haemarthrosis due to fracture through amyloid deposits in bone in Portuguese familial amyloidosis. *Ann Rheum Dis* **50**: 820-2.

Almeida MR, Aoyama-Oishi N, Sakaki Y, Holmgren G, Ulf D, Ferlini A, Salvi F, Munar-Oues M, Benson MD, Skinner M, et al (1995). Haplotype analysis of common transthyretin mutations. *Hum Genet* **96**: 350-4.

Almeida MR and Saraiva MJ (1996). Thyroxine binding to transthyretin (TTR) variants--two variants (TTR Pro 55 and TTR Met 111) with a particularly low binding affinity. *Eur J Endocrinol* **135**: 226-30 .

Almeida MR, Damas AM, Lans MC, Brower A and Saraiva MJ (1997). Thyroxine binding to transthyretin Met 119. Comparative studies of different heterozygotic carriers and structural analysis. *Endocrine* **6**: 309-15.

Almeida MR, Alves IL, Terazaki H, Ando Y and Saraiva MJ (2000). Comparative studies of two transthyretin variants with protective effects on Familial Amyloidotic Polyneuropathy: TTR R104H and TTR T119M. *Biochem Biophys Res Commun* **270**: 1024-8.

Altland K and Winter P (1996). Human plasma Transthyretin (TTR) is composed of many different molecular species with modified stability. *Neuromuscul Disord* **6**: S15.

Altland K and Winter P (1999). Potential treatment of transthyretin-type amyloidosis by sulfite. *Neurogenetics* **2**: 183-8.

Ancsin JB and Kisilevsky R (1996). Laminin interactions important for basement membrane assembly are promoted by zinc and implicate laminin zinc finger-like sequences. *J Biol Chem* **271**: 6845-51.

Ancsin JB and Kisilevsky R (1997). Characterization of high affinity binding between laminin and the acute-phase protein, serum amyloid A. *J Biol Chem* **272**: 406-13.

Ancsin JB and Kisilevsky R (1999). Laminin interactions with the apoproteins of acute-phase HDL: preliminary mapping of the laminin binding site on serum amyloid A. *Amyloid* **6**: 37-47.

Andrade C (1952). A peculiar form of peripheral neuropathy. Familial atypical generalized amyloidosis with special involvement of the peripheral nerves. *Brain* **75**: 408-27.

Andrea TA, Cavalieri RR, Goldfine ID and Jorgensen EC (1980). Binding of thyroid hormones and analogues to the human plasma protein prealbumin *Biochemistry* **19**: 55-63.

Andreoli M and Robbins J. (1962). Serum proteins and thyroxine protein interaction in early human fetuses. *J. Clin. Invest.* **41**: 1070-77.

Anesi E, Palladini G, Perffetti V, Arbustini E, Obici L and Merlini G (2001). Therapeutic advances demand accurate typing of amyloid deposits. *Am J Med* **111**: 243-4.

Aprile C, Marinone G, Saponato R, Bonino C and Merlini G (1995). Cardiac and pleuropulmonary AL amyloid imaging with technetium-99m labeled aprotinin, *Eur. J. Nucl. Med.* **22**: 1393-401.

Araki S, Shigehiro Y, Murakami T, Watanabe S, Ikegawa S, Takahashi K and Yamamura K (1994). Systemic amyloidosis in transgenic mice carrying the human mutant transthyretin (Met30) gene. *Mol Neurobiol* **8**: 15-23.

References

Artymiuk PJ and Blake CCF (1981). Refinement of human lysozyme at 1.5 Å resolution: analysis of non-bonded and hydrogen-bond interactions. *J Mol Biol* **152**: 737-62.

Asl L, Liepnieks JJ, Hamidi Asl K, Uemichi T, Moulin G, Desjoyaux E, Loire R, Delpech M, Grateaus G and Benson MD (1999). Hereditary amyloid cardiomyopathy caused by a variant apolipoprotein A1. *Am J Pathol* **154**: 221-7.

Axelrad MA and Kisilevsky R (1980). Biological characterization of amyloid enhancing factor, in Glenner GG, costa PP, and de Freitas F (eds), Amyloid and Amyloidosis, 527-533, Excerpta Medica, Amsterdam.

Baltz ML, Caspi D, Evans DJ, Rowe IF, Hind CR and Pepys MB (1986). Circulating serum amyloid P component is the precursor of amyloid P component in tissue amyloid deposits. *Clin Exp Immunol* **66**: 691-700.

Bard F, Cannon C, Barbour R, Burke RL, Games D, Grajeda H, Guido T, Hu K, Huang J, Johnson-Wood K, Khan K, Kholodenko D, Lee M, Lieberburg I, Motter R, Nguyen M, Soriano F, Vasquez N, Weiss K, Welch B, Seubert P, Schenk D and Yednock T (2000). Peripherally administered antibodies against amyloid beta-peptide enter the central nervous system and reduce pathology in a mouse model of Alzheimer disease. *Nat Med* **6**:916-919.

Bardin T, Kuntz D, Zingraff J, Voisin MC, Zelmar A and Lansaman J (1985). Synovial amyloidosis in patients undergoing long-term hemodialysis. *Arthritis Rheum* **28**:1052-8.

Bardin T, Lebail-Darne JL, Zingraff J, Laredo JD, Voisin MC, Kreis H and Kuntz D (1995). Dialysis arthropathy: outcome after renal transplantation. *Am J Med* **99**: 243-8.

Barrett AJ, Davies ME and Grubb A (1984). The place of human gamma-trace (cystatin C) amongst the cysteine proteinase inhibitors. *Biochem Biophys Res Commun* **120**: 631-6.

Baures PW, Peterson SA and Kelly JW (1998). Discovering transthyretin amyloid fibril inhibitors by limited screening. *Bioorg Med Chem* **6**: 1389-401.

Baures PW, Oza VB, Peterson S and Kelly JW (1999). Synthesis and evaluation of inhibitors of transthyretin amyloid formation based on the non-steroidal anti-inflammatory drug, flufenamic acid. *Bioorg Med Chem* **7**: 1339-47.

Bellotti V, Stoppini M, Mangione P, Sunde M, Robinson C, Asti L, Brancaccio D and Ferri G (1998). Beta2-microglobulin can be refolded into a native state from ex vivo amyloid fibrils. *Eur J Biochem* **258**: 61-7.

Benditt EP and Eriksen N (1977). Amyloid protein SAA is associated with high density lipoprotein from human serum. *Proc Natl Acad Sci U S A* **74**: 4025-8.

Benedikz E, Blondal H and Gudmundsson G (1990). Skin deposits in hereditary cystatin C amyloidosis. *Virchows Arch A Pathol Anat Histopathol* **417**: 325-31.

Bennhold H (1922). *Munch Med Wschr* **2**: 1537-8.

Benson MD, Liepnieks J, Uemichi T, Wheeler G and Correa R (1993). Hereditary renal amyloidosis associated with a mutant fibrinogen alpha-chain. *Nat Genet* **3**: 252-5.

Benson MD, Dwulet FE and DiBartola SP (1985). Identification and characterization of amyloid protein AA in spontaneous canine amyloidosis. *Lab Invest* **52**: 448-52.

Benson MD, Liepnieks JJ, Yazaki M, Yamashita T, Hamidi Asl K, Guenther B and Kluve-Beckerman B (2001) A new human hereditary amyloidosis: The result of a stop-codon mutation in the apolipoprotein AII gene. *Genomics* **72**: 272-7.

Bhatia K, Reilly M, Adams D, Davis MB, Hawkes CH, Thomas PK, Said G and Harding AE (1993). Transthyretin gene mutations in British and French patients with amyloid neuropathy. *J Neurol Neurosurg Psychiatry* **56**: 694-7.

Bianchi C, Donadio C, Tramonti G, Lorusso P and Bellitto F (1984). 99m Tc-aprotinin: a new tracer for kidney morphology and function. *Eur. J. Nucl. Med.* **9**: 257-60.

Billingsley ML, Pennypacker KR, Hoover CG, Brigati DJ and Kincaid RL (1985). A rapid and sensitive method for detection and quantification of calcineurin and calmodulin-binding proteins using biotinylated calmodulin. *Proc Natl Acad Sci USA* **82**: 7585-9.

Bladen HA, Nylen MU and Glenner GG (1996). The ultrastructure of human amyloid as revealed by the negative staining technique. J *Ultrastruct Res* **14**: 449-59.

Blake CCF and Swan IDA (1971). An X-ray study of the subunit structure of prealbumin. *J Mol Biol* **61**: 217-24.

Blake CCF, Geisow MJ, Oatley S J, Rérat B and Rérat C (1978). Structure of prealbumin: secondary, tertiary and quaternary interactions determined by Fourier refinement at 1.8 Å. *J Mol Biol* **121**, 339-6.

Blake C and Serpell L (1996). Synchrotron x-ray studies suggest that the core of the transthyretin amyloid fibril is a continuous β-sheet helix. *Structure* **4**: 989-98.

Blaner WS (1989). Retinol-binding protein: the serum transport protein for vitamin A. *Endocr Rev* **10**:308-16.

Blasko I, Apochal A, Boeck G, Hartmann T, Grubeck-Loebenstein B and Ransmayr G (2001). Ibuprofen decreases cytokine-induced amyloid beta production in neuronal cells. *Neurobiol Dis* **8**: 1094-101.

Bodovitz S, Falduto MT, Frail DE and Klein WL (1995). Iron levels modulate alpha-secretase cleavage of amyloid precursor protein. *J Neurochem* **64**:307-15

Bonar L, Cohen AS and Skinner MM. (1969). Characterisation of the amyloid fibril as a cross-beta protein. *Proc Soc Exp Biol Med* **131**: 1373-5.

Boomsma F, Veld AJM and Schalekamp ADH (1991). Not norepinephrine but its oxidation products bind spacifically to plasma proteins. *J Pharmac Experiment Therapeut* **259**: 551-7.

Booth DR, Tan SY, Booth SE, Hsuan JJ, Totty NF, Nguyen O, Hutton T, Vigushin DM, Tennent GA, Hutchinson WL and Pepys MB (1995). A new apolipoprotein Al variant, Trp50Arg, causes hereditary amyloidosis. *Q J Med* **88**: 695-702.

Booth DR, Tan SY, Booth SE, Tennent GA, Hutchinson WL, Hsuan JJ, Totty NF, Truong O, Soutar AK, Hawkins PN, Bruguera M, Caballeria J, Sole M, Campistol JM and Pepys MB (1996). Hereditary hepatic and systemic amyloidosis caused by a new deletion/insertion mutation in the apolipoprotein AI gene. *J Clin Invest* **97**: 2714-21.

Booth DR, Sunde M, Bellotti V, Robinson CV, Hutchinson WL, Fraser PE, Hawkins PN, Dobson CM, Radford SE, Blake CC and Pepys MB (1997). Instability, unfolding and aggregation of human lysozyme variants underlying amyloid fibrillogenesis. *Nature* **385**: 787-93

Borish L, King MS, Mascali JJ, Johnson S, Coll B and Rosenwasser LJ (1992). Transthyretin is an inhibitor of monocyte and endothelial cell interleukin-1 production. *Inflammation* **16**: 471-84.

Bourke MJ and Rougvie MA (1972). Cross-protein structures. I. Insulin fibrils, *Biochemistry* **11**: 2435-9.

References

Brett M, Persey MR, Reilly MM, Revesz T, Booth DR, Booth SE, Hawkins PN, Pepys M B and Morgan-Hughes JA (1999). Transthyretin Leu12Pro is associated with systemic neuropathic and leptomeningeal amyloidosis. *Brain* **122**: 183-90.

Bronfman FC, Alvarez A, Morgan C and Inestrosa NC (1998). Laminin blocks the assembly of wild-type A beta and the Dutch variant peptide into Alzheimer's fibrils. *Amyloid* **5**:16-23.

Brouwer A (1989). Inhibition of thyroid hormone transport in plasma of rats by polychlorinated biphenyls. *Arch. Toxicol. Suppl.* **13**: 440-5.

Browning MJ, Banks RA, Tribe CR, Hollingworth P, Kingswood C, Mackenzie J and Bacon PA (1985). Ten years' experience of an amyloid clinic-a clinicopathological survey. *Q J Med* **54**: 213-27.

Brzin J, Popovic T, Turk V, Borchart U and Machleidt W (1984). Human cystatin, a new protein inhibitor of cysteine proteinases. *Biochem Biophys Res Commun* **118**: 103-9.

Bucciantini M, Giannoni E, Chiti F, Baroni F, Formigli L, Zurdo J, Taddei N, Ramponi G, Dobson CM and Stefani M (2002). Inherent toxicity of aggregates implies a common mechanism for protein misfolding diseases. *Nature* **416**: 507-11.

Burton PM, Hung P, Lin T, Lovelace C and White A (1985). The effects of homogeneous human prealbumin on in vitro and in vivo immune responses in the mouse. *Int. J. Immunopharmacol.* **7**: 473-81.

Burton PM, Horner BL, Jones GH, Lin T, Nestor Jr JJ, Newman SR, Parks TL, Smith AJ and White A (1987). Immuno-enhancing activity of the amino-terminal domain of human prealbumin: isolation, characterization and synthesis. *Int. J. Immunopharmacol.* **9**: 297-305.

Burton PM, Iden S, Mitchell K and White A (1978). Thymic hormone-like restoration by human prealbumin of azathioprine sensitivity of spleen cells from thymectomized mice. *Proc. Natl. Acad. Sci. USA* **75**: 823-7.

Calvete JJ, Mann K, Schäfer W, Raida M, Sanz L and Töpfer-Petersen E (1995). Boar spermadhesin PSP-II: location of posttranslational modifications, heterodimer formation with PSP-I glycoforms and effect of dimerization on the ligand capabilities of the subunits. *FEBS Lett.* **365**: 179-82.

Camilleri P, Maskins NJ and Howlett DR (1994). β-Cyclodextrin interacts with Alzheimer amyloid β-A4 peptide. *FEBS Lett* **341**: 256-8.

Campistol JM, Shirahama T, Abraham CR, Rodgers OG, Sole M, Cohen AS and Skinner M (1992). Demonstration of plasma proteinase inhibitors in beta 2-microglobulin amyloid deposits *Kidney Int* **42**: 915-23.

Castano EM and Frangione B (1988). Human amyloidosis, Alzheimer disease and related disorders. *Lab Invest* **58**: 122-32.

Castillo GM, Ngo C, Cummings J, Wight TN and Snow AD (1997). Perlecan binds to the beta-amyloid proteins (A beta) of Alzheimer's disease, accelerates A beta fibril formation, and maintains Abeta fibril stability. *J Neurochem* **69**: 2452-65.

Castillo GM, Lukito W, Peskind E, Raskind M, Kirschner DA, Yee AG and Snow AD (2000). Laminin inhibition of beta-amyloid protein (Abeta) fibrillogenesis and identification of an Abeta binding site localized to the globular domain repeats on the laminin a chain. *J Neurosci Res* **62**:451-62.

Cerini C, Peyrot V, Garnier C, Duplan L, Veesler S, Le Caer JP, Bernard JP, Bouteille H, Michel R, Vazi A, Dupuy P, Michel B, Berland Y and Verdier JM (1999). Biophysical characterization of lithostathine. Evidences for a polymeric structure at physiological pH and a proteolysis mechanism leading to the formation of fibrils. J Biol Chem **274**: 22266-74.

Chaney MO, Webster SD, Kuo Y and Roher AE (1998). Molecular modelling of the Aβ(1-42) peptide. *Protein Eng.* **11**: 761-7.

Chanoine JP, Alex S, Fang SL, Stone S, Leonard JL, Köhrle J and Braverman LE (1992). Role of transthyretin in the transport of thyroxine from the blood to the choroid plexus, the cerebrospinal fluid, and the brain. *Endocrinology* **130**: 933-8.

Cheek, A. O., Kow, K., Chen, J. and McLachlan. (1999) Potential mechanisms of thyroid disruption in humans: interaction of organochlorine compounds with thyroid receptor, transthyretin, and thyroid-binding globulin. *J A Environ Helath Perspct* **107**: 273-8.

Chen M, Ona VO, Li M, Ferrante RJ, Fink KB, Zhu S, Bian J, Guo L, Farrell LA, Hersch SM, Hobbs W, Vonsattel JP, Cha JH and Friedlander RM (2000). Minocycline inhibits caspase-1 and caspase-3 expression and delays mortality in a transgenic mouse model of Huntington disease. *Nat Med* **6**: 797-801.

Chiti F, Bucciantini M, Capanni C, Taddei N, Dobson CM and Stefani M (2001). Solution conditions can promote formation of either amyloid protofilaments or mature fibrils from the HypF N-terminal domain. *Protein Sci* **10**: 2541-7.

Coe JE, Margossian SS, Slayter HS and Sogn JA (1981). Hamster female protein- a new pentraxin structurally and functionally similar to C-reactive protein and amyloid P component. *J Exp Med* **153**: 977-91.

Coelho T, Carvalho M, Saraiva MJ, Alves I, Almeida MR and Costa PP (1993). A strikingly benign evolution of FAP in an individual compound heterozygote for two TTR mutations: TTR Met30 and TTR Met119. *J. Rheumatol.* **20**: 179.

Cohen AS and Calkins E (1959). Electron microscope observation on a fibrous component in amyloid of diverse origins. *Nature* **183**: 1201-3.

Coimbra A and Andrade C (1971). Familial Amyloid Polyneuropathy: an electron microscope study of the peripheral nerve in five cases. *Brain* **94**: 199-206.

Colon W and Kelly JW (1992). Partial denaturation of transthyretin is sufficient for amyloid fibril formation in vitro. *Biochemistry* **31**: 8654-60.

Cooper GJS (1994). Amylin compared with calcitonin gene-related peptide: structure, biology, and relevance to metabolic disease. *Endocr. Rev.* **15**: 163-201.

Corder EH, Saunders AM, Strittmatter WJ, Schmechel DE, Gaskell PC, Small GW, Roses AD, Haines JL and Pericak-Vance MA (1993). Gene dose of apolipoprotein E type 4 allele and the risk of Alzheimer's disease in late onset families. *Science* **261**: 921-3.

Cornwell III GG, Sletten K, Johansson B and Westermark P (1988). Evidence that amyloid fibril protein in senile systemic amyloidosis is derived from normal transthyretin. *Biochem. Biophys. Res. Com.* **154**: 648-53.

Costa PP, Figueira A and Bravo F (1978). Amyloid fibril protein related to prealbumin in familial amyloidotic polyneuropathy. *Proc. Natl. Acad. Sci. USA* **75**: 4449-503.

Costa RH, Lai E and Darnell Jr (1986). Transcriptional control of the mouse prealbumin (transthyretin) gene: both promotor sequences and a distinct enhancer are cell specific. *Mol Cell Biol* **6**: 4697-708.

Costa RH, Van Dike TA, Yan C, Kuo F and Darnell Jr (1990). Similarities in transthyretin gene expression and differences in transcription factors: liver and yolk sac compared to choroid plexus. *Proc. Natl. Acad. Sci. USA* **87**: 6589-93.

References

Damas AM, Ribeiro S, Lamzin VS, Palha JA. and Saraiva MJ (1996). Structure of Val122Ile variant transthyretin – a cardiomyopathic mutant. *Acta Cryst* **D52**: 966-972.

Danesi R, Marchetti A, Bernardini N, La Rocca RV, Bevilacqua G and Del Tacca M (1990). Cardiac toxicity and antitumor activity of 4'-deoxy-4'-iodo-doxorubicinol. *Cancer Chemother Pharmacol* **26**: 403-8.

De Felice FG, Houzel JC, Garcia-Abreu J, Louzada PR Jr, Afonso RC, Meirelles MN, Lent R, Neto Vm and Ferreira ST (2001). Inhibition of Alzheimer's disease beta-amyloid aggregation, neurotoxicity, and in vivo deposition by nitrophenols: implications for Alzheimer's therapy. *FASEB J* **15**: 1297-9.

de la Chapelle A, Tolvanen R, Boysen G, Santavy J, Bleeker-Wagemakers L, Maury CP and Kere J (1992). Gelsolin-derived familial amyloidosis caused by asparagine or tyrosine substitution for aspartic acid at residue 187. *Nat Genet* **2**: 157-60.

de Vera N, Cristofol R and Rodrigues Farre E (1988). Protein binding and stability of noreepinephrine in human blood plasma. Involvement of prealbumin, alpha 1-acid glycoprotein and albumin. *Life Sci* **43**: 1277-86.

Dezutter NA, Dom RJ, de Groot TJ, Bormans GM and Verbruggen AM (1999). 99mTc-MAMA-chrysamine G, a probe for beta-amyloid protein of Alzheimer's disease. *Eur J Nucl Med* **26**: 1392-9.

Dezutter NA, Landman WJ, Jager PL, de Groot TJ, Dupont PJ, Tooten PC, Zekarias B, Gruys E and Verbruggen AM (2001a). Evaluation of 99mTc-MAMA-chrysamine G as an in vivo probe for amyloidosis. *Amyloid* **8**: 202-14.

Dezutter NA, Sciot RM, de Groot TJ, Bormans GM and Verbruggen AM (2001b). In vitro affinity of 99Tcm-labelled N2S2 conjugates of chrysamine G for amyloid deposits of systemic amyloidosis. *Nucl Med Commun* **22**: 553-8.

Diaz Lobato S, Guerrero E, Gonzalez P, Crespo M, Esteban R and Villasante C (1991). Pulmonary involvement in familial amyloid polyneuropathy type I]. *Rev Clin Esp* **189**: 335-7.

DiBartola SP, Benson MD, Dwulet FE and Cornacoff JB (1985) Isolation and characterization of amyloid protein AA in the Abyssinian cat. *Lab Invest* **52**: 485-9.

Dickson PW, Howlett GJ and Schreiber G (1985). Rat transthyretin (prealbumin). Molecular cloning, nucleotide sequence, and gene expression in liver and brain. *J Biol Chem* **260**: 8214-9.

Dickson PW, Aldred AR, Menting JG, Marley PD, Sawyer WH and Schreiber G (1987). Thyroxine transport in choroid plexus. *J. Bio.l Chem.* **262**: 13907-15.

Divino CM and Schussler GC (1990a). Transthyretin receptors on human astrocytoma cells. *J Clin Endocrinoc Metab* **71**: 1265-8.

Divino CM and Schussler GC (1990b). Receptor-mediated uptake and internalisation of transthyretin. *J Biol Chem* **265**: 1425-1429.

Drouet B, Pincon-Raymond M, Chambaz J and Pillot T (1999). Laminin 1 attenuates beta-amyloid peptide Abeta (1-40) neurotoxicity of cultured fetal rat cortical neurons. *J Neurochem* **73**: 742-9.

Dwulet FE and Benson MD (1984). Primary structure of an amyloid prealbumin and its plasma precursor in a heredofamilial polyneuropathy of Swedish origin. *Proc Natl Acad Sci U S A* **81**: 694-8.

Eanes ED and Glenner GG (1968). X-ray diffraction studies on amyloid filaments. *J Histochem Cytochem* **16**: 673-7.

Eneqvist T, Andersson K, Olofsson A, Lundgren E and Sauer-Eriksson AE (2000). The β-slip: A novel concept in transthyretin amyloidosis. *Mol Cell* **6**: 1207-18.

Engel A (1978). Molecular weight determination by scanning transmission electron microscopy. *Ultramicroscopy* **3**: 273-81.

Episkopou V, Maeda S, Nishiguchi S, Shimada K, Gaitanaris GA, Gottesman ME. and Robertson EJ (1993). Disruption of the transthyretin gene results in mice with depressed levels of plasma retinol and thyroid hormone. *Proc Natl Acad Sci USA* **90**: 2375-9.

Eriksen N, Ericsson LH, Pearsall N, Lagunoff D and Benditt EP (1976). Mouse amyloid protein AA: Homology with nonimmunoglobulin protein of human and monkey amyloid substance. *Proc Natl Acad Sci U S A* **73**: 964-7.

Ernstrom U, Petterson T and Jornvall H (1995). A yellow component associated with human transthyretin has properties like a pterin derivative, 7,8-dihydropterin-6-carboxaldehyde. *FEBS Lett.* **360**: 177-82.

Esch FS, Keim PS, Beattie EC, Blacher RW, Culwell AR, Oltersdorf T, McClure D and Ward PJ (1990). Cleavage of amyloid beta peptide during constitutive processing of its precursor. Science **248**: 1122-4.

Eulitz M and Linke RP (1982). Primary structure of the variable part of an amyloidogenic Bence-Jones Protein (Mev.). An unusual insertion in the third hypervariable region of a human Kappa-immunoglobulin light chain, *Hoppe Seylers Z Physiol Chem* **363**: 1347-58.

Eulitz M, Breurer M and Linke RP (1987). Is the formation of AL-type amyloid promoted by structural peculiarities of immunoglobulin L-chains? Primary structure of an amyloidogenic lambda-L-chain (BJP-ZIM), *Biol Chem Hoppe Seyler* **368**: 863-70.

Evans SV (1993). SETOR: hardware-lighted three-dimensional solid model representations of macromolecules *J Mol Graphics* **11**: 134-8, 127-8.

Feiner HD (1988). Pathology of dysproteinemia: light chain amyloidosis, non-amyloid immunoglobulin deposition disease, cryoglobulinemia syndromes, and macroglobulinemia of Waldenstrom. *Hum Pathol* **19**: 1255-72.

Fergunson RN, Edelhoch H, Saroff HA and Robbins J (1975). Negative cooperativity in the binding of thyroxine to human serum prealbumin. *Biochem* **14**: 282-9.

Ferrão-Gonzales AD, Souto SO, Silva JL and Foguel D (2000). The preaggregated state of an amyloidogenic protein: Hydrostatic pressure converts native transthyretin into the amyloidogenic state. *Biochemistry* **97**: 6445-50.

Finn AF Jr and Gorevic PD (1990). Clinical and biochemical correlates in primary amyloidosis. *Am J Clin Pathol* **94**: 353-5.

Floege J, Schaffer J and Koch KM (2001). Scintigraphic methods to detect beta2-microglobulin associated amyloidosis (Abeta2-microglobulin amyloidosis). *Nephrol Dial Transplant* **16**:12-6.

Fonseca C, Ceia F, Nogueira JS, Alves M, Carvalho M, Luis Mde L and Luis AS (1991). [Myocardiopathy caused by Portuguese-type familial amyloidotic polyneuropathy. Sequential morphologic and functional study of 60 patients]. *Rev Port Cardiol* **10**: 909-16.

Forloni G, Colombo L, Girola L, Tagliavini F and Salmona M (2001). Anti-amyloidogenic activity of tetracyclines: studies in vitro. *FEBS Lett*: **487**: 404-7.

Fraser PE, Nguyen JT, McLachlan DR, Abraham CR and Kirschner DA (1993). Alpha 1-antichymotrypsin binding to Alzheimer A beta peptides is sequence specific and induces fibril disaggregation in vitro. *J Neurochem* **61**: 298-305.

References

Frautschy SA, Hu W, Kim P, Miller SA, Chu T, Harris-White ME and Cole GM (2001). Phenolic anti-inflammatory antioxidant reversal of Abeta-induced cognitive deficits and neuropathology. *Neurobiol Aging* **22**: 993-1005.

Frenkel D and Solomon B (2001). Towards Alzheimer's beta-amyloid vaccination. *Biologicals* **29**: 243-7.

Fritz H and Wunderer G (1983). Biochemistry and applications of aprotinin, the kallikrein inhibitor from bovine organs. *Drug Res* **33**: 479-94.

Furuya H, Saraiva MJM, Gawinowicz MA, Alves IL, Costa PP, Sasaki H, Goto I and Sakaki Y (1991). Production of recombinant human transthyretin with biological activities toward the understanding of the molecular basis of familial Amyloidotic Polyneuropathy (FAP). *Biochemistry* **30**: 2415-21.

Ganowiak K, Hultman P, Engstrom U, Gustavsson A and Westermark P (1994). Fibrils from synthetic amyloid-related peptides enhance development of experimental AA-amyloidosis in mice. *Biochem Biophys Res Commun* **199**: 306-12.

Gertz MA, Lacy MQ, Dispenzieri A, Cheson BD, Barlogie B, Kyle RA, Palladini G, Geyer SM and Giampaolo M (2002). A multicenter phase II trial of 4'-iodo-4'deoxydoxorubicin (IDOX) in primary amyloidosis (AL). *Amyloid* 2002 **9**: 24-30.

Ghiso J, Matsubara E, Koudinov A, Wisniewski T and Frangione B (1993). The cerebrospinal fluid soluble form of Alzheimer's amyloid beta is compleced to SP-40 (apolipoprotein J), an inhibitor of the complement membrane attack complex. *Biochem J* **293**: 27-30.

Ghiso J, Wisniewski T and Frangione B (1994). Unifying features of systemic and cerebral amyloidosis. *Molec Neurobiol* **8**: 49-64.

Gianni L, Belloti V, Gianni AM and Merlini G (1995). New drug therapy of amyloidoses: Reabsorption of AL-type deposits with 4'-iodo-4'-deoxydoxorubicin. *Blood* **83**: 855-61.

Gitlin D, Kumate J, Urrsti J and Morales C (1964). The selectivity of the human placenta in the transfer of plasma proteins from the mother to fetus. *J Clin Invest* **43**: 1938-51.

Gitlin D and Gitlin JD (1975). Fetal and neonatal development of human plasma proteins. In: *The plasma proteins*. Putnam, F.W. (ed). Vol II, 2nd edition. Academic Press, New York. 264-371.

Glenner GG, Terry W, Harada M, Isersky C and Page D (1971). Amyloid fibril proteins: proof of homology with immunoglobulin light chains by sequence analyses. *Science* **172**: 150-1.

Glenner GG (1980). Amyloid deposits and amyloidosis. The beta-fibrilloses (first of two parts). *N Engl J Med* **302**:1283-92.

Glenner GG (1981). The bases of the staining of amyloid fibers: their physico-chemical nature and the mechanism of their dye-substrate interaction. *Prog Histochem Cytochem* **13**: 1-37.

Glenner GG and Wong CW (1984). Alzheimer's disease: initial report of the purification and characterization of a novel cerebrovascular amyloid protein. *Biochem Biophys Res Commun* **120**: 885-90.

Goldsbury CS, Cooper GJ, Goldie KN, Muller SA, Saafi EL, Gruijters WT, Misur MP, Engel A, Aebi U, Kistler J (1997). Polymorphic fibrillar assembly of human amylin. *J Struct Biol* **119**: 17-27.

Goldsbury C, Kistler J, Aebi U, Arvinte T, Cooper GJ (1999). Watching amyloid fibrils grow by time-lapse atomic force microscopy. *J Mol Biol* **285**: 33-39.

Goldsteins G, Andersson K, Olofsson A, Daklin I, Edvinsson A, Baranov V, Sandgren O, Thylen C, Hammastrom S and Lundgren E. (1997) Characterisation of Two Highly Amyloidogenic Mutants of Transthyretin. *Biochemistry* **36**, 5346-52.

Goldsteins, G., Persson, H., Andersson, K., Olofsson, A., Daklin, I., Edvinsson, A., Saraiva, M. J. & Lundgren, E. (1999) Exposure of cryptic epitopes on transthyretin only in amyloid and in amyloidogenic mutants. *Proc. Natl. Acad. Sci. USA* **96**, 3108-13.

Goodman DS (1984). Plasma retinol-binding protein. In: *The retinoids*, Vol. 2, MB Sporn, AB Roberts and DS Goodman (eds), Academic Press, New York, pp 41-88.

Goodman DS (1987). Retinoids and retinol-binding proteins. In: *The Harvey Lectures*. Series 81.111-32.

Gorevic PD, Prelli FC, Wright J, Pras M and Frangione B (1989). Systemic senile amyloidosis. Identification of a new prealbumin (transthyretin) variant in cardiac tissue; immunologic and biochemical similarity to one form of familial amyloidotic polyneuropathy. *J Clin Invest* **83**: 836-43.

Guijarro JI, Sunde M, Jones JA, Campbell ID and Dobson CM (1998). Amyloid fibril formation by an SH3 domain. *Proc Natl Acad SciUSA* **95**: 4224-8.

Gustavsson A, Engstrom U and Westermark P (1991). Normal transthyretin and synthetic transthyretin fragments form amyloid-like fibrils *in vitro*. *Biochem Biophys Res Commun* **175**: 1159-64.

Gustavsson Å. Engström U and westermark P (1997). Transthyretin (TTR)-derived amyloid fibrils: immunoelectron microscopy of fibrils formed *in vivo* and *in vitro* from synthetic peptides and normal Transthyretin. *Amyloid: Int J Exp Clin Invest* **4**: 1-12.

Haass C, Koo EH, Mellon A, Hung AY and Selkoe DJ (1992). Targeting of cell-surface beta-amyloid precursor protein to lysosomes: alternative processing into amyloid-bearing fragments. *Nature* **357**: 500-3.

Hagen GA and Solberg Jr LA (1974). Brain and cerebrospinal fluid permeability to intravenous thyroid hormones. *Endocrinology* **95**: 1398-410.

Haggqvist B, Naslund J, Sletten K, Westermark GT, Mucchiano G, Tjernberg LO, Nordstedt C, Engstrom U and Westermark P (1999). Medin: an integral fragment of aortic smooth muscle cell-produced lactadherin forms the most common human amyloid. *Proc Natl Acad Sci* **96**: 8669-74.

Haltia M, Prelli F, Ghiso J, Kiuru S, Somer H, Palo J and Frangione B (1990). Amyloid protein in familial amyloidosis (Finnish type) is homologous to gelsolin, an actin-binding protein. *Biochem Biophys Res Commun* **167**: 927-32.

Hamidi Asl K, Liepnieks JJ, Nakamura M, Parker F and and Benson MD (1999). A novel apolipoprotein A-1 variant, Arg173Pro, associated with cardiac and cutaneous amyloidosis. *Biochem Biophys Res Commun* **257**: 584-8.

Hamilton JA, Steinrauf LK, Braden BC, Liepnieks J, Benson MD, Holmgren G, Sandgren O and Steen L (1993). The x-ray crystal structure refinements of normal human transthyretin and the amyloidogenic Val-30-->Met variant to 1.7-A resolution. *J Biol Chem* **268**: 2416-24.

Hamilton JA, Steinrauf LK, Braden BC, Murrel JR, and Benson MD (1996). Structural changes in transthyretin produced by the Ile84Ser mutation which resulted in decreased affinity for retinal-binding protein. *Amyloid* **3**: 1-12.

Harper JD, Lansbury PT Jr. (1997). Models of amyloid seeding in Alzheimer's disease and scrapie: mechanistic truths and physiological consequences of the time-dependent solubility of amyloid proteins. *Annu Rev Biochem* **66**: 385-407.

Hawkins PN, Myers MJ, Lavender JP and Pepys MB (1988a). Diagnostic radionuclide imaging of amyloid: biological targeting by circulating human serum amyloid P component. *Lancet* **1**:1413-8.

References

Hawkins PN, Myers MJ, Epenetos AA, Caspi D and Pepys MB (1988b). Specific localization and imaging of amyloid deposits in vivo using 123I-labeled serum amyloid P component. *J Exp Med* **167**: 903-13.

Hawkins PN, Rossor MN, Gallimore JR, Miller B, Moore EG and Pepys MB (1994). Concentration of serum amyloid P component in the CSF as a possible marker of cerebral amyloid deposits in Alzheimer's disease. *Biochem Biophys ResCommun* **201**: 722-6.

Heiser V, Scherzinger E, Boeddrich A, Nordhoff E, Lurz R, Schugardt N, Lehrach H and Wanker EE (2000). Inhibition of huntingtin fibrillogenesis by specific antibodies and small molecules: implications for Huntington's disease therapy. *Proc Natl Acad Sci U S A* **97**: 6739-44.

Hengartner MO (2000). The biochemistry of apoptosis. *Nature* **407**: 770-6.

Herbert J, Wilcox JN, Pham KC, Fremeau RT, Zeviani M, Dwork A, Soprano DR, Makover A, Goodman D, Zimmerman EA, Roberts JL and Schon EA (1986). Transthyretin: a choroid plexus specific transport protein in human brain. *Neurology* **36**: 900-911.

Hermansen LF, Bergaman T, Jornvall H, Husby G, Ranlov I and Sletten K (1995). Purification and characterization of amyloid-related transthyretin associated with familial amyloidotic cardiomyopathy. *Eur. J. Biochem.* **227**: 772-79.

Skovronsky DM, Zhang B, Kung MP, Kung HF, Trojanowski JQ and Lee VM (2000). In vivo detection of amyloid plaques in a mouse model of Alzheimer's disease. *Proc. Natl. Acad. Sci.* U S A **97**: 7609-14.

Hill CS Jr, Ibanez ML, Samaan NA, Ahearn MJ and Clark RL (1973). Medullary (solid) carcinoma of the thyroid gland: an analysis of the M. D. Anderson hospital experience with patients with the tumor, its special features, and its histogenesis. *Medicine* **52:** 141-71.

Holmgren G, Ericzon BG, Groth CG, Steen L, Suhr O, Andersen O, Wallin BG, Seymour A, Richardson S, Hawkins PN and Pepys MB (1993). Clinical improvement and amyloid regression after liver transplantation in hereditary transthyretin amyloidosis. *Lancet* **341**: 1113-6.

Holt IJ, Harding AE, Middleton L, Chrysostomou G, Said G, King RH and Thomas PK (1989). Molecular genetics of amyloid neuropathy in Europe. *Lancet* **1**: 524-6.

Howlett D, Cutler P, Heales S and Camilleri P (1997). Hemin and related porphyrins inhibit beta-amyloid aggregation. *FEBS Lett* **417**: 249-51.

Howlett DR, Perry AE, Godfrey F, Swatton JE, Jennings KH, Spitzfaden C, Wadsworth H, Wood SJ and Markwell RE (1999a). Inhibition of fibril formation in beta-amyloid peptide by a novel series of benzofurans. *Biochem J* **340**: 283-9.

Howlett DR, George AR, Owen DE, Ward RV and Markwell RE (1999b). Common structural features determine the effectiveness of carvedilol, daunomycin and rolitetracycline as inhibitors of Alzheimer beta-amyloid fibril formation. *Biochem J* **343**: 419-23.

Howlett Dr (2001). Aβ oligomerization: a therapeutic target for Alzheimer's disease. *Curr Med Chem* **1**: 25-38.

Huaux JP, Noel H, Malghem J, Maldague B, Devogelaer JP and Nagant de Deuxchaisnes C (1985). Erosive azotemic osteoarthropathy: possible role of amyloidosis. *Arthritis Rheum* **28**: 1075-6.

Ikegawa S, Yi S, Ando Y and Miyazaki A (1991). Reevaluation of 134 patients with familial amyloidotic polyneuropathy (FAP) in Japan, Kumamoto focus. *In: Amyloid and Amyloidosis*, Natvig JB, Forre O, Husby G, Husebekk A, Skogen B, Sletten K, Westermark P (eds.), Kluwer Publishing, Dordrecht, pp 675-8.

Inoue S, Kuroiwa M, Saraiva MJ, Guimaraes A and Kisilevsky (1998). Ultrastructure of familial amyloid polyneuropathy amyloid fibrils: examination with high-resolution electron microscopy. *J Struct Biol* **124**: 1-12.

Inoue S and Kisilevsky R. (2001). Beta-amyloid fibrils of Alzheimer's disease: pathologically altered, basement membrane-associated microfibrils? *Ital J Anat Embryol* **106**: 93-102.

Inouye H, Domingues FS, Damas AM, Saraiva MJ, Lundgren E, Sandgren O and Kirschner DA (1998). Analysis of x-ray diffraction patterns from amyloid of biopsied vitreous humor and kidney of transthyretin (TTR) Met30 familial amyloidotic polyneuropathy (FAP) patients: axially arrayed TTR monomers constitute the protofilament. *Amyloid: Int J Exp Clin Invest* **5**:163-74.

Isaac J, Kerby JD, Russell WJ, Dempsey SC, Sanders PW and Herrera GA (1998). In vitro modulation of AL-amyloid formation by human mesangial cells exposed to amyloidogenic light chains. *Amyloid* **5**: 238-46.

Isobe T and Osserman EF (1974). Patterns of amyloidosis and their association with plasma-cell dyscrasia, monoclonal immunoglobulins and Bence-Jones proteins. *N Engl J Med* **290**: 473-7.

Jacobson DR (1992). A specific test for transthyretin 122 (Val-Ile), based on PCR-primer-introduced restriction analysis (PCR-PIRA): confirmation of the gene frequency in blacks. *Am J Hum Genet* **50**: 195-8.

Jacobson DR, McFarlin DE, Kane I and Buxbaum JN (1992). Transthyretin Pro55, a variant associated with early-onset, aggressive, diffuse amyloidosis with cardiac and neurologic involvement. *Hum Genet* **89**: 353-6.

Janssen S, Van Rijswijk MH, Meijer S, Ruinen L and Van der Hem GK (1986). Systemic amyloidosis: a clinical survey of 144 cases. *Neth J Med* **29**: 376-85.

Jantzen PT, Connor KE, DiCarlo G, Wenk GL, Wallace JL, Rojiani AM, Coppola D, Morgan D and Gordon MN (2002). Microglial activation and beta -amyloid deposit reduction caused by a nitric oxide-releasing nonsteroidal anti-inflammatory drug in amyloid precursor protein plus presenilin-1 transgenic mice. *J Neurosci* **22**: 2246-54.

Jarvis JA, Kirkpatrick A and Craik DJ (1994). 1H NMR analysis of fibril-forming peptide fragments of transthyretin. *Int J Pept Protein Res* **44**: 388-98.

Johan K, Westermark G, Engstrom U, Gustavsson A, Hultman P and Westermark P (1998). Acceleration of amyloid protein A amyloidosis by amyloid-like synthetic fibrils. *Proc Natl Acad Sci USA* **95**: 2558-63.

Johansson B, Wernstedt C and Westermark P (1987). Atrial natriuretic peptide deposited as atrial amyloid fibrils. *Biochem. Biophy Res Commun* **148**: 1087-92.

Johnson KH, O'Brien TD, Betsholtz C and Westermark P (1989) Islet amyloid, islet-amyloid polypeptide, and diabetes mellitus. *N Engl J Med* **321**: 513-518.

Kabat EA, Moore DH and Landow H (1942). An electrophoretic study of the protein components in cerebrospinal fluid and their relationship to the serum proteins. *J Clin Invest* **21**: 571-7.

Kanai M, Raz A and Goodman DS (1968). Retinol-binding protein: the transport protein for vitamin A in human plasma. *J Clin Invest* **47**: 2025-44.

Kanda Y, Goodman DS, Canfield RE and Morgan FJ (1974). The amino acid sequence of human plasma prealbumin. *J Biol Chem* **249**: 6796-6805.

References

Kaplan B, Hrncic R, Murphy CL, Gallo G, Weiss DT and Solomon A (1999). Microextraction and purification techniques applicable to chemical characterization of amyloid proteins in minute amounts of tissue. *Methods Enzymol* **309**: 67-81.

Katzman R (1986). Alzheimer's disease. *N. Engl. J. Med.* **314**: 964-973.

Kayed R, Bernhagen J, Greenfield N, Sweimeh K, Brunner H, Voelter W and Kapurniotu A (1999). Conformational transitions of islet amyloid polypeptide (IAPP) in amyloid formation in vitro. *J Mol Biol* **287**: 781-96.

Kelly JW (1996). Alternative conformations of amyloidogenic proteins govern their behaviour. *Curr Opin Struct Biol* **6**: 11-7.

Kelly JW (1998). The alternative conformations of amyloidogenic proteins and their multi-step assembly pathways. Curr *Opin Struct Biol* **8**: 101-6.

Kim TW, Pettingell WH, Hallmark OG, Moir RD, Wasco W and Tanzi RE (1997). Endoproteolytic cleavage and proteasomal degradation of presenilin 2 in transfected cells. *J Biol Chem* **272**: 11006-10.

Kishikawa M, Nakanishi T, Miyazaki A and Shimizu A (1999). Enhanced amyloidogenicity of sulfonated transthyretin in vitro, a hypothetical etiology of senile amyloidosis. *Amyloid* **6**: 183-6.

Kisilevsky R and Boudreau L (1983). Kinetics of amyloid deposition. I. The effects of amyloid-enhancing factor and splenectomy. *Lab. Invest.* **48**: 53-9.

Kisilevsky R, Lemieux L, Boudreau L, Yang DS and Fraser P (1999). New clothes for amyloid enhancing factor (AEF): silk as AEF. *Amyloid* **6**: 98-106.

Kisilevsky R (2000). Review: amyloidogenesis-unquestioned answers and unanswered questions. *J Struct Biol* **130**: 99-108.

Klabunde T, Petrassi HM, Oza VB, Raman P, Kelly JW and Sacchettini JC (2000). Rational design of potent human transthyretin amyloid disease inhibitors. *Nat. Struct. Biol.*7: 312-21.

Klunk WE, Debnath ML and Pettegrew JW (1994). Development of small molecule probes for the beta-amyloid protein of Alzheimer's disease. *Neurobiol. Aging* **15**:691-8.

Klunk WE, Debnath ML and Pettegrew JW (1995). Chrysamine-G binding to Alzheimer and control brain: autopsy study of a new amyloid probe. *Neurobiol. Aging* **16**: 541-8.

Klunk WE, Wang Y, Huang GF, Debnath ML, Holt DP and Mathis CA (2001). Uncharged thioflavin-T derivatives bind to amyloid-beta protein with high affinity and readily enter the brain. *Life Sci* **69**:1471-84.

Knops J, Lieberburg I and Sinha S (1992). Evidence for a nonsecretory, acidic degradation pathway for amyloid precursor protein in 293 cells. Identification of a novel, 22-kDa, beta-peptide-containing intermediate. *J Biol Chem* **267**: 16022-4.

Kohrle J, Hesch RD, and Leonard JL (1991). *In* The Thyroid (Braverman LE, and Utiger RD eds) 6th edition 144-189, Lippincott, Philadelphia.

Kopelman M, Cogan U, Mokady S and Shinitzky M (1976). The interaction between retinol-binding proteins and prealbumins studied by fuorescence polarization. *Biochem. Biophys. Acta* **439**: 449-60.

Kyle RA and Bayrd ED (1975). Amyloidosis: review of 236 cases. *Medicine* (Baltimore) **54**:271-299.

Kyle RA and Greipp PR (1983). Amyloidosis (AL). Clinical and laboratory features in 229 cases. *Mayo Clin. Proc.* **58**: 665-683.

Lai Z, Colon W and Kelly JW (1996). The acid-mediated denaturation pathway of transthyretin yields a conformational intermediate that can self-assemble into amyloid. *Biochemistry* **35**: 6470-82.

Lansbury PT Jr. (1992). In pursuit of the molecular structure of amyloid plaque: new technology provides unexpected and critical information. *Biochemistry* **31**: 6865-70.

Lansbury PT Jr, Costa PR, Griffiths JM, Simon EJ, Auger M, Halverson KJ, Kocisko DA, Hendsch ZS, Ashburn TT, Spencer RGS, Tidor B and Griffin RG (1995). Structural model for the beta-amyloid fibril based on interstrand alignment of an antiparallel-sheet comprising a C-terminal peptide. *Nat. Struct.Biol.* **2**: 990-8.

Lansbury PT Jr. (1997). Structural neurology: are seeds at the root of neuronal degeneration? *Neuron* **19**:1151-4.

Lansbury PT Jr and Kosik KS (2000). Neurodegeneration: new clues on inclusions. Review. *Chem Biol* 7: R9-R12.

Lashuel HA, Lai Z and Kelly JW (1998). Characterization of the transthyretin acid denaturation pathways by analytical ultracentrifugation: implications for wild-type, V30M, and L55P amyloid fibril formation. *Biochemistry* **37**: 17851-64.

Lashuel HA, Wurth C, Woo L and Kelly, JW (1999). The most pathogenic transthyretin variant, L55P, forms amyloid fibrils under acidic conditions and protofilaments under physiological conditions. *Biochemistry* **38**: 13560-73.

Lazo ND and Downing DT (1998). Amyloid fibrils may be assembled from beta-helical protofibrils. *Biochemistry* **37**: 1731-6.

Leighton B and cooper GJS (1988). Pancreactic amylin and calcitonin gene-peptide cause resistance to insulin in skeletal muscle *in vitro*. *Nature* **368**: 756-60.

Levin M, Franklin EC, Frangione B and Pras M (1972). The amino acid sequence of a major nonimmunoglobulin component of some amyloid fibrils. *J Clin Invest* **51**:2773-6.

LeVine H III (1993). Thioflavine T interaction with synthetic Alzheimer's disease beta-amyloid peptides: detection of amyloid aggregation in solution. *Protein Sci* **2**: 404-10.

LeVine H (1995). Thioflavin T interaction with amyloid β-sheet structures. *Amyloid: Int. J. Exp. Clin. Invest.* **2**: 1-6.

Lewis WD, Skinner M, Simms RW, Jones LA, Cohen AS and Jenkins RL (1994). Orthotopic liver transplantation for familial amyloidotic polyneuropathy. *Clin Transplant* **8**: 107-10.

Lim GP, Yang F, Chu T, Chen P, Beech W, Teter B, Tran T, Ubeda O, Ashe KH, Frautschy SA and Cole GM (2000). Ibuprofen suppresses plaque pathology and inflammation in a mouse model for Alzheimer's disease. *J Neurosci* **20**: 5709-14.

Lim GP, Yang F, Chu T, Gahtan E, Ubeda O, Beech W, Overmier JB, Hsiao-Ashec K, Frautschy SA and Cole GM (2001). Ibuprofen effects on Alzheimer pathology and open field activity in APPsw transgenic mice. *Neurobiol. Aging* **22**: 983-91.

Link CD, Johnson CJ, Fonte V, Paupard M, Hall DH, Styren S, Mathis CA and Klunk WE (2001). Visualization of fibrillar amyloid deposits in living, transgenic Caenorhabditis elegans animals using the sensitive amyloid dye, X-34. *Neurobiol Aging* **22**: 217-26.

Linke RP, Kerling A and Rail A (1993). Hemodialysis: demonstration of truncated beta 2-microglobulin in AB-amyloid in situ. *Kidney Int Suppl* **41**: S100-5

References

Linke CD (1995). Expression of human β-amyloid peptide in transgenic *Caenorhabditis elegans*. *Proc. Natl. Acad. Sci. USA* **92**: 9368-72.

Loun B and Hage DS (1992). Characterization of thyroxine-albumin binding using high-performance affinity chromatography. *J. Chromatog. B Biomed. Appl.* **579**: 225-35.

Lowry OH, Rosenbrough NJ, Farr AL and Randall J (1951). Protein measurement with the Folin phenol reagent. *J. Biol. Chem.* **193**: 265.

Maeda S, Gottesman ME, Constantini F, Blaner WS, Saraiva MJM, Takahashi K, Yamamura K and Shimada K (1996). Use of mouse models to analyse the molecular bases of familial amyloidotic polyneuropathy type I. *Neuromuscul. Disord.***6**: S.

Maeda S, Mita S, Araki S and Shimada K (1986). Structure and expression of the mutant prealbumin gene associated with familial amyloidotic polyneuropathy. *Mol. Biol. Med.* **3**: 329-38.

Magnus JH, Stenstad T, Kolset SO and Husby G (1991). Glycosaminoglycans in extracts of cardiac amyloid fibrils from familial amyloid cardiomyopathy of Danish origin related to variant transthyretin Met 111. *Scand J Immunol* **34**: 63-9.

Makover A, Moriwaki H, Ramakrishnan R, Saraiva MJM, Blaner WS and Goodman DS (1988). Plasma transthyretin-tissue sites of degradation and turnover in the rat. *J. Biol. Chem.* **263**: 8598-603.

Makover A, Soprano DR, Wyatt ML and Goodman DS (1989). An in situ-hybridization study of the localization of retinol-binding protein and transthyretin messenger RNAs during fetal development in the rat. *Differentiation* **40**: 17-25.

Malinchik SB, Inouye H, Szumowski KE and Kirschner DA (1998). Structural analysis of Alzheimer's Abeta (1-40) amyloid: Protofilament assembly of tubular fibrils. *Biophys J* **74**: 537-45.

Mantyh PW, Ghilardi JR, Rogers S, DeMaster E, Allen CJ, Stimson ER and Maggio JE (1993). Aluminum, iron, and zinc ions promote aggregation of physiological concentrations of beta-amyloid peptide. *J Neurochem* **61**:1171-1174.

Martone RL, Herbert J, Dwork A and Schon EA (1988). Transthyretin is synthesized in the mammalian eye. Biochem *Biophys Res Commun* **151**:905-12.

Martone R and Herbert J (1993). Transthyretin interacts with globin to form protein complexes with heme dependent solubility. *J Rheumatol* **20**: 176.

Martone RL, Mizuno R and Herbert J (1993). The mammalian pineal is a synthetic site for TTR and RBP. *J Rheumat* **20**: 175.

Masters CL, Simms G, Weinman NA, Multhaup G, McDonald BL and Beyreuther K (1985). Amyloid plaque core protein in Alzheimer disease and Down syndrome. *Proc Natl Acad Sci U S A* **82**: 4245-49.

Mathis CA, Bacskai BJ, Kajdasz ST, McLellan ME, Frosch MP, Hyman BT, Holt DP, Wang Y, Huang GF, Debnath ML and Klunk WE (2002). A lipophilic thioflavin-T derivative for positron emission tomography (PET) imaging of amyloid in brain. *Bioorg Med Chem Lett* **12**: 295-8.

Maury CP, Alli K and Baumann M (1990). Finnish hereditary amyloidosis. Amino acid sequence homology between the amyloid fibril protein and human plasma gelsoline. *FEBS Lett.* **260**: 85-7.

Mazur-Kolecka B, Frackowiak J and Wisniewski HM (1995). Apolipoproteins E3 and E4 induce, and transthyretin prevents accumulation of the Alzheimer β-amyloid peptide in vascular smooth muscle cells. *Brain Res.* **698**: 217-22.

McCutchen SL, Colon W and Kelly JW (1993). Transthyretin mutation Leu55Pro significantly alters tetramer stability and increases amyloidogenicity. *Biochemistry* **32**: 12119-27.

McLaurin J, Franklin T, Zhang X, Deng J and Fraser PE (1999). Interactions of Alzheimer amyloid-beta peptides with glycosaminoglycans effects on fibril nucleation and growth. *Eur J Biochem* **266**: 1101-10.

McLean CA, Cherny RA, Fraser FW, Fuller SJ, Smith MJ, Beyreuther K, Bush AI and Masters CL. Soluble pool of Abeta amyloid as a determinant of severity of neurodegeneration in Alzheimer's disease. *Ann Neurol* **46**: 860-6.

Merched A, Serot JM, Visvikis S, Aguillon D, Faure G and Siest G (1998). Apolipoprotein E, transthyretin and actin in the CSF of Alzheimer's patients: relation with the senile plaques and cytoskeleton biochemistry. *FEBS Lett.* **425**: 225-8.

Meretoja J (1969) Familial systemic paramyloidosis with lattice dystrophy of the cornea, progressive cranial neuropathy, skin changes and various internal symptoms. A previously unrecognised heritable syndrome. *Ann Clin Res* **1** : 314-24.

Merlini G, Ascari E, Amboldi N, Belloti V, Arbustini E, Perfetti V, Ferrari M, Zorzoli I, Marinone MG, Garini P, Diegoli M, Trizio D and Ballinari D (1995). Interaction of the anthracycline 4'-iodo-4'-deoxydoxorubicin with amyloid fibrils: Inhibition of amyloidogenesis. *Proc Natl Acad Sci USA* **92**: 2959-63.

Merlini G, Anesi E, Garini P, Perfetti V, Obici L, Ascari E, Lechuga MH, Capri G and Gianni L (1999). Treatment of AL amyloidosis with 4'-Iodo-4'-deoxydoxorubicin: an update. *Blood* **93**:1112-3.

Merz PA, Wisniewski HM, Somerville RA, Bobin SA, Masters CL and Iqbal K (1983). Ultrastructural morphology of amyloid fibrils from neuritic and amyloid plaques. *Acta Neuropathol* (Berl) **60**: 113-24.

Miroy GJ, Lai Z, Lashuel HA, Peterson SA, Strang C and Kelly JW (1996). Inhibiting transthyretin amyloid fibril formation via protein stabilization. *Proc Natl Acad Sci U SA* **93**: 15051-6.

Mita S, Maeda S, Shimada K and Araki S (1984). Cloning and sequence analysis of cDNA for human prealbumin. *Biochem. Biophys. Res. Commun.* **124**: 558-64.

Monaco HL, Mancia F, Rizzi M and Coda A (1995). Structure of a complex of two plasma proteins: transthyretin and retinol-binding protein. *Science* **268**: 1039-41.

Monji A, Tashiro K, Hayashi Y, Yoshida I and Tashiro N (1998b). The inhibitory effect of laminin 1 and synthetic peptides deduced from the sequence in the laminin alpha1 chain on Abeta40 fibril formation in vitro. *Neurosci Lett* **251**: 65-8.

Monji A, Tashiro K, Yoshida I, Kaname H, Hayashi Y, Matsuda K and Tashiro N (1999). Laminin inhibits both Abeta40 and Abeta42 fibril formation but does not affect Abeta40 or Abeta42-induced cytotoxicity in PC12 cells. *Neurosci Lett* **266**: 85-8.

Monji A, Tashiro K, Yoshida I and Tashiro N (1998a). Laminin inhibits Abeta42 fibril formation in vitro. *Brain Res* **788**: 187-90.

Morgan C and Inestrosa NC (2001). Interactions of laminin with the amyloid beta peptide. Implications for Alzheimer's disease. *Braz J Med Biol Res* **34**: 5597-601.

Mross K, Mayer U, Hamm K, Burk K and Hossfeld DK (1990). Pharmacokinetics and metabolism of iodo-doxorubicin and doxorubicin in humans. *Eur J Clin Pharmacol* **39**: 507-13.

Müller SA, Goldie KN, Bürki R, Häring R and Engel A (1992). Factors influencing the precision of

quantitative scanning transmission electron microscopy. *Ultramicroscopy* **46**: 317-34.

Munar-Qués M, Costa PP and Saraiva MJM (1990). The Majorcan focus of familial amyloidotic polyneuropathy type I. In: *Familial Amyloidotic polyneuropathy and other transthyretin related disorders*. Costa PP, Falcão de Freitas A, Saraiva MJM (eds). Arquivos de Medicina, Porto, pp 13-8.

Nagata Y, Tashiro F, Yi S, Murakami T, Maeda S, Takahashi K, Okamura H and Yamamura K (1995). A 6-kb upstream region of the human transthyretin gene can direct developmental, tissue-specific, and quantitatively normal expression in transgenic mouse. *J. Biochem.* **117**: 169-175.

Nakazato M, Kangawa K, Minamino N, Tawara S, Matsuo H and Araki S (1984). Revised analysis of amino acid replacement in a prealbumin variant (SKO-III) associated with familial amyloidotic polyneuropathy of Jewish origin. *Biochem. Biophys. Res. Commun.* **123**: 921-8.

Narindrasorasak S, Lowery D, Gonzalez-DeWhitt P, Poorman RA, Greenberg B and Kisilevsky R (1991). High affinity interactions between the Alzheimer's beta-amyloid precursor proteins and the basement membrane form of heparan sulfate proteoglycan. *J Biol Chem* **266**: 12878-83.

Narindrasorasak S, Altman RA, Gonzalez-DeWhitt P, Greenberg BD and Kisilevsky R (1995). An interaction between basement membrane and Alzheimer amyloid precursor proteins suggests a role in the pathogenesis of Alzheimer's disease. *Lab Invest* **72**: 272-82.

Naslund J, Haroutunian V, Mohs R, Davis KL, Davies P, Greengard P and Buxbaum JD (2000). Correlation between elevated levels of amyloid beta-peptide in the brain and cognitive decline. *JAMA* **283**: 1571-7.

Naylor HM and Newcomer ME (1999). The structure of human retinol-binding protein (RBP) with its carrier protein transthyretin reveals an interaction with the C-terminus of RBP. *Biochemistry.* **38**: 2647-53.

Nelson SR, Hawkins PN, Richardson S, Lavender JP, Sethi D, Gower PE, Pugh CW, Winearls CG, Oliver DO and Pepys MB (1991). Imaging of haemodialysis-associated amyloidosis with 123I-serum amyloid P component. *Lancet* **338**: 335-9.

Newcomer ME, Jones TA, Aqvist J, Sundelin J, Eriksson U, Rask L and Peterson PA. (1984). The three-dimensional structure of retinol-binding protein. *EMBO J* **3**: 1451-4.

Nichols WC, Dwulet FE, Liepnieks J and Benson MD (1988). Variant apolipoprotein AI as a major constituent of a human hereditary amyloid. *Biochem Biophys Res Commun.* **156**: 762-8.

Nichols WC, Gregg RE, Brewer HB Jr and Benson MD (1990). A mutation in apolipoprotein A-I in the Iowa type of familial amyloidotic polyneuropathy. *Genomics* **8**: 318-23.

Nilsson SF, Rask L and Peterson PA (1971). Evidence for multiple thyroxine binding sites in human prealbumin. *J Biol Chem* **246**: 6098-105.

Nordlie M, Sletten K, Husby G and Ranlov PJ (1990). Transthyretin (TTR) related fragments in a Danish family with amyloid cardiomyopathy. In: *Arquivos de Medicina, Familial Amyloidotic Polyneuropathy and other Transthyretin related disorders.* Costa PP, Freitas AF, Saraiva MJM (eds.), Porto, pp 81-5.

Obici L, Bellotti V, Mangione P, Stoppini M, Arbustini E, Verga L, Zorzoli I, Anesi E, Zanotti G, Campana C, Vigano M and Merlini G (1999). The new apolipoprotein A-I variant leu(174) --> Ser causes hereditary cardiac amyloidosis, and the amyloid fibrils are constituted by the 93-residue N-terminal polypeptide. *Am J Pathol* **155**: 695-702.

Olofsson BO, Backman C, Karp K and Suhr OB (2002). Progression of cardiomyopathy after liver transplantation in patients with familial amyloidotic polyneuropathy, Portuguese type. *Transplantation* **73**: 745-51.

Olofsson A, Ippel JH, Baranov V, Horstedt P, Wijmenga S and Lundgren E (2001). Capture of a dimeric intermediate during transthhahhayretin amyloid formation. *J Biol Chem* **276**: 39592-9.

Osserman EF, Merlini G and Butler VP Jr (1987). Multiple myeloma and related plasma cell dyscrasias. *JAMA* **258**: 2930-7.

Oza VB, Petrassi HM, Purkey HE and Kelly JW (1999). Synthesis and evaluation of anthranilic acid-based transthyretin amyloid fibril inhibitors. *Bioorg Med Chem* Lett **9**: 1-6.

Oza VB, Smith C, Raman P, Koepf EK, Lashuel HA, Petrassi HM, Chiang KP, Powers ET, Sachettinni J and Kelly JW (2002). Synthesis, structure, and activity of diclofenac analogues as transthyretin amyloid fibril. *J Med Chem* **45**: 321-32.

Palha JA, Episkopou V, Maeda S, Shimada K, Gottesman ME and Saraiva MJM (1994). Thyroid hormone metabolism in a transthyretin-null mouse strain. *J Biol Chem* **269**: 33135-9.

Palha JA, Moreira P, wisniewski T, Frangione B, and Saraiva MJ (1996). Transthyretin gene in Alzheimer's disease patients. *Neurosci Lett* **204**: 212-4.

Palha JA, Hays MT, Morreale de Escobar G, Episkopou V, Gottesman ME and Saraiva MJ (1997) Transthyretin is not essential for thyroxine to reach the brain and other tissues in transthyretin-null mice. *Am J Physiol* **272**: E485-93.

Palha JA, Fernandes R, de Escobar GM, Episkopou V, Gottesman M and Saraiva MJ (2000a) Transthyretin regulates thyroid hormone levels in the choroid plexus, but not in the brain parenchyma: study in a transthyretin-null mouse model. *Endocrinology* **141**: 3267-72.

Palha JA, Ballinari D, Amboldi N, Cardoso I, Fernandes R, Belloti, V, Merlini G and Saraiva MJ (2000b) 4'-Iodo-4'-deoxydoxorubicin (I-DOX) disrupts the fibrillar structure of transthyretin amyloid. *Am J Pathol* **156**: 1919-25.

Palha JA, Moreira P, Olofsson A, Lundgren E and Saraiva MJ (2001). Antibody recognition of amyloidogenic transthyretin variants in serum of patients with familial amyloidotic polyneuropathy. *J Mol Med* **78**: 703-7.

Palha JA, Nissanov J, Fernandes R, Sousa JC, Bertrand L, Dratman MB, Morreale de Escobar G, Gottesman M and Saraiva MJ (2002). Thyroid hormone distribution in the mouse brain: the role of transthyretin. *Neuroscience, In Press.*

Palm M, Nielsen EH and Svehag SE (1997). An in vitro cellular system for generation of AA-amyloid. *APMIS* **105**: 603-8.

Pepys MB, Hawkins PN, Booth DR, Vigushin DM, Tennent GA, Soutar AK, Totty N, Nguyen O, Blake CC, Terry CJ, *et al* (1993). Human lysozyme gene mutations cause hereditary systemic amyloidosis. *Nature* **362**: 553-7.

Pepys MB (2001). Pathogenesis, diagnosis and treatment of systemic amyloidosis. *Philos Trans R Soc Lond B Biol Sci* **356**: 203-10; discussion 210-1. Review.

Persey MR, Booth DR, Booth SE, van Zyl-Smit R, Adams BK, Fattaar AB, Tennent GA, Hawkins PN and Pepys MB (1998). Hereditary nephropathic systemic amyloidosis caused by a novel variant apolipoprotein A-I. *Kidney Int* **53**: 276-81.

Peterson PA, Nilsson SF, Osterberg L, Reask L and Vahlquist A (1974). Aspects of the metabolism of retinol-binding protein and retinol. *Vitam Horm* **32**: 181-214.

References

Peterson SA, Klabunde T, Lashuel HA, Purkey H, Sacchettini JC and Kelly JW (1998). Inhibiting transthyretin conformational changes that lead to amyloid fibril formation. *Proc Natl Acad Sci U S A* **95**: 12956-60.

Podesta A, Della Torre P, Pinciroli G, Iatropoulos MJ, Brughera M and Mazue G (1994). Evaluation of 4'-iodo-4'-deoxydoxorubicin-induced cardiotoxicity in two experimental rat models. *Toxicol Pathol* **22**: 68-71.

Power DM, Elias NP, Richardson SJ, Mendes J, Soares CM and Santos CR. (2000). Evolution of the thyroid hormone-binding protein, transthyretin. *Gen Comp Endocrinol* **119**: 241-55.

Pras M, Schubert M, Zucker-Franklin D, Rimon A and Franklin EC (1968). The characterization of soluble amyloid prepared in water. *J Clin Invest* **47**: 924-33.

Pras M, Prelli F, Franklin EC and Frangione B (1983). Primary structure of an amyloid prealbumin variant in familial polyneuropathy of Jewish origin. *Proc Natl Acad Sci USA* **80**: 539-42.

Prelli F, Pras M and Frangione B (1985). The primary structure of human tissue amyloid P component from a patient with primary idiopathic amyloidosis. *J Biol Chem* **260**: 12895-8.

Prusiner SB and Scott MR (1997). Genetics of prions. *Annu Rev Genet* **31**: 139-175.

Quintas A, Saraiva MJ and Brito RM (1997). The amyloidogenic potential of transthyretin variants correlates withtheir tendency to aggregate in solution. *FEBS Lett* **418**: 297-300.

Quintas A, Saraiva MJ and Brito RM. (1999) The tetrameric protein transthyretin dissociates to a non-native monomer in solution. A novel model for amyloidogenesis. *J Biol Chem* **274**: 32943-9.

Quintas A, Vaz DC, Cardoso I, Saraiva MJ and Brito RM (2001) Tetramer dissociation and monomer partial unfolding precedes protofibril formation in amyloidogenic transthyretin variants. *J Biol Chem* **276**: 27207-13.

Ranlov I, Alves IL, Ranlov PJ, Husby G, Costa PP and Saraiva MJM (1992). A Danish kindred with familial amyloid cardiomyopathy revisited: identification of a mutant transthyretin Methionine 111 variant in serum from patients and carriers. *Am J Med* **93**: 3-8.

Rask L, Anundi H and Peterson PA (1979). The primary structure of the human retinol binding protein. *FEBS Lett* **104**: 55-8.

Ratnaswamy G, Koepf E, Bekele H, Yin H and Kelly JW (1999). The amyloidogenicity of gelsolin is controlled by proteolysis and pH. *Chem Biol* **6**: 293-304.

Redondo C, Damas AM and Saraiva MJ (2000a). Designing transthyretin mutants affecting tetrameric structure: implications in amyloidogenicity. *Biochem J* **348**: 167-72.

Redondo C, Damas AM, Olofsson A, Lundgren E and Saraiva MJ (2000b). Search for intermediate structures in transthyretin fibrillogenesis: soluble tetrameric Tyr78Phe TTR expresses a specific epitope present only in amyloid fibrils. *J Mol Biol* **304**: 461-70.

Reilly MM and King RHM (1993). Familial amyloid polyneuropathy. *Brain Pathol.* **3**: 165-76.

Riisoen H (1988). Reduced prealbumin (transthyretin) in CSF of severely demented patients with Alzheimer's disease. *Acta Neurol Scand* **78**: 455-9.

Robbins J (1991). Thyroid hormone transport proteins and the physiology of hormone binding. *In: The Thyroid. Braverman LE and Utiger RD (eds)*. JB Lippincott Company, Philadelphia, pp 111-25.

Rosenthal CJ, Franklin EC, Frangione B and Greenspan J (1976). Isolation and partial characterization of SAA-an amyloid-related protein from human serum. *J Immunol* **116**: 1415-8.

Sambrook J, Fritsch EF and Maniatis T (1989). In: Molecular cloning: a laboratorial manual. 2nd ed. Cold Spring Harbor Laboratory, Cold Spring Harbor, New York.

Santos CR and Power DM (1999). Identification of transthyretin in fish (Sparus aurata): cDNA cloning and characterisation. *Endocrinology* **140**: 2430-3.

Saraiva MJM, Birken S, Costa PP and Goodman DS (1984). Amyloid fibril protein in familial amyloidotic polyneuropathy, Portuguese type. Definition of molecular abnormality in transthyretin (prealbumin). *J. Clin. Invest.* **74**:104-119.

Saraiva MJM, Costa PP and Goodman DS (1985). Biochemical marker in familial amyloidotic polyneuropathy, Portuguese type. Family studies on transthyretin (prealbumin) methionine-30 variant. *J Clin Invest* **76**: 2171-7.

Saraiva MJ, Costa PP, Goodman DS (1986). Genetic expression of a transthyretin mutation in typical and late-onset Portuguese families with familial amyloidotic polyneuropathy. *Neurology* **36**:1413-17.

Saraiva MJM and Costa PP (1991). Molecular biology of the amyloidogenesis in the transthyretin related amyloidoses. In: *Amyloid and Amyloidosis*. Natvig,J.B., Forre, O., Husby, G., et al. eds. Doordrecht, The Netherlands: Kluwer Academic Publishers, pp 569-74.

Sasaki H, Nakazato M, Saraiva MJM, Matsuo H and Sakaki Y (1989). Activity of a metallothionein-transthyretin fusion gene in transgenic mice. *Mol Biol Med* **6**: 345-53.

Sasaki H, Yoshioka K, Takagi Y and Sakaki Y (1985). Structure of the chromossomal gene for human serum prealbumin. *Gene* **37**: 191-7.

Sasaki H, Toné S, Nakazato M, Yoshioka K, Matsuo H, Kato Y and Sakkaki Y (1986). Generation of transgenic mice producing a human transthyretin variant: a possible model for familial amyloidotic polyneuropathy. *Biochem Biophys Res Commun* **139**: 794-9.

Schmidt ML, Schuck T, Sheridan S, Kung MP, Kung H, Zhuang ZP, Bergeron C, Lamarche JS, Skovronsky D, Giasson BI, Lee VM and Trojanowski JQ (2001). The fluorescent Congo red derivative, (trans, trans)-1-bromo-2,5-bis-(3-hydroxycarbonyl-4-hydroxy)styrylbenzene (BSB), labels diverse beta-pleated sheet structures in postmortem human neurodegenerative disease brains. *Am J Pathol* **159**: 937-43.

Schreiber G, Aldred AR, Jaworowski A, Nilsson C, Achen MG and Segal MB (1990). Thyroxine transport from blood to brain via transthyretin synthesis in choroid plexus. *Am J Physiol* **258**: R338-R345.

Schreiber G, Pettersson TM, Southwell BR, Aldred AR, Harms PJ, Richardson SJ, Wettenhall REH, Duan W and Nicol SC (1993). Transthyretin gene expression evolved more recently in the liver than in the brain. *Comp. Biochem. Physiol.* B **105**: 317-25.

Schubert D, Chevion M. The role of iron in beta amyloid toxicity. *Biochem Biophys Res Commun* **216**: 702-07.

Schwarzman AL, Gregory L, Vitek MP, Lyubski S, Strittmatter W, Enghilde JJ, Bhasin R, Silverman J, Weisgraber KH, Coyle PK, Zagorski MG, Talafous J, Eisenberg M, Saunders AM, Roses AD and Goldgaber D (1994). Transthyretin sequesters amyloid β protein and prevents amyloid formation. *Proc Natl Acad Sci USA* **91**: 8368-72.

Sebastião MP, Saraiva MJ and Damas AM (1998). The crystal structure of amyloidogenic Leu55 –> Pro transthyretin variant reveals a possible pathway for transthyretin polymerization into amyloid fibrils. *J. Biol. Chem.* **273**: 24715-22.

Sebastião MP, Merlini G, Saraiva MJ and Damas AM (2000). The molecular interaction of 4'-iodo-4'-

deoxydoxorubicin with Leu-55-Pro transthyretin 'amyloid-like' oligomer leading to disaggregation. *Biochem J* **351**: 273-9.

Seibert FB and Nelson JW (1942). Electrophoretic study of the blood response in tuberculosis. *J Biol Chem* **143**: 29-38.

Selkoe DJ, Ihara Y, Abraham C, Rasool CG and McCluskey AA (1983) in Biological Aspects of Alzheimer's Disease (Katzman R, eds), Banbury report 15, Cold Spring harbor, New York, 125-135.

Selkoe DJ (1999). Translating cell biology into therapeutic advances in Alzheimer's disease. *Nature* **399**: A23-31.

Sequeiros J, and Saraiva MJ (1987). Onset in the seventh decade and lack of symptoms in heterozygotes for the TTRMet30 mutation in hereditary amyloid neuropathy-type I (Portuguese, Andrade). *Am J Med Genet* **27**: 345-57.

Serag AA, Altenbach C, Gingery M, Hubbell WL, and Yeates TO (2001). Identification of a subunit interface in transthyretin amyloid fibrils: Evidence for self-assembly from oligomeric building blocks. *Biochem* **40**: 9089-96.

Serot JM, Christmann D, Dubost T and Couturier M (1997). Cerebrospinal fluid transthyretin: aging and late onset Alzheimer's disease. *J Neurol Neurosurg Psychiatry* **63**: 506-8.

Serpell LC, Sunde M, Fraser PE, Luther PK, Morris EP, Sangre O, Lundgren E and Blake CCF (1995). Examination of the structure of the transthyretin amyloid fibril by image reconstruction from electron micrographs. *J Mol Biol* **254**: 113-8.

Serpell LC, Goldsteins G, Daklin I, Lundgren E and Blake CCF (1996). The "edge strand" hypothesis: prediction and test of a mutational "hot-spot" on the transthyretin molecule associated with FAP amyloidogenesis. *Amyloid: Int J Exp Clin Invest* **3**: 75-86.

Shimada K, Maeda S, Murakami T, Nishiguchi S, Tashiro F, Yi S and Wakasugi S (1989). Transgenic mouse model of familial amyloidotic polyneuropathy. *Mol Biol Med* **6**: 333-43.

Shirhama T and Cohen AS (1967). High resolution electron microscope analysis of the amyloid fibril. *J Cell Biol* **33**: 679-708.

Skinner M, Shirahama T, Benson MD and Cohen AS (1977). Murine amyloid protein AA in casein-induced experimental amyloidosis. *Lab Invest* **36**: 420-7.

Sklan D and Ross C (1986). Synthesis of retinal-binding protein and Transthyretin in yolk sac and fetus in the rat. *J Nutr* **117**: 406-36.

Skovronsky DM, Zhang B, Kung MP, Kung HF, Trojanowski JQ and Lee VM (2000). In vivo detection of amyloid plaques in a mouse model of Alzheimer's disease. *Proc Natl Acad Sci U S A* **97**: 7609-14.

Sletten K, Westermark P and Natvig JB (1976). Characterization of amyloid fibril proteins from medullary carcinoma of the thyroid. *J Exp Med* **143**: 993-8.

Smeland S, Kolset SO, Lyon M, Norum KR and Blomhoff R (1997). Binding of perlecan to transthyretin in vitro. *Biochem J* **326**: 829-36.

Smith TJ, Davis FB, Deziel MR, Davis PJ, Ramsden DB and Schoenl M (1994). Retinoic acid inhibition of thyroxine binding to human transthyretin. *Biochim Byophys Acta* **1199**: 76-80.

Socolow EL, Woeber KA, Purdy RH, Holloway MT, Ingbar SH (1965). Preparation of I-131-labeled human serum prealbumin and its metabolism in normal and sick patients. *J Clin Invest* **44**: 1600-9.

Soprano DR, Herbert J, Soprano KJ, Schon EA and Goodman DS (1985). Demonstration of transthyretin mRNA in the brain and other extrahepatic tissues in the rat. *J Biol Chem* **260**: 11793-8.

Soto C, Sigurdsson EM, Morelli L, Kumar RA, Castano EM and Frangione B (1998). Beta-sheet breaker peptides inhibit fibrillogenesis in a rat brain model of amyloidosis: implications for Alzheimer's therapy. *Nat Med* **4**: 822-6.

Sousa A, Coelho T, Barros J and Sequeiros J (1995). Genetic epidemiology of familial amyloidotic polyneuropathy (FAP)-type I in Póvoa do Varzim and Vila do Conde (North of Portugal). *Am J Med Genet (Neuropsych. Genet.)* **60**: 512-21.

Sousa MM, Berglund L and Saraiva MJ (2000a). Transthyretin in high density lipoproteins: association with apolipoprotein A-I. *J Lipid Res* **41**: 58-65.

Sousa MM, Norden AGW, Jacobsen C, Willnow TE, Christensen EI, Thakker RV, Verroust PJ, Moestrup SK and Saraiva, MJ (2000b). Evidence for the role of megalin in renal uptake of Transthyretin. *J Biol Chem* **275**: 38176-8181.

Sousa MM, Vital C, Ostler D, Fernandes R, Pouget-Abadie J, Carles D and Saraiva MJ (2000c). Apolipoprotein AI and transthyretin as components of amyloid fibrils in a kindred with apoAI Leu178His amyloidosis. *Am J Pathol* **156**: 1911-7.

Sousa MM, Yan SD, Stern D and Saraiva MJ (2000d). Interaction of the receptor for advanced glycation end products (RAGE) with Transthyretin triggers nuclear transcription factor kB (NF-kB) activation. *Lab Invest* **80**: 1101-10.

Sousa MM and Saraiva MJ (2001). Internalization of transthyretin. Evidence of a novel yet unidentified receptor-associated protein (RAP)-sensitive receptor. *J Biol Chem* **276**: 14420-5.

Sousa MM, Cardoso I, Fernandes R, Guimarães A and Saraiva MJ (2001a). Deposition of transthyretin in early stages of familial amyloidotic polyneuropathy: evidence for toxicity of non-fibrillar aggregates. *Am J Pathol* **159**: 1993-2000.

Sousa MM, Yan SD, Fernandes R, Guimarães A, Stern D and Saraiva MJ (2001b). Familial amyloid polyneuropathy: receptor for advanced glycation end products-dependent triggering of neuronal inflammatory and apoptotic pathways. *J Neursci* **21**: 7576-86.

Sousa MM, Fernandes R, Palha JA, Taboada A, Vieira P and Saraiva MJ (2002). Evidence for early aggregates in transgenic mice for human Transthyretin Leu55Pro. *Submitted.*

Soutar AK, Hawkins PN, Vigushin DM, Tennent GA, Booth SE, Hutton T, Nguyen O, Totty NF, Feest TG, Hsuan JJ and Pepys MB (1992). Apolipoprotein AI mutation Arg-60 causes autosomal dominant amyloidosis. *Proc Natl Acad Sci USA* **89**: 7389-93.

Spencer RG, Halverson KJ, Auger M, McDermott AE, Griffin RG and Lansbury PT Jr (1991). An unusual peptide conformation may precipitate amyloid formation in Alzheimer's disease: application of solid-state NMR to the determination of protein secondary structure. *Biochemistry* **30**: 10382-7.

Stabilini R, Vergani C, Agostini A, Pugno Vanoni Agostini R (1968). Influence of age and sex on prealbumin levels. *Clin Chim Acta* **20**: 358-59.

Stangou AJ, Hawkins PN, Heaton ND, Rela M, Monaghan M, Nihoyannopoulos P, O'Grady J, Pepys MB and Williams R (1998). progressive cardiac amyloidosis following liver transplantation for familial amyloidotic polyneuropathy: implications for amyloid fibrillogenesis. *Transplantation* **66**: 229-33.

Stangou AJ, Heaton ND, Rela M, Jewitt D, Mathias CJ, O'Grady J, Williams RS, Pepys MB, and Hawkins PM (1999). Orthotopic liver transplantation for familial amyloidotic polyneuropathy: the U.K. experience, in Kyle Raand Gertz MA (eds). Amyloid and Amyloidosis 1998, 238-240. Parthenon, New York.

References

Stauder AJ, Dickson PW, Aldred AR, Schreiber G, Mendelsohn FA, Hudson P (1986). Synthesis of transthyretin (pre-albumin) mRNA in choroid plexus epithelial cells, localized by in situ hybridization in rat brain. *J Histochem Cytochem* **34**: 949-52

Staunter H (1991). Familial amyloid polyneuropathies. In: handbook of clinical Neurology, Vinken PJ, Bruyn GW, Klawans HL (eds). 89-115. Elsevier: Amsterdam.

Stevens FJ, Myatt EA, Chang CH, Westholm FA, Eulitz M, Weiss DT, Murphy C, Solomon A and Schiffer M (1995). A molecular model for self-assembly of amyloid fibrils: immunoglobulin light chains. *Biochemistry* **34**: 10697-702.

Stoppini M, Bellotti V, Mangione P, Merlini G, Ferri G (1997). Use of anti-(beta2 microglobulin) mAb to study formation of amyloid fibrils. *Eur J Biochem* **249**: 21-6.

Stossel TP, Chaponnier C, Ezzell RM, Hartwig JH, Janmey PA, Kwiatkowski DJ, Lind SE, Smith DB, Southwick FS, Yin HL, et al (1985). Nonmuscle actin-binding proteins. *Annu Rev Cell Biol* **1**:353-402.

Strittmatter WJ, Saunders AM, Schmechel D, Pericak-Vance M, Enghild J, Salvesen GS and Roses AD (1993). Apolipoprotein E: high-avidity binding to beta-amyloid and increased frequency of type 4 allele in late-onset familial Alzheimer disease. *Proc Natl Acad Sci U S A* **90**: 1977-81.

Styren SD, Hamilton RL, Styren GC and Klunk WE (2000). X-34, a fluorescent derivative of Congo red: a novel histochemical stain for Alzheimer's disease pathology. *J Histochem Cytochem* **48**: 1223-32.

Sullivan GM, Hatterer JA, Herbert J, Chen X, Roose SP, Attia E, Mann JJ, Marangell LB, Goetz RR and Gorman JM (1999). Low levels of transthyretin in the CSF of depressed patients. *Am J Psychiatry* **156**: 710-5.

Sundelin J, Melhus H, Das S, Eriksson U, Lind P et al (1985). The primary structure of rabbit and rat prealbumin and a comparasion with the tertiary structure of human prealbumin. *J Biol Chem* **260**: 6481-87.

Tagliavini F, McArthur RA, Canciani B, Giaccone G, Porro M, Bugiani M, Lievens PM, Bugiani O, Peri E, Dall'Ara P, Rocchi M, Poli G, Forloni G, Bandiera T, Varasi M, Suarato A, Cassutti P, Cervini MA, Lansen J, Salmona M and Post C (1997). Effectiveness of anthracycline against experimental prion disease in Syrian hamsters. *Science* **276**: 1119-22

Tagliavini F, Forloni G, Colombo L, Rossi G, Girola L, Canciani B, Angeretti N, Giampaolo L, Peressini E, Awan T, De Gioia L, Ragg E, Bugiani O and Salmona M (2000). Tetracycline affects abnormal properties of synthetic PrP peptides and PrP(Sc) in vitro. *J Mol Biol* **300**: 1309-22.

Takaoka Y, Tashiro F, Yi S, Maeda S, Shimada K, Takahashi K, Sakaki Y and Yamamura K (1997). Comparison of amyloid deposition in two lines of transgenic mouse that model familial amyloidotic polyneuropathy, type I. *Transgenic Res* **6**: 261-9.

Tanaka Y, Ando Y, Sakashita N, Tashima K, Nakazato M, Miyazaki A, Yamashita T, Ohta T, Uchino M and Ando M (1995). Binding of mutant transthyretin with HDL and LDL: a novel function of lipoprotein. *Neuromuscul Disord.***6**: S.

Tawara, S., Nakazato, M., Kangawa, K., Matsuo, H. and Araki, S. (1983) identification of amyloid prealbumin variant in familial amyloidotic polyneuropathy (Japanese type). *Biochem Biophys Res Commun* **116**: 880-8.

Teng M, Gallo G and Buxbaum J (1995). Is an amyloidogenic substrate enough? Transgenic mice producing human TTR Pro55 do not develop amyloid. *Neuromuscul Disord* **6**: S.

Teng MH, Yin JY, Vidal R, Ghiso J, Kumar A, Rabenou R, Shah A, Jacobson DR, Tagoe C, Gallo G and Buxbaum J (2001). Amyloid and nonfibrillar deposits in mice transgenic for wild-type human transthyretin: a possible model for senile systemic amyloidosis. *Lab Invest* **81**: 385-96.

Tennent GA, Lovat LB and Pepys MB (1995). Serum amyloid P component prevents proteolysis of the amyloid fibrils of Alzheimer disease and systemic amyloidosis. *Proc Natl Acad Sci U S A* **92**: 4299-303

Teplow DB (1998). Structural and kinetic features of amyloid β-protein fibrillogenesis, *Amyloid* **5**: 121-42.

Terry CJ, Damas AM, Oliveira P, Saraiva MJM, Alves IL, Costa PP, Matias PM, Sakaki Y and Blake CCF (1993). Structure of Met 30 variant of transthyretin and its amyloidogenic implications. *EMBO J* **12**: 735-41.

Thylén C, Wahlquist J, Haettner E, Sandgren O and Lundgren E (1993). Modifications of transthyretin in amyloid fibrils: analysis of amyloid form homozygous and heterozygous individuals with the Met 30 mutation. *EMBO J* **12** : 743-8.

Tomiyama T, Asano S, Suwa Y, Morita T, Kataoka K, Mori H and Endo N (1994). Rifampicin prevents the aggregation and neurotoxicity of amyloid beta protein in vitro. *Biochem Biophys Res Commun* **204**: 76-83.

Tsuzuki T, Mita S, Maeda S, Araki S and Shimada K (1985). Structure of the human prealbumin gene. *J Biol Chem* **260**: 12224-7.

Uemichi T, Liepnieks JJ, Yamada T, Gertz MA, Bang N and Benson MD (1996). A frame shift mutation in the fibrinogen A alpha chain gene in a kindred with renal amyloidosis. *Blood* **87**: 4197-203.

Vahlquist A and Peterson PA (1972). Comparative studies on the vitamin A transporting protein complex in human and cynomolgus plasma. *Biochemistry* **11**: 4526-32.

Vahlquist A, Peterson PA and Wibell L (1973). Metabolism of vitamin A transporting complex. I- Turnover studies in normal persons and in patients with chronic renal failure. *Eur J Clin Invest* **3**: 352-62.

Vahlquist A, Rask L, Peterson PA and Berg T (1975). The concentrations of retinal binding protein, prealbumin, and transferring in the sera of newly delivered mothers and children of various age. *Scand J Clin Lab Invest* **35**: 569-75.

Valleix S, Drunat S, Philit JB, Adoue D, Piette JC, Droz D, MacGregor B, Canet D, Delpech M and Grateau G (2002). Hereditary renal amyloidosis caused by a new variant lysozyme W64R in a French family. *Kidney Int* **61**: 907-12.

van Jaarsveld PP, Edelboch H, Goodman DS and Robbins J (1973). The interaction of human plasma retinol binding protein with prealbumin. *J Biol Chem* **248**: 4698-705.

Varela PF, Romero A, Sanz L, Romão MJ, Töpfer-Petersen E and Calvete JJ (1997). The 2.4 Å resolution crystal structure of boar seminal plasma PSP-I/PSP-II: a zona pellucida-binding glycoprotein heterodimer of the spermadhesin family built by a CUB domain architecture. *J Mol Biol* **274**: 635-49.

Vassar PS and Culling CF (1959). *Arch Pathol* **68**: 487-498.

Verchere CB, D'Alessio DA, Palmiter RD, Weir GC, Bonner-Weir S, Baskin DG and Kahn SE (1996). Islet amyloid formation associated with hyperglycemia in transgenic mice with pancreatic beta cell expression of human islet amyloid polypeptide. *Proc Natl Acad Sci U S A* **93**: 3492-6.

Vidal R, Frangione B, Rostagno A, Mead S, Revesz T, Plant G and Ghiso J (1999). A stop-codon mutation in the BRI gene associated with familial British dementia. *Nature* **399**: 776-81.

Vieira AV, Sanders EJ and Schneider WJ (1995). Transport of serum transthyretin into chicken oocytes - A receptor mediated mechanism. *J Biol Chem* **270**: 2952-6.

Vigushin DM, Gough J, Allan D, Alguacil A, Penner B, Pettigrew NM, Quinonez G, Bernstein K, Booth SE, Booth DR and Pepys MD (1994). Familial nephropathic systemic amyloidosis caused by apolipoprotein AI variant Arg26. *Q J Med* **87**: 149-54.

Villani F, Galimberti M, Lanza E, Rozza A, Favalli L and Poggi P (1988). Evaluation of cardiotoxicity of a new anthracycline derivative: 4'-deoxy-4'-iodo-doxorubicin. *Invest New Drugs* **6**: 173-8.

Villani F, Galimberti M and Comazzi R (1991). Early cardiac toxicity of 4'-iodo-4'-deoxydoxorubicin. *Eur J Cancer* **27**: 1601-4.

Virchow R (1854). Virchows Arch. **6**: 416-426.

Wahlquist J, Thylén C, Haettner E, Snadgren O, Holmgren G and Lundgren E (1991). Structure of transthyretin molecule in amyloid fibrils from the vitreous body in individuals with the Met30 mutation. In: *Amyloid and Amyloidosis*, Natvig JB, Forre O, Husby G, Husebekk A, Skogen B, Sletten K, Westermark P (eds), Kluwer Publishing, Dordrecht, pp 587-90.

Waits RP, Uemichi T, Zeldenrust SR, Hull MT, Field L and Benson MD (1995). Development of lines of transgenic mice expressing the human tranthyretin Ser84 variant. *Neuromuscul Disord* **6**: S.

Wakasugi S, Maeda S and Shimada K (1986). Structure and expression of the mouse prealbumin gene. *J Biochem* **100**: 49-58.

Wakasugi S, Inomoto T, Yi S, Naito M, Uehira M, Iwanaga T, Maeda S, Araki K, Miyazaki J, Takahaski K, Shimada K and Yamamura K (1987). A transgenic mouse model of familial amyloidotic polyneuropathy. *Proc Japan Acad* **63** (B), 344-7.

Wallace MR, Naylor SL, Kluve-Beckerman B, Long GL, McDonald L, Shows TB, Benson MD (1985). Localization of the human prealbumin gene to chromosome 18. *Biochem Biophys Res Commun* **129**: 753-8.

Walsh DM, Hartley DM, Kusumoto Y, Fezoui Y, Condron MM, Lomakin A, Benedek GB, Selkoe DJ and Teplow DB (1999). Amyloid beta-protein fibrillogenesis. Structure and biological activity of protofibrillar intermedia. *J Biol Chem* **274**: 25945-52.

Walsh DM, Tseng BP, Rydel RE, Podlisny MB and Selkoe DJ (2000). The oligomerization of amyloid beta-protein begins intracellularly in cells derived from human brain. *Biochemistry* **39**: 10831-9.

Walts AE, Goodman MD and Matorin PA (1985). Amyloid, carpal tunnel syndrome, and chronic hemodialysis. Am J Nephrol **5**: 225-6.

Weisner B and Roethig HJ (1983). The concentration of prealbumin in cerebrospinal fluid (CSF), indicator of CSF circulation disorders. *Eur Neurol* **22**: 96-105.

Weiss K, Welch B, Seubert P, Schenk D and Yednock T (2000). Peripherally administered antibodies against amyloid β-peptide enter the central nervous system and reduce pathology in a mouse model of Alzheimer disease. *Nat Med* **6**: 916-9.

Weiss SW and Page DL(1973). Amyloid nephropathy of Ostertag with special reference to renal glomerular giant cells. *Am J Pathol* **72**: 447-60.

Westermark P, Wernstedt C, O'Brien TD, Hayden DW and Johnson KH (1987). Islet amyloid in type 2 human diabetes mellitus and adult diabetic cats contains a novel putative polypeptide hormone. *Am J Pathol* **127**: 414-7.

Westermark P, Sletten K, Johansson B and Cornwell GG III (1990). Fibril in senile systemic amyloidosis is derived from normal transthyretin. *Proc. Natl. Acad. Sci. USA* **87**:2843-5.

Westermark P, Araki S, Benson MD, Cohen AS, Frangione B, Masters CL, Saraiva MJ, Sipe JD, Husby G, Kyle RA and Selkoe D (1999). Nomenclature of amyloid fibrils proteins. Report from the meeting of the international nomenclature committee on amyloidosis, August 8-9, 1998. Part 1. Amyloid: 63-66.

Whitehead AS, Skinner M, Bruns GAP, Costello W, Edge MD, Cohen AS and Sipe JD (1984). Cloning of human prealbumin complementary DNA. Localization of the gene to chromossome 18 and detection of a variant prealbumin allele in a family with familal amyloid polyneuropathy. *Mol. Biol. Med.* **2**: 411-23.

Wisniewski T and Frangione B (1992). Apolipoprotein E- a pathological chaperone protein in patients with cerebral and systemic amyloid. *Neurosci Lett* **135**: 235-8.

Wisniewski T, Golabek A, Matsubara E, Ghiso J and Frangione B (1993). Apolipoprotein E: binding to soluble Alzheimer's beta-amyloid. *Biochem Biophys Res Commun* **192**: 359-65.

Woeber KA and Ingbar SH (1968). The contribution of thyroxine binding prealbumin to the binding of thyroxine in human serum as assessed by immunoprecipitation. *J Clin Invest* **47**: 1710-21.

Wood SJ, MacKenzie I, Maleeff B, Murle MR and Wetzel R (1996). Selective inhibition of fibril formation. *J Biol Chem* **271**: 4086-92.

Wright JR and Calkins E (1981). Clinical-pathologic differentiation of common amyloid syndromes. *Medicine (Baltimore)* **60**: 429-48.

Yamamoto K, Hsu S, Yoshida K, Ikeda S, Nakazato M, Shiomi K, Cheng S, Furihata K, Ueno I and Yanagisawa N (1994). Familial amyloid polyneuropathy in Taiwan: identification of transthyretin variant (Leu 55 - Pro). *Muscle and Nerve* **17**: 637-41.

Yamamura K, Wakasugi S, Maeda S, Inomoto T, Iwanaga T, Uehira M, Araki K, Miyazaki, J-I and Shimada K (1987). Tissue-specific and developmental expression of human transthyretin gene in transgenic mice. *Develop Genet* **8**:195-205.

Yankner BA (1996). Mechanisms of neuronal degeneration in Alzheimer's disease. Neuron 1996 May;16(5):921-32

Yi S, Takahashi K, Naito M, Tashiro F, Wakasugi S, Maeda S, Shimada K, Yamamura K and Araki S (1991). Systemic amyloidosis in transgenic mice carrying the human mutant transthyretin (Met30) gene. Pathologic similarity to human familial amyloidotic polyneuropathy, type I. *Am J Pathol* **138**: 403-12.

Yokoi K, Ito S, Mabushi T, Miykawa K, Palha JA, Iijima H, Tsukahara S, Blaner WS, Saraiva MJM, Gottesman ME, Takahashi K, Yamamura K, Shimada K and Maeda S (1996). A mouse model for familial amyloidotic polyneuropathy (FAP) type I homozygous for the mutant transthyretin gene. *Neuromuscul Disord* **6**: S32.

Yoshioka K, Furuya H, Sasaki H, Saraiva MJ, Costa PP and Sakaki Y (1989). Haplotype analysis of familial amyloidotic polyneuropathy. Evidence for multiple origins of the Val----Met mutation most common to the disease. *Hum Genet* **82**: 9-13.

Young A, Pittner R, Gedulin B, Vine W and Rink T. (1995). Amylin regulation of carbohydrate metabolism. *Biochem Soc Trans* **23**: 325-31.

Yrjanheikki J, Keinanen R, Pellikka M, Hokfelt T and Koistinaho J (1998). Tetracyclines inhibit microglial activation and are neuroprotective in global brain ischemia *Proc Natl Acad Sci U S A* **95**: 15769-74.